Developing *Bifidobacterium*-based therapeutics to improve cancer outcome and prevent occurrence

A thesis submitted for the degree of Doctor of Philosophy (Ph.D.)

Alicia D. Nicklin, BSc, MSc

Registration number: 100324085

Date of submission: September 2024

University of East Anglia

School of Biological Sciences

Quadram Institute Bioscience

Food, Microbiome and Health

ABSTRACT

Historically, the use of microorganisms for immune modulation has been explored, but their role in cancer immunotherapy is still emerging. Recent studies, both human and preclinical, have emphasised the importance of specific gut microbes in cancer progression, including cancers outside the gastrointestinal (GI) tract. Specifically, *Bifidobacterium*, recognised for its immunogenic properties, has been linked to anti-tumour responses including boosting existing treatment efficacy.

To investigate the anti-tumour effects of *Bifidobacteria*, novel strains (or PBS as control) were orally administered to tumour-burdened mice in a range of breast cancer models. Several, but not all, strains significantly inhibited tumour growth in a PyMT-Bo1 model. One strain appeared to operate through a CD8+ T cell-driven mechanism, suggesting that strain discrepancies influence host responses. Focusing on *Bif*210, there were minimal changes in the caecal metagenome and metabolome after oral administration, likely due to *Bif*210's presence in the GI tract being transient. Taken together, with the observation that the tumours were sterile, *Bif*210 likely interacts with GI immune cells, modifying systemic and tumour-associated immune responses. While *Bif*210 increased circulatory CD8+ T memory cells, it did not offer protection for metastasis in murine models, yet potentially could act as a chemopreventive agent.

To further unlock the immunotherapeutic potential of *Bif*210, its extracellular vesicles (BEVs) were investigated. Intravenous administration of *Bif*210 BEVs to C57BL/6 mice significantly reduced melanoma tumour volumes compared to controls. Mechanistically, BEVs increased the infiltration of tumour-associated Ly6G granulocytes. *In vivo* Ly6G depletion highlighted the contrasting roles of Ly6G granulocytes to melanoma progression, it has therefore been proposed that *Bif*210 BEVs polarise these cells to an anti-tumourigenic phenotype.

Harnessing specific microbiota and microbial-derived products to modulate tumour immune responses offers a novel approach to potentially complement conventional cancer therapies. To develop this clinically, further research to evaluate efficacy in humans is imperative.

TABLE OF CONTENTS

ACKNOWLEDGEMENTS.

So many people have contributed to making my PhD journey the incredible experience it has been. First and foremost, I would like to express my deepest gratitude to my family for all their love and support. My late grandmother was immensely proud that I would be studying in Norwich, the city where she grew up before studying and starting her family in Leicester. It meant the world to me that I could share my experiences in Norwich with her through stories and photos. Those moments are memories I will forever cherish.

I owe my sincerest thanks to my supervisor, Dr. Stephen Robinson. Your guidance has shaped me not only as a researcher but also as a person. Your unwavering support, both professionally and personally, has been more than I could have ever hoped for. I have watched you grow as well, and your journey continues to inspire me, keep being the incredible person that you are. I would also like to extend my gratitude to Prof. Lindsay Hall for her invaluable scientific insights and for being a beacon of dedication to both science and outreach. A special thanks as well to Dr. Gwen Le Gall, who guided me during my first rotation in Norwich and made me feel that this PhD journey would be something truly special.

As a rotation student, I had the unique opportunity to choose the project and research group I would join. I selected the Robinson group not only because the research aligned with my interests but also because the group exuded warmth, collaboration, and coffee. Having such a supportive group is a gift that I never took for granted. I feel incredibly fortunate that every member of the Robinson group made my PhD experience truly unforgettable. In particular, I would like to thank Dr. Christopher Price, whose scientific brilliance never ceases to amaze me; Dr. Christopher Benwell, whose multitasking skills and ability to craft flawless figures are goals I aspire to reach; Nilda Ilker, for always being there to lend a hand and share a coffee; Dr. Sally Dreger, for teaching me so much; and Luke Mitchell, for being a great conference buddy. I also want to acknowledge past members, including Rhianna-lily Smith, our group's social secretary and Dr. Wesley Fowler, who took me under his wing when I first started.

Outside of the lab, I have been fortunate to meet so many incredible people who have kept me motivated. Leah, Kathy, and Rebecca, our adventures have been some of the brightest highlights of this PhD journey. Erica, your loyalty and friendship are a rare treasure. Marianthi, you have turned my final year into

something far less stressful than I ever thought possible, enriching my life in ways I can't fully express. I also want to thank my friends who have been with me since my undergraduate days. Frank, Rose, Mia, Clare, Kathy, Caroline, Olly and Dan – the memories we've made together are endless, and I look forward to many more, including our future yearly holidays.

Norwich, and the people I have met along this path, will always hold a special place in my heart.

CHAPTER ONE.

1 INTRODUCTION.

1.1 CANCER

The word cancer originated from the famous Greek physician, Hippocrates (c. 460 – c. 370 BC), who believed the appearance of a tumour; that being, a solid mass with cellular outgrowths, resembled a crab, and crab is translated to "karkinoma" in Greek (Sudhakar, 2009). Major advances in oncology research, however, did not appear until the early 20th century, which saw the development of chemotherapy and a greater awareness of carcinogens, which led to a rise of public health announcements. Since cancer is the second leading cause of mortality worldwide, behind cardiovascular disease, it is not surprising that since the 20th century, cancer research has experienced advancements at an unprecedented rate. Despite this, the vast majority of patients do not respond to therapy and risk cancer recurrence. The design of novel therapeutic approaches to tackle this issue are therefore imperative to sustain and improve human health.

1.1.1 Breast cancer statistics

Breast cancer is the most common type of cancer in the UK, with 55,000 new cases diagnosed every year, 99% of which being in women (Cancer Research UK, 2019). Over recent decades, the number of diagnosed cases also appear to be trending upwards (Baker and Mansfield, 2023). There is therefore an increasing need for the development of preventative strategies for the world's most prevalent cancer type (Bray et al., 2024).

In recent decades, the survival rate for early-stage breast cancer has dramatically improved, bringing the overall 5-year survival rate to 86% (Baker and Mansfield, 2023). Improved NHS screening programmes, heightened awareness and genetic screening have meant that most cases of breast cancer are diagnosed at an early stage, however this statistic is slashed to 25% once the cancer becomes metastatic (Cancer Research UK, 2019). Therefore, treatment strategies to prevent and treat metastasis are vital.

1.1.2 Melanoma statistics

Melanoma is the deadliest form of skin cancer due to its relatively high metastatic potential. It is the 5th most common cancer diagnosis in the UK, with over 16,000 new cases each year (UK, 2021). Melanoma has a relatively high survival rating, with 87% of patients surviving at least 10 years or more. Immunotherapy and targeted therapy have revolutionised melanoma treatment, especially in cases where the cancer has metastasised. However, additional research is vital especially as melanoma mortality rates are on the rise (Bray et al., 2024).

1.1.3 Hallmarks of cancer

One of the most pivotal papers in cancer research, by Hanahan and Weinberg (2000), defines the multi-stage process of normal/healthy cells turning cancerous (Hanahan and Weinberg, 2000). The definition of cancer is under constant review, which is highlighted in the three published hallmarks of cancer revisions (Hanahan and Weinberg, 2000, Hanahan and Weinberg, 2011, Hanahan, 2022). As of 2022 there were four newly discovered hallmarks: unlocking phenotypic plasticity; non-mutational epigenetic reprogramming; senescent cells and polymorphic microbiomes, displayed in **Figure 1.1** along with the other hallmarks.

The impact that epidermal or mucosal microbiota can have, either to local or distant tumours, is a relatively recent research area receiving great interest which will be the focus of this thesis. The revisions highlight how hallmarks also interact with other hallmarks. For example, polymorphic microbiomes are closely linked to tumour-promoting inflammation, DNA damage and sustaining proliferative signalling. In depth research discovering what drives and prevents progression of these hallmarks is paramount to develop treatment strategies, which is why this research topic will discuss the possible interventions for polymorphic microbiomes in cancer.
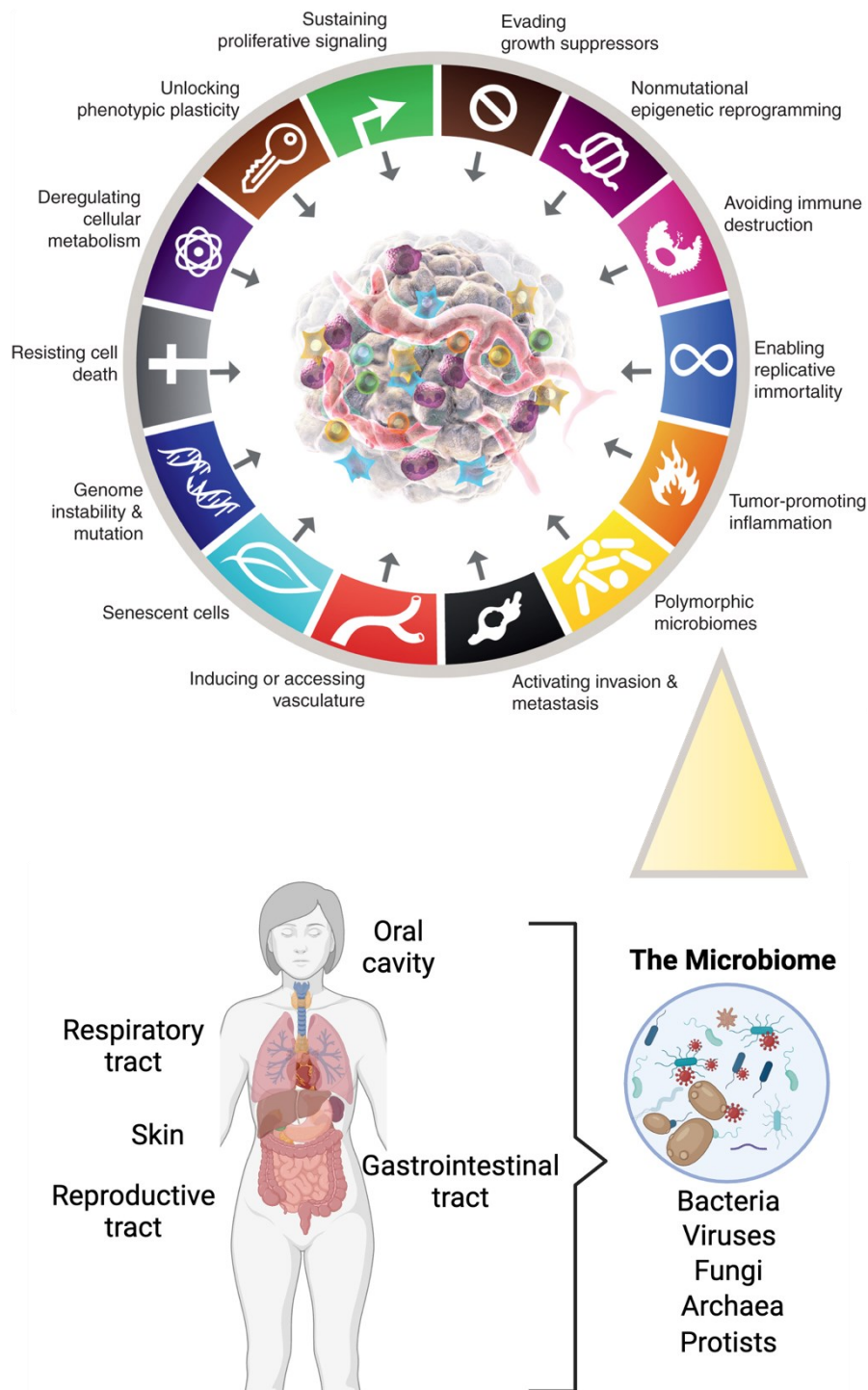
Figure 1.1 The updated 2022 revision to the key hallmarks of cancer. The hallmarks represent the multistage process that distinguishes malignant from healthy cells. The newly explored hallmark: polymorphic microbiomes will be the emphasis to this thesis. The microbiome itself is composed of trillions of microorganisms including bacteria, viruses, funghi, archaea and protists. Adapted from: "Hallmarks of Cancer: New Dimensions" (Hanahan, 2022). Created in part using BioRender.com.

1.1.4   Cancer risk factors

A person's susceptibility to developing cancer depends on three main factors: age, genetics, and the environment. All these factors drive the genetic alterations that cause the uncontrollable cancer cell growth that defines malignant tumours. The genetic alterations occur in key genes associated with the previously described 'hallmarks of cancer'. These mutations can either be inherited (germline), or somatic (occurs randomly or by exposure to environmental carcinogens).

Environmental factors play prominent roles in cancer initiation and progression, so much so that it was reported that 38% of cancer cases are preventable (Cancer Research UK., 2015). Exposure to ultraviolet rays (UV-A and UV-B), induce DNA damage and reactive oxygen species (ROS) production, promoting mutations in skin cells to increase the risk of developing skin cancers, such as melanoma (Rastrelli et al., 2014). Diet, obesity and alcohol consumption are also common influencers of cancer (Avgerinos et al., 2019, Greathouse et al., 2022). For example, The International Agency for Research on Cancer (2024) have classified alcoholic beverages as a group 1 carcinogen for breast cancer, meaning there is sufficient evidence of carcinogenicity in humans. However, comprehensive mechanisms are complicated due to the numerous physiological pathways that are involved. One mutual repercussion linking these factors is the gut microbiome (McNabney and Henagan, 2017, Wu et al., 2022). Western diets, characterised by low fibre and high fat/sugar contents, in addition to alcohol consumption, both risk factors for obesity, have been reported to induce gut dysbiosis (De Filippo et al., 2017). Gut dysbiosis is when there is a microbial composition that is not beneficial to health (Hooper et al., 2001). This emerging axis linking the gut microbiome and cancer, shall be thoroughly explored in section 1.3.8.

As well as environmental risk factors, a person's likelihood of developing cancer is largely attributed to inherited mutations in genes including oncogenes, tumour suppressor genes, and DNA repair genes. Genetic alterations in *BRCA1* and *BRCA2* genes are highly recognised to predispose people to breast and ovarian cancers (Fackenthal and Olopade, 2007). Genetic screening combined with chemo-preventative treatments including mastectomy and hysterectomy have vastly reduced cancer rates in this high-risk subset population. Research exploring novel chemo-preventative therapeutic approaches are therefore vital and can be utilised for people with high cancer susceptibility.

1.1.5 Diagnosing cancer

In the early 1940's to 50's the French surgeon, Pierre Denoix, developed a cancer stage classification system. The stages were based on pathophysiological features, with worse overall prognosis and decreased survival likelihood as stages advance. Today, similar stage classifications are used which are either a number or letter (TNM) system, displayed in tables 1.1 – 1.2. Quite often the TNM staging system is utilised by clinicians as it gives additional detail around disease progression, however, the number system is often relayed to the patient to aid communication and better understanding. Tumour/tissue biopsies are also assessed histologically and graded based on criteria in table 1.3. Grading classification is again relayed to the patient to aid their understanding around their diagnosis.

Table 1.1. Tumour stage classification based on the number system which is often used to aid diagnosis information for the patient.

Stage	Description of cancer
0	Abnormal or cancerous cells with potential to form solid tumour (carcinoma in situ).
1	Small solid tumour which has not spread from original site.
2	Large solid tumour localised to origin site.
3	Larger solid tumour which may have metastasised to lymph nodes or surrounding breast tissue.
4	Cancer cells have metastasised to at least one other organ.

Table 1.2. TNM staging classification which is often used amongst clinicians.

Classification	Description of cancer
T	Tumour size (1 – small, 4 – large).
N	Lymph nodes (0 – no cancer detected, 3 – many lymph nodes have cancer cells).
M	Metastasis (0 – not metastasised, 1 – has metastasised).

Table 1.3. Grading system used to describe histological features of tumour/tissue biopsies.

Grade	Criteria
1	Over 75% cells have tubule formation. And cells are well differentiated (small and regular). Cells have a low mitotic count.
2	10%-75% tubule formation. Cells are moderately differentiated with higher irregularity in nuclear pleomorphism. Higher mitotic count.
3	Less than 10% cells have tubule formation. Highly irregular nuclear margin and mostly single cells with no/little differentiation. High mitotic count.

1.1.6 Breast cancer physiological and molecular classification

Breast cancer can be regarded as a heterogenous disease, incorporating a collection of distinct subtypes defined by physiological and molecular classifications. For instance, tumours can either originate within the ducts, ductal carcinoma (DC), or lobules, lobular carcinoma (LC), of the breast tissue. To further characterise, tumours can be classed on whether they are non-invasive (ductal carcinoma in situ (DCIS) or lobular carcinoma in situ (LCIS)), or malignant (invasive ductal carcinoma (IDC) or invasive lobular carcinoma (ILC)), with the latter having a higher grade and thus worst prognosis (Jafari et al., 2018).

For numerous years, it has been well-established that molecular taxonomy of breast cancer has great implications to prognosis and is used in clinics to aid therapeutic approaches (Yersal and Barutca, 2014). Historically, breast tumours were molecularly classified, basing tumour cell marker expression on histological analysis. In recent years however, global gene expression profiling (GEP) has become increasingly popular to stratify subclasses of the disease to provide more accurate prognosis predictions and further tailor therapies (Rhodes et al., 2004). Molecular expression of major breast cancer subtypes is summarised in table 1.4.

The expression of sex hormone receptors for oestrogen (ER) and progesterone (PR) is apparent in Luminal A (LumA+), normal-like and Luminal B (LumB+) breast tumours. Around 70-80% of tumours are ER-positive and/or PR-positive (Bergholtz et al., 2020). The mechanism for the progression of ER+ cancers is often defined by the activation of ER-α receptor signalling by the sex hormone, ER. Resultant effects include increased cellular proliferation (Helguero et al., 2005). Similarly, when progesterone activates PRs, regulation of genes responsible for cellular proliferation and division are altered (Brisken, 2013). Generally, cancers that are

ER+ and/or PR+ are associated with better prognosis as adjuvant hormone therapies such as tamoxifen and aromatase inhibitors can be prescribed. A higher expression of the proliferation transcription marker, Ki67, which is commonly used to predict tumour growth rate, is indicative of worse overall prognosis. (Yerushalmi et al., 2010). Ki67 expression can also be used to differentiate between the hormone-receptor-positive, LumA and LumB breast cancers.

Human epidermal growth factor receptor 2 (HER2) is another pivotal protein expressed on certain tumours, those being some luminal B and all HER-enriched breast cancer subtypes. Tumours overexpressing *ERBB2*, the gene responsible for HER2 production, have increased cell proliferation and survival. Compared to HER2- tumours, HER2-enriched tumours are associated with more aggressive phenotypes and higher likelihood of recurrence. Therapies that target and inhibit HER2 are among some of the most prescribed treatments, such as the anti-HER2 monoclonal antibodies, Trastuzumab (Herceptin) and Pertuzumab (Perjeta).

Around 10-20% of breast cancers lack hormone receptors and HER2 proteins, and these are subsequently classed as triple negative, or sometimes referred to as 'basal-like' breast cancer (Bergholtz et al., 2020). Triple negative breast cancer bestows the greatest threat to cancer-free survival. This aggressive phenotype is aligned with the inability to target ERs, PRs, or HER2, resulting in a lack of effective therapies to limit cancer cell proliferation.

Table 1.4. Molecular classification of the major breast cancer subtypes based on the review by Yersal and Barutca (2014).

Subtype	Molecular expression
Luminal A (LumA)	HR+ (ER+ and/or PR+) HER2- Ki67 low
Normal-like	HR+ (ER+ and/or PR+) HER2- Ki67 low
Luminal B (LumB)	HR+ (ER+ and/or PR+) HER2+/- Ki67 high/any
HER2-enriched	HR- (ER- and PR-) HER2+ Ki67 any
Triple negative (TNBC)	HR- (ER- and PR-) HER2- Ki67 any

1.1.7 Metastasis

Metastasis occurs when cancer cells disseminate from the original (primary) tumour to distant tissues, making it the most lethal stage of cancer. Cancer cells that disseminate from primary tumours travel systemically via the blood, lymphatic system and even the nerves (Sleeman et al., 2011). Neighbouring tissues can also be infiltrated by cancer cells. Common sites of breast cancer metastasis include bone, lung, liver, axillary lymph node and ovaries, whereas melanoma tumours most commonly metastasises to the liver (Coleman and Tsongalis, 2001). How cancer cells seed to distant organs to form metastatic lesions is a multistage process defined by key hallmarks, summarised in Figure 1.2.

The first key hallmark of metastasis is an increase in cancer cell motility and invasion. Changes in cell marker expression enable cancer cells to detach from primary tumours, as well as extravasate to distant tissues. For example, enhanced metastatic potential is associated with a loss/reduced expression of E-Cadherin, an epithelial cell adhesion marker. In contrast, the marker, N-Cadherin, associated with increased cell motility is upregulated, and represents the epithelial to mesenchymal transition (EMT). Cancer cell EMT also is denoted by changes in cell morphology through cytoskeleton reorganisation and cell polarisation, both of which increase migratory properties of the cells (Brabletz et al., 2018). Transforming growth factor-beta (TGF-β) has been studied to be an important cytokine for EMT in cancer cells (Peng et al., 2022).

For cancer cells to be able to detach, the extracellular matrix (ECM) must degrade. Cancer, immune, and stromal cells all release enzymes such as matrix metalloproteinases (MMPs), cathepsins, and serine proteases that modulate the composition of proteins and carbohydrates in the ECM (Winkler et al., 2020). In response, cancer cells intravasate into the circulatory system and adhere to endothelial cells. ECM remodelling in distant organs also enhances colonisation of cancer cells, as well as immune cell infiltration (Yuan et al., 2023).

The pre-metastatic niche in distant organs governs how easy it is for cancer cells to seed and colonise (Altorki et al., 2019). An important factor shaping this is the immune system, with studies reporting that myeloid-derived suppressor cells (MDSCs) including tumour-associated macrophages (TAMs), drive growth and survival of colonising cancer cells (Swierczak and Pollard, 2020, Fu et al., 2020). In addition, cytokines, chemokines and other soluble factors released by immune- and non-immune cells in the premetastatic niche promote chronic inflammation,

angiogenesis, and remodelling of the extracellular matrix (ECM). Angiogenesis, the formation of new blood vessels, is particularly important for metastasis. Angiogenesis is driven by cytokines such as endothelial growth factor (VEGF) and TGF-β (Yehya et al., 2018). New blood vessels within the tumour not only promote primary tumour growth, but are also hyperpermeable, enabling cancer cell intravasation into the circulation. Angiogenesis also promotes cancer cell extravasation into distant organs, provides nutrients/oxygen for the metastatic lesions, as well as maintaining MDSC infiltration to the pre-metastatic niche (Zetter, 1998).
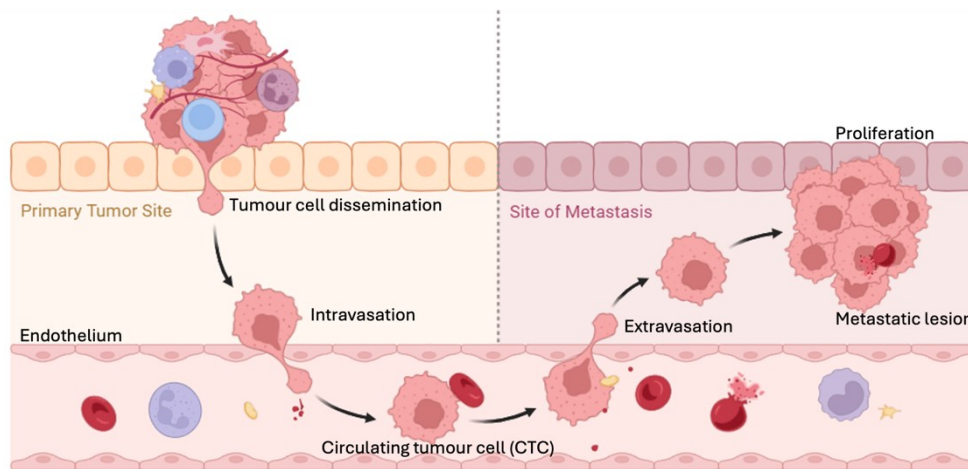
Figure 1.2 The multi-stage process of metastatic lesion formation. The primary tumour microenvironment influences the ability of cancer cells to disseminate and intravasate to a circulatory system, in this example, the blood. Platelets for example can adhere to circulating tumour cells (CTCs) to promote immune evasion hence increase CTC survival. CTCs adhere to the endothelium through selectins and integrins. Subsequently, cancer cells degrade the endothelial basement membrane by the release of matrix metalloproteases and cathepsins to enable transendothelial migration, defined as extravasation. To successfully form metastatic lesions, tumour cells then need to colonise and proliferate to the new tissue. Factors such as immune cells in the premetastatic niche influence whether cancer cells proliferate here. Adapted from "Tumour Metastasis", by Biorender.com (2023). Retrieved from https://app.biorender.com/biorender-templates.

1.1.8 Breast cancer treatment strategies

Determining a treatment strategy for cancer patients is governed by numerous factors, in particular cancer stage and grade. Other notable factors include the patient's age and ability to handle adverse treatment side effects. Palliative care may be offered for particularly vulnerable patients in late stages. For early-stage breast cancer cases (stages I - II), a lumpectomy is generally performed, involving the removal of the solid tumour and the surrounding tissue around the tumour

margins (Fisher et al., 2002). Preoperative neoadjuvant therapy in some cases is given to reduce the size of the tumour to ease resection surgery (Shien and Iwata, 2020). Radiation therapy is often offered post-surgery to eliminate any cancerous cells missed during resection and prevents reoccurrence (Fisher et al., 2002). Radiation therapy typically occurs for 5 days a week, lasting a total of 5 - 6 weeks. When multiple solid tumours exist or there are microcalcifications (calcium deposits within the tissue), complete breast removal (mastectomy) is opted for. Mastectomies are also offered to high-risk individuals, such as people with the BRCA1/2 gene mutations, as a preventative strategy (Woo et al., 2021).

Patients that are diagnosed with aggressive or metastasised breast cancer frequently are given a combination of treatments post-mastectomy. Of which include chemotherapy drugs, including oxorubicin, cyclophosphamide, paclitaxel, and carboplatin (Early Breast Cancer Trialists' Collaborative Group (EBCTCG), 2005). Endocrine therapy can also be offered for hormone receptor-positive breast cancers (ER+ or PR+), including tamoxifen and aromatase inhibitors. Such therapies are often given long-term for 5-10 years. HER2 positive cancer patients can also be treated with HER2-targeted therapies, such as rastuzumab (Herceptin), Pertuzumab (Perjeta) and T-DM1 (Kadcyla) (Greenwalt et al., 2020). Immunotherapy for the treatment of particularly hard to treat breast cancers such as triple negative has been an emerging treatment option in recent years. Immunotherapy is discussed later in more detail, as it forms the premise of potential treatments discussed in this thesis. Defining molecular subtypes of breast cancer and thus developing targeted therapies is proof of principle that research into understanding and defining a disease can dramatically improve survival rates.

1.1.9 Melanoma treatment strategies

Similarly to breast cancer treatments, melanoma treatments are offered on a patient-by-patient basis, considering the cancer stage and overall health of the patient. Surgery to excise the melanoma tumour and margins of healthy tissue around is offered at early stages (stages 0-II). Again, neoadjuvant treatment can reduce tumour volume before surgery. Radiotherapy is not commonly used post-surgery, however, can be used if the melanoma has metastasised. Again, unresectable and metastatic melanoma (stage III-IV) are much harder to treat. In recent years, targeted therapy and immunotherapy (discussed in detail later) have vastly contributed to the treatment of advanced melanoma (Pavlick et al., 2023). Drugs have been developed that target dysregulated pathways common in melanoma. Amongst these common pathways are the RAS/RAF/MAPK and

PI3K/AKT/mTOR, which promote cell division, survival, and angiogenesis (Rager et al., 2022).

1.2 THE HOST IMMUNE SYSTEM AND FUNCTION IN THE CONTEXT OF CANCER

A host's immune system is a specialised network that defends against pathogens and other factors that may harm the body, such as cancer cells. Immune responses can be broadly split into two main categories: innate and adaptive. Bone marrow-derived precursor cells become differentiated into the distinct immune cell subsets that participate in the innate and adaptive immune responses. The lineages, differentiation pathways, as well as sites of maturation are highlighted in **Figure 1.3**.

Innate immune responses are the initial line of defence and are generally non-specific. Innate immune cells are typically derived from the myeloid lineage (**Figure 1.3**) and include neutrophils, basophils, eosinophils, macrophages, mast cells, natural killer (NK) cells and dendritic cells (DCs). The innate immune response also includes plasma-associated proteins such as complement proteins, acute phase proteins, antimicrobial peptides, and mannose binding lectin, which all promote inflammation and can enhance innate and/or adaptive immune responses. Innate immune cells can be directly cytotoxic to invading pathogens, foreign bodies and other danger-associated molecules/cells by phagocytosis or through the release of extracellular components. They also interact with adaptive immune cells through antigen presentation and/or the release of soluble factors such as cytokines.

Adaptive immune cells are derived from the lymphoid lineage and offer targeted, specialised immune responses. They also provide immunological memory to prevent host damage in the event of re-exposure to antigens. Lymphoid cells including naïve T and B cells become activated by a range of antigens and signals which will be discussed, in the context of cancer, later.
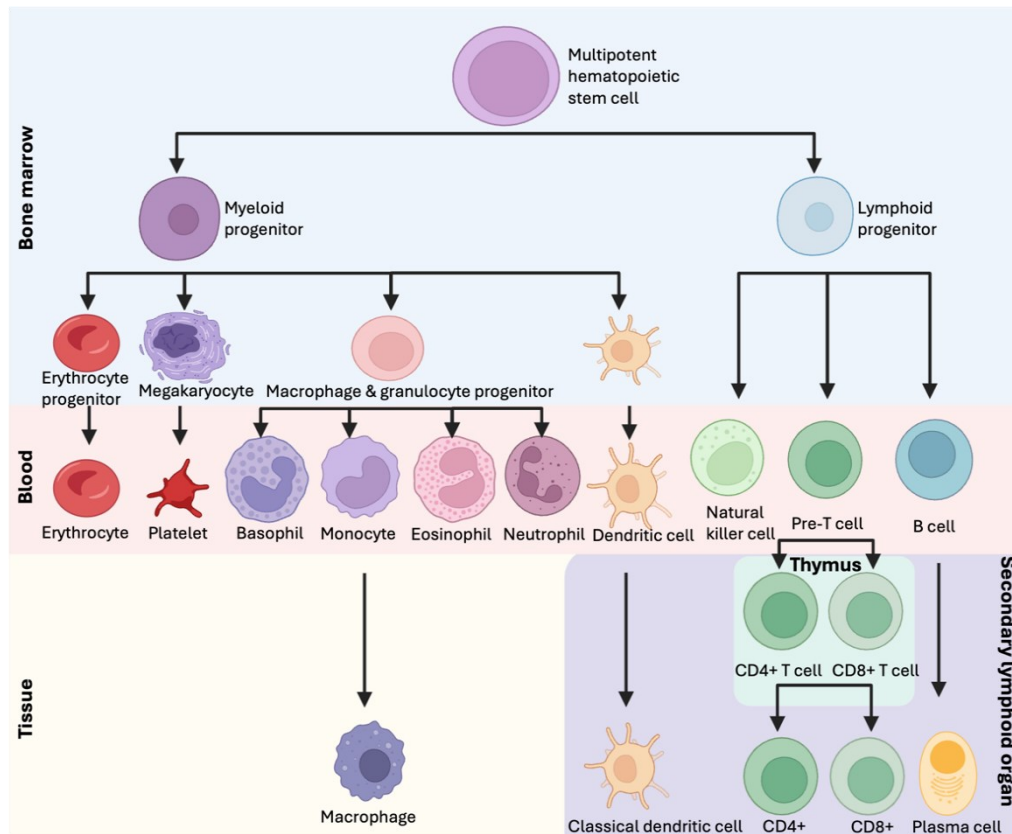
Figure 1.3 The process of haematopoiesis. All blood cells are derived from hematopoietic stem cells (HSCs) in the bone marrow. This process has two main lineages: the lymphoid and myeloid lineages. The myeloid lineage produces numerous progenitor cells that differentiate into erythrocytes, platelets, dendritic cells, granulocyte and monocyte innate immune cells. Monocytes can differentiate further in peripheral tissues to form macrophages. The lymphoid lineage generates various types of lymphocytes, including natural killer (NK), T and B cells. Pre-T cells mature further in the thymus where the majority either express CD4, known as T helper cells, or CD8, known as cytotoxic T cells. B- and T cells can become activated by antigen presenting cells in secondary lymphoid organs. The activated B cells form antibody-producing plasma cells. Adapted from: "The underestimated role of the microphthalmia-associated transcription factor (MiTF) in normal and pathological haematopoiesis" (Oppezzo and Rosselli, 2021). Created in part using BioRender.com.

1.2.1 Tumour microenvironment and the immune system

The tumour microenvironment (TME) denotes the total composition of a solid tumour, and includes tumour-, stromal-, immune-, fibroblast-, endothelial cells, cellular components, growth factors, and other soluble factors. The TME governs all factors involved in cancer cell proliferation, progression, metastasis and response to therapy.

The immune landscape is a vital element of the TME. Effective immune responses are not only killing tumour cells, but also slowing the progression of metastasis. Cancer cells, however, can evade immune-induced cell death, promoting cancer

progression. How immune cells are polarised and the ratio of pro-/anti-inflammatory signals within the TME govern whether tumour cells succumb to cell death or evade immune signals.

Immune cells interact directly with cells, including tumour, stromal and other immune cells via receptor binding or indirectly by releasing soluble factors (cytokines and chemokines). This complex web of interactions between all cells within the TME determines how immune cells are polarised and thus their functional activity. The opposing anti- and pro-tumourigenic roles of the different immune cell subtypes is discussed thoroughly below.

1.2.2 Myeloid cells in the TME

1.2.2.1 Natural killer (NK) cells

Natural killer (NK) cells make up 5–10% of circulating peripheral blood mononuclear cells (PBMCs) and play a critical role in anti-tumorigenic immunity. NK cells can release cytotoxic granules, containing granzymes and perforin, which are directly cytotoxic to tumour cells. In addition, through production of cytokines such as IFNγ and TNFα, they can enhance the functional activity of DCs resulting in increased CD8 T cell polarisation, a key cell involved in anti-cancer immunity. IFNγ also can induce anti-tumourigenic macrophage differentiation (Chistiakov et al., 2018). For these reasons, NK cell adoptive transfers have attracted attention as a potential cancer immunotherapeutic avenue.

NK cell populations within the TME have been shown to be heterogeneous, however. A recent study found 3 distinct clusters of NK cells (NK1, NK2 and NK3) with six subsets within each cluster in human blood when single-cell RNA sequencing (scRNA-Seq) and cellular indexing of transcriptomes and epitopes by sequencing (CITE-Seq) were performed (Rebuffet et al., 2024). CITE-Seq is a novel powerful tool to study immune cell subsets as combines gene expression data with surface protein marker expression. In general, NK3 cells resembled adaptive NK cells that can retain immunological memory, therefore have gained significant interest in preventing tumour reoccurrence. NK1 and NK2 clusters differed in their cytokine production and cytotoxic exerting capabilities.

1.2.2.2 Neutrophils

Neutrophil biology in the context of cancer is particularly complex and controversial. On one hand, numerous epidemiological studies suggest that high levels of circulating and tumour-infiltrating neutrophils are associated with poorer prognosis

and response to therapy (Yin et al., 2022, Sagiv et al., 2015, Schmidt et al., 2005). On the other hand, mechanistic studies in animals have found that neutrophils have an anti-cancer role. This highlights their high functional heterogeneity and plasticity (Mihaila et al., 2021). Recent studies, using transcriptomic and cell surface marker expression analysis, have clustered neutrophils into two distinct subsets: N1, anti-tumourigenic neutrophils, and N2, pro-tumourigenic neutrophils (Liu et al., 2023). Distinguishing features for each subset are depicted in **Figure 1.4**. N1 neutrophils are characterised by higher expression of the cell surface glycoprotein, Intercellular Adhesion Molecule 1 (ICAM-1), in addition to the higher production of ROS, NO and pro-inflammatory cytokines. Morphologically, N1 neutrophils exhibit hyper-segmented nuclei compared to N2 neutrophils. N2 neutrophils have higher expression of the enzyme, arginase 1 (ARG1) (Miret et al., 2019). ARG1 is responsible for converting L-arginine to urea and L-ornithine. L-arginine is essential for T cells to form the T-cell antigen receptor (TCR-CD3) complex, which when activated, sustains T cell activation and proliferation. Higher expression of ARG1 on neutrophils and other myeloid suppressor cells depletes L-arginine levels, therefore inhibits T cell effector function. In addition, N2 neutrophils produce the proangiogenic factor, VEGF, which when bound to its receptor (VEGFRs) on endothelial cells, induces pro-angiogenic signalling to promote new blood vessel growth. As discussed, angiogenesis drives cancer cell proliferation, metastasis and promotes immune evasion. N2 neutrophils also have higher expression of CXCR4 which, when bound to CXCL12, homes neutrophils to the TME. The small molecule, Plerixafor (AMD3100), has been approved for multiple myeloma and non-Hodgkin lymphoma to limit N2 neutrophil infiltration by inhibiting CXCR4-CXCL12 signalling (De Clercq, 2015).
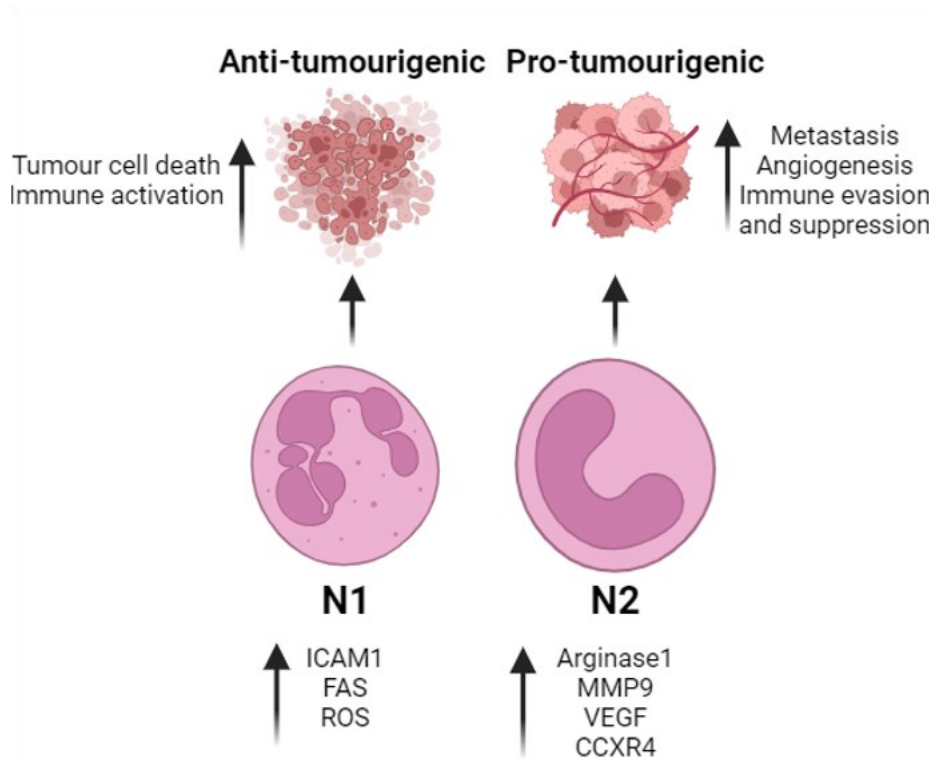
Figure 1.4 Tumour-associated granulocytes have a dual role for cancer progression. N1 neutrophils are classed as anti-tumourigenic and express markers including ICAM-1, the cell surface receptor, FAS (CD95), and higher reactive oxygen species (ROS) production. N1 also have a hypersegmented nucleus compared to N2 cells. Contrastingly N2 neutrophils are protumourigenic with markers including Arginase1 (ARG1), higher matrix metalloproteinase-9 (MMP9) production, vascular endothelial growth factor (VEGF) production, chemokine receptor type 4 (CXCR-4) expression. Adapted from (Piccard et al., 2012). Created in part using BioRender.com.

Upon stimulation via PRRs, neutrophils may undergo cellular degranulation, whereby they release components known as neutrophil extracellular traps (NETs), in a process known as NETosis (**Figure 1.5**). NETs can trap circulating cancer cells, which promotes their extravasation to distant organs (Masucci et al., 2020). The release of proteases in the NETs also increases the prevalence of EMT which drives metastasis.

Polarising neutrophils to an anti-tumourigenic phenotype is an emerging research area. Studies have shown that TGFβ to be an important driver for N2 polarisation (Fridlender et al., 2009). However, therapies that inhibit TGFβ signalling exert strong side effects, as this cytokine is essential for normal tissue homeostasis (Danielpour, 2024). On the other hand, IFNγ has been shown to promote N1 neutrophil polarisation. It is important to consider that neutrophils display different roles during tumour progression, therefore temporal considerations, in addition to

cancer stage should be reviewed closely when exploring therapies that target neutrophils.
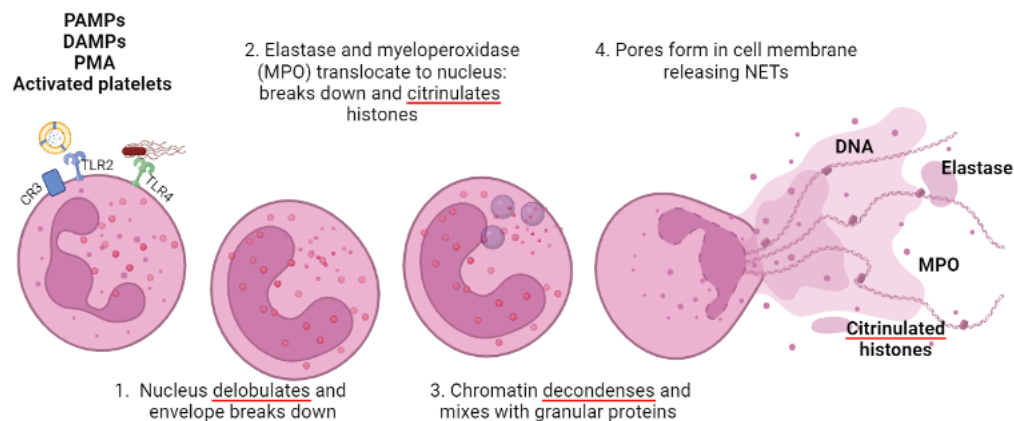
Figure 1.5 The multi-stage process of NETosis. Activated Ly6G granulocytes become activated by a range of stimuli including pathogen- and danger-associated molecular patterns (PAMPs and DAMPs), Phorbol 12-myristate 13-acetate (PMA) and activated platelets where they degranulate in a process known as NETosis. Cells release cellular contents such as DNA, elastase, myeloperoxidase (MPO) and citrullinated histones. Adapted from: "Immune modulation of some autoimmune diseases: the critical role of macrophages and neutrophils in the innate and adaptive immunity" (Navegantes et al., 2017). Created using BioRender.com

1.2.2.3   Macrophages

Macrophages, along with dendritic cells, are among the most vital cells for presenting antigens to T cells. Macrophages are a highly heterogenous immune cell population with distinct functions that are governed by inflammatory signals. Previous literature has clustered tumour associated macrophages as 'M1' (proinflammatory) or alternate 'M2' (immunosuppressive) macrophages, with the latter being pro-tumourigenic (Mills et al., 2000, Martinez and Gordon, 2014). However, recent studies have emphasised that this binary characterisation does not represent the plasticity of different activation and polarisation states (Lv et al., 2021). Terminology of subsets should therefore be standardised to aid consistency across studies and clinical understanding. In general, macrophages (M1) that are classically activated produce higher levels of ROS and NO that can directly inhibit cancer cell growth. They present antigens via major histocompatibility complex (MHC) class I molecules to other cells, interact with co-stimulatory receptors (e.g. CD80 and CD86), and produce cytokines that collectively control T cell responses. For example, M1 macrophages promote CD8 T cell responses through antigen presentation and production of IL-12 and Type-I interferon (IFN) (Weiss et al., 2017). In contrast, alternatively activated macrophages (M2) produce anti-

inflammatory cytokines such as IL-10, IL-2 and TGFβ that can promote Treg cells (Jaynes et al., 2020). Macrophages can also directly inhibit T cells through PD-L1 and PD-1 signalling. In addition, M2 macrophages can stimulate tumour-associated angiogenesis through secretion of VEGF. Immunosuppressive M2 macrophages therefore are a prominent target for cancer immunotherapy. Currently, there are numerous ongoing clinical trials that exploit macrophage heterogeneity during cancer development, for example by enhancing co-stimulatory macrophage-T cell signalling, inhibiting macrophage development (through preventing colony stimulating factor-1 signalling), and limiting macrophage recruitment by blocking chemokines such as CCR2 (Mantovani et al., 2022).

1.2.2.4 Dendritic cells

DCs, like macrophages, are involved in antigen presentation and are undoubtedly the most important cells for bridging innate and adaptive immune responses. Research over the past two decades has uncovered the two major dendritic cell subsets in tumour biology; conventional dendritic cells type 1 (cDC1) and type 2 (cDC2).

cDC1s, characterised by expression of CD103, are a particularly important subset of dendritic cells as they exert crucial anti-cancer immune responses (Ng et al., 2018). In tumour tissues, cDC1s sample tumour-associated antigens (TAAs) and present them via MHC class I or class II molecules. cDC1s have superior antigen presenting abilities compared to cDC2s (Murphy and Murphy, 2022). cDC1s then migrate to tumour draining lymph nodes down a chemokine gradient via CCR7 chemokine receptor binding to CCL19 and CCL21 (Lee et al., 2024). Inside the lymphoid tissue, cDC1s bind to naïve CD8+ T cells via MHC class 1 molecule and co-receptors (CD80, CD86). Pro-inflammatory cytokines such as IL-12 are also released. Signalling pathways are activated that promote CD8+ T cell proliferation and priming, subsequently expanding the cytotoxic T lymphocyte population. cDC1s also activate naïve CD4+ T cells to activate T helper cells via MHC class II interactions (Lei et al., 2023).

Overall, an increased presence of cDC1s has been associated with higher infiltration of CTLs, T helper 1 cells and thus better overall survival and response to ICI therapy. As a result, therapies have focussed on increasing cDC1 infiltration and activity, for example by increasing expression of CCR7, TLR agonists to increase activation, and research into cDC1 vaccines.

1.2.3 Lymphoid cells in the TME

1.2.3.1 T cells

T cells form a crucial part of the adaptive immune system and in recent years have been at the forefront of cancer immunotherapy research. As discussed, the two major T cell subsets that exist in blood and tissues are: CD4+ and CD8+. Interactions with antigen presenting cells and growth factor signals determine their activation and polarisation, and thus role, in the TME.

As discussed, T cell priming primarily exists within tumour draining lymph nodes, where cDCs express tumour antigens on MHC molecules (**Figure 1.6**). Macrophages also are important in shaping T cell activation and polarisation (Mantovani et al., 2022). MHC class I binds to naïve CD8+ T cells, whilst MHC class II binds to naïve CD4+ T cells. Co receptors on APCs (CD80, CD86) also bind to CD28 or CTLA4 on T cells and are crucial for effective T cell activation.

The cytokine environment within the TME heavily influences T cell subset polarisation. Activated CD4+ T cells clonally expand depending on the cytokine and antigen exposure into the following subsets: T helper 1 (Th1), T helper 2 (Th2), T helper 17 (Th17), T follicular helper, and T regulatory cells (Treg) (Basu et al., 2021). New emerging evidence has suggested that CD8 effector T cells can be divided into subsets in a similar manner to CD4+ T cell subset classifications (Koh et al., 2023). Subsets are defined by the type of cytokines produced. Most research, especially in the context of cancer, has focussed on cytotoxic T cells (CTLs), however these additional emerging subsets appear to have distinct functions. Further research is vital to better understand the therapeutic potential and role of these cells during cancer progression and therapy responsiveness.

Once activated, T cells infiltrate tumours down a chemokine gradient. Tumour and other cells within the TME secrete chemokines such as CCL9, CCL10 and CCL5 which are vital for T cell homing to the tumour site (Lanitis et al., 2017). Upon transmigration through the endothelial cell barrier, activated tumour-specific T cells are re-exposed to tumour antigens.

CTLs are amongst the most potent anti-cancer immune effectors. CD8+ effector cells are directly cytotoxic to tumour cells as they release proteolytic enzymes (**Figure 1.6**), including perforin and granzyme B, upon cellular degranulation. Together, these enzymes form pores in the tumour cell membrane, and cleave intracellular components. In addition, FasL expressed on CTLs can bind to Fas on

tumour cells, inducing tumour cell apoptosis (Fu et al., 2016). CTLs also have potent indirect anti-tumorigenic effects through the release of cytokines, mainly TNFα and IFNγ, which shape the tumour-immune landscape. These cytokines polarise immune cells such as macrophages, DCs and neutrophils to M1, cDC1 and N1 phenotypes, respectively (Cox et al., 2011).

Amongst the CD4+ T cell subsets, Th1 cells are involved in anti-tumourigenic immunity by producing cytokines such as IFNγ that activate CTLs and M1 macrophages. On the other hand, Th2 and Th17 cells have been implicated in suppressing Th1 cell responses and thus tumour cell immune evasion (Tay et al., 2021). In addition, TH17/Th2-derived cytokines may promote angiogenesis (Kwee et al., 2018). Tregs are the T cell subset most studied to suppress immune responses within the TME. In healthy, noncancerous tissues, Tregs are crucial to prevent autoimmunity and chronic inflammation, whereas Tregs in the TME can support tumour growth (Vignali et al., 2008). Tregs are characterised by the expression of CD4, CD25, and the transcription factor FOXP3. By producing the anti-inflammatory cytokines, IL-10, TGFβ and IL-35, Tregs inhibit CTL functions and enhance MDSC polarization (McRitchie and Akkaya, 2022). In addition, Tregs have a high IL-2 demand, an important cytokine for T cell proliferation, thus reducing IL-2 availability for anti-tumourigenic T cells. Highly immunosuppressive Tregs have a high expression of the receptors CTLA-4 and PD-1 that regulate Treg function. CTLA-4 has been found to interact with CD80/CD86 on APCs, activating signalling pathways that decrease the ability of APCs to present antigens to effector T cells and thus creating an immunosuppressive environment (Sobhani et al., 2021).

As previously discussed, T cells have inbuilt signalling pathways, termed immune checkpoints, that function to prevent over-activation and unregulated immune responses. Cancer cells, however, have exploited this mechanism, leading to immune evasion and their uncontrolled proliferation (**Figure 1.6**). The discovery of the immune checkpoints, cytotoxic tumour lymphocyte antigen 4 (CTLA-4) and programmed cell death-1 (PD-1)/programmed cell death-ligand 1 (PD-L1), in the 1990s has been at the forefront of immunotherapeutic research which will be discussed in section 1.2.5. (Krummel and Allison, 1995, Ishida et al., 1992). PD-1 is expressed on T cells and binds to one of its ligands, PD-L1 or PD-L2, expressed on tumour cells as well as immune- and non-immune cells. PD-1 expression is also increased upon chronic antigen exposure, as well as IFNγ. This interaction ultimately leads to T cell exhaustion and death (Jiang et al., 2015). Tumour cell

mutations and pro-inflammatory cytokines within the TME can promote PD-L on tumour cells, enhancing T cell exhaustion and immune evasion (Yu et al., 2020). CTLA-4 on the other hand is constitutively expressed on T cells and binds to CD80 and CD86, inhibiting the binding of CD28 on T cells, the co-stimulatory receptor required for adequate T cell activation (Waldman et al., 2020). Therefore, CTLA-4 binding prevents T cell activation and again results in T cell exhaustion.
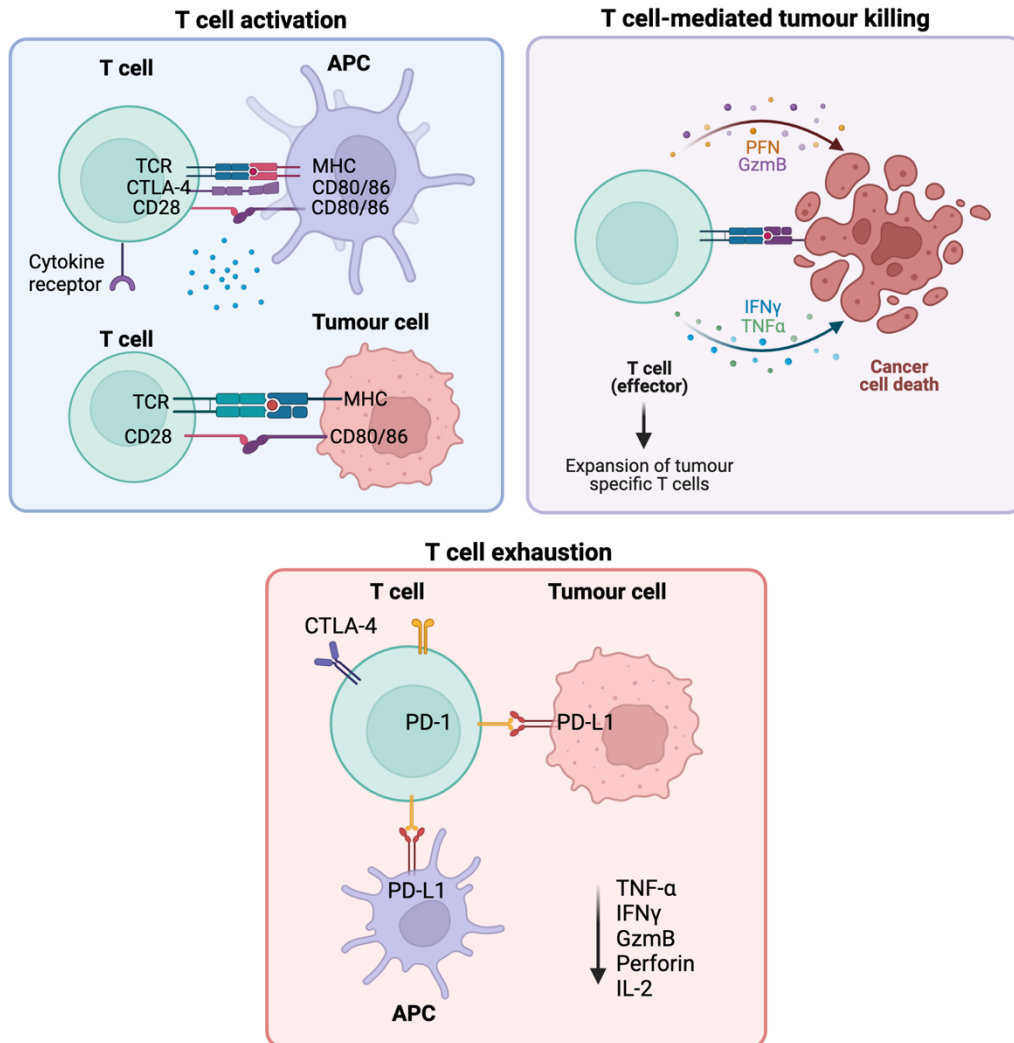
Figure 1.6 T cells are important players within the tumour microenvironment. Multiple steps and processes govern how T cells function within the tumour microenvironment. The way T cells are activated depends on antigen presentation as well as external factors such as cytokines and chemokines. Cells that are polarised to effector CD8 T cells can directly kill tumour cells with the release of cytotoxic granules including perforin (PFN) and granzyme B (GzmB) as well as proinflammatory cytokines. T cell exhaustion through interactions with Programmed cell death protein 1 (PD-1) and Cytotoxic T-lymphocyte associated protein 4 (CTLA-4) are major drivers of immune evasion and numerous intervention treatments to combat this have and are being developed. Adapted from "T Cell Activation in Cancer", by Biorender.com (2023). Retrieved from https://app.biorender.com/biorender-templates.

Many activated T cells exhaust and die over time. However, a small subset remain, which differentiate into memory T cells by undergoing a complex multistage reprogramming of metabolic and gene expression profiles (Barnaba, 2022). Memory T (Tmem) cells are crucial to quickly respond in the event of re-exposure to the same antigen and thus offer protection against cancer recurrence. Three

major Tmem subsets exist, with key markers and functions displayed in table 1.5. Cytokines such as IL-2, IL-7 and IL-15 are important for the proliferation, maintenance and survival of Tmems (Benichou et al., 2017).

Table 1.5 Memory T cell subsets and their roles in offering immunological memory within tumour tissue. Marker expression was adapted from the graphical illustration presented by (Benichou et al., 2017).

Memory T cell subset	Markers (human)	Markers (mouse)	Function
Central memory (Tcm)	CD45RO+ CD45RA- CD62L+	CD44+ CD62L+ CCR7+	Immunosurveillance of lymphoid tissue and provide long-lived memory. Upon re-exposure rapidly proliferate.
Effector memory (Tem)	CD45RO+ CD45RA- CD62L- CCR7-	CD44+ CD62L- CCR7-	Reside in peripheral tissues and respond instantly to re-exposure to antigens. Short-lived.
Tissue resident memory (Trm)	CD45RO+ CD45RA- CD62L- CCR7- CD103+ CD69+	CD44+ CD62L- CCR7- CD103+ CD69+	Reside permanently in tissues, offering long-lived memory. Become rapidly activated upon re-exposure.

1.2.3.2   B cells

Akin to other immune cells, B cells have complex contrasting roles during cancer progression, governed by factors within the TME. However, numerous studies on a range of cancers have suggested that B cells are associated with an overall positive prognosis (Wouters and Nelson, 2018, Petitprez et al., 2020, Cabrita et al., 2020).

B cells bind to TAA through B cell receptors. Upon internalisation, B cells then present the antigen on MHC class II molecules. Interactions with CD4+ T helper cells facilitate B cell activation, forming plasma cells that can rapidly produce tumour-specific antibodies. Antibodies can directly kill tumour cells (antibody-dependent cell cytotoxicity) or indirectly through complement system activation (Mamidi et al., 2017, Petitprez et al., 2020). In addition, by coating tumour cells with antibodies (opsonisation), the effectiveness of phagocytotic cells increases. Studies have previously shown that antibody-producing plasma cells increase the polarisation and phagocytic capabilities of cDC1s and M1 macrophages

(Suchanek et al., 2023). Antibodies can also target growth factors that promote tumour proliferation, metastasis, and angiogenesis. For example, antibodies produced by plasma cells can target VEGF, therefore inhibit angiogenesis (Mahmood et al., 2020). Functional and transcriptomic studies on B cells have also suggested that there are B regulatory cells (Bregs) (Fillatreau et al., 2002, Yanaba et al., 2009). Bregs produce higher levels of anti-inflammatory cytokines such as IL-10, IL-35, TGF-β, that limit anti-tumorigenic T cell responses and promote Tregs (Lv et al., 2019).

An aggregation of B cells in close proximity to T cells within tumours are classified as tertiary lymphoid structures and are associated with increased survival and response to immunotherapy (Cabrita et al., 2020). The high degree of tumour heterogeneity and production of tumour neoantigens, however, make it difficult for plasma cells to produce tumour-specific antibodies, which subsequently leads to immune evasion.

Numerous clinically approved cancer treatment strategies have exploited monoclonal antibodies for years. Examples include Trastuzumab which is a monoclonal antibody, targeting HER2, commonly used in the treatment of breast cancer (Cameron et al., 2017). Other B cell therapies include Ofatumumab that lead to B cell and thus complement system activation. Another common approved treatment for cancers such as non-Hodgkin lymphoma and chronic lymphocytic leukaemia is Rituximab which is a monoclonal antibody to deplete abnormal B cells (Bergantini et al., 2020).

1.2.4 Pattern-recognition receptor activation and cancer

In 2011, the Nobel Prize in Physiology or Medicine was awarded to Bruce A. Beutler and Jules A. Hoffmann for the discovery of Toll-like receptors in mammalian cells and how their activation orchestrated innate immune activation (Beutler, 2002, Hoffmann et al., 1999). The discoveries came after decades of work which transpired from the discovery of the receptor, Toll, in the fruit fly Drosophila melanogaster (Lemaitre et al., 1996). This conserved mechanism recognises microbial products across different species. Numerous different TLRs exist in mammals, 10 in humans and 12 in mice, and the signalling pathways and thus immune responses differ slightly depending on the highly conserved MAMP/DAMP activators (Akira et al., 2001). Without TLRs activating innate immune responses and subsequently feeding into adaptive immune activation, the threat to life from microbial attack would be substantial (Pasare and Medzhitov, 2004).

Currently, a total of three compounds which induce TLR activation are approved for cancer patients. Monophosphoryl lipid A (MPL) is the substantially less toxic lipid A derivative of LPS yet mediates TLR activity via similar cytokine-inducing responses. MPL has been used as an adjuvant in the development of cancer vaccines. Bacillus Calmette-Guérin (BCG) treatment, an immunotherapy consisting of a weakened form of the strain *Mycobacterium bovis,* is the most successful treatment for non-muscle invasive bladder cancer and has been employed for over three decades. Although BCG's exact mechanisms of action are still to be elucidated, it is apparent there is crosstalk between members of the innate immune system, mainly granulocytes with CD4+ and CD8+ lymphocytes (Redelman-Sidi et al., 2014). Tumour cells may also internalise BCG, leading to antigen presentation and further interactions with the immune system as well as potential direct cytotoxic effects (Redelman-Sidi et al., 2014). Imiquimod can be used as a topical treatment for melanoma *in situ*, and metastatic melanoma in combination with other treatments. Imiquimod consists of viral nucleic acids which activate TLR7 responses in immune cells, producing viral-associated effector cytokines, such as IFN-α (Wang et al., 2005).

1.2.5   Immunotherapies for cancer

The concept of treating cancer by intercepting and modulating immune responses has been around for decades. For example, live attenuated *Mycobacterium bovis* was approved for non-muscle-invasive bladder cancer in the 1970's and is now the gold standard treatment. Over the past decade, four major classes of immunotherapies have emerged: immune checkpoint blockade, cytokine therapy, cell therapy, and vaccines.

The discovery of cell surface proteins on T cells that essentially employ a 'brake' on T cell activation, function and proliferation came in the 1990's. James P. Allison, Tasuku Honjo, and their colleagues, uncovered key functions of CTLA-4 and PD-1 in T cell biology, respectively (Krummel and Allison, 1995, Ishida et al., 1992). It wasn't until 2011, however, that the first ICI was approved for clinical use; a CTLA-4 blockade drug, Ipilimumab (Yervoy), approved by the FDA to treat metastatic melanoma as well as other cancers (Beer et al., 2017). A few years later in 2014, the FDA approved Pembrolizumab (Keytruda) and nivolumab (Opdivo), both of which block PD-1 signalling and thus prevent T cell exhaustion. Combination therapies of both CTLA-4 and PD-1 blockade are very common for stage IV melanoma patients, however, adverse effects from immune system overstimulation are observed (Klein-Brill et al., 2024).

Since the 1990's, two FDA approved therapies that harness cytokines have been used in clinics, one being IFN-α2b as a treatment for hairy cell leukaemia, renal cell cancer and melanoma, and IL-2 to treat metastatic renal cell carcinoma and metastatic melanoma (Jiang et al., 2016, Xiong et al., 2022). IFN-α2b can directly induce apoptosis in cancer cells as well as increase the activity of anti-tumourigenic macrophages, NK cells, and CTLs. Similarly, IL-2 increases CTLs and NK cell activity, however, depending on the dose, also regulate T cell responses.

There are two uses for vaccines in cancer treatment. One being to prevent cancer by targeting known cancer-causing viruses. The other are therapeutic vaccines used to induce anti-tumorigenic immune responses. Human papillomavirus (HPV) and hepatitis B (HBV) vaccines have been used for several years to prevent mostly cervical and liver cancers, respectively. The Sipuleucel-T (Provenge) vaccine has also been approved for the treatment of metastatic prostate cancer. The main principle of this vaccine is to use the patient's isolated APCs, which have been 'tumour activated' by culturing *ex vivo* with prostate cancer antigens and activating cytokines, before re-infusing back to the patient (Anassi and Ndefo, 2011).

One of the greatest breakthroughs in cellular cancer therapies was Chimeric Antigen Receptor T-cell (CAR-T) therapy, approved in the late 2010's for hematologic malignancies (Barros et al., 2022). It harnesses the patient's isolated T cells which are then genetically altered to express surface receptors (CARs) that recognise tumour antigens. Upon re-infusion into the patient, circulating CAR-T cells become activated and proliferate upon tumour cell challenge. Intense research for solid tumours is ongoing, however, there are numerous additional obstacles including tumour antigen heterogenicity (Guzman et al., 2023). Employing adoptive transfer of alternative immune cells such as NK cells are under clinical trials (Page et al., 2024). Therapies also include CAR-NK cell therapy which have shown promising results for haematological-based malignancies (Bachier et al., 2020, Imai et al., 2005). One trial isolated NKs from cord blood and transduced with a retroviral vector to express CAR-CD19, IL-15, and an inducible caspase-9-based suicide gene (iC9) as an added safety feature (Liu et al., 2018). However, there have been considerable limitations for NK cell clinical translatability. For example, to gain adequate quantities, cells are expanded *ex vivo*, which can be challenging. In addition, cytokines added *ex vivo,* to prime immune cells and enhance their tumour-killing capacity, have resulted in states of cell-cytokine dependency that cannot be sustained *in vivo.* (Liu et al., 2021). Storage conditions have also limited their ability to expand *in vivo*.

A common therapeutic approach used to treat metastatic and aggressive cancers is a combination of the immunotherapies as well as conventional therapies.

1.2.6 Personalised treatment approaches

Providing targeted treatment approaches for individual cancer patients is a rapidly emerging research area. Utilising a patient's own immune cells in therapies such as Sipuleucel-T (vaccine for prostate cancer) and CAR T cell therapy, previously described, are examples of personalising a cancer treatment.

Personalisation also can combine a patient's genomic, metabolomic and even microbiome data to offer a complex overview of the tumour microenvironment as well as host responses that affect treatment efficacy. Stratifying patients based on response rates for immunotherapy for example, then comparing genotypes and tumour immune cell infiltrations between responders and non-responders, provides future pipelines for prescribing these therapies to specific patient subsets. An example of this is CTLA-4 blockade (Ipilimumab) which can be prescribed to patients suffering from non-small cell lung cancer. This option is not available however if there are mutations in the genes, epidermal growth factor receptor (EGFR) and anaplastic lymphoma kinase (ALK) (Gainor et al., 2016). As next-generation sequencing (NGS) has improved and developed drastically in recent years, somatic variants in tumours can much more easily be identified. This will therefore guide targeted therapy with the greatest effectiveness and with the fewest side effects.

1.3 THE GUT MICROBIOME

The collection of trillions of bacteria, fungi and viruses that reside in the gastrointestinal tract, is referred to as the gut microbiome and is responsible for many physiological functions of the host (Qin et al., 2010b). Bacteria are, by far, the most studied members of the microbiome. Analysing the bacterial composition and functional activity aims to unravel the microbiome-host interactions (Lozupone et al., 2012).

When the gut microbiome is in a state known as eubiosis, the communities are in balance and exert health promoting properties. One important function is energy regulation as the gut microbiota metabolise dietary components such as complex carbohydrates and plant-derived secondary metabolites. The gut microbiome also controls local and systemic immune responses, which shall be discussed in more detail later. Other functions include, but are not limited to: nutrient absorption,

vitamin synthesis and protection against invading pathogens. On the other hand, when the gut microbiome is disrupted, known as dysbiosis, these functions are impaired. Numerous environmental factors such as medical treatments (especially antibiotic use), disease, aging, and diet all promote the transition to gut dysbiosis. Many disease aetiologies and pathogenesis can be linked to gut dysbiosis, highlighting the bi-directional relationship of disease and the gut microbiome.

To confirm microbial dysbiosis, infection, or assess the microbial composition, microbiological techniques such as culturing were traditionally employed. However, not only are culturomics time-consuming, but information regarding non-culturable bacteria is lost. High-throughput DNA sequencing revolutionized microbiome research as techniques such as 16S rRNA sequencing effectively identified specific bacterial species in intestinal samples. Further developments in DNA sequencing came after the introduction of shotgun metagenomic sequencing, which can distinguish between different strains. The number of microbiome publications has reflected the technological developments as since around 2008, publications have gone from below one hundred to several thousands in present day (Petersen Jillian and Osvatic, 2018). This has led to better understanding of microbiome-host interactions on a population level by allowing very large cohorts to be assessed. For example, there are two major microbiome research initiatives: Human Microbiome Project (HMP) (Proctor et al., 2019), founded by the NIH in the US, as well as the MetaHIT (Metagenomics of the Human Intestinal Tract) (Qin et al., 2010a), which is European led. Both studies analyse the composition of microbiomes and their roles in health and disease. They also provide publicly available reference genomes to aid analysis and accurate taxonomic identification for other microbiome studies.

1.3.1 Immune responses within the gastrointestinal tract

The gut microbiota is an important player in regulating host immune responses, both locally and distant to the GIT. It is therefore not surprising that the gut houses the largest population of immune cells in the body, which predominantly reside in structures termed the gastro-associated lymphoid tissue (GALT) (Rivera and Lennon-Duménil, 2023). The general architecture of the gut including the GALT is presented in **Figure 1.7**. The mucus layer is the first initial line of defence as it acts as a physical barrier and contains antimicrobial peptides produced by Paneth and epithelial cells (Mowat, 2003). In addition, microbial-derived products, food and metabolites can be sampled by the APCs, dendritic cells and macrophages, in the lamina propria. Microfold (M) cells are dotted throughout the epithelial layer and

can transport antigens across the epithelial lining to Peyer's patches (PPs) or lymphoid follicles that reside beneath them (Calder, 2013). The area called the Subepithelial dome (SED), that resides above PPs and beneath the epithelial lining, has a concentrated population of APCs and is pivotal for antigen sampling.

Peyer's patches primarily reside in the small intestine, particularly the ilium. They are composed of a T cell zone surrounding a germinal centre which are the sites of T and B cell maturation, respectively. Lymphocyte maturation occurs through recognition of pathogen-associated molecular pattens presented by APCs that interact with receptors on T and B cells. T cells differentiate to T helper cells, including follicular T helper cells. B cells, with the aid from follicular T helper cells, can differentiate into primarily plasma cells that produce immunoglobulins (Igs). IgA is particularly important for mucosal defence against invading pathogens and maintaining gut barrier integrity. In allergic responses or during parasitic infection, however, plasma cells may undergo class switching to produce IgE rather than IgA. Dysregulation of IgA and IgE production can create immune dysfunction. Chemokines facilitate the homing and extravasation of immune cells from the blood to the Peyer's patches. Antigen-specific, mature immune cells then leave Peyer's patches through drainage into the lymphatic system, including in the mesenteric lymph nodes that reside in the large intestine. Mesenteric lymph nodes, similarly, to Peyer's patches, are also the site of antigen presentation. Of note, Treg cells are vital for immune tolerance and are generated within mesenteric lymph nodes.

Early studies showing the importance of the GALT in immunity discovered that GF mice had poor adaptive immune responses due to perturbations in B and T cell development (Lamousé-Smith et al., 2011). Specifically, GF mice had dysfunctional Treg and Th17 cells in the gut along with morphologically small Peyer's patches. There is a fine balance between the ratio of Treg and Th17 cells in the gut. Th17 cells are pro-inflammatory and defend against invading pathogens to maintain gut barrier integrity, whereas Tregs dampen immune responses and promote tolerance. Consequently, GF mice have shown greater susceptibility to colonisation of pathogens such as *Shigella* (Round and Mazmanian, 2009). Recolonising GF mice with specific microbial members, termed gnotobiotic models, is an important tool to reveal direct immune-microbial/microbial product interactions. For example, GF mice that were colonised by different species and strains of *Bifidobacteria* isolated from infants, had profound differences in systemic immune responses. Some strains induced a Th1 over Th2 systemic response when immune stimulated due to the production of certain cytokines, such as IFN-

γ compared to IL-4, whilst other strains favoured a Th2 response (Ménard et al., 2008). This highlights the importance of considering functional differences between strains and species when analysing microbiome data. Understanding how microbiota members interact with the complex web of immune cells encompassed within the architecture of the GI tract is important so therapeutics can be designed to modulate systemic immune responses.
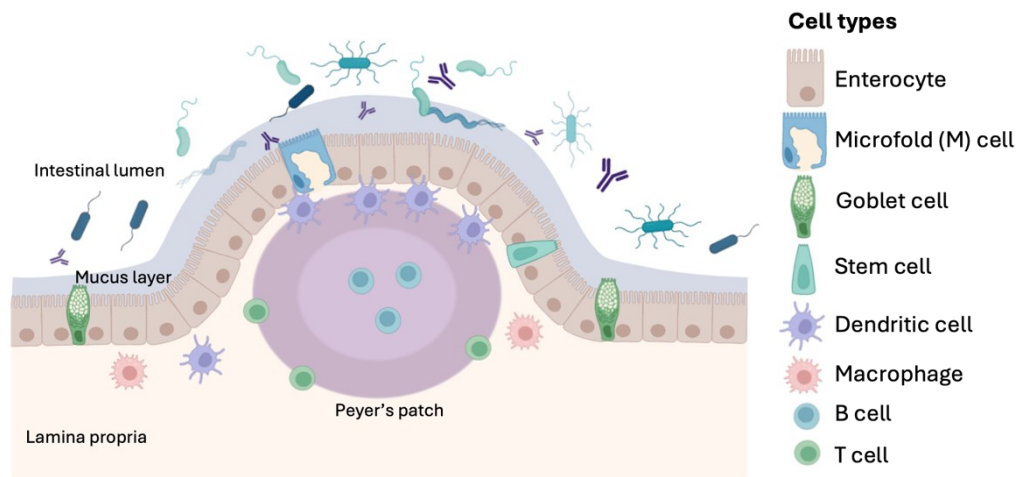
Figure 1.7 The architecture of the gastrointestinal tract lining. The intestinal lumen contains trillions of microorganisms. The gastrointestinal barrier is made up of a mucous layer and enterocytes that aim to prevent translocation of microorganisms to the lamina propria layer. Specialised cells also form part of the intestinal lining which include microfold (M) cells, mucin-producing goblet cells, and stem cells that maintain the epithelial barrier. Immune cells in the lamina propria such as macrophages and dendritic cells sample microorganisms where they can antigen present to adaptive immune cells that reside in the specialised lymphoid structures such as Peyer's patches. T cells can then maintain immune tolerance to microorganisms, and B cells within the germinal centre interact with T cells and produce immunoglobulins that are secreted into the intestinal lumen. Adapted from "Small Intestine Villus Background (Layout)", by Biorender.com (2023). Retrieved from https://app.biorender.com/biorender-templates.

1.3.2   Gut microbial-derived metabolites

Understanding how members of the microbiome influence host immune and metabolic function is vital to developing future therapeutics and design interventions. One of the major links underpinning microbiome-host interactions is from the various microbial-derived metabolites. Key metabolites that have gained significant interest for modulating host immune responses include short-chain fatty acids (SCFAs), bile acids, phenolic acids, tryptophan metabolites, amino acid metabolites and vitamins.

SCFAs are arguably the most studied gut-derived metabolite, as they have been proposed to have health-promoting effects including being anti-inflammatory, anti-tumorigenic, and antimicrobial. SCFAs include propionate, butyrate and acetate, and are produced by members of the genera *Bacteroides*, *Firmicutes*, and *Lactobacillus,* as well as others. SCFAs regulate levels of anti-microbial peptides, mucous secretion and tight junctions between intestinal epithelium, and subsequently the integrity of the gut barrier (Paone and Cani, 2020). If gut barrier integrity is impaired, this can promote systemic inflammatory responses and carcinogenesis (Lazar et al., 2018). In addition, SCFAs interact with G-protein-coupled receptors (GPCRs) expressed on cells such as colonic epithelium and immune cells. In the context of immunity, SCFA-GPCR signalling influences chemotaxis, therefore immune cell infiltration, cytokine production, gene expression which influences differentiation, proliferation and immune cell function (Tan et al., 2014). In the gut, SCFAs are known to induce anti-inflammatory responses, for example through regulating the Treg population (Smith et al., 2013). Beyond the gut, a small proportion of SCFAs can enter the circulation and tissues, where they can exert systemic immunomodulatory effects (Bloemen et al., 2009).

Aside from SCFAs, there are notable microbial-derived metabolites known to regulate immune responses. For example, iondole-3-lactic acid (ILA), produced from tryptophan by members of *Lactobacillus* and *Bifidobacterium*, has been shown to have profound effects for immune development in infants as well as immune regulation in adults (Yu et al., 2023). One study found that *Lactobacillus plantanium*-derived ILA upregulated IL-12 production by DCs which in-turn caused CD8 T cell priming. The CD8 T cells displayed anti-tumourigenic activity and ILA was shown to reduce overall tumour burden in a mouse model of colon carcinogenesis (Zhang et al., 2023).

Certain gut microbial metabolites have been associated with increased risk of disease. For example, elevated trimethylamine N-oxide (TMAO) levels have been associated with increased risk of CVD (Tang et al., 2013, Wu et al., 2019). Foods such as eggs, dairy and red meat contain high amounts of choline, phosphatidylcholine and carnitine, which are metabolised to trimethylamine (TMA) by certain members of the microbiome. *Prevotella* and *Bacteroides* have been shown to be efficient TMA producers (Wu et al., 2020). TMA then enters the circulation where it undergoes oxidation in the liver to TMAO. It should be highlighted, however, that whilst the link between TMAO and CVD has not been proven to be causative, it could be correlative (Canyelles et al., 2023). Even so,

studies have aimed to modulate the gut microbiota through prebiotics (Cheon et al., 2023, Li et al., 2021) and probiotics (Ramireddy et al., 2021) to reduce the abundance and effects of TMA-producing bacteria.

GIT metabolite assessment is a vital functional readout of the microbiome. However, the function of a large proportion of metabolites is yet to be known, especially in the context of disease and systemic effects. It is therefore vital to assess metabolic effects in disease states and post-interventions such as 'probiotic' administrations.

1.3.3 Gastrointestinal barrier function

Gastrointestinal barrier function is essential for protection against pathogen colonisation as well as stopping toxins, bacteria and food products from entering the bloodstream. If the barrier is compromised, termed 'leaky gut', then these components stimulate immune cells around the body which can lead to immune overstimulation leading to chronic inflammation or even sepsis. The production of pro-inflammatory cytokines leads to various pathologies including autoimmune diseases, allergies, non-alcoholic liver disease, metabolic disorders such as obesity, and cancer. A study found that increased intestinal permeability accelerated breast cancer progression due to changes in systemic immune responses and chronic inflammation (Shrout et al., 2022).

To maintain gut barrier integrity, the tight junction proteins (occludins and claudins) that hold colonic epithelial cells together, need to be intact and highly expressed. Also, there should be a thick layer of mucus (produced by goblet cells) and a high turnover of epithelial cells. Inflammation, however, can lead to epithelial cell apoptosis due to the production of pro-inflammatory cytokines and ROS. As discussed, the gut microbial communities heavily regulate gastrointestinal inflammation. For example, increased species diversity with high abundances of specific microbial members, such as *Bifidobacteria*, can produce metabolites including SCFAs, which are anti-inflammatory, increase tight junctional protein expression and are energy sources for colonic epithelial cells. In addition, microbes themselves can directly improve gut barrier function through immune cell interactions, such as upregulating Treg cells and secretory IgA. An example study found that a strain of *B. bifidum* increased trans-epithelial resistance in Caco-2 cell monolayers (Al-Sadi et al., 2021). The strain also enhanced the intestinal epithelial barrier in mice, and thus protection against DSS-induced colitis.

1.3.4 Gut microbiota changes throughout life, health and disease

Historically, there have been disparities in the literature for when the first microbial members colonise the host. Some say it occurs *in utero* (Jiménez et al., 2005, Han et al., 2009, Obiero et al., 2022), whilst others argue the foetus is in sterile conditions until labour. Even so, the labour/birth is the first considerable dose of external microbes, which is why mode of delivery is an important gut microbiome influencer. It has been shown that infants born via a vaginal birth are exposed to a higher abundance, and more diverse microbes than infants born via caesarean section. In addition, breast-fed babies receive human milk oligosaccharides that are predominantly metabolised by the bacterial genera, *Bifidobacteria*. A study found that the faeces of breastfed infants had significantly higher levels of *Bifidobacterium* compared to formula-fed infants (Ma et al., 2020). Transition to solid food diets and environmental conditions also shape an infant's microbiome. The renowned 'hygiene hypotheses' proposes that infants exposed to more microbial antigens, for example by exposure to pets, and living in rural areas or multiple child homes, are less likely to develop allergies and autoimmune conditions, which can be attributable to gut microbiome modulations (Scudellari, 2017, Stiemsma et al., 2015). Many studies have shown that the establishment of the gut microbiome in the first few years of life are vital for the overall health and physiological functions of the host throughout a lifetime.

During these early years, the composition of the microbiome is predominantly *Bifidobacterium*. By the age of three, our microbiome stabilises and resembles more of an adult's microbiome enterotype. As we age, levels of *Bifidobacterium* decrease as our diet shifts from a milk-based to a more complex diet containing nondigestible carbohydrates and plant secondary metabolites. The most dominant phyla in the adult gut microbiota, representing 90% of the total are *Firmicutes* (which includes members of *Lactobacillus*, *Clostridium*, *Ruminococcus*, and *Faecalibacterium genera),* and *Bacteroidetes* (examples include *Bacteroides* and *Prevotella)*. Other prominent phyla include Actinobacteria (such as Bifidobacteria) and *Proteobacteria* which includes many opportunistic pathogens. A less prominent but noteworthy genera is *Akkermansia*, of the phylum, *Verrucomicrobia*, which has been associated with immune and metabolic function.

The disease status of the host has also been associated with shifts in microbiome composition (Blumberg and Powrie, 2012, Hooper et al., 2012). This is thought to be a bidirectional relationship as the disease could accelerate gut microbial dysbiosis and in-turn, gut dysbiosis could fuel disease progression. Diseases that

occur near the gut, most commonly inflammatory bowel diseases (IBD), have the closest association with the gut microbiome, a link that has been heavily studied. IBD patients often have distinct microbial signatures compared to healthy individuals, for instance *Enterobacteriaceae*, including certain invasive and potentially pathogenic strains of *E. coli*, are prominent in IBD patients (Darfeuille-Michaud et al., 1998). Likewise, *Fusobacterium nucleatum* levels are elevated in people with ulcerative colitis, which increases the risk of developing colorectal cancer (Ou et al., 2022, Su et al., 2020). However, proving whether the associations of the microbiota with disease progression and initiation are causative or correlative is very difficult. For instance, *Fusobacterium nucleatum* was found to be destructive to intestinal epithelial cells by inducing the IL-17F/NFκB inflammatory signalling pathway, exasperating ulcerative colitis (Chen et al., 2020). However, it is still unknown whether ulcerative colitis conditions fuel the prevalence of *Fusobacterium nucleatum*.

For the past decade, research into linking diseases that are distant from the GIT to the microbiome has boomed. Pathologies that root from immune and metabolic dysfunction, such as cardiovascular disease, Alzheimer's and cancer are major examples and contribute to an unprecedented burden to human health services (Chen et al., 2022, Helmink et al., 2019, Masenga et al., 2022). By understanding how the microbiome can fuel or alleviate disease pathology, therapeutic strategies can be developed. For instance, a clinical trial showed that atopic dermatitis (AD) symptoms were mitigated in patients that received faecal microbiota transplants (FMTs) from healthy stool donors compared to placebos (Mashiah et al., 2022). However, the study was conducted using a small cohort (9 patients). The high interindividual variability that exists in microbiome composition and function means that large sample sizes are required for reliable results.

1.3.5 Diet and the gut microbiota

Studies have shown that the gut metagenome of family members tend to cluster more closely together than non-family members (Yatsunenko et al., 2012). Therefore, researchers hypothesised whether there was a genetic element influencing gut microbial composition. Studies on monozygotic and dizygotic twins, however, confirmed that genetically identical twins did not show higher microbiome similarity than non-identical, and that there was high variability between individuals (Turnbaugh et al., 2009, Yatsunenko et al., 2012). Researchers concluded that environmental influences, most notably diet, have an even greater impact on the microbiome than genetics. In addition, migrant studies have shown that the

microbial genomic composition shifts when individuals move to different countries, where they adopt new dietary habits (Copeland et al., 2021, Vangay et al., 2018).

Shortly after the introduction of the term 'probiotics', 'prebiotics' were introduced. Prebiotics are defined as non-digestible functional foods that are selectively fermented by microorganisms to increase their growth/activity, and in-turn exert health-promoting effects to the host (Gibson and Roberfroid, 1995). Major examples used in the food industry include small carbohydrates, termed oligosaccharides (3-10 glycoside-bond linked monosaccharides). In the food industry, human milk oligosaccharides or their synthetic analogues are added to infant milk formula to support the growth of the most dominant genera in the infant's gut, *Bifidobacteria* (Basavaiah and Gurudutt, 2021).

Non-digestible carbohydrates including fibre are the most widely used gut microbiome modulators, however, plant bioactive compounds have also gained a lot of attention. Studies have found that polyphenols, the coloured secondary metabolites of plants, are metabolised by certain members of the commensal microbiome (Alves-Santos et al., 2020, Zhang et al., 2018). The cocoa-derived polyphenol, flavanols, were found to enhance *Lactobacillus* and *Bifidobacterium* growth while reducing abundance of *Clostridium perfringens* (Sorrenti et al., 2020). Flavanols, as well as other polyphenols, have therefore shown to positively influence the host immune system through a prebiotic-driven mechanism (Martín and Ramos, 2021, Lordan et al., 2020).

To further develop the health-promoting effects of prebiotics and probiotics, symbiotics were formed. Symbiotics combine beneficial bacteria with prebiotics, to enhance the growth and survival of probiotics within the harsh conditions of the GIT (Swanson et al., 2020). In addition, certain prebiotics favour the growth of specific bacterial species/strains, therefore machine learning models can help predict optimum prebiotic/probiotic combinations (Westfall et al., 2021). More in-depth characterisation of the symbiotic-derived metabolites produced and their impacts to human health/disease prevention is paramount.

Aside from enhancing the gut microbiome composition, diet can negatively impact microbial communities beneficial to health, leading to dysbiosis. A high-fat diet is amongst the most studied dietary factor to negatively influence microbial communities. One study found that high-fat diets decreased *Bacteroidetes* and increased both *Firmicutes* and *Proteobacteria* members, independently of obese status in a genetically modified mouse model (Hildebrandt et al., 2009). A

decreased *Bacteroidetes* to *Firmicute* ratio has been associated with a reduction in metabolites such as short chain fatty acids, which have anti-inflammatory effects in the gut so promote immune homeostasis (Bahar-Tokman et al., 2022).

Changes to dietary habits that modulate the gut microbiome have been found to be transient and reversible (Leeming et al., 2019). Therefore, to maintain health promoting effects, dietary interventions should have long-term acceptability when implemented. This also highlights how diets with detrimental effects can be reversed rapidly upon interventions. In addition, it is crucial to appreciate the high inter-individual variability to diet-induced gut microbiome modulations. An example dietary study with fermentable carbohydrates found that the variation in gut microbial species were higher between individuals rather than pre- and post-dietary intervention (Walker et al., 2011).

1.3.6 Bifidobacterium

Bifidobacteria is the genus which falls within the *Bifidobacteriaceae* family, which is part of the *Bifidobacteriales* order and all this forms the *Actinobacteria* phylum. Among *Bifidobacteria*, other members of *Actinobacteria* include *Streptomyces*, which are used to produce antibiotics, and *Mycobacterium*, which includes species responsible for tuberculosis. Bacteria within *Actinobacteria* phylum are all Gram-positive, meaning they have a thick peptidoglycan cell wall. Historically, 'Gram-positive' bacteria were distinguishable by their blue/purple appearance under the microscope which was due to the bacteria retaining a crystal violet/iodine complex when tested with a Gram stain developed by Hans Christian Gram in 1884 (Coico, 2005). Within the phylum, there is large morphological differences. *Bifidobacteria* are rod-shaped with two branching elements, previously described as bifurcated, which contributes to the etymology of the name '*Bifidobacteria*'.

Genomes of *Actinobacteria* members exhibit large genetic diversity and have relatively high guanine and cytosine contents (> 50% G+C) compared to members of other bacterial phyla (Ventura et al., 2007). The large genetic diversity can be attributable to bacterial species adapting to distinct environmental conditions. For instance, *Bifidobacteria* are best adapted to the GIT of mammals, but other sources include the oral cavity, food produce, insects and sewage, all of which can be linked back to GITs.

Amongst the *Bifidobacterium* genus, there are six phylogenetic clusters that contain 29 known species (Ventura et al., 2006). There is also large genetic diversity between and within species of *Bifidobacteria*, which are responsible for

the diverse effects seen in human health. *B. bifidum, B. longum, B. breve, B. adolescentis,* and *B. animalis* are amongst some of the most studied species (O'Callaghan and van Sinderen, 2016, Quigley, 2017). In the adult gut, the prominent species are *Bifidobacterium longum subsp. longum*, *Bifidobacterium adolescentis,* and *Bifidobacterium pseudocatenulatum*. In recent years, there are ongoing research efforts to isolate and identify novel strains of *Bifidobacterium* and characterise any host-modulating effects.

1.3.7 *Bifidobacterium* in the treatment of disease

Certain members of *Bifidobacterium* have been classed as probiotics, so products like probiotic supplements and functional foods containing these strains can be marketed with specific health claims. Examples of commercially available probiotic strains include *Bifidobacterium animalis subsp. lactis* BB-12, *Bifidobacterium longum* BB536, *Bifidobacterium infantis* 35624 and *Bifidobacterium bifidum* Bb-02 (Lewis et al., 2016). Health claims not only focus on supporting gastrointestinal health, but certain strains also may reduce body fat, improve metabolic health, and modulate the gut-brain axis (Bonfrate et al., 2020, Groeger et al., 2013, Jungersen et al., 2014).

As Bifidobacteria is the dominant genus that colonises an infant's GIT, a time of significant immune priming and tolerance, *Bifidobacterium* strains were hypothesised to treat infant- as well as immune-related illnesses (Lewis et al., 2016, Stuivenberg et al., 2022). Allergic diseases, such as allergic asthma, atopic eczema, allergic rhinitis, and food allergies, are caused by over activation of the immune system. Numerous human studies have shown that *Bifidobacterium* strains play a crucial role in preventing and alleviating allergic symptoms, particularly in early life (Enomoto et al., 2014, Kim et al., 2010, Nogueira and Gonçalves, 2011, Anania et al., 2021, Strisciuglio et al., 2023). An example study found that *Bifidobacterium lactis* Bb-12 supplementation in formula milk significantly reduced atopic eczema symptoms in infants (Isolauri et al., 2000). Another randomised, double-blind study with the same strain also reported that atopic eczema symptoms were reduced, this time in infants whose mothers received the probiotic (Dotterud et al., 2010). Even though there are numerous studies promoting the allergy-alleviating potential of Bifidobacterium, possibly by promoting a Th1 and Treg over Th2 response, the strains, dose and timing of the dose are important to consider (Miraglia Del Giudice et al., 2017, van der Aa et al., 2011). For example, *Bifidobacterium* has been shown to reduce incidences of

asthma in infants, but no effect was seen in infants in a study when mothers received the probiotic (Dotterud et al., 2010).

In recent years, Bifidobacterium has shown great potential to treat the life-threatening disease, necrotizing enterocolitis (NEC). NEC is the leading cause of premature neonatal death whereby inflammation consumes the gastrointestinal tract which eventually leads to tissue death and perforations, which can promote sepsis and bacteraemia (Alsaied et al., 2020). In a retrospective study, rates of NEC were compared before and after routine probiotic administration. The study administered *Lactobacillus* and *Bifidobacterium* probiotics to high-risk premature neonates and found a significant decreased risk of NEC (7.5% to 3.1 %) and late-onset sepsis (22.6% to 11.5%) after probiotic use (Robertson et al., 2020).

In addition, *Bifidobacterium* members are paramount for energy metabolism as well as immune regulation. *Bifidobacterium longum subspecies infantis* has been found to alleviate severe acute malnutrition in Bangladeshi infants in a single-blind, placebo-controlled trial (SYNERGIE). The study not only found increases in body weight after microbial supplementation but also decreases in markers for intestinal inflammation (Barratt et al., 2022).

On the contrary, it is important to assess, in depth, all health effects of *Bifidobacterium* supplementation as not all members are classed as probiotic. For example, one study found that *Bifidobacterium* members such as *B. dentium* were detrimental to oral health by promoting dental cavities (Manome et al., 2019). *Bifidobacteria* species can metabolise carbohydrates, even in high fluoride concentrations, producing acids such as acetate which acidifies and erodes enamel. Another possible risk factor of live bacteria administrations is the risk of immune system overstimulation, which is seen in life-threatening diseases such as sepsis. A systematic review of pre-term neonatal sepsis cases uncovered 25 out of 32 cases detected strains that matched the strains in the probiotic supplementation (Kulkarni et al., 2019). However, this does not mean that probiotic administration caused sepsis, as co-morbidities and factors including gut surgeries attributed to the risk of sepsis, independently. It is therefore vital to monitor patients taking probiotics as well as finding alternatives with higher safety profiles e.g. postbiotics.

1.3.8 The microbiome and cancer link

The global cancer burden attributable to infectious agents is large, as around 16% of cancer cases have been found to be caused by viruses, bacteria or parasites

(de Martel et al., 2012). One of the most notable cancer-causing infectious agents is *Helicobacter pylori* (H. pylori) that infects the stomach lining. *H. pylori* infection causes chronic inflammation, by producing cytokines such as TNFα and IL-1, ROS, and virulence factors, all of which damage the stomach lining. Persistent gastritis leads to DNA damage and modulates cell signalling, and thus increases the risk of gastro-associated cancers (Wotherspoon et al., 1991).

Other microbial members, in particular *Escherichia coli* (Arthur et al., 2012), *Fusobacterium nucleatum* (Gur et al., 2015) *and Campylobacter jejuni* (He et al., 2019)*,* to name a few, have been implicated with increased cancer risk and progression, mainly colorectal carcinogenesis. Many mechanisms have been proposed, and include the release of genotoxic metabolites, virulence factors and direct interactions with immune and colonic epithelial cells, which can lead to dampened anti-cancer functions and oncogenic transcriptional changes. However, numerous studies have also investigated the cancer-protective role of the commensal microbiota, which shall be discussed in detail.

Epidemiology data have proposed that the gut microbiome is associated with cancers distant from the gastrointestinal tract. One such case control study found that 48 newly diagnosed post-menopausal breast cancer patients had statistically significant reduced gut microbiome α-diversity and a distinct microbial composition, measured as β-diversity, compared to 48 post-menopausal control patients (Goedert et al., 2015). An advantage of this study was that gut microbial composition was analysed before breast cancer treatment commenced, as it has been shown that common treatments including chemotherapy and radiotherapy can induce gut dysbiosis (González-Mercado et al., 2020, Zhao et al., 2023). In the study, breast cancer patients had higher levels of *Clostridiaceae*, *Faecalibacterium*, and *Ruminococcaceae*; and lower levels of *Dorea* and *Lachnospiraceae.* Another study found that levels of *C. coccoides, F. prausnitzii,* and *Blautia* were significantly different depending on cancer stage and histoprognostic grade (Luu et al., 2017). A common factor shared between the gut microbiome and breast cancer is oestrogen metabolism, however additional research into the mechanistic link is needed. In addition, there is mounting evidence to suggest that microbiome differences across patients are associated with response rates to ICI therapy. Bacterial members such as *Bifidobacterium*, *Akkermansia muciniphila*, and *Faecalibacterium* have been linked to improved responses in a range of cancers (Andrews et al., 2021, Chaput et al., 2017, Routy et al., 2018, Zheng et al., 2019).

Additional evidence to support the gut microbiome-cancer axis is observed with increased cancer risk and progression in humans after antibiotic-induced gut microbiota perturbations (Kilkkinen et al., 2008). Preclinical studies have aimed to uncover how microbiome depletion drives progression of certain cancers. One of the first studies by Viaud and colleagues showed that antibiotic-treated and GF mice had reduced IL-17 production by spleenocytes upon chemotherapeutic (CTX) treatment (Viaud et al., 2013). CTX suppresses Treg cells and in-turn promotes the differentiation of the IL-17 producing T cell, pathogenic Th17. The study summarised that the efficacy of CTX was dependent on the commensal microbiota. Another study showed increased infiltration of mast cells in breast tumour stromal regions with antibiotic administrations in C57BL/6 mice (McKee et al., 2021). In support of this, mice with commensal dysbiosis showed an increased frequency of mast cells in mammary tissues and breast tumours, which was accompanied by greater cancer cell dissemination compared to controls (Feng et al., 2022). Another study showed that antibiotic-treated and GF mice had impaired immune responses compared to control mice after CpG-oligonucleotide immunotherapy and platinum chemotherapy (Iida et al., 2013). The study summarised that commensal bacteria were crucial for myeloid cell function including ROS and TNFα production which can be cytotoxic to tumour cells Together, these findings signpost the crucial role of the microbiome for immune function during cancer progression, metastasis and treatment efficacy.

Since numerous studies have associated microbiome depletion with worse cancer outcome, studies that use biotherapeutics to target cancer have emerged in recent years. Baruch et al. and Davar et al. were the first in-human clinical trials to test whether faecal microbiota transplantation (FMT) influenced response to anti–PD-1 immunotherapy in metastatic melanoma patients (Baruch et al., 2021, Davar et al., 2021). The studies utilised faecal microbiota preparations from anti-PD-1 responders then transplanted to non-responders. Both studies reported patients receiving FMTs boosted their anti-PD-1 responses through immune-dependent mechanisms. Arguably, some say that transferring whole faecal microbiome preparations have safety concerns, however, both clinical trials certified the safety, as well as effectiveness of the FMTs.

Analysing microbiome composition in healthy vs cancer patients and treatment responders vs non-responders is not only important for developing future biotherapeutics, but may possibly be used as a predictive biomarker to aid diagnosis and/or treatment efficacy. A recent study used a diagnostic tool to

characterise a patient's 'microbiome community score', which could help identify people who may benefit from microbiome-based intervention to improve their response to ICI therapy (Derosa et al., 2024). The study analysed metagenomic sequencing of faecal samples from 245 people with lung cancer and stratified patients into two groups. Group one showed higher resistance to ICI and contained 37 microbes, such as members of *Enterocloster*, *Streptococcaceae* and *Lactobacillaceae* families, whilst group two included 45 bacterial species from families such as *Lachnospiraceae* and *Oscillospiraceae*, associated with positive responses. *Akkermansia muciniphila* abundance was also incorporated into the scores, as many studies have proposed this species has anti-cancer properties (Derosa et al., 2022). Researchers say that the final patient-specific score, in most cases, could predict response to ICI in a range of cancers, including kidney cancer.

1.3.8.1 *Focussing on the Bifidobacterium and cancer link*

As previously discussed, perturbations in the gut microbiome, particularly through the depletion of commensal bacteria, have been widely associated with cancer progression and reduced treatment efficacy. This has led to studies aimed at restoring gut homeostasis through supplementation with targeted microbial species. *Bifidobacterium* members, as examined above, have immunomodulatory effects, and therefore research has proposed they could promote cancer protection.

Bifidobacterium, being a prominent member of an adult's GI tract, has been associated with adapting immune responses in GI-associated carcinogenesis. One study showed that two *B. breve* strains were able to reduce MC38 colon tumour volumes compared to controls by enhancing the CD8^{+}/Treg, and the effector CD8^{+}/Treg ratio (Yoon et al., 2021). In corroboration, another study showed that certain strains of *Bifidobacterium* induced apoptosis in colon cancer cells *in vitro,* which was accompanied by modulations to expression of genes regulating cell cycle, apoptosis and inflammation (Asadollahi et al., 2020). For *in vivo* confirmation, colon tumour size and number were reduced in mice administered *Bifidobacterial* strains. In addition, *Bifidobacterium* has been shown to reduce oxidative stress in part by increasing expression and activity of the host's antioxidant enzymes, such as superoxide dismutase, glutathione peroxidase and catalase (Lin et al., 2022, Vitheejongjaroen et al., 2022). Since elevated ROS can damage DNA and alter cellular signalling, *Bifidobacterium* has been proposed to prevent CRC initiation (Liang et al., 2023, Shang et al., 2024).

One of the first studies to highlight how a specific member of the microbiome could alter tumour associated-immune responses distant to the GIT was Sivan and colleagues (Sivan et al., 2015). The study noticed that genetically identical C57BL/6 mice housed in two different facilities, Jackson Laboratory (JAX) and Taconic Farms (TAC), had distinct microbiomes and different rates of melanoma tumour growth. Mice housed in the JAX laboratory had less aggressive tumours with higher infiltrations of intratumoural CD8 T cells, as well as improved anti–PD-L1 efficacy. At the genus level, *Bifidobacterium* was more abundant in JAX mice and levels were significantly positively correlated with tumour-specific CD8 T cells. For proof of concept, commercially available *Bifidobacterium* mixes of *B. breve* and *B. longum* were orally administered which reduced tumour volumes in TAC mice. Mechanistically, *Bifidobacterium* supplementation altered gene expression in isolated intratumoural DCs. Genes involved in CD8 T cell activation and tumour immune infiltration were upregulated. Supportive evidence in humans has reported increased abundance of *Bifidobacterial* members, including *B. longum,* in ICI responders compared to non-responders, before treatment commenced (Matson et al., 2018).

Studies have aimed to divulge *Bifidobacterium's* health-promoting mechanisms. One such study showed that the metabolite inosine, produced by *B. pseudolongum*, improved efficacy of ICI therapy in a range of murine cancer models, including CRC and melanoma (Mager et al., 2020). The ICI therapy, induced permeability of the gastrointestinal tract which allowed translocation of the microbiome-derived metabolite, inosine. Inosine could then interact with adenosine 2A receptor ($A_{2A}R$) on T cells, which enhanced Th1 cell activation and effector function. Other metabolites, notably SCFAs, are generated by *Bifidobacteria*. As discussed SCFAs offer protection for cancer initiation, protection and recurrence. One study found that the gut microbiota was essential for CD8 T cells to confer a memory T cell response upon antigen rechallenge (Bachem et al., 2019). In particular, the gut microbiota metabolite, butyrate, promoted recall responses of memory $CD8^+$ T cells. Certain Bifidobacterium species produce small amounts of butyrate, however, Bifidobacterium supplementation has been shown to greatly elevate butyrate levels through cross-feeding (Rivière et al., 2016). The lactate and acetate produced by Bifidobacterium feed other butyrate producing bacteria, therefore may protect against cancer recurrence by promoting Tmem cell differentiation. In corroboration, CRC patients who received daily probiotic (*Bifidobacterium lactis* Bl-04 and *Lactobacillus acidophilus* NCFM) administrations had higher abundances

of butyrate producing members of the phylum, Firmicutes, in the tumour tissue biopsies compared to control CRC patients. In addition, potentially harmful members associated with CRC, such as *Fusobacterium*, were reduced with probiotic intervention (Hibberd et al., 2017).

1.3.9 Tumour microbiome

Sequencing technology developments have not only shed light on microbial communities within the gut, but also have exposed microbial communities within tissues once considered sterile. Solid tumours from multiple sites have been shown to contain microbial genetic material. Bacteria may colonise tumours through invasion of mucosal barriers, such as leaky gastrointestinal barriers. The conditions within the TME also facilitate growth of specific bacterial colonies, as conditions can be hypoxic, immune suppressive and harbour metabolites.

Not surprisingly, intratumorally bacterial load depends on anatomical location. For instance, a study found that over 60% of bone, pancreatic and breast tumours had detectable levels of bacteria, compared to just 14% of melanoma tumours (Nejman et al., 2020). In addition, composition of bacteria is proposed to differ between tumour sites. One study expanded on this further to suggest that different subsets of breast cancer had differing microbial signatures (Banerjee et al., 2018). If this is true, microbial signatures could aid clinical diagnoses and prognostics.

Even though sequencing has revealed the presence of microbial DNA in tumours, studies have tried to uncover whether the bacteria are viable. One such study showed that cultured MMTV-PyMT breast tumours had significantly more colonies than normal breast tissue and environmental control (Fu et al., 2022). 97.25% of the bacteria were found in the cytosol of tumour cells, whereby bacteria would reorganise the actin cytoskeleton, so cancer cells appeared to resist shear stress and enhance their chance of surviving in circulation. This was apparent as intracellular bacteria positively correlated with lung metastasis and the microbiome of the lung mets resembled that of the primary breast tumour.

The presence of the tumour microbiome is strongly debated. A possible explanation for this discrepancy could be due to inconsistencies amongst the bacterial detection protocols, including histological methods, qPCR and DNA sequencing. Improving sensitivity of qPCR assays may therefore be beneficial. DNA sequencing low microbial biomass samples such as tumours, either by whole genome or 16S rRNA sequencing, has been found to lead to false positive bacterial taxonomic signals. One study assessed the presence of the brain microbiome by

adapting pre- and post-sequencing bioinformatic pipelines (Bedarf et al., 2021). The protocol used environmental and bioinformatic controls, as well as comparing against absolute bacterial copy numbers from qPCR targeting the 16S rRNA gene. The study found off-target amplicons due to the presence of high-host DNA, as well as environmental contamination from reagents or sequencing steps. Risk of contamination in samples with low microbial biomass is a critical concern. For example, the ongoing debate of the sterility of the placenta led to a study finding that the major sources of bacterial DNA in samples were acquired during labour and from laboratory equipment during DNA extraction (de Goffau et al., 2019). Recently, a paper, originally published in 2020, designed a machine learning model to predict cancer type based off microbial signatures, however this was retracted in June 2024 (Poore et al., 2024). Re-analysis of the data by the study by Gihawi et al. (2023) found that the original analysis had reported human reads as bacterial. In addition to this taxonomic misclassification, the original study used normalised data instead of raw reads to classify tumour types, which when used in a machine learning model, gave false distinctions in the microbial signatures. It is therefore important to consider sequence data processing and assembling to remove potential off-target amplification of host DNA as well as correct controls to eliminate contaminants. This highlights the need for studies to have adequate environmental controls as well as normal (non-tumourigenic) tissue samples taken at the time of sampling.

There is a large amount of conflicting evidence for the presence of microbiomes in cancers such as breast and melanoma. However, improvements to sequence data processing and the use of robust controls have led to more reliable microbiome assessments. If a tumour contains a specific microbiome, the next crucial steps are to decipher how these microbes affect tumour progression.

1.4 BACTERIAL EXTRACELLULAR VESICLES

Bacterial extracellular vesicles (BEVs) are nano-sized particles (20-400 nm) that contain bioactive molecules, including proteins, lipids and nucleic acids, secreted from a parent bacterium (Jahromi and Fuhrmann, 2021). Extracellular vesicle (EV) release is not only specific to bacteria but also all domains of life, and is thought to serve as an export system for biological material (Nickel, 2010, Rodrigues et al., 2014, Buzas, 2023, Chang et al., 2021). For example, EVs from eukaryotic cells, including cancer and immune cells, release their cargos which can act locally or travel systemically around the body. EVs have multiple biological functions

including intra- or inter-species communication. In particular, BEVs are involved in bacterial defence, antibiotic resistance, environmental signalling, biofilm formation, host interactions including immunomodulation, and exchange of genetic/biological material (Macia et al., 2020); (Manning and Kuehn, 2011); (Manning and Kuehn, 2011).

BEVs can be classified depending on whether they are derived from Gram-negative or Gram-positive bacteria. The differences in cell wall structures determine how these vesicles are formed. Gram-negative bacteria have a thin peptidoglycan membrane (1 - 3 nm thick) with an outer cell wall consisting of LPS and phospholipids. Whereas Gram-positive bacteria lack LPS in their outer wall, but instead possess a much thicker peptidoglycan layer (20 – 80 nm thick) containing teichoic acids (Silhavy et al., 2010). It was thought that this thick peptidoglycan layer impaired vesicle formation hence why Gram-positive BEVs were discovered much later. Consequently, most of the literature has focussed on BEVs, or commonly referred to as outer membrane vesicles (OMVs), secreted from Gram-negative bacteria. Unlike outer membrane blebbing in Gram-negative bacteria, the cytoplasmic membrane on Gram-positive bacteria blebs in an elusive mechanism which appears to be species-specific.

Vesicle production occurs throughout the growth cycle of a bacterium; however, specific mutations enable increased EV production and secretion. Such mutations can occur in endogenous enzymes such as autolysins in the cell membrane which can break down peptidoglycan, thus enabling easier vesicle release (Stentz et al., 2022a). In addition, vesicle size, abundance and cargo load fluctuate throughout the growth cycle (Bryant et al., 2017).

It is believed that the cargo load of BEVs differs between strains of the same species of bacteria (Kim et al., 2020, Kaparakis-Liaskos and Ferrero, 2015). Functionally, this may mean that the host effects from BEVs are also strain specific. An example of the general composition of BEVs derived from the Gram-positive bacterium, *Bifidobacterium*, is depicted in **Figure 1.8**.
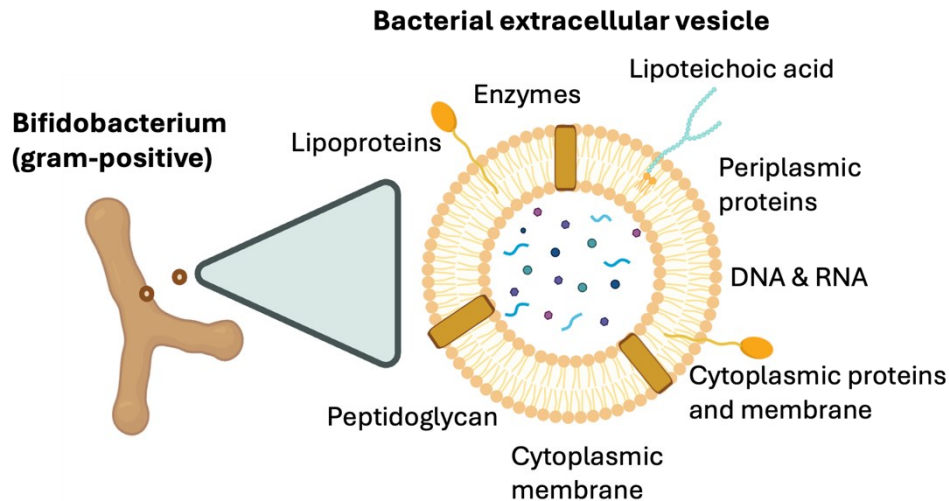
Figure 1.8 The composition of Gram-positive bacterial extracellular vesicles (BEVs). The nanosized, membrane-bound particle contains an array of proteins, nucleic acids, lipids and metabolites derived from the parent *Bifidobacterium.* Adapted from (Amatya et al., 2021). Created in part using BioRender.com.

1.4.1 BEVs as an immunomodulator

BEVs are enriched in conserved ligands, so called molecular- or pathogen-associated molecular patterns (MAMPs/PAMPs), which are recognised by intracellular and extracellular host pattern-recognition receptors (PRRs). The type of PRRs that are activated, and thus the signalling cascade, are dependent on the parent bacterium that BEVs are derived from.

BEVs from Gram-negative bacteria contain LPS which activates TLR4 signalling. For example, OMVs from *E. coli* were shown to significantly increase TLR4 mRNA levels in endothelial cells compared to PBS, however, no other TLRs (TLR1-9) were activated. The subsequent activation of TLR4 initiated the NF-κB signalling pathway. Downstream effects included IL-8 production and neutrophil infiltration. Whereas Gram-positive bacterial-derived BEVs have significant levels of peptidoglycan so were shown to activate TLR2 signalling. BEVs isolated from *B. longum* activated TLR2 ligand on macrophage-like RAW 264.7 cells, and resultant pro-inflammatory effects included IL-6 production (Kurata et al., 2022). In addition, TLR2 ligand on DCs have been shown to sense *Bacteroides fragilis OMVs,* triggering phagocytosis of the OMVs (Shen et al., 2012).

In addition to cell surface receptor activation, BEVs from both Gram-negative and Gram-positive bacteria have been shown to deliver their cargo load components directly into the cytosol of host cells (Bomberger et al., 2009, Gurung et al., 2011, Jin et al., 2011). The studies proposed the mechanism to be dependent on BEVs

fusing with the host cell's lipid membrane, specifically lipid raft components. One study showed *Pseudomonas aeruginosa* delivered virulence factors by fusing to cell membranes, resulting in host cell death (Bomberger et al., 2009).

Another family of PRRs are nucleotide-binding domain (NOD)-like receptors (NLRs) that reside in the cytosol of cells, including immune cells. NLRs respond to intracellular infection hence are activated by internalised BEVs. NLRs also respond to increased ROS and other cellular stresses (Almeida-da-Silva et al., 2023).

The NLRs, NOD1 and NOD2, recognise peptidoglycan on bacterial cell walls. Upon NOD1 and NOD2 activation, NF-κB and MAPK pathways are activated, causing pro-inflammatory effects such as IL-6 and TNFα production (Caruso et al., 2014). BEVs secreted by a variety of Gram-positive and Gram-negative bacteria have been shown to function, though not exclusively, through NOD1 and NOD2 signalling pathways (Irving et al., 2014, Thay et al., 2014).

Other NLRs form multi-protein inflammasome complexes (NLRP1, NLRP3 or NLRC4). Activated inflammasome complexes then cleave pro-caspase 1 forming active caspase-1 which consequently activates specific molecules, depending on the inflammasome activated. Active gasdermin D (GSDMD) can be formed which leads to a form of cell death known as pyroptosis. Cells with activated inflammasomes can also produce active IL-18 and IL-1β. BEVs have been shown to activate inflammasome signalling pathways in a species-specific mechanism. For example, S*almonella typhimurium*-derived OMVs were shown to activate NLRC4 inflammasome, which was dependent on the bacterial flagellin. Whereas the same study showed that OMVs derived from *Escherichia coli* that lacked flagellin, caused IL-1β secretion from macrophages through NLRP3 inflammasome activation (Yang et al., 2020).

In addition to the canonical inflammasome signalling, Gram-negative BEVs have also been implicated in non-canonical inflammasome signalling (Vanaja et al., 2016, Yang et al., 2019b). The pathway involves intracellular LPS detection that causes activation of the caspases 4 and 5 in humans, or caspase 11 in mice. As a result, active GSDMD is formed and thus cellular pyroptosis occurs.

Other PRRs such as TLR9 and retinoic acid-inducible gene I (RIG-I)-like receptors can sense genetic material in the cytosol (Lind et al., 2022). Since BEVs contain DNA and RNA and can be endocytosed by host cells, numerous studies have shown activation of TLR9 and RIG-I-like signalling pathways (Tsatsaronis et al., 2018, Ye et al., 2018, Song et al., 2022).

Collectively, the composition, structure and source of BEVs orchestrates the signalling pathways activated and ultimately the immune-modulatory responses.

1.4.2 The migration of BEVs – from the gastrointestinal tract to distant organs

Although the majority of BEVs/OMVs are produced in the gastro-intestinal tract by the host's microbiota, many tracking studies have found BEVs in the systemic circulation, peripheral tissues and distant organs in humans (Park et al., 2017, Nikkari et al., 2001, Païssé et al., 2016). Other sites of BEV/OMV production include the pulmonary respiratory tract and oral cavity, which have distinct microbiomes. When microbiome-rich sites experience dysregulation, there is a change in OMV/BEV composition (Park et al., 2017).

BEVs produced within the gut lumen have been shown to translocate to the lamina propria through the gastrointestinal barrier (Stentz et al., 2018). As discussed, numerous factors affect the permeability of this barrier and previous studies have shown that BEVs derived from certain bacterial members can increase or decrease gut permeability by affecting tight junction expression (Alvarez et al., 2016, Elmi et al., 2016, Turkina et al., 2015). In addition, immune cells within the lamina propria can also phagocytose BEVs which are able to escape then enter the circulation. BEVs can also cross the colonic epithelium through transcellular mechanisms. BEVs have previously been shown to be endocytosed by host cells. Whilst most endocytic pathways lead to lysosome degradation, BEVs have been shown to avoid this via caveolin-dependant endocytosis.

Enzymes such as proteases and glycosidases, enriched in BEVs, have been proposed to be involved in their transport from a microbiome site to distant tissues. For example, Surve and colleagues found that BEVs isolated from a strain of Group B *Streptococcus* migrated to the uterus after it was administered to the vaginal opening of mice, potentially affecting the incidence of pre-term births (Surve et al., 2016).

The mode of BEV administration in studies is therefore important to consider as this influences the levels of BEVs entering systemic circulation and travelling to the tissue of interest. Choi et al. (2017) found that intraperitoneal (IP) injection dramatically increased production of pro-inflammatory cytokines in the spleen by 5-fold compared to oral administration. Other routes may include intravenous, intratracheal, intratumorally and subcutaneous.

1.4.3 BEVs and pathogenesis

Until recent years, studies have focussed on BEVs/OMVs acting as accelerators of disease pathogenesis. As previously discussed, the host response to bacterial extracellular vesicles differs depending on the genus, species, or even strain of the parent bacterium. Members of bacteria which have been heavily studied to drive pathogenesis of certain disease include *Helicobacter pylori* (*H. pylori)* and *pathogenic E. coli (David et al., 2022).* OMVs derived from these strains were tracked to the brain where they were found to accelerate amyloid beta peptide (Aβ) plaque formation in the hippocampus of mice after 3-weeks of oral administration. In the same study, the OMVs were found to activate complement C3/C3RA signalling. Studies have also found *H. pylori* OMVs to contain virulence factors found in the parent bacterium, including CagA and VacA, which disrupt gastrointestinal barrier integrity and lead to gastric-associated cancers (González et al., 2021).

In addition, OMVs isolated from *Bactereroides* and *Prevotella* bacteria have been shown to accelerate pulmonary fibrosis in mice by inducing pro-inflammatory and -fibrotic responses (Yang et al., 2019a). In particular, the OMVs activated TLR-MyDD88 pathways, leading to increased IL-17B production in macrophages and Th17 cell development, thus driving pulmonary fibrosis pathogenesis. OMVs isolated from the Gram-negative bacterium, *Fusobacterium nucleatum*, accelerated the migration of head and neck squamous cell carcinomas (HNSCCs) *in vitro*, which they then confirmed *in vivo* by observing increased lung metastatic nodules when OMVs were injected intratumorally (Chen et al., 2024). *Fusobacterium nucleatum* OMV-treated mice had increased markers of EMT in the lungs, a key hallmark of metastasis.

LPS in Gram-negative bacterial OMVs can cause host toxicity, however bioengineering steps can be employed to reduce this. For example, detergent treatments or genetic modifications in BEVs can increase the biosafety profile (Cluff, 2010). However, genetic modifications are not always successful and detergent treatments can deplete other lipids, altering host immunomodulatory effects. Utilising BEVs derived from Gram-positive bacteria, that lack LPS, could therefore be advantageous.

Studies have also highlighted OMV/BEV's involvement in driving antibiotic resistance. Studies show that OMV cell surface proteins called porins, together with the enzyme, β-lactamase, could hydrolyse β-lactam antibiotics, decreasing the

bacteria's susceptibility to antibiotics (Kim et al., 2020). Genes involved in antibiotic resistance within OMVs can be acquired by other species via horizontal gene transfer (HGT).

1.4.4 BEVs in the treatment of disease

The immuno-stimulatory and regulatory nature of BEVs makes them potential candidates to treat immune related disorders. Intervention studies assessing BEVs for disease alleviation are sparse, however. The most prominent medical use of BEVs is in vaccine development. BEVs activate humoral and innate immune responses, making them useful adjuvants in vaccines by enhancing immune efficacy and long-lasting immunological memory. There are two OMV-based vaccines available in the clinic: Bexsero® by Novartis, and VA-MENGOC-BC® by the Finlay, both of which are against *N. meningitidis* serogroup B (MenB) which cause meningococcal disease. In addition, OMVs isolated from *B. pertinus* biofilms, responsible for whooping cough, had higher immunogenicity and lower lung epithelial cell adherence than current acellular vaccines in preclinical trials (Carriquiriborde et al., 2021). In the study, OMVs initiated strong Th1/Th2/Th17 as well as tissue resident memory responses in the lungs.

Since the more recent discovery of Gram-positive BEVs, emerging research has focused on exploring the potential of BEVs derived from probiotic and commensal bacteria. Research has focussed on BEV-host effects localised to the gastrointestinal tract. For example, BEVs isolated from the probiotic strain *Escherichia coli Nissle 1917 (EcN)* was found to upregulate tight junctional protein expression and thus increase transepithelial resistance in a gut epithelium cell line (Alvarez et al., 2019). Another study also found that *A. muciniphila* derived BEVs protected against DSS-induced inflammatory bowel disease in mice. As discussed, the genus *Bifidobacterium* has been studied to hold numerous health-promoting effects. There are very few studies that have investigated the disease-alleviating potential of *Bifidobacterial* BEVs. One study found that *B longum* KACC 91563 BEV's alleviated food allergy-induced intestinal issues in mice by increasing mast cell apoptosis, without affecting T cell activity (Kim et al., 2016). More studies have characterised Lactobacillus-derived BEVs (Al-Nedawi et al., 2015, Behzadi et al., 2017, Domínguez Rubio et al., 2017). For example, one study reported that *L. plantarum* WCFS1 derived BEVs improved host defences against antimicrobial resistance pathogens (Li et al., 2017).

As previously discussed, one of the most prominent examples of microorganisms in cancer treatment is using live, attenuated BCG bacteria to treat non-muscle-invasive bladder cancer (Redelman-Sidi et al., 2014). However, a recent study found that EVs derived from BCG are as, or more, effective at stimulating IL-6, IL-8, and GM-CSF production from epithelial bladder cancer cells (Gellings et al., 2023). This could offer safer treatment options compared to live bacteria, especially for immunocompromised patients. One study reported that the hepatic adenocarcinoma HepG2 cells incubated with BEVs, isolated from *L. rhamnosus,* had increased *Bax/Bcl-2* ratio which is associated with increased apoptosis. Additional research to investigate the mechanisms involved in *L. rhamnosus* BEV-associated cancer cell death is therefore warranted.

Another major therapeutic potential of BEVs is their use in drug delivery platforms. BEVs make ideal drug delivery candidates as they are relatively stable under physiological conditions, can encapsulate a range of biological material, and are modifiable (Herrmann et al., 2021). Adding therapeutic agents to BEVs can be achieved either before EV isolation, as the parent bacterium will incorporate this into the vesicles, or post EV isolation via processes such as electroporation or sonication (Alves et al., 2015, Baker et al., 2014). In addition, parent bacteria can also be genetically modified to change expression of therapeutic related genes. Genetic modifications and cell surface molecule alterations, such as adding surface antibodies, can increase the specificity by targeting cells and tissues of interest (Caruana and Walper, 2020, Kim et al., 2008).

1.5 AIMS AND OBJECTIVES

Conclusive evidence has shown that the gut microbiome is involved in fundamental aspects of the immune system, including immune-related pathologies. Emerging research has uncovered that cancer, a disease heavily influenced by immune responses, is associated with the gut microbiome. A loss of certain commensal bacteria, often regarded as beneficial to host-health, has been associated with cancer initiation, progression and resistance to treatment. Further research is therefore paramount to determine whether commensal bacteria could be used to treat cancers distant from the gastrointestinal tract. Emerging research over the past few years has uncovered certain microbial members to exert anti-cancer effects, however, none have yet reached the clinic. Often, there is a gap in mechanistic data, and administrations of consortiums or cocktails of bacteria do not consider functional differences that exist between strains. In addition,

administration of live bacteria may not be the only potential of using commensal microorganisms for the treatment of cancer, as bacteria release other bioactive molecules, including BEVs.

In broad, this thesis aims to uncover the therapeutic potential of novel *Bifidobacterial* strains in the context of cancer. Research aims shall be met by employing breast cancer and melanoma mouse models. Novel strains of *Bifidobacterium* shall be administered orally to assess whether modulating the gut microbiome affects breast cancer initiation, progression and metastasis. Techniques such as flow cytometry, metabolomics, and metagenomics will assess immune, metabolite and gut microbial changes, respectively. In addition, to fully assess the therapeutic potential of *Bifidobacterium*, BEVs isolated from a novel strain shall be administered intravenously in a melanoma mouse model. Systemic and tumour immune responses will subsequently be assessed.

Assess whether novel strains of *Bifidobacteria* slow tumour growth in a range of breast cancer mouse models.

Genomic and phenotypic characterisation of novel *Bifidobacteria* strains.

Characterise *Bifidobacterium*-host interactions by assessing any immune, metabolomic and metagenomic modulations.

Determine the potential of *Bifidobacterium* oral administration to prevent breast cancer occurrence and prevent and/or slow metastasis.

Assess whether *Bifidobacterium*-derived BEVs could slow cancer growth when administered intravenously (bypassing the gut microbiota).

CHAPTER TWO.

2 MATERIALS AND METHODS.

2.1 CELL CULTURE FOR *IN VITRO* AND *IN VIVO* STUDIES

All tumour cell lines were cultured in high glucose Dulbecco′s Modified Eagle′s Medium (DMEM) (Thermofisher) supplemented with 10% foetal bovine serum (FBS) (Hyclone, Thermofisher) and 100 units/ml penicillin/streptomycin (Thermofisher).

Cells were seeded in polystyrene cell culture treated flasks pre-coated with 0.1% porcine gelatin (Sigma). Cells were subcultured every 2-3 days, when 70% confluency was reached. 0.25% trypsin-EDTA was used for cellular detachment and all medium was prewarmed prior to use. Cells were incubated in the following conditions: 37°C, 5% C0$_2$ and 95% humidity.

2.1.1 Cancer cell preparation for *in vivo* tumour studies

All cells were routinely tested for mycoplasma and prior to *in vivo* administrations. Tumour cell lines, grown as previously described, were detached with 0.25% trypsin-EDTA. To wash cells, cells were centrifuged at 300 g for 5 minutes, resuspended in sterile PBS and counted. Desired volume of cell suspension was transferred to new 15 mL centrifuge tubes. After centrifugation was repeated, cells were resuspended in appropriate volume of 1:1 ratio of ice-cold sterile PBS and Matrigel (Thermofisher, cat. 354234) for implantation in the mammary gland or PBS only for subcutaneous injections. To prevent the setting of Matrigel prior to administrations, cell suspensions and the needle were kept on ice.

2.2 ANIMALS

The use of mice in this study was approved by the UK Home Office (HMO) and the European Legal Framework for the Protection of Animals used for Scientific Purposes (European Directive 86/609/EEC). All procedures were carried out by trained personal license holders and approved under the HMO project license protocol PP8873233. Specific pathogen free (SPF) and germ-free C57BL/6 mice, as well as MMTV-PyMT mice were taken from colonies maintained at University of East Anglia's Disease Modelling Unit.

All experiments used mice aged 8-12 weeks which were mixed prior to treatments commencing to homogenise microbiomes between cages. Each cage was ventilated, and mice were subjected to 12-hour light/dark cycles with access to sterilised water and standard chow *ad libitum.*

2.2.1 Maintenance and breeding of MMTV-PyMT+ mice

MMTV-PyMT mice on a congenic C57BL/6 genetic background were purchased from the Jackson Laboratory (stock No. 022974). Hemizygous MMTV-PyMT females spontaneously develop mammary tumours therefore breeding MMTV-PyMT+ males with non-carrier females were performed.

To confirm MMTV-PyMT transgenic status, DNA genotyping from ear biopsies were routinely performed. To extract DNA, ear biopsies were digested overnight at 56°C in lysis buffer (Tris-HCl (50mM, pH 8.5); EDTA (10 mM, pH 8); NaCl (100 mM); SDS (0.2%)) supplemented with proteinase K (100 ug/mL) (Sigma). 100 μL of isopropanol was added to precipitate DNA from each sample. After centrifugation (2600 g, 30 minutes) isopropanol was removed by inverting the plate and evaporation. Precipitated DNA was then resuspended in Tris-EDTA buffer (Tris-HCl (10 mM, pH 7.5); EDTA (1 mM, pH 8)). PCR reaction mixes and DNA outlined in table 2.1 were loaded into 96-well PCR plates and ran according to conditions in table 2.2 on a 96-well block thermocycler (Bioer Technology). PCR products were run on a 1.8% agarose gel containing ethidium bromide at 90 V then subsequently imaged using a BioDoc-IT Transilluminiator (UVP) to confirm genotypes, example seen in **Figure 2.1**.

Table 2.1. Reagents for MMTV-PyMT transgene PCR

Reagent	Volume per well (μL)
MegaMix-Blue (Cat. 2MMB-100, Clent Lif Science) a PCR master mix containing Taq polymerase, MgCl2, dNTPs and blue agarose loading dye.	10
P1 (5' - CAAATGTTGCTTGTCTGGTG – 3') (100 μM)	0.8
P2 (5' - GTCAGTCGAGTGCACAGTTT – 3') (100 μM)	0.8
P3 (5' – GGAAGCAAGTACTTCACAAGGG – 3') (100 μM)	0.8
P4 (5' – GGAAAGTCACTAGGAGCAGGG – 3') (100 μM)	0.8
DNA	0.5

Table 2.2. Steps and conditions for MMTV-PyMT transgene PCR

Step	Temperature (°C)	Hold time (mm:ss)	Cycles
Initial activation	94	03:00	1
Denaturation	94	01:00	35
Annealing	60	02:00	
Extension	72	01:00	
Elongation	72	03:00	1
Cooling	16	Indefinitely	
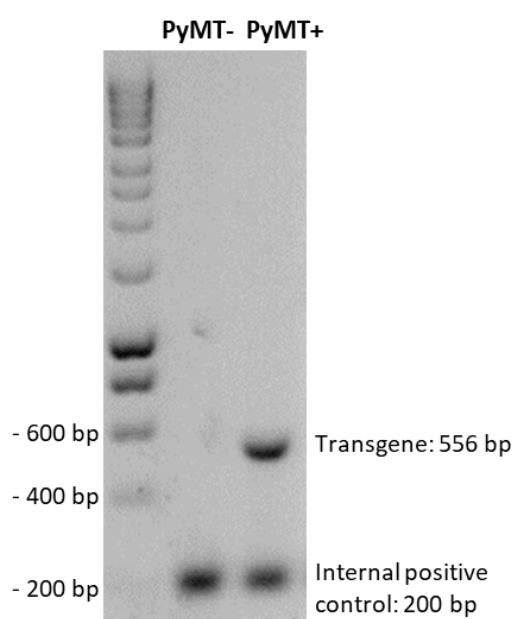
Figure 2.1 Example gel electrophoresis of PCR assay targeting MMTV-PyMT transgene (556 base pairs). DNA was isolated from MMTV-PyMT-negative and MMTV-PyMT-positive mice. Successful reactions are denoted by the presence of an internal positive control band at 200 base pairs (bp).

2.2.2 Calculating tumour volume

Resected tumours were placed in bijous containing RPMI-1640 Medium (Merck, Cat. 51536C), weighed and volumes measured using digital callipers and the following formula:

$$Tumour\ Volume = (Tumour\ Width)^2 \times Tumour\ Length \times 0.52$$

2.2.3 Assessing tumour growth and occurrence in a spontaneous breast cancer model (MMTV-PyMT)

To assess if *Bif*210 could be used as a chemopreventative agent, the time for tumours to develop in MMTV-PyMT+ mice were tracked. Tumour growth was also measured by digital callipers to assess long-term *Bif*210 supplementation on overall tumour burden. Oral administrations of *Bif*210 occurred twice weekly and commenced when mice were aged 8-weeks. Mice were sacrificed, by procedures previously described, when tumours reached 1000 cm^3 (or until experimental time limits defined in project license protocols were reached).

2.2.4 Orthotopic breast cancer models

Breast tumour cells (prepared as previously described) were orthotopically injected into the abdominal mammary gland (number 4). Surgery was performed under aseptic conditions with pre- and post-surgery care given to all animals in accordance with Laboratory Animal Science Association (LASA) guidelines (2017). Treatment regimens and model durations are detailed in table 2.3. Tumour growth was tracked on treatment days by digital callipers and volumes calculated as previously described. On pre-determined end point dates, or when tumours ≥ 1000 cm^3, animals were sacrificed by exposure to increasing CO_2 concentrations and tissues harvested.

Table 2.3. Orthotopic breast tumour mouse model experimental details

Cell line	Number of cells injected	Day treatment commenced	Model duration (days)
PyMT-Bo1	1×10^5	7	15
BRPKp110	5×10^5	10	21
EO771	2×10^5	10	26

2.2.5 Gastrointestinal permeability assessment in non-tumour and tumour bearing, aged mice

To assess the gastrointestinal permeability of mice *in vivo*, non-tumour bearing (MMTV-PyMT-) and tumour bearing (MMTV-PyMT+) 17-week (aged) mice were orally administered fluorescein isothiocyanante labelled dextran (FITC-dextran, Sigma-Aldrich, cat. 46944) at a concentration of 44 mg/100 g body weight. PBS oral administrations acted as controls to measure background fluorescence. After 2 hours, mice were sacrificed by rising levels of CO_2 and blood immediately collected by cardiac puncture using a 21G needle. Serum was prepared by

allowing blood to coagulate at room temperature for 30 minutes then centrifuging at 2600 g for 15 minutes at 10°C. FITC-dextran standards ranging from concentrations of 0.125 – 16 µg/mL were prepared. 100 µL standards/serum samples were loaded to wells of a non-tissue culture-treated 96-well plate and fluorescence measured using a fluorescence microplate reader (excitation: 485nm, emission: 528nm).

2.2.6   Breast tumour resection model

To assess tumour cell dissemination and seeding to distant organs, a model was developed based on the PyMT-Bo1 orthotopic breast cancer model (previously described in section 2.2.4). Primary tumours were resected under aseptic surgery conditions when tumour weights were estimated to be around 600 – 1000 mg (days 12 - 14). Care was taken during surgery to remove all primary tumour to prevent regrowth. The surrounding blood vessels were clamped with haemostat forceps and detached using disposable cautery pens. Analgesic was administered for 3 days post-resection. Metastases were allowed to develop for 4 weeks then animals were sacrificed, and organs prepared for histology. Animals which experienced primary tumour regrowth were sacrificed prior to this.

2.2.7   Experimental metastasis models

To examine if BEVs affected metastasis formation, 1×10^6 B16-F10 cells were administered intravenously via the tail vein. Intravenous BEV administrations commenced on day 3, every 3 days, for a total of 4 administrations. Animals were sacrificed (as previously described) on day 14.

To examine if *Bif*210 affected breast tumour metastasis formation, 8×10^5 PyMT-Bo1 cells were administered intravenously via the tail vein. Oral administrations of *Bif*210 commenced alongside tumour cell administration and occurred every 2-3 days. Animals were sacrificed (as previously described) on day 13.

Lungs (the favoured site for cancer cell colonisation after tail vein injections), and livers were harvested, and prepared for: histology (section 2.6); *in vivo* bioluminescence imaging (section 2.2.8); and/or surface nodule enumeration.

2.2.8   *In vivo* and *ex vivo* bioluminescence imaging for PyMT-Bo1-Luc-GFP cell quantification

PyMT-Bo1 cells were previously tagged with GFP and firefly luciferase by our collaborators in the Weilbaecher lab (Washington University, St. Louis, USA), aiding the identification of circulating/metastatic GFP and luciferase tagged PyMT-

Bo1 cells in tissues and blood. Luciferase, an enzyme tagged on the cancer cells, converts the substrate luciferin, in a bioluminescence (light emitting) reaction. For *in vivo* detection, animals received IP injection of 2 mg/dose of VivoGlo™ luciferin (Promega, cat. P1041, diluted in sterile PBS). After 10-minute incubation, animals were anaesthetised with 2-3% isofluorane/oxygen and imaged using the Bruker In Vivo Xtreme (Bruker, Billerica, MA, USA). Bruker settings were as follows: exposure time (10-120 seconds), field of view was 19 cm, fStop was 1.1, focal plane was 5 mm. For *ex vivo* assessment of metastatic burden in the lungs and livers, animals were sacrificed (rising levels of CO_2) and the lungs/livers were placed in 1.5 mL VivoGlo™ luciferin (300 µg/mL) of a 24 black-side well imaging microplate and incubated for 2 minutes then imaged as described.

To quantify bioluminescence emission, which is proportional to metastatic burden, Bruker images were analysed using ImageJ 1.52a to calculate densitometry readings of bioluminescence regions.

2.2.9 Subcutaneous melanoma model

4×10^5 B16-F10 cells were injected subcutaneously into the flank of C57BL/6 mice. BEVs, administered intravenously (IV) via the tail vein, commenced once tumours became palpable on day 6, then on days 9 and 12 post-tumour implantation. Animals were sacrificed on day 14 as previously described.

2.2.10 *In vivo* depletion of Ly6G cells

To assess if anti-tumourigenic activity of BEVs were due to increases in granulocytes, Ly6G cells were depleted in a B16-F10 melanoma model (previously described). 200 µg/per mouse of InVivoMAb anti-mouse Ly6G (Clone:1A8, 2B Scientific Limited, cat. BE0075-1-25MG) or the InVivoMAb rat IgG2a isotype control (anti-trinitrophenol, 2B Scientific Limited, cat. BE0089-25MG) were administered by intraperitoneal (IP) injection every 2 days (commencing 1 day prior to the first BEV administration).

2.3 CULTURING *BIFIDOBACTERIUM*

Bifidobacterium strains "210", "506", "80", "8809", previously isolated by Lindsay Hall's group (Quadram Institute Bioscience, UK), were grown in DeMan, Rogosa and Sharpe (MRS) media (Thermo Scientific™, cat. CM0359B) supplemented with 50 µg/mL L-Cysteine Hydrochloride (Sigma Life Science, Cas. 52-89-1). Cultures were grown in humidified anaerobic conditions at 37°C for 48/72 hours before subculturing and/or experimental use.

2.3.1 Lyophilisation of Bifidobacterium strains

Bif cultures (20 mL) were added to 250 mL MRS-cysteine media and grown in anaerobic conditions at 37˚C for 22-26 hours until optical density was 1.5 - 1.8; indicative of the late exponential growth phase. To remove media, cultures were centrifuged (4000 rpm, 10 minutes, brake speed 3) and washed in sterile PBS, twice. Bacteria were resuspended in 15 mL sterile PBS and 1.2 mL of which were transferred to sterile 2 mL ChromaVial short thread vials (Chromex Scientific). Parafilm ensured a tight seal around vials which were incubated overnight at -80˚C. Parafilm lids were pricked twice using a 25-gauge needle. Lyophilisation occurred in a Modulyo® freeze dryer for 48 hours. Lyophilised bacteria were stored at -80˚C. To reconstitute lyophilised *Bif,* sterile water and PBS to give a final CFU of around 1×10^{10}/mL were added.

2.3.2 Growth curve generation

To predict the growth of *Bifidobacterium* strains, inoculums were prepared with a 1:10 inoculation of bacterial cultures in MRS-cysteine media. 100 µL of each inoculum (timepoint = 0 hours) were added to wells of a sterile, non-tissue culture-treated 96-well microplate in replicates of 6. PBS were added to surrounding empty wells to prevent sample evaporation. Stratus (Cerillo) microplate reader measured optical densities at 600 nm (OD_{600nm}). Average readings of medium only wells were subtracted from each sample reading to account for background absorbance. Absorbance readings were plotted every 2-hours for 48 hours.

Since bacterium growth cycles depend on numerous conditions, including culture volumes, it was also important to generate growth curves for cultures grown in 50 mL centrifuge tubes (resembling growth conditions used for oral gavage preparation). Inoculums were prepared as described and 1 mL bacterial cultures were collected every 2 hours for 48 hours for measurement of optical densities (OD_{600nm}) using the CO 8000 Biowave spectrophotometer (Avantor®).

Non-viable bacteria increase optical density; therefore, it was important to enumerate colony forming units (CFU) at 2-hour timepoints, which represent viable bacteria. Every 2 hours, 100 µL bacterial cultures were serially diluted (1:10 in sterile PBS giving final concentrations of $10^{-3} – 10^{-11}$/mL). 20 µL spots were plated on MRS-cysteine agar plates and incubated in anaerobic conditions at 37˚C for 48 hours. Bacterial colonies were counted, and CFU/mL calculated based on the following formula:

$$CFU/mL = \frac{Number\ of\ colonies\ \times dilution\ factor}{Volume\ plated\ (mL)}$$

2.3.3 Preparation of acid-killed *Bifidobacterium*

To induce bacterial cell death yet conserve molecular structures, bacteria were acid-killed. Acid-killed bacterial cultures were prepared by Christopher Price (Robinson Lab, Quadram Institute, UK). Lyophilised bacteria were reconstituted in sterile PBS, then Peracetic acid (Sigma) (final concentration of 0.4%) was immediately added. After 1 hour incubation at RT, bacteria were washed three times in sterile PBS by centrifugation described in section 2.3.1 and then resuspended to give a final concentration of around 1×10^{10} CFU/mL for subsequent oral administration to mice. Acid-killed bacteria were plated on MRS-cysteine agar as previously described and incubated under anaerobic conditions at 37˚C for 48 hours to confirm successful bacterial killing.

2.3.4 BEV isolation from *Bif*210

BEVs were isolated, concentrated and purified by Anne Jordan (Quadram Institute Bioscience, UK) with the protocol adapted from Stentz et al. (2022a). Briefly, *Bif*210 (5% inoculation in 500 mL filtered vegan RCM media) was grown for 20 hours at 37°C in humidified anaerobic conditions. Cultures were centrifuged (7000 g, 1 hour at 4°C) and supernatant filtered through 0.22 µM polyethersulfone (PES) bottle top vacuum filter system (Sartorius). Supernatants were concentrated using a counterflow ultrafiltration system which involved running sample through a Vivaflow® 50R cassette (100 kDa molecular weight cut-off, Sartorius) which was connected to a peristaltic pump (Sartorius) and a Vivaspin 500 centrifugal concentrator (Sartorius). 500 mL PBS was then run through the ultrafiltration pump system. Filtrate was collected and 10 mL PBS added then filtered and centrifuged for 5 minutes at 4000 rpm. Filtered solution was then centrifugation at 4000 rpm for 40 minutes. BEVs were further purified using size-exclusion chromatography with qEVoriginal 35 nm columns (Izon), used according to manufacturer's instructions. After a final filter-sterilisation step using 0.22 µm PES membranes (Sartorius), aliquots were stored at -80°C until required.

2.4 ASSESSING MICROBIAL COMPOSITION AND ACTIVITY

2.4.1 DNA extraction

Genomic DNA was extracted from bacterial monocultures, intestinal contents, faeces and tumours using a commercially available kit (FastDNA™ Spin Kit for Soil, MP Biomedicals, SKU: 116560200). Around 50 mg of sample was used, following manufacturer's instructions, with an additional bead beating step using a FastPrep (MP Biomedicals, USA), protocol previously described by (Kellingray et al., 2017). DNA concentrations were evaluated using Qubit® dsDNA broad range assay kit (Thermo Fisher Scientific, cat. Q32850) with a Qubit® 2.0 Fluorometer, following manufacturer's instructions.

2.4.2 De novo hybrid assembly of novel bacterial strains

Extracted genomic DNA from bacterial species were diluted 5 ng/μL in ultrapure water for Illumina sequencing and 50 ng/μL for nanopore sequencing, both of which were performed in-house (Quadram Institute, UK).

Nanopore sequencing files were run through NanoFilt v2.8.0 which trimmed long reads. Reads were excluded if the minimum length was below 1000 bp as well as a read quality score below 7. Trimming and filtering of paired-end Illumina reads were performed using Fastp v0.23.4. Unicycler v0.5.0 assembled the trimmed/filtered Illumina and nanopore files to output complete genomes. Bandage v0.8.1 was used to visualise the genomes and CheckM v1.1.6 was used to assess completeness and quality.

2.4.3 Culturing tumours from MMTV-PyMT+ mice to identify viable bacteria

To assess whether there was any presence of a tumour microbiome in our murine models, culture techniques were used to identify any viable bacteria in tumours from MMTV-PyMT+ mice. Mammary tumours from different anatomical locations (thoracic, abdominal, and inguinal) were resected in sterile conditions. To reduce bacterial contamination, all reagents, lab user personal protective equipment, surfaces and tools were autoclaved and (where possible) UV sterilised. Tumour tissue samples were manually homogenised in 1 mL sterile PBS to > 1 mm^3 pieces using scalpels. 100 μL tumour lysates were spread on selective agar plates. To increase the likelihood of identifying aerobic bacteria, a range of selective agars were utilised including Columbia blood agar (CBA) (Oxoid) + 5% horse blood; Man Rogosa Sharpe (MRS) agar (Oxoid); brain heart infusion (BHI) agar (Oxoid) and cultured at 37°C in aerobic conditions. For anaerobic bacterial identification,

selective agars including MRS agar (+ 50mg/L-cysteine), BHI agar (+ 50mg/L-cysteine), Peptone Yeast Extract Glucose Starch (PYGS) agar (Thermo) were used and incubated in anaerobic conditions at 37˚C. Surgical tools dipped in sterile PBS were also plated to act as an environmental control. Mouse skin swabs were plated to confirm agar plates and conditions successfully supported growth of microorganisms. Aerobic plates were grown at 37°C + 5% CO_2 for 5 days and anaerobic plates were grown at 37°C + 5% CO_2 for 3 days.

2.4.4 Culturing gastrointestinal compartments from germ-free mice

Germ-free mice, maintained and sacrificed in sterile conditions, as previously described, were used to assess the viability of *Bif*210 in the gastrointestinal tract. *Bif*210 (CFU/mL of 6.03^{10}) was orally administered, and mice were sacrificed after 6, 24 and 48 hours. Contents of the different compartments of the gastrointestinal tract (small intestine, caecum and upper and lower large intestines) were collected under sterile conditions and 50 mg were homogenised in sterile PBS (1:10). 100 µL were spread on MRS-cysteine agar and incubated in anaerobic conditions at 37˚C for 48 hours. Colonies were manually counted, and CFU/g calculated using the following formula:

$$CFU/g = \frac{Number\ of\ Colonies \times Dilution\ Factor}{Volume\ Plated\ (in\ mL) \times Weight\ of\ Sample\ (in\ g)}$$

2.4.5 Real-time polymerase chain reaction (qPCR) for *Bif* quantification

To relatively quantify levels of *Bifidobacterium* in mouse faecal/gastrointestinal material, experimental outlines described in figure legends, as well as in tumours, I used quantitative PCR (qPCR) targeting the housekeeping *GroEL* gene. The *GroEL* gene is conserved across different *Bifidobacterium* species, allowing for species-level discrimination Primers specific to *B. pseudocatenulatum* used in previous studies were used and listed in table 2.4 (Junick and Blaut, 2012).

Table 2.4. Primer details to identify *B. pseudocatenulatum* (*Bif*210) by qPCR

Bifidobacterium strains	Primers	Sequence (5' to 3')	Size (base pairs)
B. pseudocatenulatum	Forward	AGCCATCGTCAAGGAGCTTATCGCAG	325
	Reverse	CACGACGTCCTGCTGAGAGCTCAC	

A SYBR Green dye detection method was used to relatively quantify *Bif*210 levels in DNA samples. General principle being that the higher the levels of target gene, the increased binding of SYBR Green I dye, which is proportional to fluorescence intensity. Reagents (detailed in table 2.5) were added to wells of a Axygen® 96 well PCR microplate. 480 ng of target DNA was added per well. Standards ranging from final concentrations of 0.0002-20 ng/μL were prepared by serially diluting DNA isolated from *Bif*210 monocultures in RNA-ase free water. Samples/standards were run in duplicates. RNase-free water acted as a negative control.

Table 2.5. Reagents details for SYBR Green qPCR targeting the *Bif*210 *GroEL* gene

Reagent	Volume per well (μL)
LightCycler® 480 SYBR Green I Master (Roche Diagnostics, cat. 0470751600)	12.5
Forward primer (10 μM)	2.5
Reverse primer (10 μM)	2.5
RNA-ase free water	7.3

After a brief centrifuge (1500 g 2 minutes), the sealed plate was loaded onto LightCycler® 480 system (Roche Diagnostics) and ran under the following conditions detailed in Table 2.6.

Table 2.6. qPCR conditions for the detection of *Bif*210 *GroEL* gene using the LightCycler® 480 system (Roche Diagnostics)

Step	Cycles	Target (°C)	Acquisition mode	Hold (hh:mm:ss)	Ramp rate (°C/s)
Initial activation	1	95	None	00:05:00	4.40
Amplification	45	94	None	00:00:15	2.20
		64	None	00:00:15	2.20
		72	Single	00:00:15	4.40
Melting curve	1	95	None	00:00:05	4.40
		65	None	00:01:00	2.20
		97	Continuous		0.11
Cooling	1	40	None	00:00:30	2.20

2.4.6 Metagenomic sequencing of the mouse caecum

Caecum DNA (extracted as previously described) was diluted in sterile H_2O to give a final concentration of 5 ng/µL. Illumina Nextera Flex library construction was performed in-house (Dave Baker and colleagues, Quadram Institute Bioscience, UK). To determine the microbial species in the metagenomic caecal DNA pre-prepared libraries, Shotgun Whole Genome Sequencing (WGS) was then outsourced to Source BioScience which used NovaSeq S4 lane sequencing. Data (FASTQ) files containing the raw reads were processed, trimmed, assembled and classified by Dr Raymond Kui (Quadram Institute Bioscience, UK).

MicrobiomeAnalyst v2.0 was utilised for visual representation of the marker genes in processed shotgun sequence files. Default settings were applied for data inspection that excluded singletons and constant values. Also default data filtering settings excluded features with a count lower than 4 in less than 20% of samples as well as features with low variance (based on inter-quartile ranges). Total sum scaling was applied to normalise count data.

2.4.7 Caecal contents ^{1}H NMR analysis

100 mg of caecal matter was prepared for ^{1}H NMR analysis by adding 600 µL NMR buffer (18.3 mM Na_2HPO_4, 80.9 mM K_2HPO_4 and 1 mM TSP (sodium 3-(trimethylsilyl)-propionate-d_4) in D_2O (deuterium oxide)) and homogenising for 1 minute using sterile pellet pestles attached to a cordless motor. After centrifugation (17,000 g at 4°C for 5 minutes), caecal waters were transferred to microcentrifuge tubes and stored at −20℃ until further analysis.

550 µL caecal waters were transferred to NMR tubes, immediately followed by ^{1}H NMR analysis using the Bruker Avance III 800 MHz spectrometer, equipped with an inverse triple resonance z-gradient probe. Dr Gwenaelle Le Gall and Dr Trey Koev (University of East Anglia, UK) aided with spectra generation. All ^{1}H NMR spectra acquired on the 800 MHz spectrometer were obtained using 256 scans, a spectral width of 9615 Hz, acquisition time of 0.83 s, using Bruker's 'noesygppr1d' pulse sequence, featuring selective low-power pre-saturation (p16 = 1.0 ms) on the residual H_2O peak frequency during relaxation delay and mixing time for effective solvent suppression. Spectra were apodised using 0.1 Hz line broadening and referenced using the TMSP peak at 0.0 ppm. Recycle delay was set to 10 s, the mixing time used was 0.1 s, and the ^{1}H π/2 rf pulse was 9.08 µs.

2.4.8   ¹H NMR spectral analysis for untargeted metabolomics

The metabolites were quantified using the NMR Suite v7.6 Profiler (Chenomx®, Edmonton, Canada). NMR spectral processing TOPSPIN 2.0 software was used for baseline and phase correction. The chemical shift indicator, TSP (concentration = 1 mM), peak was automatically calibrated for each spectra using Chenomx Processor software, aiding metabolite concentration determination. Metabolites were identified and concentrations (mM) calculated using Chenomx Profiler (V8.6) containing libraries of pre-selected metabolite profiles.

2.5   FLOW CYTOMETRY

2.5.1   Tumours and lung preparation

Resected tumours and lungs were manually homogenised to 0.5 mm³ pieces. Tumours and lungs were digested in 10 mL collagenase solutions (1% 1X DNase, Sigma-Aldrich, cat. D4263-1VL; 20 mg collagenase type IV for tumours or type I for lungs, Sigma-Aldrich, cats. C0130 and 17100017, respectively; 1 mg hyaluronidase; 10 mL Hanks' Balanced Salt Solution (HBSS)) at 37°C for one hour. Digested tumours and lungs were passed through 70 µM strainers to remove cellular debris. After centrifugation at 300 g, 4°C for 5 minutes, cells were incubated in 10 mL red blood cell lysis buffer (final concentration of 0.82% (w/v) ammonium chloride, 0.12% (w/v) sodium bicarbonate, 0.02% (v/v) 0.5M pH8 EDTA in Millipore water)) for 5 minutes at RT.

After a washing step with ice-cold PBS, cells were resuspended in FACS buffer (2% FBS in PBS) and counted using the Countess™ 3 Automated Cell Counter (Invitrogen™). Cells were resuspended in appropriate volumes of FACS buffer to give a concentration of 10^7 cells/mL. 100 µL of cell suspension were transferred to wells of a 96-well PCR plate.

2.5.2   Lymph node preparation

Lymph nodes were passed through 70 µM strainers with 2 mL PBS then 100 µL of cell suspensions directly loaded to wells of a 96-well PCR microplate.

2.5.3   Blood preparation

Blood, collected by cardiac puncture using 23G EDTA-coated needles, were immediately placed in microcentrifuge tubes containing 50 µL EDTA to prevent blood coagulation. After centrifugation as described, red blood cells were lysed,

which was repeated 2 – 3 times; until cells were visibly free from red components. Cells were washed, counted and resuspended as previously described.

2.5.4   Fluorescence staining of cellular markers

Fluorescence minus one controls (FMOs) were prepared using pooled cell suspensions which would aid identification of positive populations in downstream analysis. To prevent non-specific antibody binding, cells were resuspended in 100 µL TruStain FcX™ anti-mouse CD16/32 antibody (1:200 in FACS buffer, cat. 101320, BioLegend) and incubated for 10 minutes on ice. Centrifugation was repeated and cells were incubated in 100 µL appropriate antibody solution detailed in Table 2.7 for 30 minutes on ice in the dark. At this stage, cells were also stained with LIVE/DEAD™ Fixable Red or Blue (Thermo, Cat. L34971/ L23105, 1:400). After which, cells were washed with 100 µL FACS buffer. If intracellular staining was not required, cells were fixed with 100 µL 4% paraformaldehyde (PFA) for 30 minutes on ice then centrifuged and resuspended in 200 µL FACS buffer and stored at 4°C until analysis. If intracellular staining was required, see section below.

2.5.5   Intracellular staining for flow cytometry

To stain for transcription factors or nuclear proteins, such as FoxP3 and Ki67, the Foxp3 Transcription Factor Staining Buffer Set (eBioscience™, Cat. 00-5523-00) was used according to manufacturer's instructions. After overnight incubation in 200 µL fixation/permeabilization solution, plates were centrifuged (400 g, 5 minutes, RT) and cells resuspended in 100 µL 5% rat serum (eBioscience™, Cat. 24-5555-93) in 1X permeabilization buffer for 15 minutes at RT. Directly conjugated antibodies for detection of intracellular antigen(s), displayed in Table 2.7, were added and incubated for 30 minutes in the dark. 200 µL of 1X permeabilization buffer was added to each well. After centrifugation was repeated, cells were resuspended in an appropriate volume of FACS before analysis.

2.5.6   Flow cytometry data collection and analysis

AbC™ Total Antibody Compensation Bead Kit (Thermo, Cat. A10497) was used according to manufacturer's instructions to prepare single stained controls for compensation to account for any fluorescence spill-over into other fluorescence channels.

All single stained controls, FMOs and samples were run on the LSRFortessa™ (BD BioSciences). 10,000 events were recorded for single stained controls and between 100,000 – 200,000 events were recorded for FMOs and samples. Singles

were run first, and laser voltages were adjusted so that fluorescence intensities of positive populations were around 10^3-10^4 whilst fluorescence intensities of negative populations were around 10^2. Subsequently, compensation was calculated and applied to all samples. FlowJo (v10.9.0, BD) computer software was used to display cells and gate specific populations based on forward and side scatter (FSC, SSC), and fluorescence emissions. The gating strategy used to gate immune cell populations is presented in supplementary table 9.1.

Table 2.7. Details of fluorophore-conjugated antibodies identifying key cell surface and intracellular markers specific to immune cell subsets, with a focus on lymphocyte identification.

Cell Populations					
Cell population	Antigen	Fluorophore	Supplier details	Clone	Dilution
Leukocyte	CD45	PerCP-Cy5.5	eBioscience, Cat. 45-0451-82	30-F11	1:200
		BUV395	BD, Cat. 564279	30-F11	
Lymphoid cells	CD3e	APC	Thermo, Cat. 17-0031-81	145-2C11	
T-helper cells	CD4	FITC	eBioscience, Cat. 11-0043-81	RM4-4	
Cytotoxic T lymphocytes	CD8a	APC-Cy7	Thermo, Cat. A15386	53-6.7	
B cells	CD19	BV650	BioLegend, Cat. 115541	6D5	
Natural killer cells	NK1.1	PE-Cy7	BioLegend, Cat. 108713	PK136	
Regulatory T cells	FoxP3	eFlour450	Thermo, Cat. 48-5773-82	FJK-16s	1:100
T-effector	CD44	eFlour450	Thermo, Cat. 48-0441-82	IM7	1:200
T-memory	CD62L	BV605	BioLegend, Cat. 104438	MEL-14	
Natural killer cells	NK1.1	PE-Cy7	BioLegend, Cat. 108713	PK136	
Tissue resident memory T cells	CD103	BV711	BioLegend, Cat. 121435	2E7	
	CD69	FITC	Biolegend, Cat. 104505	H1.2F3	
Tumour cells	GFP	GFP-PE-Cy7	BioLegend, Cat. 338014	FM264G	1:100
	Luciferase	AF647	Abcam, Cat. ab237252	EPR17789	1:100
	Pan-cytokeratin	AF488	Thermo, Cat. 53-9003-80	AE1/AE3	1:200

Central memory T cell	CCR7	PE	Biolegend, Cat. 120105	4B12	
γδ T cells	TCR γ/δ	APC/Fire™ 750	BioLegend, Cat. 118136	GL3	
Pan-myeloid/cDC2	CD11b	BV605	BD, Cat. 563015	M1/70	
Monocytes	Ly-6C	eFluor450	Invitrogen, Cat. 48-5932-82	HK1.4	
Granulocytes	Ly6G	APC-Cy7	BD, Cat. 560600	1A8	
N1 neutrophils	ICAM-1	PE	BioLegend, Cat. 116107	YN1/1.7.4	
Pan-macrophages	F4/80	AF700	BioLegend, Cat. 123129	BM8	
		APC	Invitrogen, Cat. 17-4801-82	BM8	
M1 macrophages	MHCII	PE-Cy7	Invitrogen, Cat. 25-5321-82	M5/114.15.2	1:200
		AF594	BioLegend, Cat. 107650	M5/114.15.2	
M2-macrophages	CD206	FITC	BioLegend, Cat. 141704	CO68C2	
		AF594	Biolegend, Cat. 141726	C068C2	
Pan-DCs	CD11c	BUV395	BD, Cat. 564080	HL3	
cDC1 cells	CD103	BV711	BioLegend, Cat. 121435	2E7	
Immunosuppressor myeloid cells	Arg-1	APC	Invitrogen, Cat. 15943214	A1exF5	
Activated neutrophils/M1 macrophages	CD64	FITC	Biolegend, Cat. 139315	X54-5/7.1	
TLR2 receptor	CD282	PE-Cy7	BioLegend, Cat. 153011	QA16A01	

2.6 HISTOLOGY

2.6.1 Tissue processing and embedding for formalin-fixed, paraffin-embedded (FFPE) tissues

Explanted mouse tissues were fixed in 4% PFA at 4°C for 24 hours, followed by storage in 100% ethanol at 4°C. Tissues were processed in the Leica Tissue Processor ASP300S (Leica Biosystems) following steps in Table 2.8.

Table 2.8. Leica tissue processor reagents and settings

Step	Reagent	Duration (minutes)
1	70% ethanol	60
2	80% ethanol	90
3	90% ethanol	120
4	100% ethanol (3 changes)	60
5		90
6		120
7	Xylene (3 changes)	30
8		60
9		90
10	Paraffin wax (3 changes)	120
11		60
12		120

Tissues were embedded in paraffin wax using the embedding station EG1150H (Leica Biosystems) and cooled overnight at 4°C. FFPE tissues were sectioned at 4 µm thickness using a rotary microtome (Leica Biosystems, RM2235) then mounted onto positively charged glass slides (Thermo Fisher) and incubated at 37°C overnight to affix.

Sections were deparaffinized in xylene (Sigma-Aldrich, 534056) (two changes for five minutes each) then rehydrated in decreasing concentrations of ethanol (EtOH, 100%, 80% and 70% for two minutes each) then into dH$_2$O and stained as required. Alternatively, sections were stained using an automated multistainer (Leica Biosystems, ST5020) as per manufacturer's instructions.

2.6.2 Cryo-sectioning mouse tissues

Explanted mouse tissues were placed in tubes and immediately snap frozen in liquid nitrogen and stored at -80°C. Tissues were sectioned to 5 µm thickness using a Cryostat NX70 (Thermo Fisher) and stored at -80°C.

2.6.3 Haematoxylin and eosin (H&E) staining to assess tissue morphology

FFPE sections were deparaffinised and rehydrated as previously described and frozen tumour sections were air dried for 10 minutes at room temperature, transferred to running tap water for 30 seconds then placed in Mayer's Haematoxylin for five minutes. Sections were rinsed in running tap water until blue, drained and Eosin was added for 20 seconds. Excess Eosin was blotted off sections, rinsed in running tap water, followed by gradual dehydration (50% EtOH, 70% EtOH, 80% EtOH, 95% EtOH, twice 100% EtOH, and twice Histoclear). Sections were mounted on glass coverslips (24x50 mm, thickness: 0.13-0.16 mm) with Neo-Mount™ (Sigma-Aldrich, cat. 1090160100) and allowed to air dry. Alternatively, sections were stained using an automated multistainer (Leica Biosystems, ST5020) as per manufacturer's instructions.

2.6.4 Immuno-fluorescence on frozen tissue sections

Frozen tissue sections were air-dried for 10 minutes then fixed in 4% PFA for 10 minutes. Slides were placed in a foil-covered Coplin jar and washed in PBS 0.3% triton-X100 for 1 hour then in PBLEC solution (PBS, 1% Tween20, 0.1 mM $CaCl_2$, 0.1 mM $MgCl_2$, 0.1 mM $MnCl_2$) for 30 minutes with gentle agitation. Tissues were outlined with a hydrophobic PAP pen to prevent solution spill-over. Tissues were blocked in Dako serum-free protein block for 30 minutes at RT in a humidified chamber. After removal of blocking solution, 40 µL of primary antibody (diluted in PBLEC) (in Table 2.9) was added and incubated overnight at 4°C in a humidified chamber. Primary antibody was removed, and slides washed in PBS 0.3% triton-X100 3 times, 5 minutes each. 40 µL of appropriate fluorescent conjugated secondary antibody (diluted in PBLEC) (in Table 2.10) was added and incubated for 2 hours at RT in the dark. The secondary antibody was removed and washing steps were repeated. To help remove autofluorescence, slides were blocked in Sudan Black B (0.1% in 70% ethanol) for 5 minutes then rinsed in a continuous flow of water until clear flow through. Slides were mounted onto glass coverslips (24x50 mm, thickness: 0.13-0.16 mm) using Fluoromount-G™ with DAPI (Thermo Fisher Scientific, Cat. 495952).

Table 2.9. List of primary antibody details for immunohistochemistry

Antibody	Manufacturer	Clone	Specificity	Dilution
Endomucin	Santa Cruz, Cat.	Sc-65495	Rat	1:500
Ki-67	Abcam, Cat. ab15580	Polyclonal	Rabbit	1:200

Table 2.10. List of fluorescence-conjugated secondary antibodies for immunohistochemistry

Fluorescence conjugated molecule	Manufacturer	Clone	Specificity	Dilution
Alexa 594	Invitrogen	A21209	Rat	1:1000
FITC 488	Invitrogen	A21206	Rabbit	1:1000

Slides were imaged using the Zeiss AxioImager M2 microscope (at 20X magnification). Blood-vessel density was examined by manually counting endomucin-positive vessels per mm^2 in 3 representative Regions of Interest (ROIs) per tumour section, averaged over 2 sections per tumour. Proliferation index was measured by counting Ki67-positive cells as a percentage of total cells (DAPI-positive) using ImageJ^{TM} software. Again, quantification was the average of 3 ROIs per tumour section, with 2 sections per tumour.

2.7 ASSESSING BACTERIAL EXTRACELLULAR VESICLE-HOST RESPONSES

2.7.1 MTS assay to assess cell viability

B16-F10 cells were seeded (2000 cells/100 µL per well) in a flat bottom cell-culture treated 96-well plate and incubated at 37˚C for 24 hours. After which, media was replaced with media containing 1 µL BEVs (final concentration 10^9) or 1 µL PBS and incubated at 37˚C for 24 hours. For bone marrow cells, 1 X 10^6 cells/100 µL RPMI + 1% FBS per well) were seeded in flat bottom cell-culture treated 96-well plates and BEVs (final concentration 10^9) or PBS were incubated for five hours. For bone marrow cell/tumour cell co-cultures, B16-F10 cells were seeded and incubated for 24 hours as previously described. Media was replaced and bone marrow cells +/- BEVs were added as previously described.

After which, 20 µL MTS solution was added per well and incubated for 1 hour. Absorbance (A492 nm) was measured using a microplate reader (Biotec, USA).

The average media only value was subtracted from each sample. Cell viability was presented as a percentage compared to control (PBS-treated) cells.

2.7.2 HEK-Blue™ hTLR activation assays

To assess if BEVs activated TLR-dependent NFκB, the human embryonic kidney reporter cell-lines, HEK-Blue™ hTLR2 and HEK-Blue™ hTLR4, were used. The basic principle is that cells were modified to have an inducible gene for secreted embryonic alkaline phosphatase (SEAP) production under the promoter region of the downstream targets of TLR2 and TLR4 signaling pathways, therefore SEAP production could be measured by coulorimetric assessment in the presence of detection medium. HEK-Blue hTLR2 and HEK-Blue hTLR4 (Invivogen) were cultured in RPMI1640 medium supplemented with 10% FBS (Hyclone, Thermofisher), 1% Penicillin-Streptomycin (Thermofisher), and 100 µg/mL Normocin (Invivogen) and additionally treated with 1 x HEK-Blue™ selection cocktail (Invivogen). Cells were seeded at 5×10^4 cells per well in 96-well plates containing HEK-Blue detection media along with experimental interventions that included PBS for controls, BEVs, and respective positive controls (Bacillus subtilis lipoteichoic acid (LTA-BS) for TLR2 and LPS for TLR4)) all purchased from Invivogen. After overnight incubation at 37°C, absorbance was measured at 650 nm using a microplate reader (Biotec, USA).

2.7.3 Bone marrow cell isolation

Mice were euthanised as previously described. Under sterile conditions, femoral and tibia bones were removed, and the marrow compartments were flushed with sterile PBS using a 23G needle. Cells were centrifuged (300 g, 5 minutes) and resuspended in 10 mL ice-cold sterile 0.2% NaCl for 30 seconds to lyse red blood cells. Osmotic homeostasis was restored by adding 10 mL 1.6% ice-cold NaCl. This was repeated once, and cells centrifuged as described and resuspended to give the desired concentration.

2.7.4 Bone marrow cell incubation with BEVs for cell marker expression analysis

Murine bone marrow cells isolated as previously described, were seeded at a density of $1 \times 10^6/100$ µL in a 96-well sterile, non-tissue culture treated microplate. Cells were either incubated with media supplemented with 1 µL sterile PBS (control) or BEVs (final concentration 10^9) for five hours then cellular marker expression was assessed by flow cytometry. For the assessment of extracellular

DNA release, 100 ng/mL Phorbol 12-Myristate 13-Acetate (PMA) was used as the positive control and incubated for five hours.

2.7.5 Myeloperoxidase (MPO) activity in tumours and blood

When neutrophils undergo a process known as NETosis, this releases the enzyme, MPO. To assess if BEVs induced NETosis, MPO activity was measured in tumour lysates from BEV and PBS-treated animals (experiment plan in section 2.2.9). In addition, MPO activity was assessed in 200 uL mouse blood incubated with BEVs (final concentration 10^9) for 2 hours. Myeloperoxidase (MPO) Activity Assay Kit (Colorimetric) (Abcam, cat. ab105136) was performed on both tumour lysates and blood according to manufacturer's instructions.

2.8 STATISTICAL ANALYSIS

All graphs and statistical significance analysis were generated using GraphPad Prism V10.1.1 software. Data was displayed as means ± SEM (standard error of the mean). Details of statistical tests performed are specified under each of the corresponding graphical illustrations. In general, if two independent groups with equal variance (Gaussian distribution) were compared, two-tailed unpaired student's T test was performed. If Gaussian distribution was not met, an appropriate nonparametric test such as Mann-Whitney U test was performed to determine p values between selected groups. When more than two independent groups were compared, ordinary one-way and two-way analysis of variance (ANOVA) followed by Tukey's and Dunnett's multiple comparison tests were performed to determine p values between selected groups. If Gaussian distribution was not met and there were more than two independent groups, an appropriate nonparametric test such as Kruskal-Wallis would be performed. Values were considered statistically significant if $p < 0.05$, meaning there was at least a 95% probability the results were not due to chance. Statistical significance was denoted by *$p < 0.05$, **$p < 0.01$, ***$p < 0.001$, ****$p < 0.001$. If no p value annotation was given, assume no statistically significant differences between groups.

CHAPTER THREE.

3 CHARACTERISING NOVEL STRAINS OF *BIFIDOBACTERIUM* AND ASSESSING THEIR EFFECT ON BREAST TUMOUR GROWTH.

Bifidobacterium members as previously discussed have been widely studied for their health-promoting potential (O'Callaghan and van Sinderen, 2016). Within the genus there is high genetic, and thus functional, diversity (Lugli et al., 2014). However, there are many strains yet to be discovered. Therefore, culturomics techniques were employed by our collaborators, the Hall lab (Quadram Institute Biosciences, UK/Technical University of Munich, Germany), to identify novel strains, primarily isolated from human faecal samples. Having a large 'Bifidobacteria bank' unlocks an untapped potential to investigate the use of strains to ameliorate disease progression. However, identifying ideal candidates for treatment strategies then characterising the microbial-host effects is challenging.

This chapter primarily explores the work undertaken in the Robinson lab to identify and characterise novel *Bifidobacterial* strains that are potentially suitable for breast cancer treatment strategies. The complexity of the gut microbiome and interactions with gastrointestinal lymphoid cells, combined with the added complexity of tumour-associated immune responses, suggests that *in vivo* mouse models are the most effective method for screening potential *Bifidobacterial* treatment candidates. *In vitro* systems, although having advanced since the introduction of 3D-organoid culture systems (Wang et al., 2022, Puschhof et al., 2021), cannot effectively and reliably model the spatially separated and highly complex microbiome-immune-breast tumour axis.

3.1 NOVEL STRAINS OF BIFIDOBACTERIUM SLOW BREAST TUMOUR GROWTH IN A PYMT-BO1 MOUSE MODEL IN A SPECIES-SPECIFIC MANNER

Previous data from the Robinson lab observed that breast tumour growth accelerated when mice were administered antibiotics in a PyMT-Bo1 breast cancer model (McKee et al., 2021). A proposed mechanism for the protumourigenic antibiotic response was the loss of protective microbiota rather than the introduction of a pathobiont. Subsequent research has therefore focussed on restoring gut homeostasis and assessing whether this offers any tumour protecting qualities.

Four newly discovered strains of Bifidobacterium from the species *B. bifidum* (*Bif*80), *B. animalis* (*Bif*506), *B. pseudocatenulatum* (*Bif*210) and *B. longum subsp. Longum (Bif*8809), isolated by the Hall lab, plus a mix of all four strains (*Bif* cocktail) were administered orally thrice weekly, for a total of four administrations. Experimental design and conceptualisation were created by Christopher Price (Quadram Institute Bioscience, UK) and the lab work and analysis was a collaborative endeavour.

Three out of the four strains significantly decreased breast tumour volume by over 50%. There were no significant decreases in tumour size in groups administered *Bif*8809 or the *Bif* cocktail compared to PBS (controls). One of the limitations of working with live bacteria is that bacterial cultures must be prepared immediately prior to administrations, therefore doses could only be determined retrospectively. Evaluating the doses, seen in **Figure 3.1**, *Bif*8809 had the highest CFU/mL (viable bacteria). Since *Bif*8809 had the highest viability yet lacked anti-tumourigenic activity, this may have outcompeted the other strains in the cocktail, which failed to reduce tumour volumes. *Bif*8809 had magnitudes higher viability compared to the other strains, and it is not known whether a dose this high could have offset any tumour response or even exerted adverse effects. The dose administered is not physiologically relevant and magnitudes higher used in probiotic studies. As discussed, controlling the dose due to fluctuations in the growth of live bacteria is challenging and administrations need to be optimised moving forward.

As previously highlighted, the tumour immune microenvironment is particularly important for tumour progression and the microbiome has been associated with modulating tumour immune responses. Tumour-associated lymphocyte populations were assessed by flow cytometry to help uncover the bacteria-driven mechanism. There were differences in levels of tumour infiltrating NK cells, with

*Bif*210-treated mice having significantly higher levels compared to *Bif*8809, *Bif*80 and the cocktail. NK cells can actively kill cancer cells in a non-specific innate immune way, so higher levels may offer protection. In addition, it has been previously highlighted that T cell polarisation is extremely important in the tumour microenvironment. The highest ratio of cytotoxic T cells (CD8+) compared to T helper cells (CD4+) were in tumours derived from *Bif*210-treated mice. The other strains, *Bif*80 and *Bif*506, which offered reductions in tumour volumes, did not display differences in CD8+ T cells or large increases in NK cells. This highlights that the host modulating effects are strain dependent. The anti-tumourigenic effects of Bif80 and Bif506 warrants further investigation.

To improve the reproducibility and precision of this animal experiment, multiple experiments with fewer animals, referred to as block randomisation, could have been employed. This is superior to using one experiment with more animals as there are variables such as the cage effect which could heavily influence statistical significance.

Altogether, *Bif*210 showed the greatest potential to modulate CD8+ T cell responses and increased NK cells, both have been well studied for their cancer-killing abilities. *Bif*210's CD8-driven mechanism was investigated by Christopher Price (unpublished thesis, 2024, Quadram Institute Bioscience, UK). Key findings were that *Bif*210 supplementation significantly reduced breast tumour volumes in the BRPKp110 model (supplementary Figure 9.1) which was associated with increased activity of tumour infiltrating CD8 T cells (supplementary Figure 9.2).
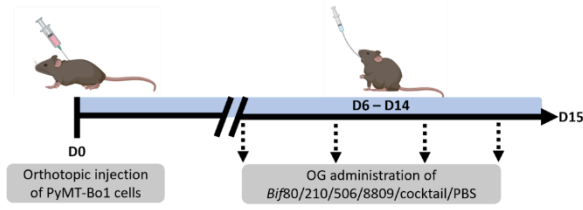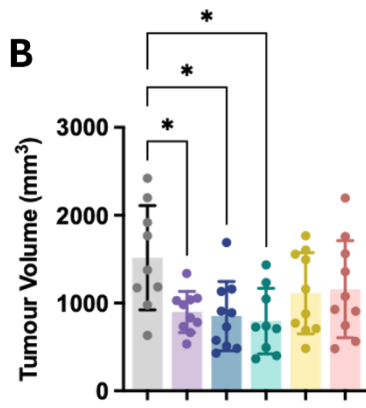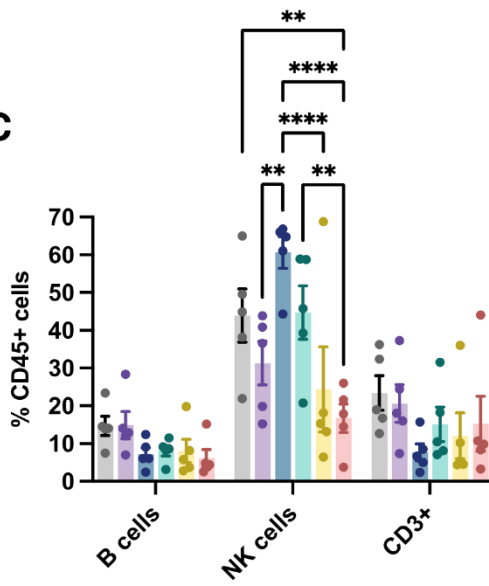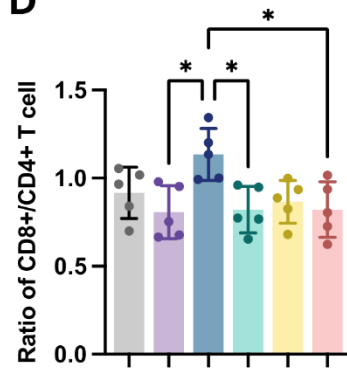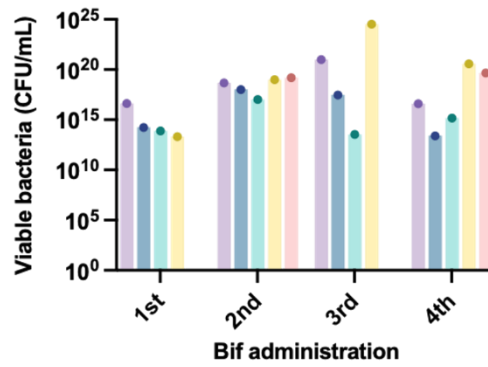
Figure 3.1 Oral administration of certain members of Bifidobacterium influences breast tumour growth in C57BL/6 mice. (A) Experimental outline of PyMT-Bo1 breast cancer model including the Bif dosing regimen. Bif oral administration began once a palpable tumour had formed (6 days post-PyMT-Bo1 orthotopic implantation) for a total of 4 administrations every 48/72 hours. (B) Data shows mean (±SEM) resected tumour volumes (day 15) from control (PBS) (n=9), Bif80 (n=10), Bif210 (n=10), Bif506 (n=9), Bif8809 (n=10), Bif cocktail (n=10) treated mice. Flow cytometric analysis of tumours (n=5 per group) targeting (C) lymphocytes (CD3+ and B cells) as a percentage of total immune cells (CD45+). (D) Ratio of CD8+ T cells over CD4+ T cells in tumour samples. (E) Levels of viable bacteria (CFU/mL) for each Bif species administered per oral gavage. Statistical significance was calculated by one-way ANOVA with Tukey's multiple comparisons. * ($p < 0.05$).

3.2 *BIF*80 AND *BIF*506 AS POTENTIAL ANTI-TUMOURIGENIC AGENTS REQUIRES FURTHER INVESTIGATION.

*Bif*80 (*B. bifidum*) and *Bif*506 (*B. animalis*) treatment showed significant reductions in PyMT-Bo1 tumour volumes compared to controls. To explore their potential therapeutic properties further, I assessed whether the strains also affected the growth of BRPKp110 HR+ luminal A-like tumours. Similarly to the previous orthoptic PyMT-Bo1 experiment, the treatments commenced once a palpable tumour formed (day 10), occurring thrice weekly. *Bif*80-treated mice had comparable tumour volumes to *Bif*506-treated. Tumours from control mice exhibited an average increase of over 200 mm³. This increase was largely attributable to two mice, each with tumours exceeding 1000 mm³. Although these differences were not statistically significant, it may be valuable to repeat *Bif*80 and *Bif*506 treatments in the BRPKp110 model to reliably conclude whether these species exerted any anti-tumorigenic effects. Luminal A-like and luminal B-like models show distinct differences in gene expression profiles as well as the tumour immune landscape. One major difference is that luminal A-like tumours have reduced expression of proliferation-related genes, making them less aggressive. Tumour volumes in **Figure 3.2** were around 350 – 600 mm³, which were considerably smaller than the PyMT-Bo1 tumours (**Figure 3.1**). It is therefore important to consider tumour stage and size when comparing treatments.

To evaluate the immune populations in luminal A-like tumours and determine whether *Bif* treatments induced any immunological changes, flow cytometry was employed. Flow cytometric analysis revealed few changes in tumour-associated myeloid cell populations between the treatment groups. However, similarly to *Bif*210, *Bif*506 showed an, albeit non-significant, increase of CD8+ cells, as well as significant increases in CD3+ cells. Expression of CD107a, a marker of cellular

degranulation and thus CD8+ and NK cell activation, was quantified. There were minimal differences observed, which may suggest that while *Bif*506 treatment increases CD8+ levels in tumours, it does not enhance CD8+ activity or function.
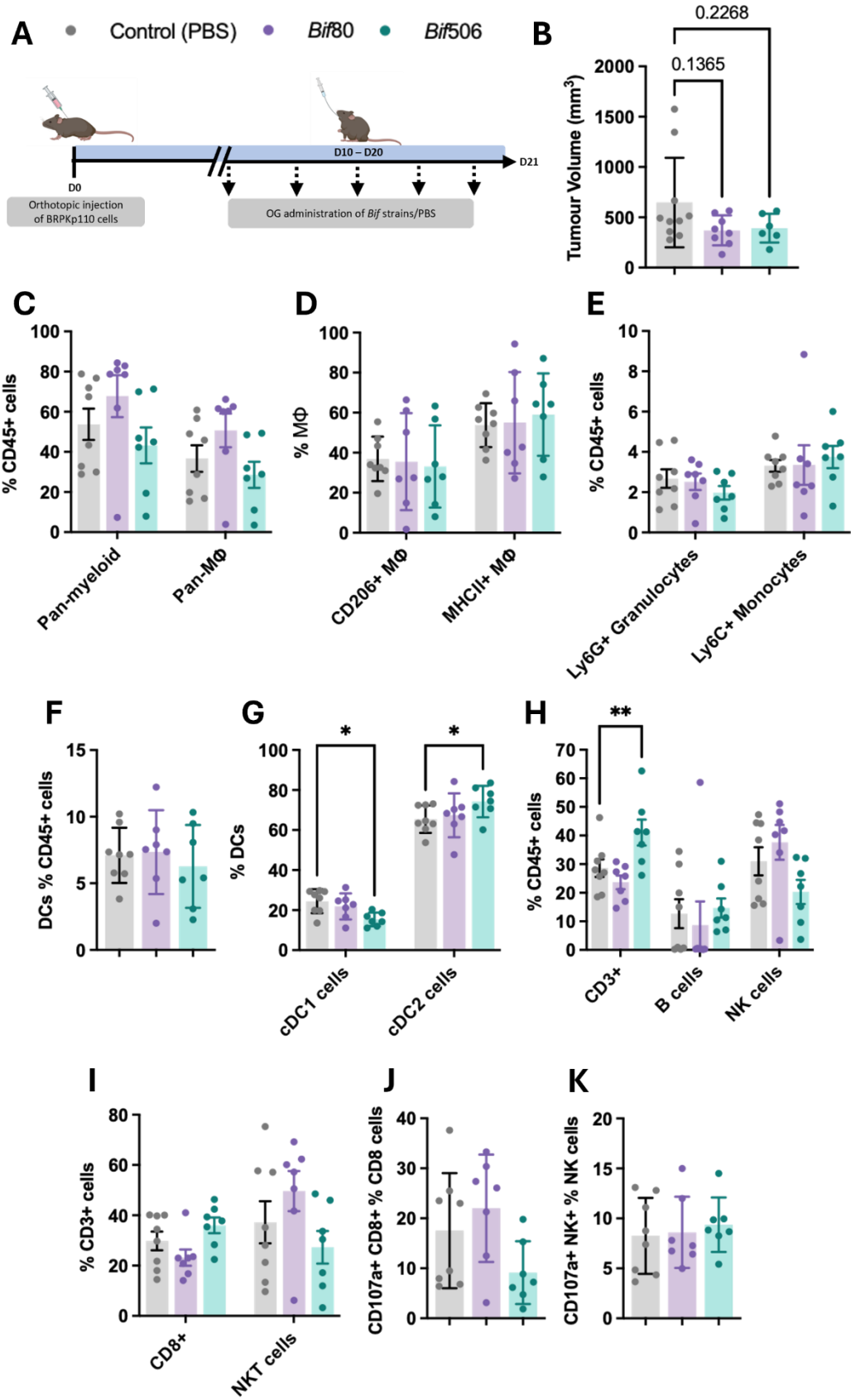
***Figure 3.2* Bif*80 and* Bif*506 oral administration does not significantly alter tumour volumes or tumour-associated immune populations in C57BL/6 mice.** *(A) Experimental outline of BRPKp110 breast cancer model including the* Bif *dosing regimen.* Bif *oral administrations began once a palpable tumour had formed (10 days post-BRPKp110 cell orthotopic implantation) for a total of 5 administrations every 48/72 hours. (B) Data shows mean (±SEM) resected BRPKp110 tumour volumes in mice orally administered PBS (n=10),* Bif*80 (n=8),* Bif*506 (n=7). Flow cytometric analysis of tumours (n=7/8 per group) assessing (C) myeloid (CD11b), macrophage (F4/80+) including (D) macrophage polarization, (E) granulocytes (Ly6G+), monocytes (Ly6C+), (F) dendritic cells (CD11c+) including (G) dendritic cell polarization, (H) lymphocytes (CD3+, B cells), NK cells including (I) CD3+ cell polarization (CD8+, NKT cells), (J+K) CD8+ and NK+ cell activation (CD107a+). Statistical significance was calculated by one-way ANOVA with Tukey's multiple comparisons. * (p < 0.05), **(p < 0.01).*

3.3 *De novo* genome assemblies and characterisation of the novel *Bifidobacterium* strains

All four *Bifidobacterial* genomes were successfully assembled as at least 80% of the genome was annotatable (Table 3.1). Bacterial genome sizes (total size of scaffolds) were estimated to be between 2.09 - 2.31 Mbp (Table 3.1), which falls within the range of other *Bifidobacterial* members (~1.9-3.2 Mbp) (Lugli et al., 2014). NG50 displayed in Table 3.1 is indicative of genome assembly quality, as it represents the length of the shortest contig which together on its' own, or with equal, or longer contigs, contains 50% of the genomic content. *Bif*210 and *Bif*80 both had very high NG50 values which provides highly accurate genome annotation and genome organisation information. LG50 is the number of contigs required to give this NG50 score. *Bif*506 genome assembly needed 8 contigs to cover 50% of the genome. Guanine + cytosine (GC) content of each bacterium is listed in Table 3.1. GC content is highly variable between bacterial genera, with *Bifidobacterium* having a relatively high percentage of genomic GC (55 to 67%) (Lee and O'Sullivan, 2010). GC content also varies between species of the same genus – as seen in Table 3.1. GC content can give an insight into evolutionary adaptation, thermal stability, chances of mutation and gene expression/amino acid composition.

Once genome assemblies are obtained, bioinformatic software can predict the function of genes. I used eggNOG-mapper v2 to functionally annotate the four novel strains of *Bifidobacteria*. Genes were then classified by function according to categories of clusters of orthologous genes (COGs) displayed in **Figure 3.3** (Tatusov et al., 2000). *Bif*80 and *Bif*8809 had higher total COGs compared to *Bif*210 and *Bif*506. All strains had a substantial portion of genes associated with metabolism, particularly categories C (Energy Production and Conversion), E (Amino Acid Metabolism and Transport), and G (Carbohydrate Transport and

Metabolism). *Bif*8809 and *Bif*210 displayed higher proportion of genes dedicated to carbohydrate transport and metabolism, for example to produce short chain fatty acids.

Cell processing and signalling functions show slight variations, with strains *Bif*80, *Bif*506 and *Bif*8809 having a higher proportion of genes involved in cell wall/membrane biogenesis (M) compared to *Bif*8809. Since all strains other than *Bif*8809 displayed anti-tumourigenic activity, the functional properties of the genes coding for cell wall/membrane biogenesis may warrant further investigation. In addition, there was a slight reduction in proportion of genes associated with signal transduction (T) in the *Bif*210 genome.

All strains show a substantial proportion of genes that are poorly characterised. Further work should therefore aim to uncover the function of these currently unknown COGs to better understand *Bifidobacterial* biological pathways.

Table 3.1. Quality assessments of the *de novo* genome assemblies of *Bif*210 (*B. pseudocatenulatum*), *Bif*80 (*B. bifidum*), *Bif*506 (*B. animalis*) and *Bif*8809 (*B. longum* subsp. longum) using the tool GenomeQC

	*Bif*210	*Bif*80	*Bif*506	*Bif*8809
Number of contigs	2	2	38	10
Total size of contigs (bp)	2312665	2152576	2094221	2329522
% of estimated genome that is useful	100.5	93.6	83.0	99.9
Longest contig (bp)	2273104	1603541	308200	1001298
Shortest contig (bp)	39561	549035	3100	179
NG50	2273104	1603541	85322	785318
LG50	1	1	8	2
%A	21.5	18.5	17.3	19.9
%C	28.2	31.7	32.7	29.9
%G	28.4	31.2	32.9	30.2
%T	22.0	18.6	17.1	20.0

A

*Bif*210

2,273,104 bp

39,561 bp

*Bif*80

1,603,541 bp

549,035 bp

*Bif*506

308,200 bp   189,670 bp

173,237 bp   138,926 bp   120,604 bp

118,795 bp   92,774 bp   85,322 bp   84,062 bp

77,198 bp   66,309 bp   59,477 bp   48,372 bp   46,450 bp

39,569 bp   39,114 bp   36,588 bp   35,666 bp   31,564 bp   30,807 bp

30,685 bp   27,692 bp   27,037 bp   24,756 bp   20,998 bp   20,794 bp   20,720 bp

19,734 bp   15,314 bp   13,515 bp   9,349 bp   8,266 bp   7,318 bp   6,735 bp   6,377 bp

5,186 bp   3,949 bp   3,100 bp

*Bif*8809

325,678 bp

185,738 bp   56 bp

1,001,298 bp   5,413 bp

55? bp

785,318 bp

2,442 bp
2061,025 bp
22,602 bp

B

Metabolism
- C - Energy Production and Conversion
- E - Amino Acid Metabolism and Transport
- F - Nucleotide Metabolism and Transport
- G - Carbohydrate Metabolism and Transport
- H - Coenzyme Transport and Metabolism
- I - Lipid Transport and Metabolism
- P - Inorganic Ion Transport and Metabolism
- Q - Secondary Metabolites Biosynthesis, Transport and Catabolism

Information Storage and Processing
- A - RNA Processing and Modification
- B - Chromatin Structure and Dynamics
- J - Translation, Ribosomal Structure and Biogenesis
- K - Transcription
- L - Replication, Recombination and Repair

Cell Processing and Signaling
- D - Cell Cycle Control and Mitosis
- M - Cell Wall/Membrane/Envelope Biogenesis
- N - Cell Motility
- O - Post-translational Modification, Protein Turnover, Chaperones
- T - Signal Transduction Mechanisms
- U - Intracellular Trafficking, Secretion and Vesicular Transport
- V - Defense Mechanisms

Poorly Characterised
- S - Function Unknown

*Bif*80 — Total = 1657 COGs

*Bif*210 — Total = 1524 COGs

*Bif*506 — Total = 1517 COGs

*Bif*8809 — Total = 1759 COGs

Figure 3.3 De novo hybrid genome assemblies and gene predictions of four newly discovered Bifidobacterium strains. (A) Graphs depicting the visualisation of the genome assemblies of B. bifidum, B. pseudocatenulatum, B. animalis, B. longum ssp. longum created using Bandage software. Each genome assembly displays the number of contigs with the number of base pairs contained in each contig. (B) De novo assembled genomes were run through eggNOG-mapper v2 software to functionally annotate the genomes. Graphs depict the gene predictions which were characterized based on Clusters of Orthologous Genes (COGs) and grouped into distinct classifications: metabolism; information, storage, and processing; cell processing and signalling; and poorly characterised groups.

3.4 Using genome assemblies to assess safety profiles of *Bifidobacterium* strains for use in clinics.

There are numerous safety concerns to consider when administering microorganisms or microbial products to humans in clinical settings, especially to cancer patients who are often immunocompromised. We must therefore acknowledge and explore these safety concerns associated with the use of *Bifidobacteria.*

One of the largest global threats is antibiotic resistance, as in 2019 it was estimated that over 4.95 million deaths were attributable to antimicrobial resistant infections globally (Walsh et al., 2023). One possible concern for probiotic use is whether the bacteria harbour antibiotic resistance genes (ARG) within their genomes. A potential threat is the transfer of ARG from probiotics to pathogens and pathobionts (potentially pathogenic bacteria), subsequently leading to infections resistant to treatment (Koutsoumanis et al., 2021). The newly discovered *Bifidobacterium* strains were screened through a database containing known ARGs; the Comprehensive Antibiotic Resistance Database (CARD) to identify ARGs in the assembled genomes, which are displayed in Table 3.2. One of a frequently exploited strains of *Bifidobacterium* in the food industry*, B.animalis subsp. lactis BB-12*, was also screened for comparison.

All *Bifidobacterium* strains contained the gene *rpoB,* which is associated with resistance to rifamycin. Mutations in *rpoB* reduces the affinity of rifamycin, commonly used to treat tuberculosis (TB), to bind to RNA polymerase and thus has reduced bacterial growth inhibitions. One of the biggest concerns to human health is promoting multidrug-resistant TB (Patel et al., 2023). However, it has been proposed that not all *rpoB* mutations lead to rifamycin resistance (Watanabe et al., 2011). The gene, *erm(X)* was identified in *Bif*210's genome, which aligns with others who identified the gene in strains of the species*, B. thermophilum* and *B. animalis* (van Hoek et al., 2008b).

It is relatively common for all bacteria to have the presence of at least one ARG. However, to fully assess the risk of transferring ARGs, *in silico* genomic evaluation needs to be combined with laboratory-based experiments. Experiments need to assess how likely it is for horizontal gene transfer across different species to occur. For example, in the food industry if a microorganism is to gain Qualified Presumption of Safety (QPS) status by the European Food Safety Authority (EFSA), the transfer of resistance needs to be unlikely (Koutsoumanis et al., 2021).

In addition, identifying minimum inhibitory concentrations (MICs), indicates how functional the ARG gene is. To assess the complete risk to the microbiome post-supplementation, the 'resistome' (number of resistance genes) can be evaluated using *in vitro* colon models and eventually human trials (Montassier et al., 2021).

Table 3.2. Antimicrobial resistance gene identification by screening genome assemblies of *Bifidobacterium* strains against CARD which uses known ARG in reference genomes. For quality control, contigs < 20,000 base pairs were excluded from analysis. Table describes AMR gene family, and the drug associated with predicted resistance as well as how closely the identified gene aligns with the reference ARG gene.

Bacterial strain	Antimicrobial resistance gene and family	Drug class	Percentage identity of matching region
*Bif*80	*vanY* - glycopeptide resistance gene cluster	glycopeptide antibiotic	50.27
	rpoB - rifamycin-resistant beta-subunit of RNA polymerase	rifamycin antibiotic	91.47
	ileS - antibiotic-resistant isoleucyl-tRNA synthetase	mupirocin-like antibiotic	99.37
*Bif*210	*erm(X)* - erm 23S ribosomal RNA methyltransferase	macrolide antibiotic, lincosamide antibiotic, streptogramin antibiotic, streptogramin A antibiotic, streptogramin B antibiotic	90.14
	rpoB – rifamycin-resistant beta-subunit of RNA polymerase	rifamycin antibiotic	98.48
*Bif*506	*rpoB* – rifamycin-resistant beta-subunit of RNA polymerase	rifamycin antibiotic	93.17
*Bif*8809	*rpoB* – rifamycin-resistant beta-subunit of RNA polymerase	rifamycin antibiotic	92.65
Bifidobacterium animalis subsp. lactis BB-12	*rpoB* - rifamycin-resistant beta-subunit of RNA polymerase	rifamycin antibiotic	92.66
	tet(W) - tetracycline-resistant ribosomal protection protein	tetracycline antibiotic	96.87

3.5 Assessing the growth kinetics of *Bif*80, *Bif*210, *Bif*506 and *Bif*8809.

When utilising microorganisms for *in vivo* applications, it is important to understand the bacterial growth kinetics so that administrations can be optimised. Growth curves (**Figure 3.4A**) of strains grown in 96-well microplates, show that exponential growth starts from around 10 hours onwards. Strains *Bif*8809 and *Bif*80 are the fastest growers, evident from the steepest gradient until the point of plateau at around 30 hours. The growth of *Bif*210 and *Bif*506 slows and reaches stationary phase at around 36/38 hours.

Small culture volumes in 96-well plates do not represent the same growth experienced in larger 50 mL vessels used to grow strains for *in vivo* administrations. Growth curves in **Figure 3.4B** show that strains potentially reach exponential phase quicker (~ 4 hours) when grown in a starting volume of 40 mL. The stationary phase is also reached quicker, from around 10-12 hours. However, the plate reader had a maximum optical density (OD) reading of 2.0, therefore the exponential/stationary phases were somewhat unknown. OD did not decrease at 48 hours, apart from strain 80 which displayed a small drop. However, OD cannot accurately represent viable bacteria as bacteria in the death phase also contribute to increased turbidity, hence high OD readings. Subsequently, viable bacteria over 48 hours were assessed by measuring colony forming units per mL of culture (CFU/mL), displayed in **Figure 3.4C**. In agreement with the growth curve in **Figure 3.4B**, the highest CFU/mL for all strains were at 10-12 hours. Decreases overtime were seen, however, viable bacteria were still detectable for all strains at around 44 and 46 hours (similar time to oral gavage preparation).
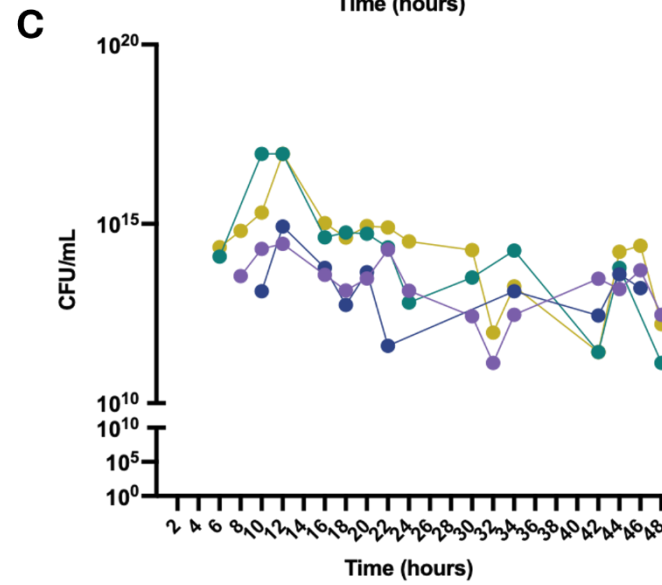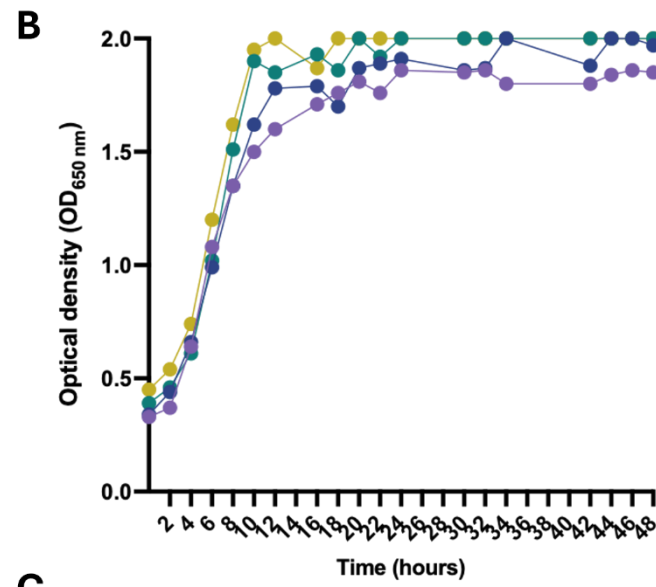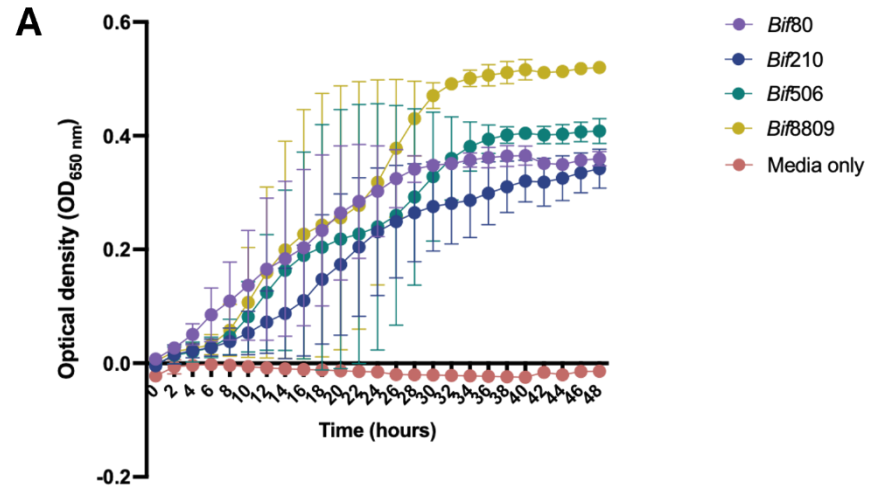
Figure 3.4 Growth curves of four newly discovered strains of Bifidobacterium. (A) Each point represents average optical densities (OD650 nm) (+/- SEM) of 100 μL of bacterial cultures (N=3) grown in 96-well microplates measured every 2 hours for 48 hours using an automatic plate reader. Media only control (red) confirmed media was free from bacterial contamination. (B) Bacterial cultures (20 mL) were grown, and 1 mL aliquots were taken for optical density (OD650 nm) measurement as well as (C) cultured on MRS-cysteine agar at 2-hour intervals where possible until 48 hours post bacterial inoculation. Colony forming units per mL (CFU/mL) represent viable Bifidobacterium and calculated based on the number of colonies counted per dilution over the volume of culture plated.

3.6 OPTIMISING *BIF*210 PREPARATION TO IMPROVE DOSE CONSISTENCY.

Due to the dose inconsistencies of *Bif* administrations throughout the PyMT-Bo1 experiment (**Figure 3.1**), coupled with the retrospective dose quantifications, I sought to optimise how I prepared *Bifidobacterium* for *in vivo* use. The probiotic industry tends to utilise lyophilised bacterial preparations therefore, I developed methods to obtain lyophilised *Bif*210 at around a 10^{10} CFU/mL dose. The dose was chosen based off the pilot data showing that these doses significantly reduced tumour volumes and is consistent with doses used in other probiotic studies.

It was important to identify a timepoint where the bacteria have high viability and stability. It is also important that the point of lyophilisation is consistent across batches to limit fluctuations in viability, as well as bacterial metabolite and product secretion.

Growth kinetic data (in **Figure 3.4**) suggested that *Bif*210's exponential growth phase was between 4 – 12 hours and the largest drop in viable bacteria (CFU/mL) was at 22 hours. Bacteria in the exponential phase experience rapid growth however when nutrients deplete and bacteria compete for nutrients/space, they enter the stationary phase. Therefore, lyophilisation preparation was chosen to begin at the start of the stationary phase as it would yield more consistent CFU's between batches compared to the exponential phase, which varies, and bacteria have less competition and stress compared to the later stationary phase.

To assess whether the growth phase timepoint affected viability during lyophilisation preparation, CFU/mL (pre- and post-lyophilisation) at 2-hour intervals throughout the growth cycle were assessed (in **Figure 3.5**). Viability of *Bif*210 post-lyophilisation did not decrease when bacteria were between 18-27 hours of growth. There was a considerable reduction in the viability of *Bif*210 post-lyophilisation when the growth cycle was at the 16-hour timepoint, likely during the exponential

growth phase. As discussed, rapidly dividing bacteria can have decreased stability. There was also a large decrease at 48 hours which was likely when the bacteria were entering the death phase and competing for nutrients and space. It was therefore decided that lyophilisation would start at around 21 – 27 hours which yielded the highest CFU/mL and showed high bacterial stability. To fully understand the growth cycle of reconstituted *Bifidobacteria,* future experiments could plot the growth curve and assess whether the bacteria are actively growing (have an exponential phase) after being reconstituted. As even though, high CFU's were obtained from reconstituted *Bif*210, the growth stage of this bacteria when inoculated in media is unknown.

An important benefit of using lyophilised bacteria is that multiple, separate experiments could utilise the same batch of lyophilised *Bifidobacteria*, maintaining consistency. I first, however, needed to confirm that viability was not impaired during long-term storage, so I conducted shelf-life testing. It was confirmed that the viability of lyophilised *Bif*210 did not decrease after short (5-days) or long (30-day) storage when sealed vials were kept at -80˚C. By eliminating exposure to moisture and storing at low temperatures, it has been shown that lyophilised bacteria can last for several years. Several factors, however, such as the bacterial strain and lyophilisation efficacy affect longevity therefore, additional testing over several months may be beneficial.

A dose response study was initially setup, however, model-specific issues occurred so tumour volumes were not possible to record. However, **Figure 3.5** shows that lyophilised *Bif*210 doses can be modified by diluting. Using the same batch of lyophilised *Bif*210, high doses (~10^{14} CFU/mL) medium doses (~10^{10} CFU/mL) and low doses (~10^{6} CFU/mL) were all prepared and had considerably less dose variability than live bacteria.
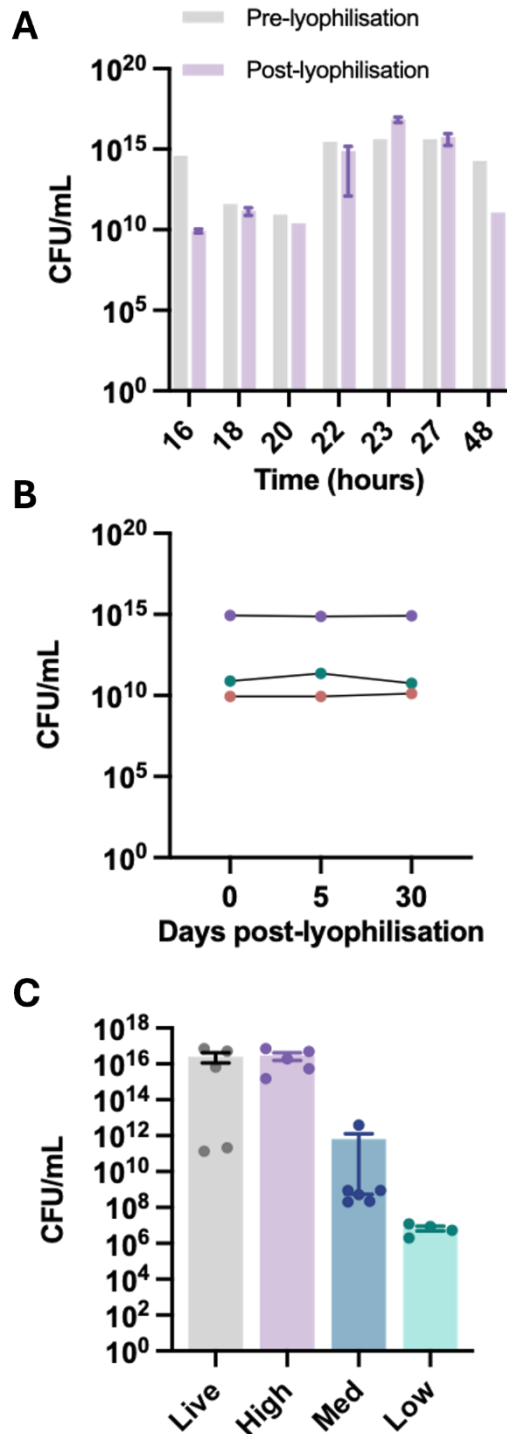
Figure 3.5. Lyophilised Bif210 as an alternative to live culture preparations. (A) Viable bacteria (CFU/mL) were quantified pre-lyophilisation (purple) and post-lyophilisation (grey) at different timepoints of Bif210's growth. Post- and pre- lyophilisation CFU/mL were compared to choose the optimum timepoint when lyophilisation would commence to maximize viable bacteria post-lyophilisation. (B) Three different batches of lyophilised Bif210 were prepared and CFU/mL were calculated from reconstituted vials at days 0, 5 and 30 post-lyophilisation to measure any loss of viability upon storage at -80˚C. (C) Bars represent average CFU/mL (+/- SEM) of a live culture or reconstituted Bif210 at different doses (high/medium/low). Graph depicts how doses of Bif210 can be altered by diluting reconstituted Bif210 (1 mL for high, 10^{-1} for medium, 10^{-2} for low). Lyophilised Bif210 doses can be determined pre-administration and have less variability than live cultures.

3.7 Bacteria including *Bif*210 are absent in mouse breast tumour tissue.

To fully understand the mechanism driving *Bif*210's anti-tumourigenic activity, I assessed whether *Bif*210 was indirectly or directly changing the tumour microbiome, or if indeed such existed. To assess the tumour microbiome, tumours derived from MMTV-PyMT+ mice were homogenised and plated on a range of selective agars. Tumours derived from MMTV-PyMT+ mice were chosen to culture over tumours from orthotopic models as although we performed the surgery as aseptically as possible, I wanted to eliminate possible external sources of contamination. In addition, the growth of MMTV-PyMT tumours better resembles human breast cancer pathology, and the longer model duration may have allowed a potential microbiome to develop.

Different bacterial species have differing nutrient and oxygen requirements, I therefore utilised a range of selective media in both aerobic and anaerobic conditions, which maximised the possibility of bacteria being cultured. For example, Columbian blood agar + 5% horse blood was used as this promotes growth of even the most demanding bacteria with complex needs. Details of the other selective medias are detailed in section 2.4.3.

Mice have 10 mammary glands in total (5 on each side) and MMTV-PyMT+ mice can develop tumours at any one of these sites. Three tumours per location (thoracic, abdominal, inguinal) were plated to assess if anatomical location could influence the presence of a tumour microbiome. Results in **Figure 3.6** show that all tumours cultured were free from microbial colonies on all selective agars cultured in both aerobic and anaerobic conditions. Swabs of mouse hair/skin were also plated to act as a positive control and confirmed nutritional quality of the selective medias, growing conditions and plating technique all could support the growth of microorganisms.

Numerous microorganisms are very difficult to culture. Non-viable/culturable bacteria could be present in the tumour microbiome, especially if mice had a leaky gastrointestinal barrier. To examine the presence of non-viable/culturable bacteria or bacterial products, I employed qPCR targeting the 16S rRNA gene on DNA isolated from the same MMTV-PyMT+ tumours I used for culturing. 16S rRNA qPCR is a very common technique to assess the total microbial load in a sample as it targets the highly conserved regions of the 16S ribosomal RNA gene present in all bacteria and archaea. Cycle threshold (CT) values were compared between

tumour DNA and control (salmon sperm which acts as a non-template control), with CT values being inversely proportional to the quantity of 16S rRNA, hence bacteria. Bacterial DNA standards, prepared using DNA isolated from *Bif*210 monocultures, and converted to copy numbers, were used to create a standard curve. As the CT values of tumour samples were too low to calculate the absolute quantification of bacterial loads using the standard curve, the standards represented positive controls. DNA extracted from tumour samples had considerably less bacteria than the lowest standard (10^2 bacterial copy numbers), displayed in **Figure 3.6**. In addition, CT values of tumour DNA samples were similar to the average control value, which further confirms MMTV-PyMT+ tumours from mice housed in our conditions are sterile.

To thoroughly investigate the presence of a tumour microbiome, I assessed whether any bacterial translocation to the tumour occurred when mice were supplemented with high doses (~10^{10} CFU/mL) of *Bif*210. qPCR targeting a *B. pseudocatenulatum* housekeeping gene (*groEL*) was performed using DNA from tumours derived from C57BL/6 mice that received *Bif*210 treatment or control (PBS). Tumours spiked with known concentrations of isolated pure *Bif*210 DNA confirmed that qPCR could detect levels of *Bif*210 as low as 0.002 ng in the presence of tumour DNA. The three tumours examined (**Figure 3.6**) had similar levels of *B. pseudocatenulatum* gene expression as tumours from control (PBS) mice and as water.

As discussed, the gut barrier functions to prevent bacteria from translocating from the lumen to the circulation. However, if the gut barrier integrity is impaired for example, from high tumour burden, disease or through ageing, bacteria are more likely to translocate. To confirm culturomics and qPCR results, I examined the gut barrier integrity of aged, non-tumour and tumour-bearing mice. The quantity of FITC-dextran detected in the serum (measured by fluorescence intensity) is proportional to the permeability of the gut. Results in **Figure 3.6** show that aged non-tumour and tumour-bearing mice had very similar intensities of fluorescence as the PBS-administered mice, which represent background fluorescence. I have therefore confirmed that mice housed in the same conditions used for our tumour experiments have very little gastrointestinal permeability. Collectively, with the tumour culturomics and qPCR results, this strongly suggests that *Bif*210 is not directly interacting with tumour, or tumour-associated, cells.
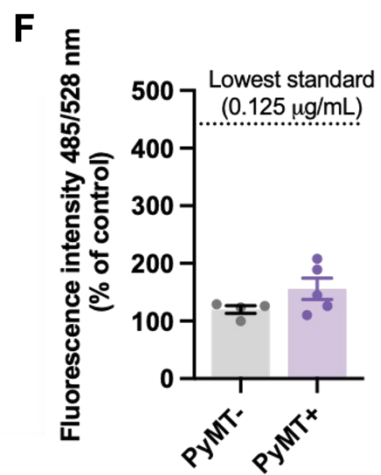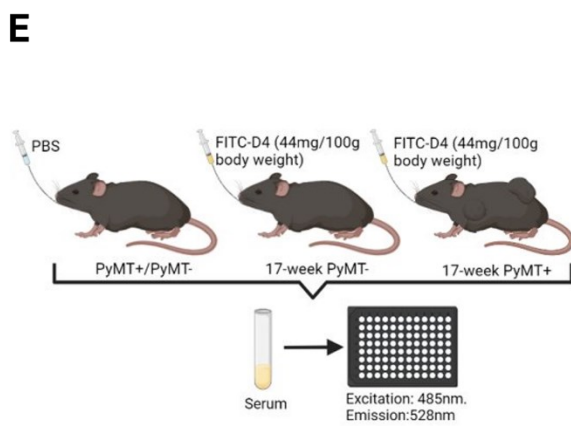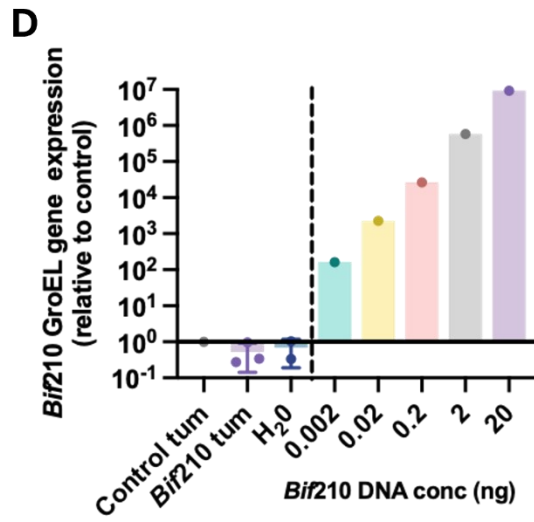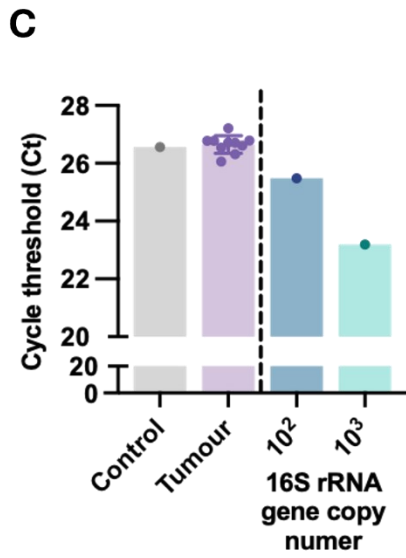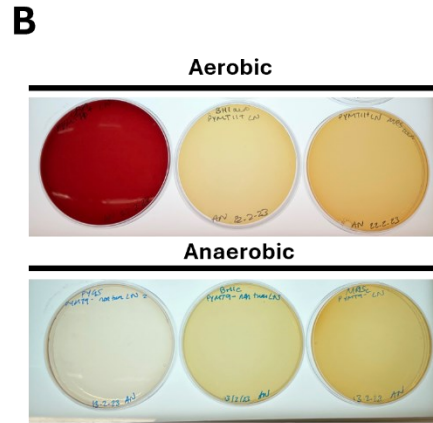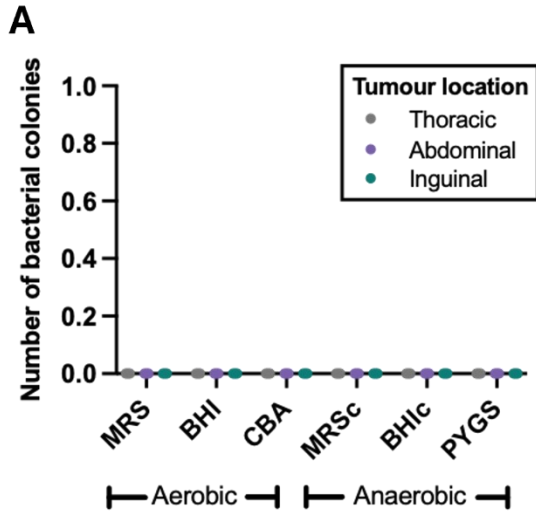
Figure 3.6. There is no evidence of a breast tumour microbiome in the breast cancer murine models tested. (A) Tumours at different anatomical sites (thoracic, abdominal, inguinal, each n=3) from MMTV-PyMT mice were extracted, homogenized in sterile conditions then cultured. (B) Example plates showing no bacterial colonies were cultured on selective agar plates (MRS, BHI, CBA, MRSc, BHIc, PYGS) in aerobic or anaerobic conditions. (C) DNA was isolated from the MMTV-PyMT+ tumours (n=10) and qPCR targeting the bacterial gene, 16S rRNA was performed. Each bar presents cycle threshold number which is inversely proportional to level of 16S rRNA gene copy number. No template control was used to detect contamination or non-specific amplification. (D) qPCR targeting B. pseudocatenulatum-specific groEL gene. Bars represent average groEL gene expression relative to tumour DNA from control (PBS-treated) mice. Bif210-treated animals were from a BRPKp110 breast cancer model and were orally administered Bif210 the night before sacrifice. Control tumuor samples were spiked with known concentrations of purified Bif210 DNA (0.002 - 20 ng). (E) Gut permeability of aged (17-week-old), tumour- (MMTV-PyMT+) and non-tumour bearing (PyMT-MMTV-) mice was assessed using FITC-Dextran. FITC-Dextran was orally administered (44 mg/ 100g body weight) and sacrificed 2 hours later. If guts were permeable, FITC would be detectable in serum. (F) Bars represent average fluorescence intensity (Ex. 485, Em. 528 nm) (+/- SEM) of serum collected from MMTV-PyMT- (n=4) and MMTV-PyMT+ (n=5) mice treated with FITC/dextran expressed as a percentage compared to mice orally administered PBS. Fluorescence intensity of serum samples was below the lowest standard (0.125 ug/mL) indicating mice had a strong barrier integrity.

3.8 Mouse gut metabolome mostly unchanged with *Bif*210 administrations.

As previously highlighted, one of the main functions of the gut microbiome is to metabolise complex carbohydrates and other dietary components. These subsequent metabolites have many physiological functions such as energy release, nutrient absorption, and immunomodulation, all of which play an important role in the context of cancer. To assess if the metabolome of tumour-burdened mice treated with *Bif*210 was distinctly different from PBS-treated mice, caecal metabolites were assessed by ^{1}H NMR spectroscopy. Dr Trey Koev (of University of East Anglia, UK) aided with the running of samples and training in NMR analysis was obtained from Dr Gwenaelle Le Gall (of University of East Anglia, UK).

Principle component analysis (PCA) (displayed in **Figure 3.7**) shows little separation between the two groups along PCA1 (x axis). PCA1 accounts for the majority (25.4%) of the variance, this therefore suggests the metabolome of the two groups is similar. However, there is some separation along PCA2. The PCA plot also shows that *Bif*210 caecal samples did not cluster as tightly together as the control caecum, suggesting there was higher variation within the *Bif*210 group.

A non-parametric T test with a corrected FDR (q<0.05) found no significant differences in metabolite concentrations between the two groups. However,

general trends in metabolite concentrations are observed in the heatmap which displays the top 30 most differentially significant metabolites (**Figure 3.7B**).

Cluster analysis confirms metabolomes within each treatment group are most similar. Of note the short chain fatty acid, propionate, was on average more abundant in *Bif*210-treated caecum. *Bifidobacterium* strains have been shown to produce SCFAs through fermentation of carbohydrates, however levels and compositions of SCFAs is strain specific. Other than propionate, no other SCFAs were noticeably increased in *Bif*-treated mice. Propionate has been shown to modulate immune responses in the gut leading to systemic immunomodulation. One study found that the sodium salt of propionate inhibited JAK2/STAT-3 signalling and increased intracellular ROS, leading to cell cycle arrest and apoptosis in both ER-negative, HER2-expressing (JIMT-1) and ER-positive (MCF7) cells (Park et al., 2021). In addition, myo-inositol, a dietary metabolite derived from the gut microbiota but is also synthesised from glucose in the body, was more abundant in *Bif*210 caeca. Myo-inositol has been found to have anti-inflammatory effects and potentially anti-cancer properties by inhibiting cell proliferation through cell cycle arrest (Bizzarri et al., 2016)

Anti-tumour activity of *Bif*210 could also be driven by a collective decrease in the proportion of certain metabolites. Metabolites such as choline, betaine and trehalose were more abundant in control caeca and there has been contradictory research showing these compounds to be associated with both cancer progression, as well as cancer inhibition (Grinde et al., 2014, Sun et al., 2016, Wu et al., 2022, Xu et al., 2009).

Even though there was no statistical increase or decrease in specific metabolites, the anti-tumourigenic properties of *Bif*210 could still be through shaping metabolites as a collective and subsequently alter complex interactions with immune cells, microbial composition and gut epithelial cells. Also, the sample size in the control group was small (n=5) which may have led to unreliable statistical significance.

Metabolite profiling displays a snapshot in time. Caecal samples were collected 24 hours post the final *Bif*210 administration, therefore metabolites measured at additional timepoints are likely to differ depending on *Bif*210's colonisation time.
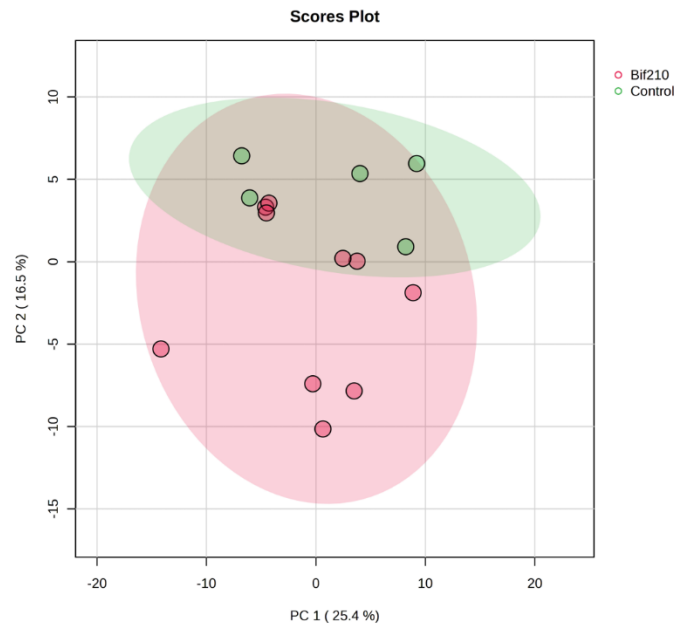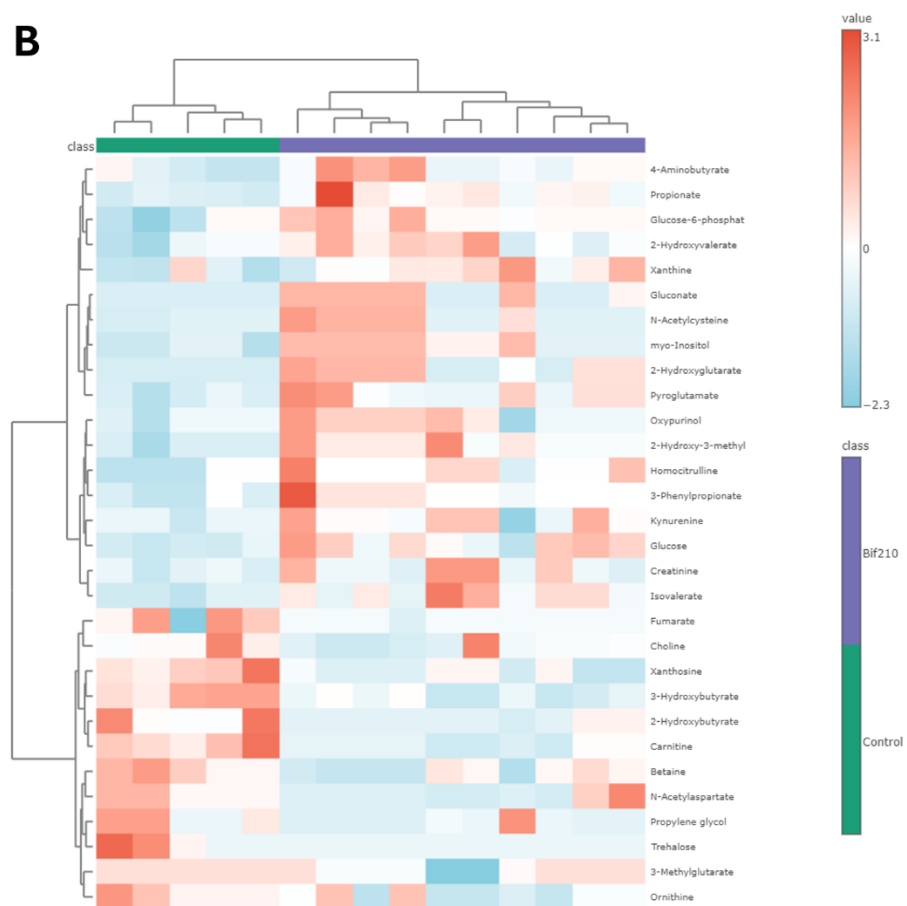
Figure 3.7 Small amount of variability of caecal metabolites between control and Bif210 treated mice, however no significantly different metabolite abundances. Mice were orally administered PBS (control) or Bif210 for the duration of the BRPKp110 model (total of five treatments total). Caecal metabolites were analysed by ^{1}H NMR. (A) Principal component analysis (PCoA) plot displays the variability between metabolic profiles in control (green) and Bif210 (red) treated mice. Distinct clustering within each group is observed. (B) Heatmap and cluster analysis of T-test (Wilcoxon rank-sum test) of the top 30 differentially abundant metabolites in caecum samples from control and Bif210-treated mice.

3.9 *Bif*210 ELICITS FEW CHANGES TO THE MOUSE GUT METAGENOME

To assess whether *Bif*210 modulated the murine gut microbial composition, caecal DNA from tumour-bearing mice treated with PBS (control), *Bif*210 or *Bif*8809 were analysed by shotgun metagenomic sequencing. Combining metagenomic data with metabolomic data generates a more detailed view of the functional properties of a microbiome. Caecal DNA was outsourced for shotgun metagenomic sequencing and Dr Raymond Kui (Quadram Institute Bioscience, UK) processed raw reads (FATQ files), performing taxonomic profiling as discussed in section 2.4.6. The processed data was subsequently presented and interpreted by me with the aid of MicrobiomeAnalyst v2.0.

Shotgun sequencing results revealed that very little *Bifidobacterium* were detected in all caecal samples, including *Bif*-treated mice. *Bifidobacterium* was not present in the top 30 most abundant genus displayed in **Figure 3.8A**. It has previously been reported that C57BL/6 mice have very low/undetectable levels of endogenous *Bifidobacterium*, however, *Bif*210 nor *Bif*8809 administrations did not greatly increase levels. It should be noted that caecal samples were collected 24 hours post the final *Bif*210 administration, which may exceed the colonisation time of *Bifidobacterium*. *Bif*210/8809 may have also died before reaching the caecum. I assessed the viability (CFU/mL) of the bacterial culture and confirmed that *Bif*210/8809 were viable at the time of administrations.

The relative abundance of different microbial genera across control, *Bif*210, and *Bif*8809 caeca in **Figure 3.8** shows there is not a single genus that greatly dominates. Slakia are amongst the highest abundance in control and *Bif*210 groups. Overall, the microbial community composition between *Bif*210 and control appears somewhat similar. Staphylococcus appears to be more abundant in a few *Bif*210/8809 samples compared to controls. Overall, there are no striking differences in bacterial relative abundance at the genus level in *Bif*210 caecum compared to the two groups (control and *Bif*8809) that did not reduce tumour

volume. In addition, relative abundance at the species-level (supplementary figure 9.4) also appeared relatively unchanged in *Bif*-treated groups compared to controls.

In addition, the alpha diversity (Shannon index) in **Figure 3.8B** of the microbial species is highest in the *Bif*8809 group and lowest in the *Bif*210 group. However, there is no significant differences between groups. It has been suggested that increased alpha diversity is linked to health-promoting effects.

The beta diversity (Bray Curtis) presented in a PCoA (Principal Coordinates Analysis) plot (**Figure 3.8C**) describes if differences in microbial community composition exists between samples/groups. The microbial communities in all groups appear not to be distinct, as there is no clear separation observed in the PCoA plot (**Figure 3.8C**). There was little variation within groups too, as samples within the same group clustered closely together, especially within the control group. The PCoA plot captured 64.5% of the total variation (PCo1 = 43% and PCo2 = 21.5%). This means that samples displaying higher separation on PCo1 have higher variation. It may therefore be interpreted that samples in *Bif*210 group had the most separation from *Bif*8809, although ellipses overlap indicating there is still little variation.

A
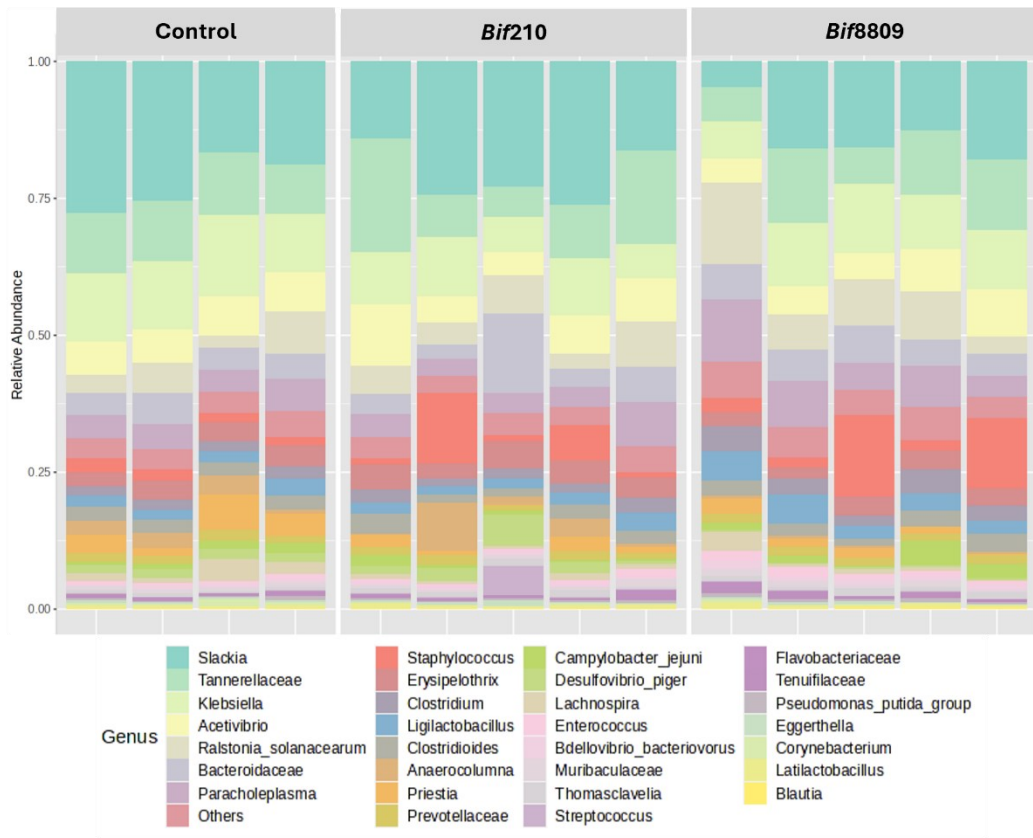
B
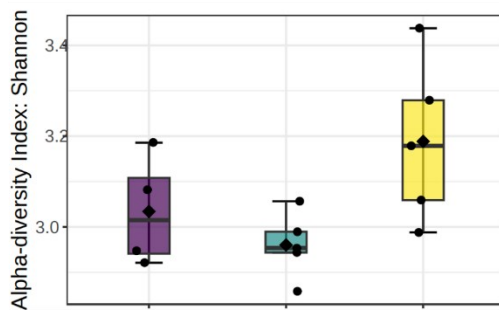
C
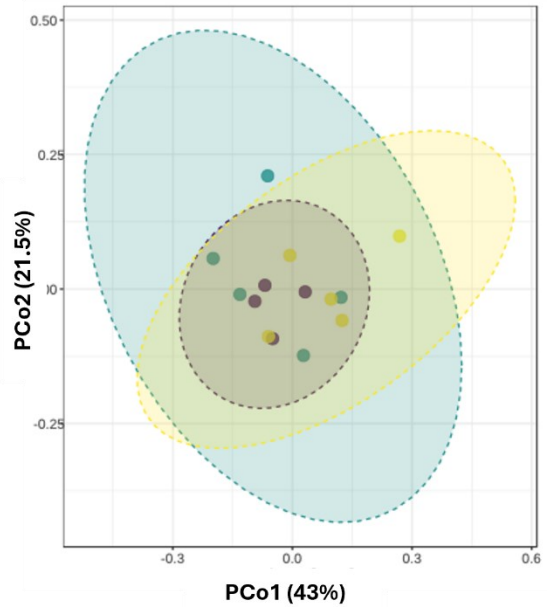
Figure 3.8 No obvious differences in commensal gut microbiota in Bif-treated compared to control PBS-treated tumour-bearing mice. (A) Stacked bar chart of the relative abundance of the top 30 most prevalent bacterial genus present in caecal samples from control (n=4), Bif210 (n=5) and Bif8809 (n=5) supplemented mice. (B) Box plot showing the alpha diversity (Shannon index) of microbial species in caecum samples from control, Bif210 and Bif8809 mice. (C) Principal component analysis plot (PCoA) showing the beta diversity (Bray Curtis index) of microbial species between control, Bif210 and Bif8809 caecal samples.

3.10 THE COLONISATION OF *BIF*210 IN THE MOUSE GUT IS TRANSIENT AND SHORT-LIVED.

Because the metagenomic sequencing results showed low relative abundance of *Bif* in caecal samples, I investigated the colonisation efficacy of *Bif*210 in the murine gastrointestinal tract. A housekeeping gene specific to the species, *B. pseudocatenulatum*, *groEL*, was used to target *Bif*210 for quantitative PCR. The *groEL* gene can be used to discriminate between different species of *Bifidobacterium*, unlike the universal bacterium gene, 16S rRNA, which shares high similarity between *Bif* species (Junick and Blaut, 2012).

I monitored levels of *Bif*210 in faeces every 2 hours post-*Bif*210 oral administration for the first 8 hours, then at 24- and 48-hours. To examine if long-term administration increased the colonisation efficacy of *Bif*210, the experiment was repeated using the same mice after a total of five administrations. Five administrations represented the typical dosing routine in the BRPKp110 model. Results in **Figure 3.9A** showed that *Bif*210 levels in faeces peaked at 4-6 hours, consistent with the gastrointestinal transit time of a C57BL/6 mouse (Padmanabhan et al., 2013). *Bif*210 levels at 24 hours was relatively higher compared to pre-*Bif* administration, however little differences were seen at 48 hours. Of note, absolute levels of *Bif*210 were not measured, therefore the quantity of *Bif* in faeces after 24 hours was unknown. Relative levels of *Bif*210 did not differ after long-term administration at any measured time-point.

DNA was isolated from faeces, however the region where *Bif*210 may colonise is unknown. By identifying the region of the GIT where *Bif*210 persists the longest, metabolites and host immune responses in this area can be effectively assessed. qPCR results in **Figure 3.9D** indicate that *Bif*210 levels in the caeca are comparable to those in the large intestines. Minimal *Bif*210 was observed in the small intestines, one sample at 24 hours exhibited higher levels which could have been a result of caecal contents spill-over. Examining immune responses should therefore focus on mesenteric lymph nodes in the large intestine. I have also

provided evidence that measuring caecal metabolites (section 3.8) was an appropriate site to assess *Bif*-induced metabolic effects.

qPCR identified *Bif*210 at 24 hours post-administration. However, it was unclear whether the bacteria were viable, as qPCR detects both live and dead bacteria, as well as bacterial products and fragments. To identify levels of viable bacteria post-administration, I utilised a germ-free mouse model, which was generated and maintained in sterile housing. To confirm sterility, I plated skin/intestinal swabs on selective agar seen in **Figure 3.9G**. SPF mice could not be used as these harbour numerous other bacterial species that grow on the selective agar, MRS. Sections of the gastrointestinal tract were cultured at 6 hours, when *Bif*210 groEL gene expression in faeces peaked, in addition to 24- and at 48-hours. Contrary to qPCR results, GF mice had no detectable *Bif*210 colonies from 24 hours onwards. The highest levels of *Bif*210 at 6 hours were in the large intestine, possibly due to *Bif*210 still being transported out of the body. However, even the highest levels were magnitudes lower compared to the dose administered (6.03^{10} CFU/mL).

From these results, it may be concluded that survival of *Bif*210 is poor. In addition, *Bif*210 does not appear to colonise the mouse intestinal tract, potentially exerting a transient effect instead.
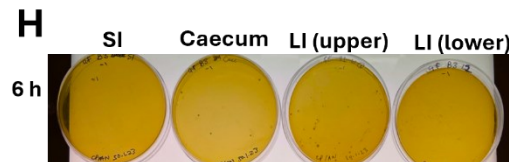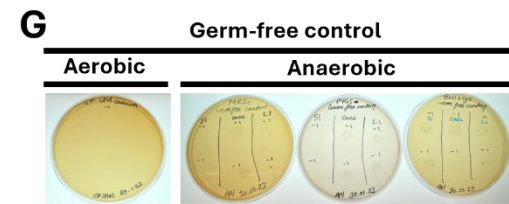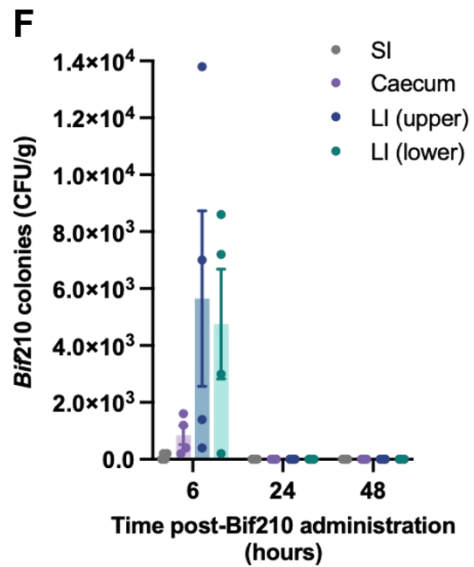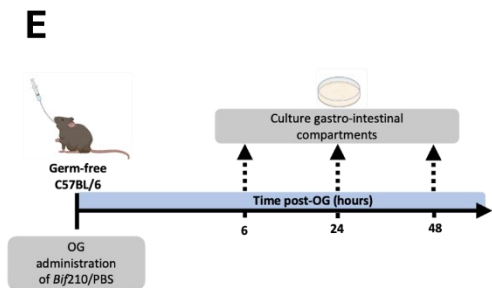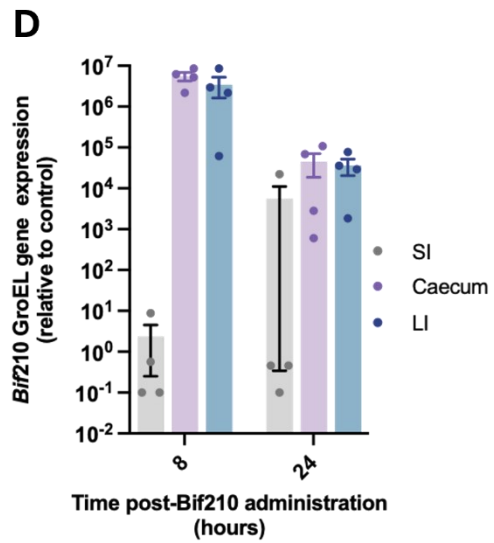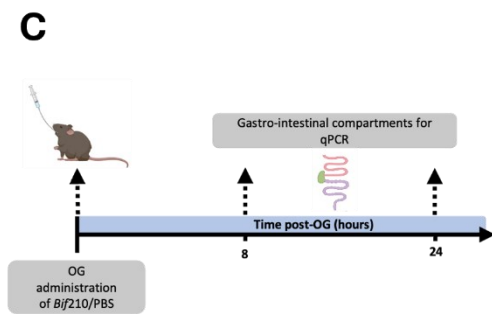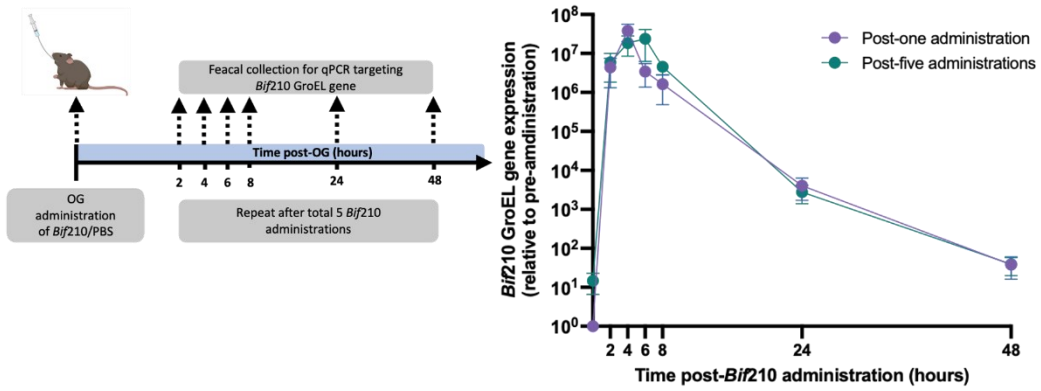
Figure 3.9. Persistence of *Bif*210 within the murine gastrointestinal tract is transient. To track *Bif*210 levels in faeces, mice (n=5) were administered *Bif*210, and faeces were collected every 2 hours until 8 hours then at 24- and 48-hour timepoints for subsequent DNA extraction. To examine long-term *Bif*210 administration, faecal collection was repeated after a total of 5 *Bif*210 administrations with (A) experimental outline detailed. (B) Normalised faecal DNA was prepared for SYBR Green qPCR targeting *B. pseudocatenulatum* housekeeping (*groEL*) gene. Graph represents relative expression of *groEL* gene relative to control faecal sample that was collected from the same mice prior to *Bif*210 administrations. Relative quantification was calculated using cycle threshold (CT) values. (C) To examine the location of *Bif*210 colonisation, qPCR targeting *B. pseudocatenulatum groEL* gene was repeated using normalised DNA isolated from small intestinal, caecal and large intestinal contents. (D) Bar graph represents relative expression of *groEL* gene in intestinal contents (n=4) at 8 and 24 hours post *Bif*210 administration relative to control (non-*Bif*210-treated faecal sample). Samples were run in duplicates and CT values averaged. Relative quantification was calculated using CT values. (E) Experimental outline for germ-free (GF) experiment that involved orally administering Bif210 (n=4) then plating small intestinal, caecal, upper/lower large intestinal contents of (H) MRS-cysteine agar plates. (G) Intestinal contents from control mouse (administered sterile PBS) were plated on MRS and grown aerobically or MRS-cysteine, PYGS, BHI-cysteine and grown anaerobically to confirm sterility of GF mice. (F) Bar graph representing number of colony forming units (CFU) per gram (g) of intestinal contents at 6-, 24- and 48-hour timepoints.

3.11 ANTI-TUMOURIGENIC ACTIVITY OF *BIF*210 IS NOT DEPENDENT ON ITS VIABILITY OR ADMINISTRATION FREQUENCY.

I have shown that the colonisation of *Bif*210 is short-lived and immuno-modulation may therefore be transient. For this reason, I tested different dose regimens of *Bif*210 to find the optimum administration frequency. Conventionally, administrations were every 48-72 hours but as *Bif*210 does not survive for 24 hours in the GI tract, everyday administrations were tested. To stay within the HMO project license protocol (PP8873233), administrations were not allowed to exceed this. In addition, as levels of viable *Bif*210 cultured from germ-free intestines was considerably less than the dose administered, it was hypothesised that non-viable bacteria may offer anti-tumourigenic properties.

To conserve *Bif*210's structure, hence PAMPs which may be interacting with immune cell receptors, bacteria were killed with peracetic acid (section 2.3.3). Other techniques to kill bacteria include high pressures and temperatures that in turn denature proteins and modify sugar composition. We proposed structure alterations may inhibit immune cell interactions/receptor binding. Successful bacterial death was confirmed by plating on nutrient agar, which yielded no colonies.

Tumour burden was significantly decreased in all *Bif*-treated groups compared to controls from day 13 (after the first *Bif* administration) up to tumour resection. Final tumour volumes in the *Bif*-treated groups were under half that of tumours in the control (PBS) group (**Figure 3.10**). No significant differences in tumour volumes were seen between the *Bif* treatments, suggesting that there were no added benefits of more frequent administrations or the use of live bacteria.

Administering non-viable bacteria for the treatment of cancer could be classed as a 'postbiotic'. New research is emerging displaying how metabolically inactive bacteria or bacterial products exert health benefits to the host, such as shaping microbiome composition (Motei et al., 2023). The acid-killed bacteria were metabolically inactive in the gut, however, metabolites produced in culture, as well as bacterial products, such as extracellular vesicles, exopolysaccharides and bacterial cells may all modulate immune responses.
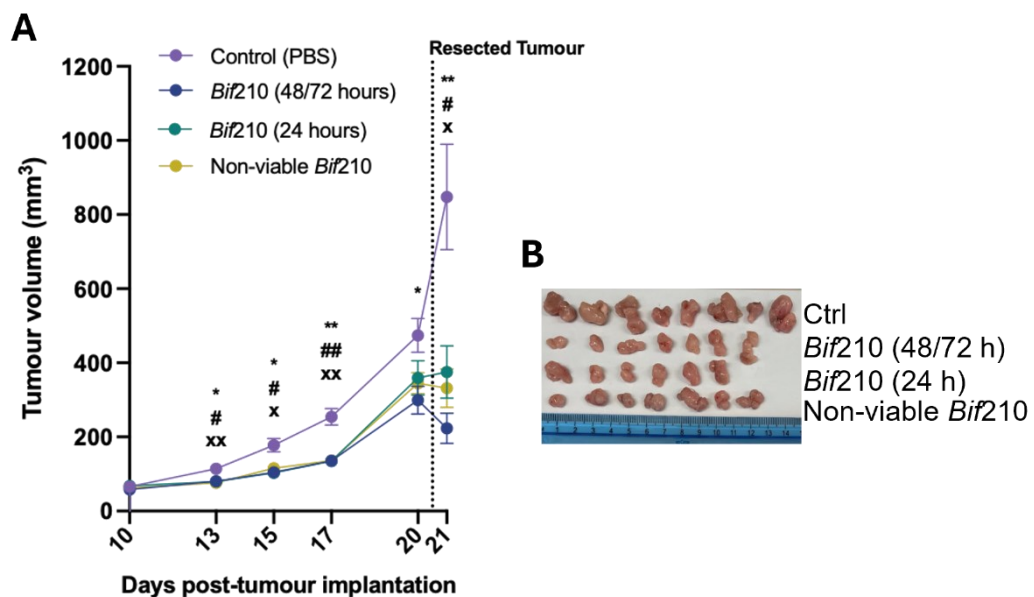
Figure 3.10. Live and non-viable *Bif*210 inhibited breast tumour growth by similar degrees. (A) Average BRPKp110 breast tumour volumes (+/- SEM) tracked from day 10 post-tumour cell implantation into the mammary fat pad. PBS (control, n=8) or *Bif*210 administrations (*Bif*210 every 48-72 hours, n=7; *Bif*210 every 24 hours, n=7; and acid-killed, non-viable *Bif*210 every 48-72 hours, n=9) commenced from day 10. Statistical significance was determined using one-way ANOVA and Tukey's multiple comparisons test. "*" denotes the difference between control (PBS) and *Bif*210 (48/72 hours). "#" denotes the difference between control (PBS) and *Bif*210 every day. "X" denotes the difference between control (PBS) and non-viable *Bif*210. */#/x $p<0.05$, **/##/xx $p<0.01$. (B) Image of representative resected tumours from each group.

3.12 DISCUSSION

Modulating the gut microbiome in cancer patients is an emerging treatment avenue that offers a relatively cost effective and safe approach. Human epidemiology data suggests microbiome influences cancer patient outcome and response to therapy (Goedert et al., 2018, Goedert et al., 2015, Jackson et al., 2018, Zhu et al., 2018). Two recent clinical trials suggested FMTs could combat anti-PD1 therapy resistance for the treatment of advanced melanoma (Baruch et al., 2021, Davar et al., 2021). In addition, animal studies have mechanistically shown the immunomodulatory properties of bacteria such as *Bifidobacteria* and their ability to prime anti-cancer responses (Sivan et al., 2015, Chen et al., 2021). Furthermore, ablating potentially beneficial microbes through antibiotic administrations was shown to accelerate breast tumour growth and ablate anti-tumourigenic immune responses in mouse models (Iida et al., 2013, McKee et al., 2021). Our work has therefore employed a targeted treatment approach to enrich the microbiome with *Bifidobacterium* to slow cancer progression.

*Bif*210, a strain of *B. pseudocatenulatum*, inhibited tumour volumes in breast cancer mouse models (**Figure 3.1** and **Figure 3.10**). Interestingly, different *Bifidobacterium* species appeared to elicit slightly altered tumour immune responses. *Bif*210 was the candidate which appeared to enhance CD8+ T cell function, a major player in anti-cancer immunity. Two other strains of the species (*B. bifidum* and *B. animalis*) also reduced PyMT-Bo1 tumour volumes however no significant decreases were seen in a BRPKp110 model. A strain of *B. longum* failed to inhibit breast cancer growth in a PyMT-Bo1 model. This highlights the need to consider strain differences in studies that analyse microbiome data. Further work is essential to uncover functional differences that exist between species/strains and characterise the induced host immune responses. It is unknown whether additional *B. pseudocatenulatum* strains exert anti-tumourigenic effects. Identifying strains that have no effect could help identify small differences within the genome responsible for altered *in vivo* responses.

*Bif*210's presence within the mouse gastrointestinal tract was transient. I also observed few metabolomic and metagenomic differences between control and *Bif*210 caeca. Taken together with the observation that acid-killed *Bif*210 elicited similar reductions in tumour volumes compared to controls as live bacteria, *Bif*210 could be offered as a postbiotic. A postbiotic is defined by the International Scientific Association of Probiotics and Prebiotics (ISAPP) as "a preparation of inanimate microorganisms and/or their components that confers a health benefit

on the host" (Salminen et al., 2021). One double-blind, placebo-controlled human study showed that 90-day supplementation with a *B. breve BB091109* postbiotic, consisting of mostly b-glucans, significantly reduced chronic inflammatory markers (IL-6, Plasma C-reactive protein, TNFα) and improved endocrine function in healthy perimenopausal women (Motei et al., 2023). Another randomised, double-blind, placebo-controlled study found that heat-killed *Bifidobacterium longum CECT 7347 (ES1)* reduced symptom severity as much as the live strain in IBS sufferers (Srivastava et al., 2024). It is unknown whether heat-killed *Bif*210 would elicit the same effects *in vivo* as acid-killed *Bif*. We chose acid killing to preserve the protein and carbohydrate structures on the bacterium's surface which may be interacting with PRR on immune cells. To examine whether the anti-tumourigenic effects of postbiotics are whole cell-dependent, future experiments could administer cell-free supernatant or heat-killed *Bif*210 to tumour-bearing mice. Results would therefore determine whether properties are due to bacterial products/metabolites or from the cells directly interacting with immune cells. One study found that cell-free supernatant from Lactobacillus fermentum significantly decreased proliferation of colorectal cancer cells in 3D culture models (Lee et al., 2020). An additional benefit of using postbiotics as an alternative to live bacteria, is that they are safer which is especially important for cancer patients who tend to suffer from immunosuppression induced by treatments such as radiotherapy and chemotherapy (Li et al., 2023).

A controversial mechanism that links altered microbiome with cancer progression is the presence of a breast tumour microbiome. There are several studies that have identified specific microbial signatures in solid breast tumours compared to non-cancerous surrounding tissue (Nejman et al., 2020, Banerjee et al., 2018). However, viable bacteria was not detected in MMTV-PyMT-derived tumours (**Figure 3.6**). Since many bacteria are difficult to culture, I also employed qPCR, which again showed no signs of bacteria or bacterial fragments. Administering *Bif*210 at doses around 10^{10} CFU/mL could have increased the likelihood of bacteria translocating into the blood then systematically to the tumour. It has recently been proposed that probiotics locally interact with the TME, exerting anti-tumourigenic effects (Bender et al., 2023). However, *Bif*210 was not detected in tumours and the gastrointestinal barrier integrity was intact in aged, tumour-bearing mice. We propose *Bif*210 modulates immune responses within the GALT which in-turn shape systemic and tumour-associated immune responses. Further work assessing interactions between *Bif*210 and gastro-associated immune cells

that modulate systemic responses is essential. Future experiments include isolating immune cells, particularly DCs, from GF and *Bif*210 gnotobiotic mouse models. Co-cultures of DCs and T cells would assess the ability of *Bif*210-primed DCs to enhance T cell effector function. Humanised GF mouse models have recently been developed and could increase the translatability to studying human host-microbiome responses. The model was developed by irradiating, immune deficient, GF mice which were transplanted human liver, thymus and bone marrow (Wahl et al., 2024). Interactions of specific microbiome members with human immune cells can therefore be studied.

A few considerations should be acknowledged before advancing to clinical trials in humans. Even though the use of postbiotics is considered safer than live microorganisms, especially in immunocompromised patients due to the low risk of active infection, the safety profile should still be assessed. An important safety consideration is the transfer of antibiotic resistance genes to potentially pathogenic members of the microbiome. *Bif*210's genome was found to contain *erm(X)* gene that is associated with resistance against macrolide, lincosamide and streptogramin (MLS) antibiotics. Previous studies found that only animal derived *Bifidobacteria* hold the erm(x) gene (van Hoek et al., 2008a), however, a recent study has identified human sources too (Luo et al., 2015). Additional work should assess the risk of *erm(x)* horizontal gene transfer from *Bif*210 to other microbial members.

An additional important consideration is the optimum *Bif*210 dose, which needs to be evaluated first in mice then humans. The dose administered to mice was around $10^{10} - 10^{11}$ CFU/mL however, a dose response study was not performed. According to EU guidelines (Directive 2001/83/EC) any product intended to prevent or treat disease requires marketing authorization. Rouanet et al. outlines the difficulties in obtaining marketing authorisation for microbiome-based therapies as assessing efficacy and safety profiles for products that do not go systemically is challenging (Rouanet et al., 2020).

For the anti-tumourigenic properties of *Bif*210 to be translatable to clinics, differences between mice and humans need to be carefully considered. An important difference between humans and mice is that humans have endogenous *Bifidobacterium* unlike SPF mice. *Bif*210's effects could be dampened by endogenous *Bifidobacterium*. Likewise, when *Bif*210 was administered with other members of *Bifidobacterium* as part of a cocktail, no reduction in tumour volume

was observed, which may be attributable to *Bif*210 being outcompeted. *Bif*210's colonization efficacy in humans may also be different compared to mice. One study orally administered *Bifidobacterium breve UCC2003* for the first 3 days then detected viable colonies in faeces, caecum and large intestine on day 31 (Fanning et al., 2012). The study used BALB-C mice, unlike C57BL/6 mice used in this study, which have slight difference in gut morphology and microbiomes (Gama et al., 2020, Guan et al., 2022). The same study found that exopolysaccharides on the *Bif*'s surface increased the bacterium's tolerance to bile, acid and facilitated the persistence within the murine intestines.

The human gut microbiome is far more complex than SPF mice. Not only do humans have much higher microbial alpha diversity, but they also exhibit longer transit times and different gastrointestinal architecture. There are also large intraspecies and interspecies variations in immune responses and metabolism. In addition, human solid tumours have high heterogeneity due to cancer cell mutations. It is therefore very common for humans to display large ranges in treatment efficacy. Results from clinical trials have shown that large proportions of breast cancer patients are non-responders to ICI therapy (Adams et al., 2019, Blomberg et al., 2023, Winer et al., 2021). Many factors, in particular the tumour immune landscape, influence whether a patient responds to ICI therapy. It is therefore paramount to consider the genetic, metabolic and immunogenic differences that exist between humans and mice. For these reasons, it is unknown whether *Bif*210 will have dramatic reductions, or any effect, in humans.

Cluster analysis of responders vs non-responders in human trials then analysing the factors that drive variability could help elucidate *Bif*210's mechanism. Predicting a patient's response to microbiome-based therapies such as *Bif*210 using artificial intelligence could also aid clinical applications. This patient-by-patient microbiome intervention would be part of the exciting push for personalised cancer treatments in clinics. Additional work could aim to characterise host immune responses to additional *Bif* strains using in silico analysis and *in vitro/ex vivo* functional immune assays. This could offer an untapped potential of *Bifidobacterial* strains to modulate immune responses in a personalised manner.

Our work highlights how a 'generally regarded as safe' microbial member modulates tumour immune responses to inhibit breast tumour growth in mice. This chapter further confirms the functional heterogeneity between members of the same genus. Further work elucidating the *Bif*210-specific mechanism as well as

identifying additional anti-tumorigenic strains are paramount. We are, however, by no means suggesting that *Bif*210 supplementation could replace existing cancer treatments, we hope it will offer a multifaceted approach; combined with pre-existing treatments.

Chapter Four.

4 Investigating the oncological treatment potential of *Bif*210: from chemoprevention to metastasis.

*Bif*210 has shown strong potential as a neoadjuvant treatment for breast cancer that may slow primary tumour growth before lumpectomy surgery. As discussed, breast cancer rates have been on the rise, therefore preventative strategies are paramount. Other than mastectomy surgeries offered to genetically predisposed, high-risk individuals, one of the major preventative strategies for breast cancer is dietary intervention. Dietary intervention modulates the gut microbiome which may attribute to lowered breast cancer risk. Taken together with *Bif*210's immunomodulatory properties, as well as research indicating the associations between the gut microbiome and breast cancer aetiology, I sought to investigate whether *Bif*210 could be utilised as a chemopreventitive agent.

In addition, breast cancer metastasis to distant organs unfortunately drives overall mortality rates and slashes the chances of cancer-free survival considerably. Despite advances of treatments that slow primary tumour progression, treatments that tackle metastasis show low response rates and overall ineffectiveness. It is important to consider key drivers of metastasis to identify potential treatments. This chapter therefore explores whether *Bif*210 could offer protection against metastasis initiation and progression. Modelling metastasis with *in vivo* models holds great challenges, and the key hallmarks involved in metastasis can easily be lost. It was vital to employ numerous murine metastasis models to represent human physiology as closely as possible.

4.1 ORTHOTOPIC TRANSPLANTATION OF BREAST TUMOURS IN MICE CANNOT MODEL CHEMOPREVENTION.

As *Bif*210 was observed to slow primary tumour growth in breast cancer murine models (BRPKp110 and PyMT-Bo1), the subsequent aim was to assess whether *Bif*210 could prevent or slow breast cancer occurrence. *Bif*210 was therefore administered before orthotopic injection of BRPKp110 cells, and the percentage of tumour-free animals were tracked over time. The first control and *Bif*210-treated mice to develop palpable tumours were 7 days post-tumour cell implantation. The majority of mice developed palpable tumours by day 8, followed by the entirety by day 9. There were no considerable differences in tumour onset time between control and *Bif*210-treated mice. It is, however, apparent that orthotopic breast cancer models cannot accurately and effectively compare chemoprevention strategies. Actively metabolising BRPKp110 cells were implanted directly into the mammary tissue therefore cellular events involved in tumour initiation and progression were lost. In addition, tumour occurrence is profoundly rapid (9 days) so treatment effects may be insufficient for observable differences. Orthotopic models are appropriate to assess whether interventions affect the tumour growth rate rather than cancer prevention.

To assess whether *Bif*210 is a suitable chemopreventative agent, a GEM model would be more appropriate. A GEM model would develop *de novo* tumours and model the multi-stage process of tumour development (Fluck and Schaffhausen, 2009). An ideal chemopreventative agent should successfully slow tumour initiation by adapting key events such as focal inflammation and basement membrane integrity (Le Magnen et al., 2016).
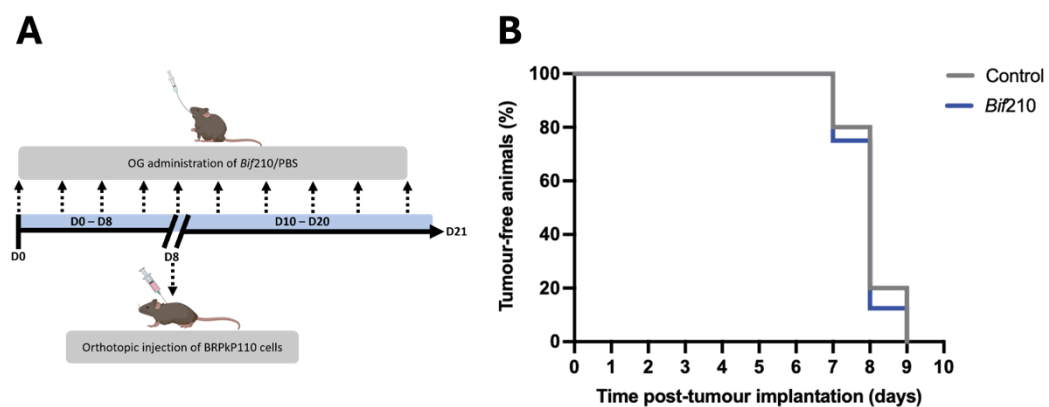
Figure 4.1 Orthotopic models could not assess *Bif*210's effects on chemoprevention. (A) Experimental design showing oral gavage (OG) of *Bif*210 occurring five times before orthotopic BRPKp110 tumour cell implantation and continued until mice were sacrificed (day 21). (B) Mice were monitored daily for palpable tumours and graph shows percentage of tumour-free animals at each day post tumour cell implantation for control PBS- (n=10) and *Bif*210-treated (n=8) mice.

4.2 UTILISING A SPONTANEOUS MURINE BREAST CANCER MODEL TO ASSESS *BIF*210'S POTENTIAL AS A CHEMOPREVENTIVE AGENT.

MMTV-PyMT+ transgenic mice have the oncogenic gene, polyoma middle T-antigen (PyMT), which mimics key signalling pathways activated by human oncogenes expressed in breast cancer patients. The PyMT gene is under control of the promoter, MMTV, which is expressed in the mouse mammary epithelium, therefore, MMTV-PyMT+ mice can spontaneously develop breast tumours in every mammary gland. MMTV-PyMT+ mice first develop hyperplastic early lesions which form into non-invasive mammary adenomas, which resembles ductal carcinoma in situ (DCIS) in humans. It progresses into early carcinoma and the tumours become invasive. Eventually, overt carcinoma occurs which features malignant tumours with high metastatic potential, favouring the lungs for metastatic lesion formation. The slow progression of overt carcinoma in mice, that molecularly and histopathologically resemble human breast cancer, make this an excellent model to study tumour initiation. I assessed whether *Bif*210 intervention could slow malignant tumour formation in MMTV-PyMT+ mice.

*Bif*210 oral administrations commenced pre-tumour initiation, when animals were aged 8-weeks as this represented adulthood in mice. There was a significant, albeit modest, delay in tumour onset time (average number of days) in *Bif*210-treated MMTV-PyMT+ mice. The first control-treated MMTV-PyMT+ mouse to develop a palpable tumour was aged 81 days, whilst it was 98 days for the first *Bif*210-treated mouse (**Figure 4.2C**). The median time for a palpable tumour to form was 116 compared to 126 days for control and *Bif*210-treated mice, respectively.

As *Bifidobacterium* species have been shown to modify metabolism and weight management, both of which are associated with breast tumour initiation, the weight of control and *Bif*210-treated mice was compared. The average weight of mice was approximately equal (22.5 g compared to 21.7 g for the *Bif*210 group, seen in **Figure 4.2B**). The weight was compared after 4-weeks of *Bif*210 administrations and before tumour initiation so that tumour weight and carcinogenesis would not be a variable between the two groups.

There was a significant decrease in the average tumour burden (cumulative volume of each tumour/s per animal) with *Bif*210 twice weekly oral administrations. Three mice in the *Bif*210 group had considerably slower rate of tumour growth compared to other mice. All mice had to be sacrificed before 25 weeks to comply with project licence protocol, therefore the full duration of the tumour growth (when tumours reached 1000 mm^3) could not be assessed in these mice. There was an increased number of control mice which exhibited higher tumour growth rate compared to *Bif*210 mice.
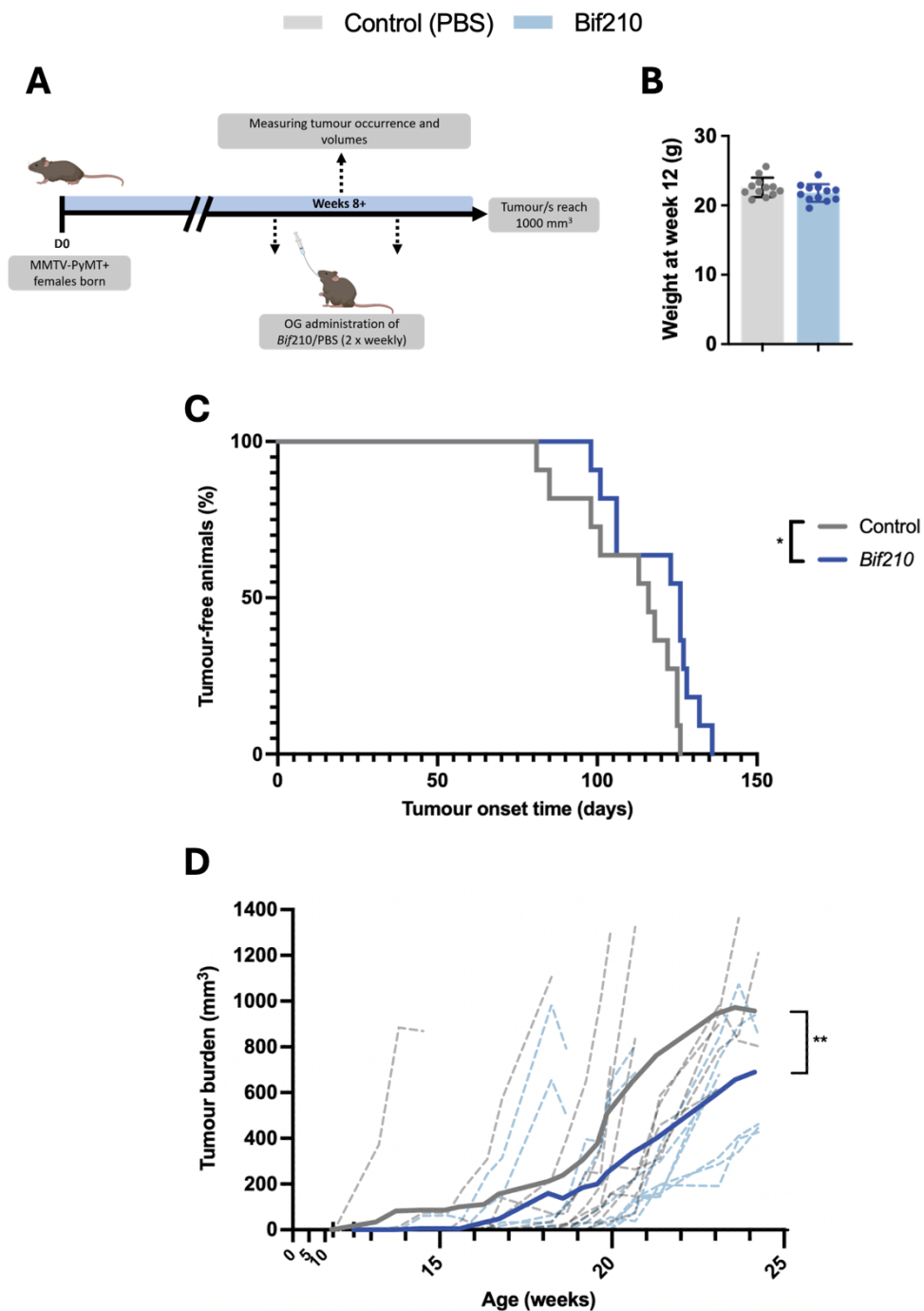
Figure 4.2 *Bif*210 acted as a chemopreventative agent and slowed breast tumour growth in a MMTV-PyMT model. (B) Experimental plan detailing that oral gavage (OG) commenced when MMTV-PyMT+ mice were 8-weeks old and continued twice weekly. Mice were sacrificed when tumour/s reached 1 cm^3. Tumour burden of each mouse was monitored twice weekly using calliper measurements. (B) Average body weights (g) of control (PBS) and *Bif*210 mice at 12-weeks old did not differ. (C) Survival plot displaying percentage of tumour-free MMTV-PyMT+ mice in control (PBS) (n=11) and *Bif*210-treated (n=11) groups plotted against time (days) for the first palpable tumour to arise. "*" Denotes statistical significance (p<0.05) from a log-rank (Mantel-Cox) test. (D) Average total tumour burden (sum of tumour volume mm^2) for (PBS) (n=11) and *Bif*210-treated (n=11) groups plotted overtime until resection. Tumour volumes were measured *in vivo* 1-2 times per week and at resection using digital callipers. Dotted lines display total tumour burden for each individual. "**" Denotes statistical significance (p<0.01) of total tumour burden at experimental endpoint from a two-tailed unpaired T test.

4.3 *Bif*210 INDUCES SYSTEMIC IMMUNOLOGICAL MEMORY BUT NOT TISSUE RESIDENT MEMORY IN ORTHOTOPIC BREAST CANCER MODELS.

Immunological memory is induced when leukocytes are exposed to antigens and subsequently undergo proliferation and polarisation, and a proportion of these activated cells differentiate into memory cells. The major purpose of memory cells is to rapidly respond upon re-exposure to the antigen. By providing immunological memory, Tmem cells are essential to prevent cancer recurrence. As discussed, effector CD8 T cells have been studied to be the major players in anti-tumourigenic immunity (Barnaba, 2022). CD8 Tmem cells are a heterogeneous population offering numerous different mechanisms of protection.

CD8 T effector memory (Tem) cells can be identified by high expression of CD44 and low expression of CD62L. Tem cells rapidly respond to tumour cell rechallenge by proliferating and differentiating into effector cells that directly kill tumour cells. There were, however, no significant differences in the Tem population (as a percentage of total CD8 T cells) in the tumour draining lymph nodes (TDLNs) and tumours from control and *Bif*210-treated mice (seen in **Figure 4.3**). Tumour-presenting DCs migrate and interact with naïve T cells in TDLNs, making it the primary site for tumour-specific T cell activation and proliferation. In addition, higher levels of memory T cells within tumours have been associated with lower risk of cancer recurrence (Barnaba, 2022). While there were no increases in Tem cells within tissues, there were significant increases in circulating Tems in *Bif*210-treated mice in both BRPKp110- and PyMT-Bo1-tumour bearing mice. *Bif*210 may therefore prime CD8 T cells to increase their differentiation to Tems, whilst

inflammatory signals within tissues override this. It is unknown how *Bif*210 may be priming these CD8 T cells, however. Further work is necessary to evaluate whether *Bif*210-primed Tems in circulation have higher cytotoxicity than Tems derived from control mice upon tumour cell rechallenge.

Central memory T cells (Tcm), defined by their expression of CD44+ and CD62L+, mostly reside in lymphoid organs as CD62L acts as a homing signal to lymph tissues. Unlike Tems, Tcms offer long-term immunological memory and hence sustained cancer protection. Upon antigen re-exposure, cells undergo high degrees of proliferation, not just immediate effector function. Tcm cell populations in the TDLNs from control- and *Bif*210-treated mice did not differ (**Figure 4.3**).

The third major memory T cell subset that I assessed were tissue-resident memory T cells (Trm). Trm cells reside in peripheral tissues, for example the tumour. They provide long-term, tissue-specific immunological memory and tailor effector responses accordingly. Enhancing Trm populations within tumours and TDLNs could therefore offer protection against primary tumour recurrence. I however, observed no significant differences in Trm levels in TDLN and tumours from control- and *Bif*210-treated mice. *Bif*210 may therefore offer systemic immunological memory without affecting tissue-resident immunological memory responses.
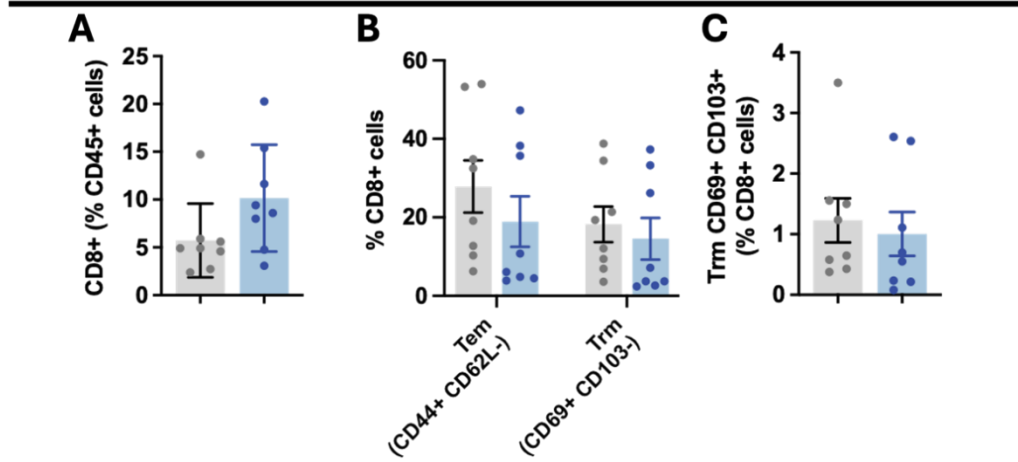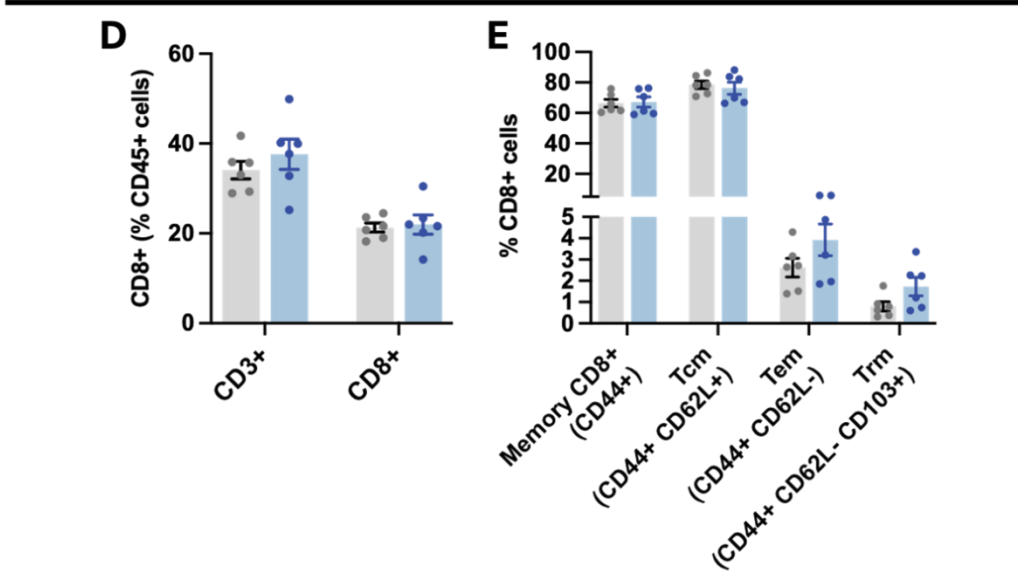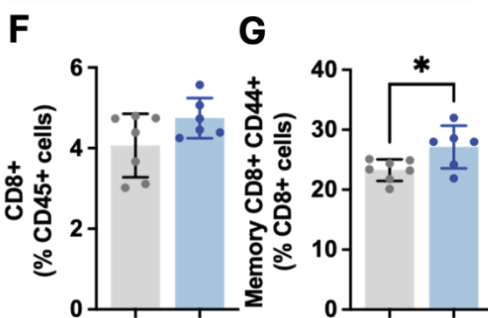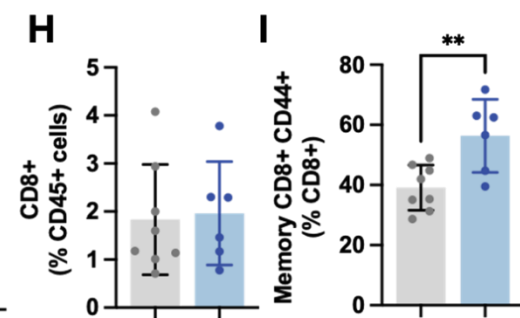
Figure 4.3 Assessing tumour resident and systemic immunological memory with *Bif*210 treatment. Flow cytometric analysis of CD8 T cell infiltration as a percentage of total immune (CD45+) cells in (A) BRPKp110 tumour, (B) BRPKp110 tumour draining lymph node (TDLN) and blood from (F) PyMT-Bo1 and (H) BRPKp110 tumour-bearing mice. Flow cytometric analysis of the polarisation of different subsets of memory CD8 T cells including central memory (Trm), effector memory (Tem) and tissue-resident memory (Trm) as a percentage of total CD8 T cells in (B-C) BRPKp110 tumour, (E) BRPKp110 tumour draining lymph node (TDLN) and blood from (G) PyMT-Bo1 and (I) BRPKp110 bearing mice. Two-tailed unpaired T tests were performed, and statistical significance is denoted by ** (p<0.05), ** (p<0.01).

4.4 OPTIMISING MURINE BREAST CANCER METASTASIS MODELS.

Breast cancer subtypes and murine cell-lines have differing metastatic potentials. It was important to identify the orthotopic breast cancer model most likely to metastasise. Consequently, the overarching aim was to develop a resection model whereby tumours are resected post-tumour cell extravasation, allowing for the assessment of *Bif*210 treatment effects on metastatic burden. Circulating tumour cells (CTCs) in the blood were compared in a LumA+ BRPKp110 and LumB+ PyMT-Bo1 orthotopic model with/without *Bif*210 treatment. To aid CTC identification and quantification, BRPKp110 and PyMT-Bo1 cells were tagged with GFP and GFP and luciferase, respectively. Flow cytometry was used for the identification of non-immune (CD45-) tagged cells, which were classified as CTCs.

Fewer than 0.1% of non-immune cells were GFP+ and hence CTCs in the blood from BRPKp110-tumour bearing mice. Whereas up to 0.47% of CTCs (GFP+Luc+ non-immune cells) were identified in the PyMT-Bo1 model. In both models, there were no significant differences in CTCs between the control and *Bif*210-treated mice. The absence of a non-tumour bearing control used for comparison means that it cannot conclusively be confirmed that GFP+ non-immune cells are in fact CTCs in these tumour-bearing samples. There were low levels of false positive CTCs in the non-tumour bearing control of the PyMT-Bo1 model. All PyMT-Bo1-tumour bearing mice, but one in the *Bif*210 group, had considerably higher proportion of GFP+Luc+ non-immune cells than the non-tumour bearing control, hence most likely exhibited tumour cell extravasation.

Metastasis was further confirmed in the PyMT-Bo1 model as tumour cells were identified in the lungs (seen in **Figure 4.4E**), which are the first site of metastatic lesion growth. However, approximately 2 out of 7 lungs in the control group and 3 out of 9 lungs in the *Bif*210-treated group had similar levels of Luc+GFP+ cells as the non-tumour-bearing lungs. Again, no significant differences were witnessed between treatment groups. Tumour cell identification could be optimised in future

experiments by incorporating a CD45 cell depletion step pre-antibody staining to enrich the non-immune, hence the tumour cell, population.

Due to increased levels of circulating tumour cells in the PyMT-Bo1 model, these cells were used in further experiments to model metastasis. The low metastatic burden presented by mice in the orthotopic model also highlights the necessity to model metastasis in additional *in vivo* models to fully investigate whether *Bif*210 offers any protection.
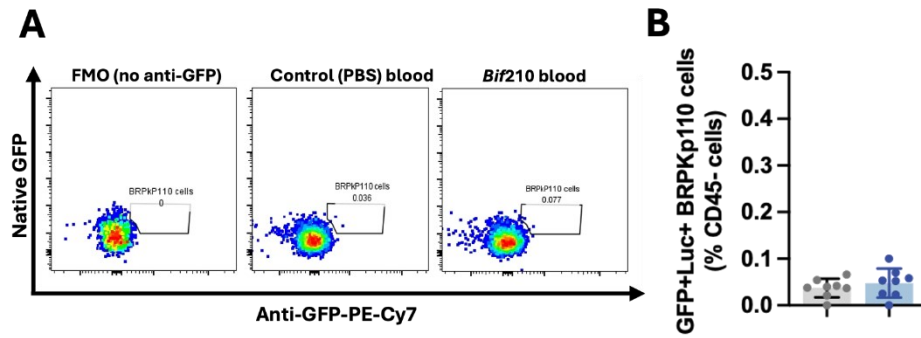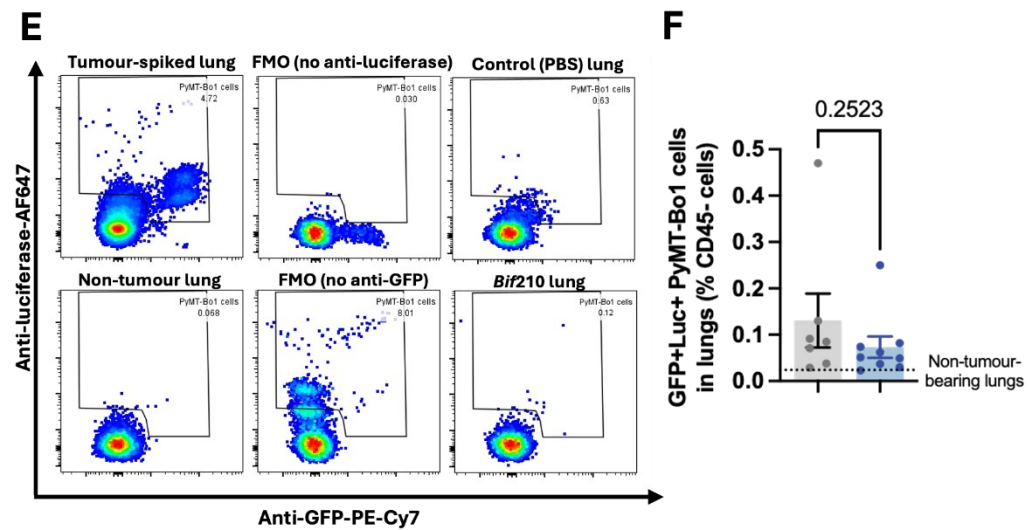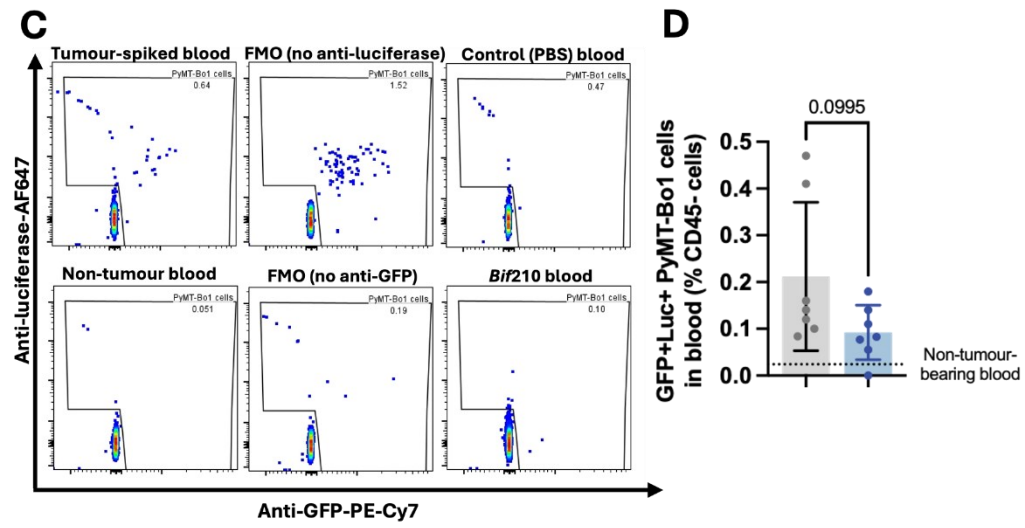
Figure 4.4 PyMT-Bo1 tumour model shows higher metastatic potential than BRPKp110 model. (A) Dot plot of flow cytometric analysis to identify circulating tumour cells in blood derived from BRPKp110 tumour bearing mice. Fluorescence minus one (FMO) blood sample stained in the absence of anti-GFP-PE-Cy7 aided the gating of GFP+BRPKp110 cells. (B) Bar graph enumerating percentage of BRPKp110 cells (positive for GFP-PE-Cy7) of total non-immune cells (CD45-negative) in the blood from control (PBS-treated) (n=8) and *Bif*210-treated (n=8) mice. Dot plot of flow cytometric analysis to identify (C) circulating tumour cells in blood and in (E) lungs derived from PyMT-Bo1 tumour-bearing mice. Blood and lung FMOs stained in the absence of anti-GFP-PE-Cy7 and anti-luciferase-AF647 aided the gating of GFP+Luc+PyMT-Bo1 cells. Tumour cell spiked blood and lung samples acted as positive controls. Blood and lungs from non-tumour bearing mice also aided gating. Bar graph enumerating percentage of PyMT-Bo1 cells (positive for GFP-PE-Cy7 and luciferase-AF647) of total non-immune cells (CD45-negative) in the blood from control (PBS-treated) (n=7) and *Bif*210-treated (n=7) mice. (F) Bar graph enumerating percentage of PyMT-Bo1 cells (positive for GFP-PE-Cy7 and luciferase-AF647) of total non-immune cells (CD45-negative) in the lungs from control (PBS-treated) (n=7) and *Bif*210-treated (n=9) mice. Statistical significance was determined by two-tailed unpaired student's T test

4.5 *Bif*210 TREATMENT EXERTS NO PROTECTION AGAINST METASTASIS IN A PyMT-Bo1 TUMOUR RESECTION MODEL

I have previously shown that PyMT-Bo1 cells were able to disseminate from the primary tumour. In addition, this cell line was derived from a bone metastatic lesion of a MMTV-PyMT+ mouse, and thus, it has been selected for its invasive potential. The PyMT-Bo1 orthoptic model is aggressive and the total model duration is just 15 days. This allows limited time for metastatic colonies to form in distant tissues/organs. Resecting the primary tumour will therefore provide additional time for metastatic lesions to form without having the rate determining step of excessive primary tumour growth.

I completed numerous optimisation experiments to assess the most effective surgery to resect all the primary tumour to prevent regrowth. Guidance and training in these difficult surgeries prior to this experiment were obtained from the Weilbaecher lab (Washington University, St. Louis, USA). It has been well-established that tumour size is positively associated with the likelihood of metastasis (Westenend et al., 2005). Previous experiments performed by the Weilbaecher lab revealed that the minimum tumour weight required for tumour cell dissemination was at least 600 mg. We aimed to resect tumours when they were equal sizes across the control and treatment groups. In addition, under the HMO project license protocol PP8873233, tumour volumes should not exceed 1000 cm^3, equivalent to around 1200 mg, therefore daily monitoring was implemented so that resections would begin before tumours reached protocol limits. In addition, tumours around 800 – 900 mg were technically challenging to resect as they were prone to haemorrhaging. Taken together, I aimed to perform resections when

tumours reached 600 - 800 mg. Resections were staggered over multiple days to prevent differing tumour sizes affecting metastatic burden. To predict when tumours reached 600 mg, I measured tumour volumes using digital calliper measurements then predicted the weight based off our previous data of tumour volumes/weights in the orthotopic model experiments. After the tumours were resected, the model continued, and animals were sacrificed one month post-date of resection.

There were 8 out of 14 and 6 out of 12 successful resections in the PBS-treated control and *Bif*210 groups, respectively (**Figure 4.5B**). Unsuccessful resections were defined by regrowth of primary tumour or if humane end points were reached due to adverse effects of the surgical procedure. As resections were staggered over days 12/13/14, resected tumour volumes were comparable between control and *Bif*210-treated groups, therefore would not be a variable for metastatic burden. Despite aiming for a minimum tumour weight of 600 mg for resections, around three successfully resected tumours were considerably smaller (around 400 mg). Despite this, metastatic lesions were identified in all lung sections.

The number of lung metastatic nodules, post-normalisation to the lung section area presented in **Figure 4.5B**, were not significantly different between control and *Bif*210-treated mice. Between 4 to 17 and 5 to 14 lung metastatic nodules were counted for control and *Bif*210-treated lung sections, respectively. Even though the number of metastatic nodules were consistent between groups it is worth noting that 2 mice in the *Bif*210-treated group were sacrificed prior to 30 days post-resection (the pre-determined endpoint). The 2 mice displayed clinical signs of metastasis and had reached humane end points clearly defined in the HMO project licence. The metastatic burden in these animals vastly exceeded the rest of the groups, as seen with *in vivo* bioluminescence imaging (data not shown). The luciferase signal was not observed in all the mice, apart from the 2 described, even though metastatic lesions were identified. To improve sensitivity, future experiments may therefore require optimisation of the luciferase-tagged cancer cells, so they emit a stronger signal. Due to the relatively low sample sizes of successful resections, particularly in the *Bif*210 group, as well as comparable lung metastatic burden, it cannot be concluded that *Bif*210 negatively impacts metastasis.
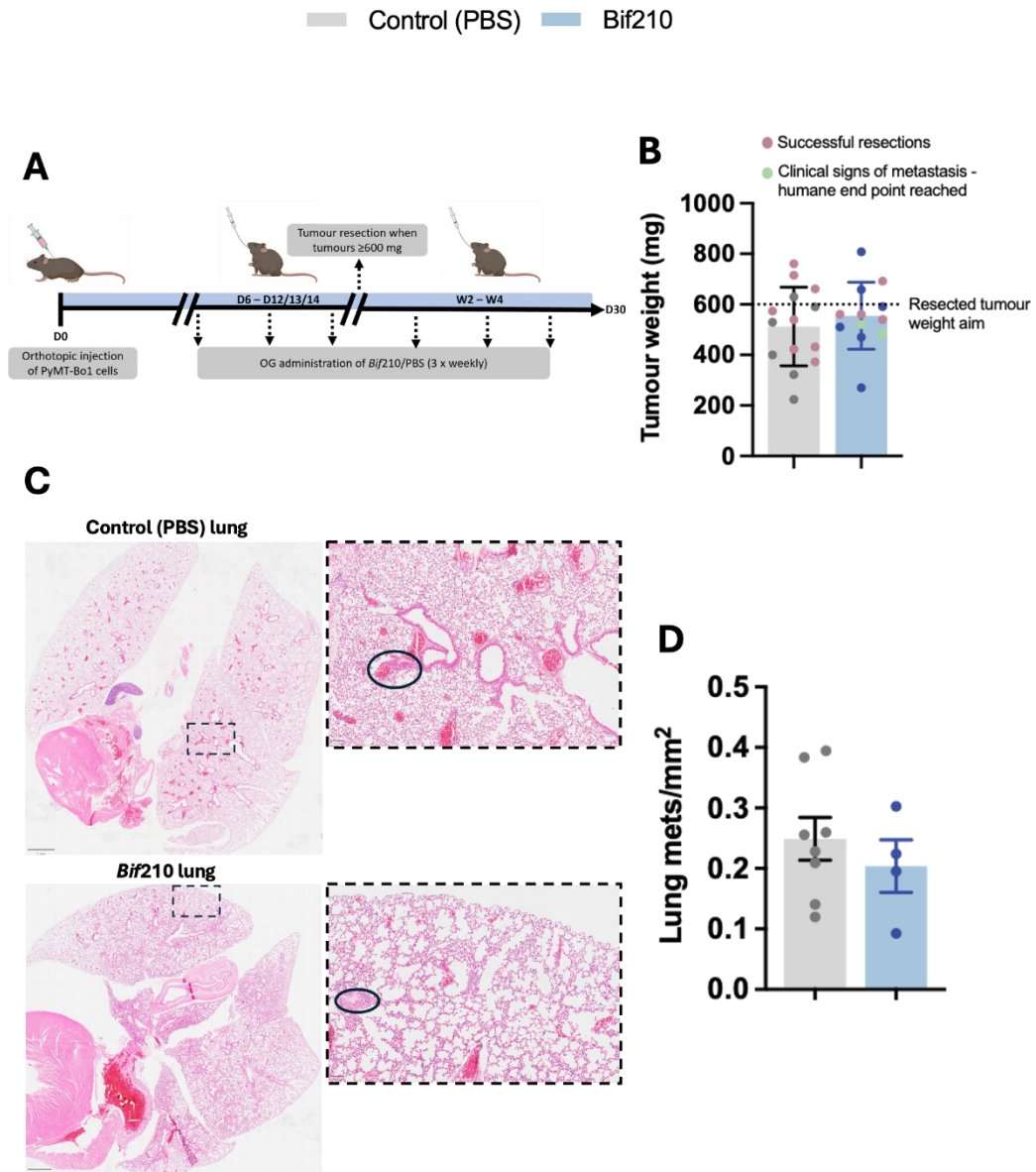
Figure 4.5 Assessing whether *Bif*210 treatment alleviates metastatic burden in a PyMT-Bo1 tumour resection model. (A) Experimental plan of PyMT-Bo1 resection model. 1×10^5 PyMT-Bo1 tumour cells were orthotopically injected into the abdominal mammary gland of C57BL/6 mice. Oral gavage (OG) of PBS (control) (n=14) or *Bif*210 (n=12) commenced when tumours became palpable (day 6) thrice weekly. Tumours were resected on days 12/13/14 when tumour weights were predicted to weigh at least 600 mg then sacrificed and lungs harvested 30 days post tumour resection. (B) Average resected tumour weight for control and *Bif*210-treated mice. Two mice showing clinical signs of metastasis (denoted in green) were sacrificed as humane end points were reached. Successful resections (pink) were mice that were sacrificed 30 days post tumour resection and lungs were harvested. Unsuccessful resections were due to human end points reached due to adverse effects from the resection surgery. (C) Representative images of whole lung sections stained with haematoxylin and eosin. Scale bars show 1 mm and 800 µm for control and *Bif*210 lung sections, respectively. Black ovals indicate lung metastatic lesions which appear as atypical cell clusters, with disordered cellular and nuclei arrangements. (D) Number of lung metastatic (mets) nodules and area of each lung section were identified. Bars represent average lung mets per mm^2 of lung section for control (n=8) and *Bif*210-treated (n=4) tumour resected mice.

4.6 *Bif*210 TREATMENT HAD NO EFFECT ON METASTATIC BURDEN IN MMTV-PYMT+ MICE

As discussed, the MMTV-PyMT model closely resembles human breast cancer progression, compared to orthotopic models. The MMTV-PyMT model has high metastatic potential as mice readily develop multi-focal breast tumours as well as metastatic lesions, especially in the lungs. To assess whether *Bif*210 could alleviate metastatic burden, *Bif*210 was orally administered twice weekly to MMTV-PyMT+ mice when they reached adulthood (from 8-weeks) until a tumour reached 1000 mm^3. Tumour volumes were monitored using digital callipers, as it was important to euthanise mice when tumours were consistent between intervention groups, as tumour size has been correlated with metastatic burden (as mentioned above).

As circulating cancer cells disseminate and form metastatic lesions first in the lungs, I sectioned and performed H&E staining on this organ. Counting metastatic lesions (mets) is a good measure of metastatic burden, however, to ensure the area of lung sections were taken into consideration, I calculated number of mets per mm^2. There were no significant differences in number of lung metastatic nodules per mm^2 of lung sections between interventions (control/PBS-treated and *Bif*210), seen in **Figure 4.6C**. To remove bias, sample identification was blinded during histological examination. Every sample which had noticeably larger metastatic lesions were noted (data not shown), however, very few samples had this, and they were spread evenly across interventions. Therefore, metastatic lesion area was not measured. However, future analysis could display metastatic lesion area (mm^2) of lung section area (mm^2), in addition to the number of mets.

As discussed, it was important to assess metastatic burden when the primary tumour burden was consistent across treatment groups. As seen in **Figure 4.6D**, the tumour burden between control and *Bif*210-treated mice were on average equal. To assess whether tumour burden did affect metastatic burden, I plotted the simple linear regression of these two variables. In the MMTV-PyMT model, tumour burden did not influence, or could predict, lung metastatic burden as seen by the low R^2 value (0.0135) in **Figure 4.6E**.

The mammary gland and lungs harbour differing immune environments; therefore, it is important to assess whether immunogenic interventions affect metastasis in both locations. Since MMTV-PyMT+ mice develop breast tumours at multifocal sites and have a total of five pairs of mammary glands, the number of tumours per

mouse was also assessed (**Figure 4.6F**). There were no significant differences between the number or breast tumours in control and *Bif*210-treated MMTV-PyMT+ mice. However, the mode number of tumours in the control group was five per mouse compared to four in the *Bif*210 group. In addition, two *Bif*210-treated mice had just one breast tumour per mouse.
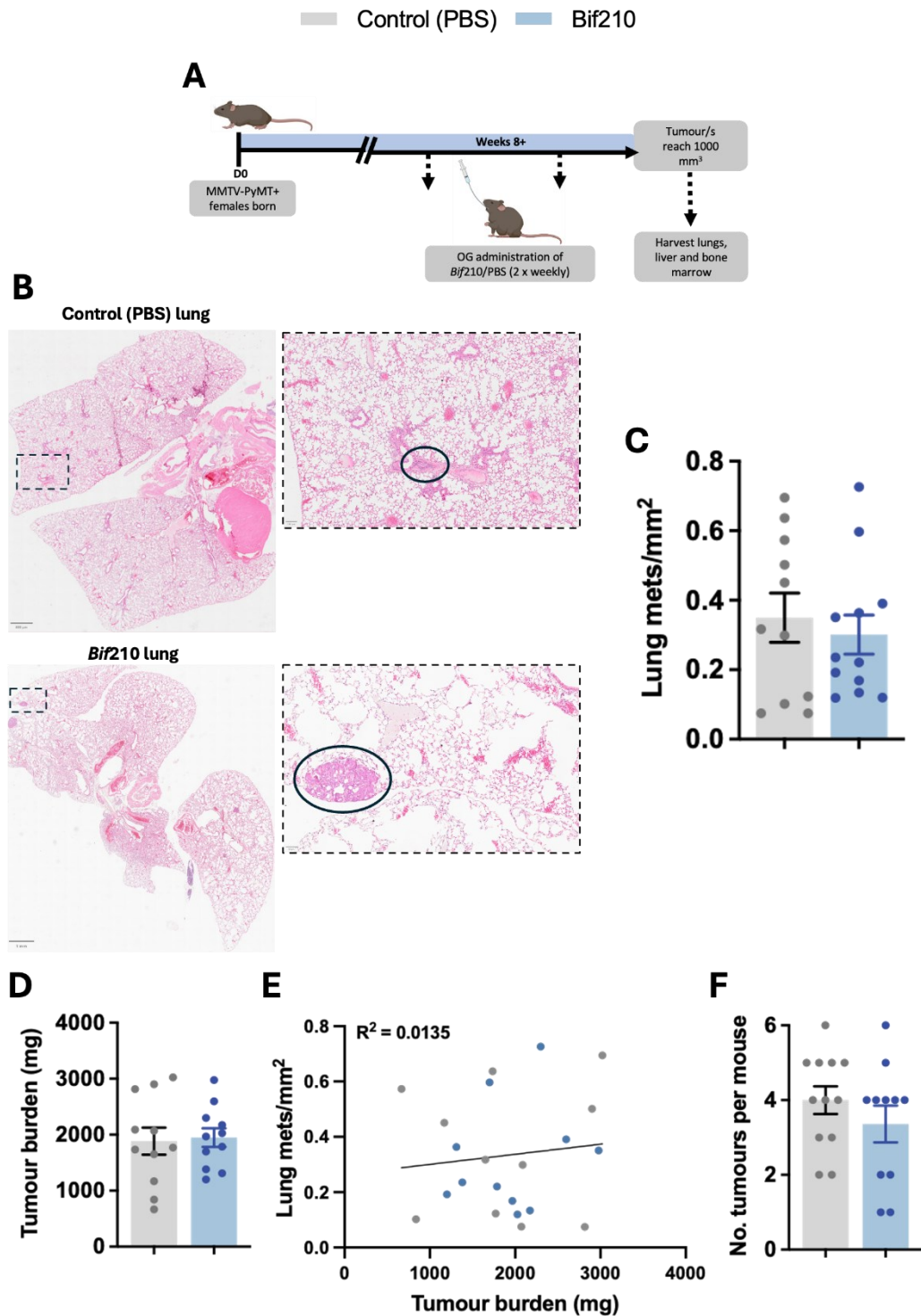
Figure 4.6 Assessing whether *Bif*210 treatment alleviates metastatic burden in the highly metastatic, spontaneous MMTV-PyMT model. (B) Experimental plan detailing that oral gavage (OG) of PBS (control) or *Bif*210 commenced when MMTV-PyMT+ mice were 8-weeks old and continued twice weekly. Mice were sacrificed when tumour/s reached 1 cm^3 and lungs and bone marrow were harvested to identify tumour cells/metastatic lesions. Representative images of whole lung sections stained with haematoxylin and eosin. Scale bars show 800 μm and 1 mm for control and *Bif*210 lung sections, respectively. Black ovals indicate lung metastatic lesions which appear as atypical cell clusters, with disordered cellular and nuclei arrangements. (D) Number of lung metastatic (mets) nodules and area of each lung section were identified. Bars represent average lung mets per mm^2 of lung section for control (n=11) and *Bif*210-treated (n=12) tumour resected mice. (D) Bars represent average tumour weight (mg) in control and *Bif*210-treated mice. (E) Simple linear regression graph to assess whether tumour burden correlated with lung metastatic burden. Line of best fit and coefficient of determination (R^2) were calculated. (F) Graph displays the total number of tumours per MMTV-PyMT+ mouse.

4.7 OPTIMISING THE QUANTIFICATION OF CIRCULATING TUMOUR CELLS IN THE BONE MARROW OF MMTV-PYMT+ MICE

One disadvantage of the MMTV-PyMT metastasis model is that, unlike the orthotopic PyMT-Bo1 model, which utilises antibodies against GFP or luciferase, the tumour cells are not tagged, making them significantly more challenging to identify. Methods to quantify tumour cell burden in MMTV-PyMT+ mice, other than relatively subjective histological techniques, was therefore investigated. In general, cells in the bone marrow lack cytokeratin, an epithelial protein found on the cytoskeleton. Tumour cells on the other hand are cytokeratin positive, therefore tumour cells that have disseminated to the bone marrow can be identified using an anti-pan cytokeratin antibody. The antibody used for staining (clone AE1/AE3) identified a range of cytokeratin (CK) types expressed on breast carcinoma cells (CK 7, 8, 5/6, 14, 18, and 19).

To confirm CK-positive events were truly breast cancer cells, bone marrow aspirates from MMTV-PyMT- were included. Flow cytometry results in **Figure 4.7** show that there were around 5-6% cytokeratin-positive cells of total non-immune cells in the bone marrow of these mice. Non-specific binding or autofluorescence could have contributed to these positive events in the non-tumour bearing control. In addition, plasma and megakaryocytes are cytokeratin-positive and small quantities may be present in bone marrow aspirates. Cytokeratin-positive, non-tumour cells can be excluded if methods such as histology that examines the cellular morphology are performed, however, conventional flow cytometry cannot do this (de Manzoni et al., 2002). Even though the few tumour-bearing samples processed displayed >6% cytokeratin-positive cells of total non-immune cells,

these differences were very minor and therefore unclear whether biologically relevant. Unfortunately, there was a facility-wide issue that affected the viability of the bone marrow cells during flow cytometry preparation for repeat experiments. The repeat experiments had numerous MMTV-PyMT+ bone marrow samples as well as tumour-spiked bone marrow controls. PyMT-Bo1 cells grown in culture were used to spike bone marrow cultures for antibody validation. A lack of repeat experiments also meant that statistical analysis could not be performed.
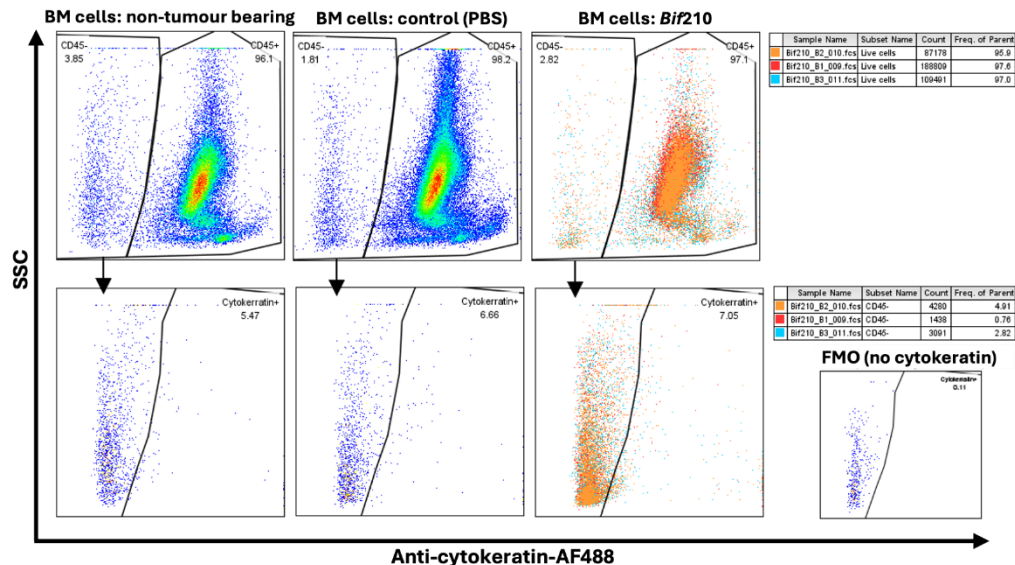
Figure 4.7 Attempt to identify disseminated tumour cells in bone marrow. Dot plots depict bone marrow cells derived from tumour-bearing MMTV-PyMT mice assessed by flow cytometry. Bone marrow cells were stained with LIVE/DEAD™ fixable dead cell dye, anti-CD45-PerCP-Cy5.5 and anti-cytokeratin-AF488. To identify tumour cells, CD45- then cytokeratin+ cells were gated and compared against a non-tumour bearing control.

4.8 CANCER CELL BURDEN IN LUNGS AND LIVER DID NOT DIFFER WITH *BIF*210 TREATMENT IN AN EXPERIMENTAL PYMT-BO1 METASTASIS MODEL

To examine whether *Bif*210 affects cancer cell seeding in distant organs and metastatic lesion growth, PyMT-Bo1 cells were injected intravenously (via the tail vein). In BrCa patients and mouse models, lungs are generally the first organ of metastatic growth followed by the liver, so these organs were chosen for metastatic burden analysis. PyMT-Bo1 cells were chosen over BRPKp110 cells because of their greater metastatic potential. *Bif*210 was orally administered on the same day as cancer cell administrations because it was hypothesised that the immune cells could be stimulated/polarised by *Bif*210 in the presence of cancer cells, before any lesion growth occurred, which may offer immunological memory.

Due to weak bioluminescence signals *in vivo,* lungs and liver were extracted and placed in a luciferin bath and imaged *ex vivo*. A disadvantage of this, however, is that metastatic burden could not be tracked longitudinally. All lungs displayed metastatic growth compared to a non-cancer bearing lung, that displayed the background fluorescence naturally emitted by lung tissue, as seen in **Figure 4.8B**. Bioluminescence was quantified using densitometry analysis. There were no significant differences in bioluminescence densitometry in lungs between control and *Bif*210-treated animals. Within each group there was considerable variance, with a range of high and low metastatic burdened lungs.

Unlike the lungs, there were two livers in the control group and one liver in the *Bif*210 group which displayed no measurable bioluminescence compared to the non-tumour bearing liver (**Figure 4.8D**). The signal from the tagged cancer cells may have been too weak to be detectable so it cannot be concluded whether these livers were cancer cell free. All mice had detectable cancer cells in the lungs, despite not all having detectable levels in the liver, therefore it can be confirmed that the PyMT-Bo1 cell injections were performed correctly. These mice may have had a slower rate of metastatic growth. Again, there were no strong differences in bioluminescence signals between the control and *Bif*210-treated livers. However, the *Bif*210 group had a slightly lower average signal, with high variability, as two livers showed high signals while one had no detectable signal. There were two livers with no detectable signal in the control group therefore no differences were observed between the two groups.
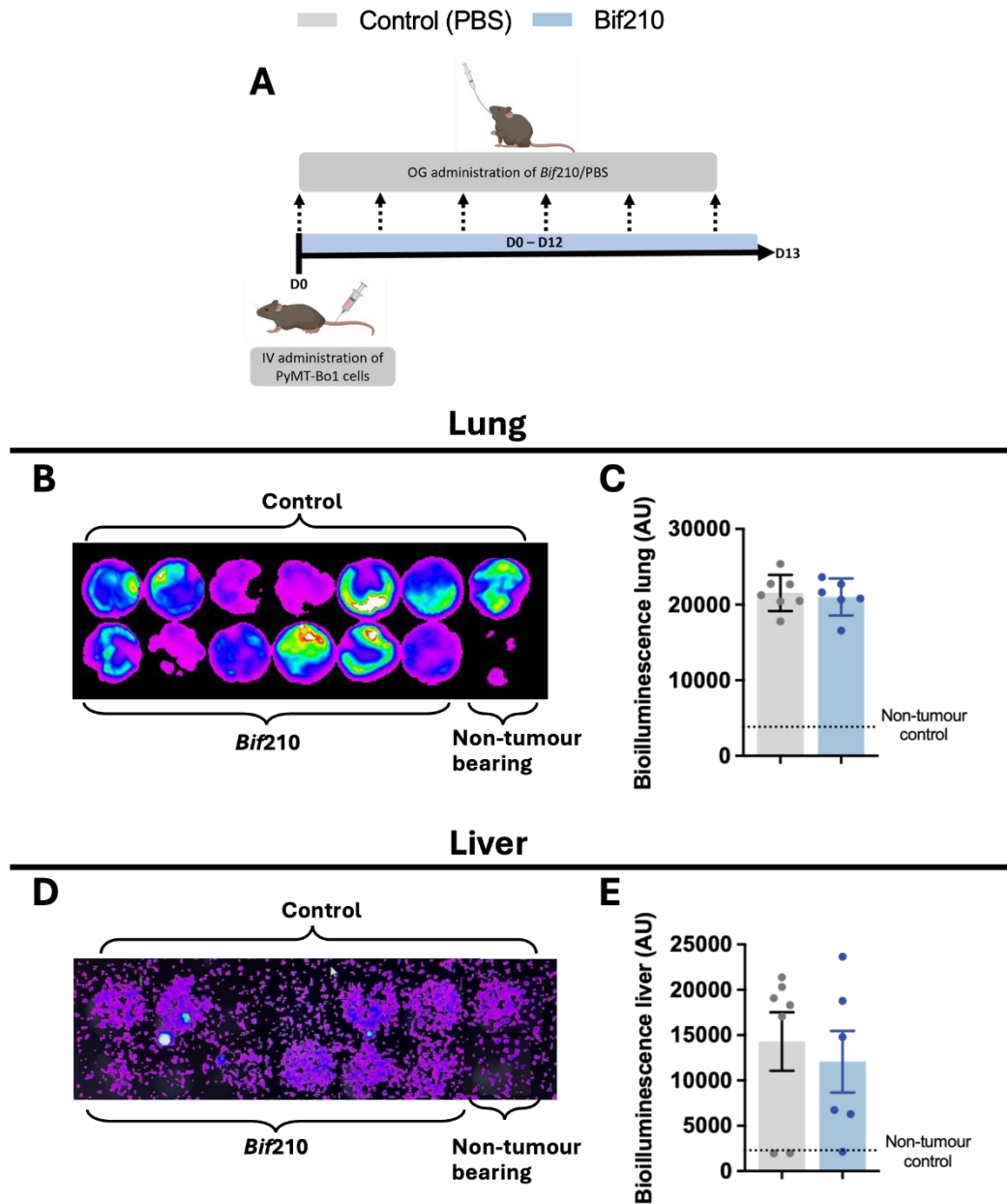
Figure 4.8 *Bif*210 supplementation does not affect lung and liver metastatic burden in a breast cancer experimental metastasis mouse model. (A) Experimental outline shows C57BL/6 mice were intravenously administered PyMT-Bo1 breast cancer cells in the tail vein to represent circulating cancer cells and cancer cell seeding to distant organs (lungs and liver) during metastasis. Oral administrations/gavage (OG) of *Bif*210 (n=6) or PBS (n=7) occurred on the same day as tumour cell administration then every 2-3 days for a total of 6 administrations. Bioluminescence images of excised (B) lungs and (D) liver submerged in a luciferin bath from control (PBS-treated) and *Bif*210-treated PyMT-Bo1-tumour bearing mice. Bioluminescence is proportional to tumour burden since PyMT-Bo1 cells were tagged with luciferase. A lung and liver from a non-tumour bearing mouse was included to measure background bioluminescence levels. Bar graphs display bioluminescence levels in (C) lungs and (E) livers quantified by measuring densitometry measurements from images.

4.9 DISCUSSION

Metastasis is a complex, multistage process and is the leading cause of cancer-related mortality (Baker and Mansfield, 2023). Historically, one of the most fundamental concepts in understanding metastasis was Stephen Paget's 'seed and soil' hypothesis in 1889 (Paget, 1889). He proposed that cancer cell metastasis is not random, instead can be targeted to specific tissues/organs. The general principle being that metastasis relies on how easy it is for cancer cells (the seed) to disseminate and grow in the distant organ (the soil). Understanding how external factors, in this case the gut microbiome, can influence the pre-metastatic niche (i.e. the soil) as well as cancer cell extravasation to the circulation is paramount to aid developments of microbial-based therapeutic interventions.

The few studies that have examined whether the gut microbiome is associated with metastasis of cancers distant from the gastrointestinal tract, have suggested that antibiotic-induced gut dysbiosis is associated with metastasis (McKee et al., 2021, Viaud et al., 2013, Gao et al., 2020). Albeit research is sparse and despite existing research suggesting that the genus *Bifidobacteria* slows primary tumour burden, effects on metastasis are relatively unknown. This chapter therefore focussed on whether a newly discovered stain of *Bifidobacteria*, *Bif*210, known to slow primary tumour growth, modified breast cancer metastatic burden as well as tumour initiation.

*Bif*210 did not significantly alter metastatic burden in a range of murine breast cancer models. Likewise, McKee and colleagues found that the number of PyMT-Bo1 metastatic lesions in the lungs were unchanged when the microbiome was modified, albeit through antibiotic use. However, antibiotics did increase the overall metastatic area, suggesting the gut microbiota may affect metastatic proliferation rather than cancer cell extravasation and seeding rate to distant organs (McKee et al., 2021). Upon visual inspection of the metastatic lesions in these results, there were no apparent differences in lesion area therefore further analysis was not pursued. One study found that members of *Faecalibacterium* were elevated in faeces of metastatic melanoma patients with higher rates of overall survival. Specific microbiota members, other than *Bifidobacteria*, may therefore be associated with metastatic progression. Results presented in chapter one (section 3.9) has shown that *Bif*210 exerts little modulation to the microbiome composition, therefore the incorrect population may have been targeted.

Modelling metastasis in mice is extremely challenging, as metastasis is a complex process that typically develops over several months or years. The different models that were utilised in these experiments have distinct advantages and disadvantages, summarised in Table 4.1.

Additionally, there are key differences in metastatic progression between humans and mice. In humans, cancer heterogeneity is substantial, involving genetic, epigenetic, phenotypic, and microenvironmental factors that all attribute to metastatic initiation and progression. This heterogeneity exists not only between patients but also within primary tumours and metastatic lesions. For example, tumour cells can exhibit metabolic plasticity, allowing them to survive under various conditions. The immune microenvironment of the primary tumour and pre-metastatic niche is highly variable between individuals and tissues and is distinct from that of mice. Furthermore, in humans, disseminated cancer cells may adapt to their local environment but remain unable to proliferate, a state known as dormancy. Dormant cancer cells are often resistant to therapy, and a small proportion can become reactivated, leading to the formation of metastatic lesions (Park and Nam, 2020). Mouse models cannot encapsulate the complex process of cancer cell dormancy and reactivation, therefore treatments that aim to offer long-term protection against metastasis and cancer recurrence cannot accurately be compared. Consequently, the true effects of *Bif*210 in the context of metastatic progression in humans cannot be concluded from murine models.

Our results employed three different metastasis models (Table 4.1), all of which had slightly dissimilar *Bif*210 dosing regimens. One model (MMTV-PyMT) administered *Bif*210 before overt carcinogenesis, hence metastasis occurred, whilst the other two administered *Bif*210 post- and simultaneously to the time of tumour cell administration. One study found that a dysbiotic microbiome modified normal mammary tissue before tumour implantation in mice, by activating and expanding fibroblasts (Feng et al., 2022). The study found a significantly enhanced number of activated fibroblasts that resulted in extracellular matrix remodelling in the gut dysbiosis group. It was therefore important to assess whether *Bif*210 affected metastasis at multiple stages of carcinogenesis.

Table 4.1 Assessing the advantages and disadvantages of murine metastasis models utilised in this chapter to investigate the treatment potential of *Bif*210.

Model	Advantages	Disadvantages
Primary tumour resection model (PyMT-Bo1 cells)	• PyMT-Bo1 cells have high metastatic potential. • Assesses tumour cell dissemination from the primary site. • Resections allow time for metastatic tumour growth compared to orthotopic models. • Tumour cells can be tagged so can track metastatic burden longitudinally without sacrifice and easier to quantify.	• High rate of primary tumour regrowth. • Location of orthotopic injection could influence rate of metastasis – difficult to control. • Metastatic burden may be low therefore hard to detect micro metastases.
MMTV-PyMT model	• Long-term – able to administer multiple treatments. • Clinically relevant as histologically and molecularly resembles human breast cancer. • Highly metastatic, especially to the lungs. • Slow rate of primary tumour growth so allows time for metastatic lesions to form.	• Difficult to surgically remove tumours (as tumours can occur in all mammary glands), therefore cannot model metastasis post-lumpectomy/mastectomy. • Non-tagged cancer cells - difficult to identify CTCs/DTCs and assess metastatic burden longitudinally *in vivo*. • Mouse genetic background (C57Bl/6J MMTV-PyMT) can influence metastatic burden.
Tail vein model (PyMT-Bo1 cells)	• Each animal has same number of cancer cells administered so can compare circulating cancer cell colonisation. • Good model for assessing whether treatment affects pre-metastatic niche. • Tumour cells can be tagged so can track metastatic burden longitudinally without sacrifice and easier to quantify.	• Bypasses early metastasis stages: only measures circulating tumour cell seeding and metastatic growth rate, not how tumour cells disseminate from the primary tumour and intravasate into circulation. • The least relevant to metastatic progression in humans.

Breast tumours have the highest rate of bone marrow metastasis compared to other tumour types; therefore, it was important to assess whether *Bif*210 could prevent this (La Gioia et al., 2022). In addition, numerous studies value breast tumour dissemination to bone marrow as a prognosis factor for overall survival and risk of relapse (Hartkopf et al., 2014, Sai and Xiang, 2018, Steeg, 2006). Flow cytometry was used to identify cytokeratin-positive, and hence (presumed) disseminated tumour cells, in the bone marrow. The non-tumour-bearing control had similar levels of cytokeratin-positive cells compared to tumour-bearing samples. In addition, due to unforeseen circumstances, additional repeats were unable to be analysed. The presence of disseminated tumour cells in the bone marrow of MMTV-PyMT tumour-bearing mice therefore could not conclusively be

confirmed. Studies have suggested that disseminated tumour cells can be detected in the bone marrow at early stages, before metastasis is detected, which raises questions about the sensitivity of the protocol (Ditsch et al., 2002, Vlems et al., 2003). In humans, disseminated tumour cells occupy specialised niches, either the perivascular or endosteal areas, where they can reside in a dormant state. It may take several months or years for disseminated tumour cells to form micro-metastases, overt bone metastases or re-enter circulation (Pan et al., 2017). The MMTV-PyMT model duration may therefore be insufficient to adequately compare differences in disseminated tumour cells in the bone marrow. The intracardiac model, whereby tumour cells are injected into the left ventricle of the heart, exhibits overt bone metastasis. To effectively compare whether *Bif*210 affects metastatic outgrowth in the bone, future experiments could therefore utilise this method.

I have shown that there was no correlation between overall tumour burden and lung metastatic burden in MMTV-PyMT+ mice. Particularly in murine models, increased primary tumour weight has been shown to positively correlate with metastatic burden (Rutkowski et al., 2014, Westenend et al., 2005, Miyawaki et al., 2023). As the primary tumour grows, the extent of vascularisation and tumour-associated stromal regions expands, facilitating metastasis (Horimoto et al., 2012, Westenend et al., 2005). However, this is model-dependent and is not directly translatable to human carcinogenesis. In humans, other factors such as angiogenesis, the immune environment and genetics exert greater profound metastatic effects than tumour weight. In experiments presented in this chapter, animals were sacrificed, or tumours were resected in the MMTV-PyMT model and the PyMT-Bo1 model, respectively, once tumours reached equal volumes to avoid potential bias in cancer cell dissemination. Since I have shown that tumour burden is not directly proportional to tumour weight in the MMTV-PyMT model, a future experiment could be adapted so the defined endpoint is a timepoint post palpable tumour formation.

*Bif*210 modestly, yet significantly, delayed tumour onset time and slowed tumour growth rate in a MMTV-PyMT+ model. As previously discussed, there is mounting evidence suggesting the cancer-protective effects of prebiotics, such as polyphenols (Alves-Santos et al., 2020). Studies have suggested that polyphenols exert their health-promoting effects through gut microbiome modulation, including targeting the growth of specific members, in particular *Bifidobacteria* (Lordan et al., 2020, Sorrenti et al., 2020, Martín and Ramos, 2021). We have therefore further

supported the hypothesis that certain strains of this genus could act as chemopreventive agents.

To comply with project license protocols, twice weekly administrations were chosen instead of thrice weekly (used previously in our orthotopic models) for the MMTV-PyMT models. Previous results, however, in section 3.10 revealed that *Bif*210 viability in the murine GI tract was non-existent 24 hours post-administration. Future work could therefore aim to investigate the optimum *Bif*210 administration frequency to delay tumour onset and reduce burden. Colonisation efficacy and microbiome modulation after long-term *Bif*210 exposures in humans also warrants investigation.

Despite no differences in metastatic burden, *Bif*210 offered increased systemic immunological memory through induction of CD44+ CD8+ T cells in the blood of tumour-bearing mice. There was little evidence to suggest that *Bif*210 enhanced the tissue resident memory CD8 T cell population in lymph nodes and tumours. Consequently, this may have contributed to the lack of resistance against metastasis. Though not assessed, reduced abundance in CD8 Trm cells in tumours may also increase the likelihood of tumour recurrence. There are numerous other sites where tumour-specific immunological memory offers protection, including the spleen, tumour adjacent mucousal tissue and pre-metastatic niches (lungs, liver, etc.), which were not analysed but would aid understanding of *Bif*210's systemic immunological effects. To effectively examine the induction of CD8 Tmems, future work could utilise OT-I mice. T cells in OT-I mice express a transgenic T cell receptor (TCR) that is specific for the ovalbumin (OVA) peptide presented by MHC class I molecules (H-2Kb). Engineered tumour cells can also present OVA and upon OVA presentation, T cells become primed and activated. Activated, OVA-specific T cells differentiate into effector cells, with a small subset differentiating into Tmems. Adoptive transfer experiments could assess whether Tmems derived from *Bif*210-treated OT-1 mice offer carcinogenesis protection compared to control-treated OT-I mice when rechallenged with OVA-tumour cells.

Numerous other immune populations have been implicated with metastasis progression. An immunosuppressive environment, abundant in MDSCs, such as protumourigenic neutrophils and M1 macrophages, in distant organs facilitates cancer cell seeding and proliferation. On the contrary, anti-tumourigenic immune populations, such as CD8 T cells, prevent metastatic lesion proliferation and

formation. However, CD8 T cells may promote cancer cell dormancy (Aqbi et al., 2018, Min and Lee, 2023). *Bif*210 is a highly immunogenic member of the microbiome, and I have previously shown that *Bif*210 modulates immune environments at distal sites. Future experiments could therefore assess whether *Bif*210 modifies immune populations in the pre-metastatic niches.

There are numerous non-immune cells associated with cancer cell extravasation, dissemination and proliferation in distant tissues/organs. For example, cancer-associated fibroblasts (CAFs) can promote EMT, angiogenesis and release chemokines, proteases and growth factors. By assessing the activation levels of these cells and the associated key hallmarks, such as EMT by quantifying E-cadherin, N-cadherin and vimentin levels, additional metastatic effects of *Bif*210 could be assessed. It is important to fully understand *Bif*210's effects on the host because, as previously discussed, murine models do not fully represent human metastatic physiology and may have incorrectly suggested a lack of metastatic implications.

I have shown that *Bif*210 supplementation alone did not affect metastasis progression, however it is unknown whether *Bif*210 would mediate metastasis in combination with conventional therapies. The two clinical trials that utilised FMTs in advanced melanoma, found that FMTs from anti-PD1 responders into non-responders increased efficacy of anti-PD1 therapy (Baruch et al., 2021, Davar et al., 2021). Huang and colleagues showed that FMTs offered protection for cancer progression and increased overall survival in a colon cancer model when combined with anti-PD1 therapy more so than the therapies alone, suggesting a synergistic effect (Huang et al., 2022). In addition, *Bif*210 supplementation may restore commensal microbial homeostasis during a state of dysbiosis induced by existing therapies. It has previously been highlighted that common cancer therapies induce negative gastrointestinal implications. Since numerous studies have shown that commensal dysbiosis can drive tumour cell dissemination in mice, future studies could utilise conventional therapies combined with *Bif*210 to promote gut eubioisis, and thus examine metastatic burden.

Overall, I have shown that *Bif*210 offered no protection against metastasis but modestly delayed primary tumour initiation in a spontaneous murine breast cancer (MMTV-PyMT) model. *Bif*210 supplementation may therefore be valuable in high-risk people and as part of neoadjuvant therapies in early breast cancer stages, before overt carcinogenesis.

CHAPTER FIVE.

5 INVESTIGATING THE POTENTIAL OF BACTERIAL EXTRACELLULAR VESICLES (BEVs) ISOLATED FROM *BIF*210 AS A NOVEL ANTI-CANCER IMMUNOTHERAPEUTIC.

The use of BEVs in the treatment of disease is a novel and booming research area (Stentz et al., 2022b, Jahromi and Fuhrmann, 2021, Shen et al., 2012). Literature has traditionally focussed on the use of Gram-negative BEVs due to their earlier discovery, whilst much less is known about the use of Gram-positive BEVs. There is therefore an untapped potential to uncover the BEV-host effects from such bacteria, including BEVs derived from the highly immunogenic bacterial genus, *Bifidobacteria.*

Our collaborator, Anne Jordan in the Hall lab (Quadram Institute Bioscience, UK), successfully isolated BEVs from *Bif*210, the strain of *Bifidobacteria* that significantly slowed breast tumour progression in murine models. There is limited research investigating the host effects of *Bifidobacterial* BEVs, but studies have proposed of their immunogenic properties (Kurata et al., 2022, Alessandri et al., 2019). Studies have shown that BEVs pass through the gastrointestinal barrier, albeit in small quantities. BEVs can also be administered intravenously, unlike live bacteria, due to their increased safety profile. Aiming to unlock the full therapeutic potential of *Bif*210, our experimental setup shall include administering the BEVs intravenously, bypassing the gut microbiome to maximise the amount of BEVs that reach the tumour. Different administration routes of *Bifidobacterium*-based therapeutics could offer additional clinical treatment opportunities as well as uncovering mechanistic data.

5.1 INTRAVENOUS ADMINISTRATION OF *Bif*210 EXTRACELLULAR VESICLES INHIBITS MELANOMA B16-F10 TUMOUR GROWTH.

Since the tumour suppressive potential of live and non-viable *Bif*210 has been shown, we wanted to explore whether *Bif*210-derived bacterial products could elicit an immune response to combat tumour growth. Bacterial extracellular vesicles (BEVs) have been well studied to modulate host immune responses; therefore, I assessed effects of *Bif*210 BEVs in tumour-burdened mice. I employed a B16-F10 melanoma tumour model, where isolated BEVs were administered intravenously to mice, commencing six days post subcutaneous injection of tumour cells. The timing coincided with formation of palpable tumours, mimicking the clinical scenario for patients. Intravenous administration was chosen to maximize systemic circulation and direct delivery of BEVs to the tumour. Previous work in the Robinson lab has demonstrated minimal differences in melanoma tumour volumes following intraperitoneal administration of *Bacteroides thetaiotaomicron* OMVs, whereas intravenous injections led to significant reductions in tumour volumes (Christopher Price, 2024, unpublished thesis). In addition, an advantage of using BEVs over live bacteria is the increased safety profile, as likelihood of life-threatening immune overreactions, such as septic shock, is unlikely. There were significant reductions in tumour volumes following BEV administrations (seen in **Figure 5.1**), evident as early as day 12 (after two administrations of 10^9 BEVs). The optimal dose selected for subsequent experiments was 10^9 BEVs per mouse, however, lower concentrations (10^7 and 10^5) still exhibited significant inhibition of melanoma tumour growth.
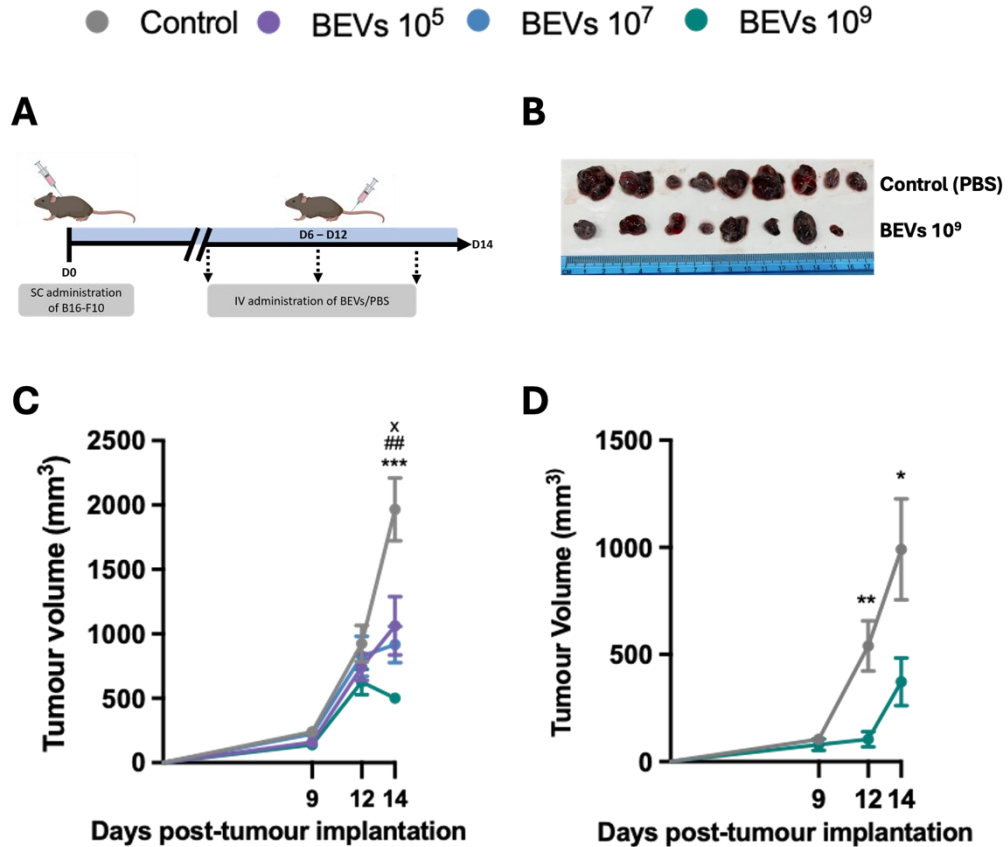
Figure 5.1 *Bif*210 BEV administration slows melanoma B16-F10 tumour growth in mice. (A) Illustration of B16-F10 melanoma model. Cells were subcutaneously injected, and BEV administrations commenced 6 days post-tumour implantation, every 3 days, before mice were sacrificed (day 14). (B) Representative tumours from control PBS-treated and BEV-treated mice. Tumour volumes were measured by tumour width^2 x tumour length x 0.52. (C) Tumour volumes in a BEV-dose response study using BEV doses of 10^5, 10^7, 10^9 per mouse. (D) Tumour volumes (mm^3) (+/- SEM) in live mice (days 9 and 12) and on resected tumours (day 14) in control and BEV-treated (10^9 BEVs per dose) groups. Two-way ANOVA with Dunnett's multiple comparisons test and multiple unpaired T tests was performed for (C) and (D) respectively and statistical significance is denoted by * / x (P<0.05), ** / ## (P<0.01), *** (P<0.005). "x" denotes the difference between control and BEVs 10^5, "#" denotes the difference between control and BEVs 10^7, "*" denotes the difference between control and BEVs 10^9.

5.2 *Bif*210 BEVs do not directly alter proliferation in vivo and tumour cell metabolic activity in vitro.

To assess whether BEVs affected tumour cell proliferation, tumour sections (obtained from the BEV experiment described above) were immunolabelled for the proliferation marker Ki67. Determining a tumour's Ki67 index via immunohistochemical assessment is a very common practice in the clinic, aiding prognostic indications. A higher ratio of Ki67-positive cells (indicating cells not in

the G0 phase of the cell cycle) is associated with increased tumour proliferation, which correlates with poorer prognosis and higher rates of metastasis in melanoma patients (Ladstein et al., 2010). There were no differences in the percentage of Ki67-positive cells between control and BEV-treated tumours which could imply BEV treatment had no effect on tumour cell cycle arrest. To further assess whether BEVs altered tumour cell proliferation, exerting direct cytotoxic effects, B16-F10 cells were incubated with BEVs *in vitro* at different concentrations for 24 hours and cell viability was assessed with the MTS assay. MTS, a tetrazolium salt, is converted to the coloured product formazan by viable cells, therefore, increased absorbance indicates higher cell metabolic activity which is proportional to the quantity of proliferating/viable cells. BEV concentrations at all doses had no effect on cell viability compared to the cell only or vehicle (PBS) controls (seen in **Figure 5.2**). BEVs may therefore exert their anti-tumourigenic effects via an indirect mechanism, such as adapting the tumour immune environment, rather than exerting direct tumour cytotoxic effects.
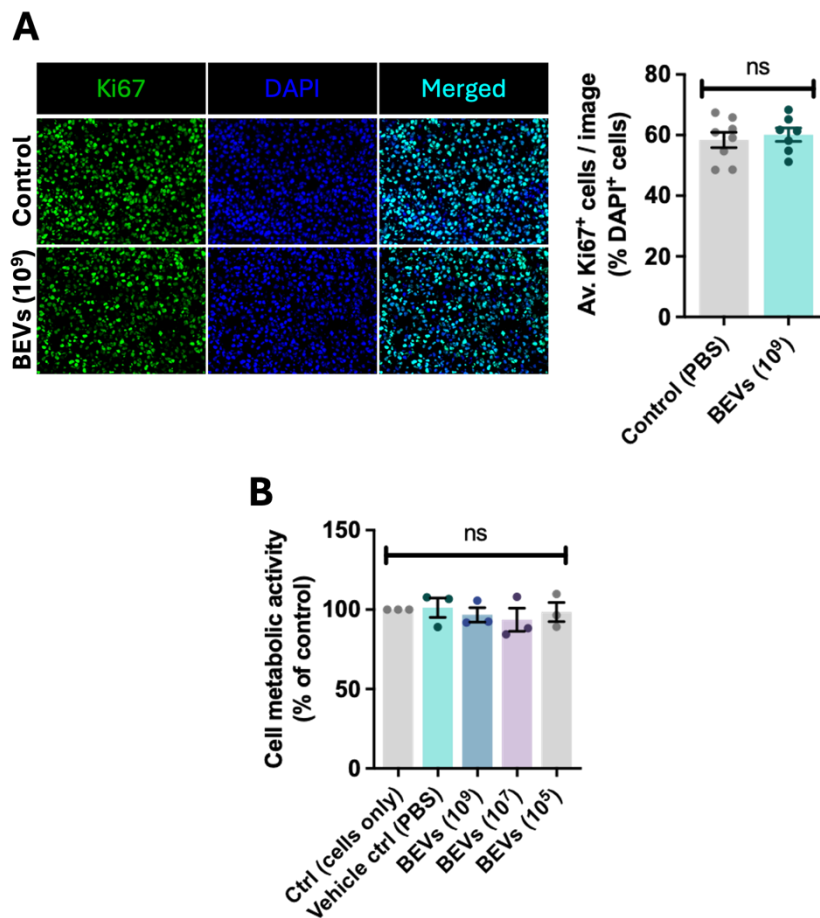
Figure 5.2 BEVs do not directly alter proliferation rate or B16-F10 metabolic activity. (A) Immunofluorescence images of tumour sections (20x magnification) stained with the proliferation marker, anti-Ki67 (green), and the nuclear stain, DAPI (blue). B16-F10 tumours were collected from control (PBS-treated) (n=8) and BEV-treated (n=7) mice. Each data point displays the average count of Ki67-positive cells as a percentage of total cells (DAPI-positive) from 3 regions of interest per tumour section, and 2 sections per tumour. Bars represent the average percentage of Ki67-positive cells of DAPI-positive cells (+/-SEM) per treatment group. (B) MTS assay (N=3) on B16-F10 tumour cells incubated with different concentrations of BEVs for 24 h (in replicates of 6). Bars represent average cell metabolic activity (+/-SEM) expressed as a percentage (average optical density (OD) at 492 nm of intervention / OD at 492 nm of control (cells only).

5.3 THE ADMINISTRATION OF *BIF*210 BEVS IS ASSOCIATED WITH INCREASED INFILTRATION OF LY6G+ GRANULOCYTES IN B16-F10 TUMOURS.

Given previous research highlighting the immunomodulatory nature of BEVs, it was crucial to compare immune populations within B16-F10 tumours from control (PBS) and BEV-treated mice. Immune cells within tumours exert distinct functional properties, including immunosurveillance and tumour suppression, depending on their type and polarisation. On the other hand, many immune cell subsets, including MDSCs and regulatory T cells, are immunosuppressive, and thus promote tumour growth. To investigate any BEV-induced effects to the tumour-immune landscape, I utilised flow cytometry targeting key immune cell populations and cellular markers to characterise their polarisation.

Our analysis revealed a significant increase in tumour associated Ly6G+ granulocytes in mice administered BEVs. This upward trend in Ly6G+ cells was consistent across three independent experiments (as seen in **Figure 5.3B**). Notably, other myeloid and lymphoid cell infiltrations remained unchanged (**Figure 5.3A, C-E**). Cytotoxic CD8+ T cells are recognised as important players in anti-tumorigenic immunity, however, the polarisation of T cells and dendritic cells towards conventional type 1 dendritic cells, which favour CD8+ T cell polarisation, showed no significant differences in BEV-treated mice.

Our results therefore suggest that *Bif*210 BEVs may modulate the tumour microenvironment by promoting increased infiltration and/or survival of Ly6G+ granulocytes.

153
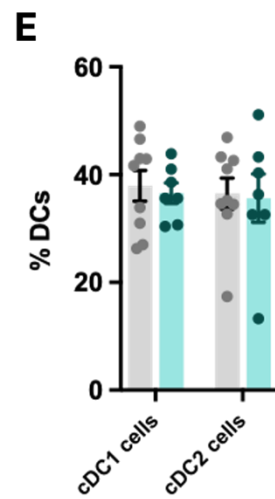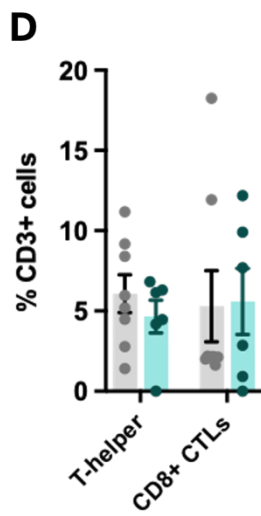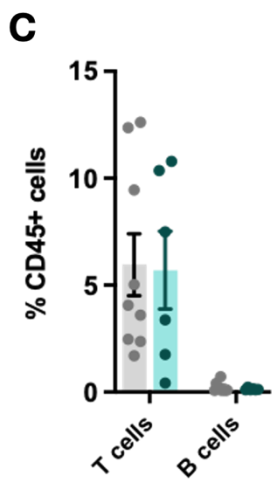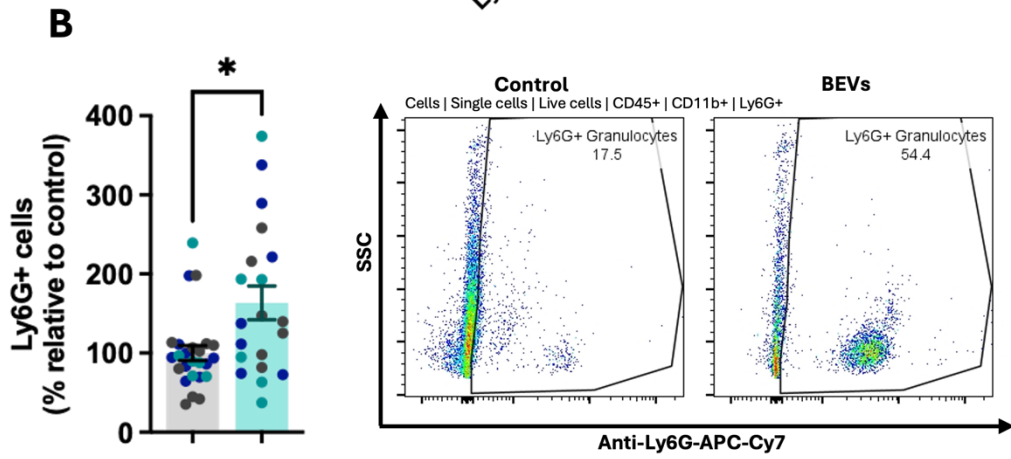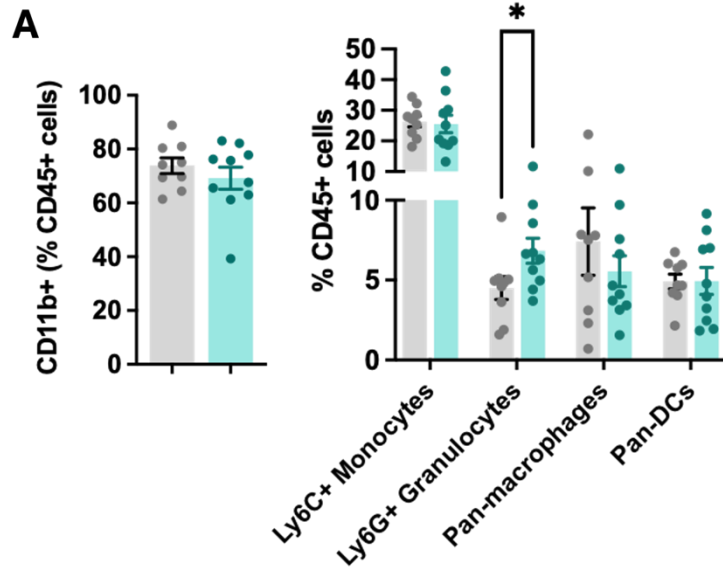
Figure 5.3 Tumour associated Ly6G+ granulocytes significantly increased in *Bif*210 BEV-treated mice. (A) Flow cytometric analysis of myeloid and (C) lymphocyte populations in tumours resected from control (PBS-treated) and BEV (10^9/dose)-treated mice, displayed as a percentage of total immune cells (CD45+). Multiple unpaired T tests were performed, and statistical significance is denoted by * (p<0.05). (B) Graph displays mean Ly6G+ granulocytes (+/- SEM) in tumours measured by flow cytometry from three independent experiments (N=3). Each sample is expressed relative to the respective control group average. Matched sample colours indicate experimental repeat (n>6). Dot plots display a shift in Ly6G+ cells in representative tumours after BEV administrations compared to control. Mann-Whitney non-parametric T test was performed, and statistical significance is denoted by * (P<0.05). (D) Polarisation of T cells: T-helper (CD4+) and cytotoxic T lymphocytes (CTLs) (CD8+) as a mean percentage (+/- SEM) of total T cells (CD3+) in tumours. (E) Polarisation of dendritic cells (DCs) in tumours displayed as mean (+/-SEM) conventional type 1 (cDC1) (CD103+) or conventional type 2 dendritic cells (cDC2) (CD11b+) as a percentage of total dendritic cells (CD11c+).

5.4 Ly6G depletion in a B16-F10 tumour model highlights the complex role Ly6G granulocytes exert in the tumour microenvironment.

Given the observed increased infiltration of tumour-associated Ly6G granulocytes after BEV administrations *in vivo*, I assessed the activity of these cells using a Ly6G+ depletion antibody. Two groups (PBS-treated and BEV-treated) received intraperitoneal injections of anti-Ly6G, while the other two groups received an isotype control, IgG2A. Ly6G+ cells were depleted 24 hours before the first BEV administration to prevent any BEV-induced expansion and activation of Ly6G+ cells. Due to the rapid turnover of Ly6G granulocytes, anti-Ly6G treatments were administered every two days. Successful depletion was confirmed (**Figure 5.4D**) by flow cytometry as <1% Ly6G-positive cells were detected in anti-Ly6G-treated blood samples compared to the isotype controls.

Depletion of Ly6G+ cells in both PBS and BEV groups led to reduced tumour volumes, aligning with studies such as Valencia et al. (2021). Findings suggest that Ly6G granulocytes in control mice may have a pro-tumorigenic role, potentially promoting B16-F10 primary tumour growth. Consistent with our prior findings, BEVs (with isotype control) resulted in significant reductions in tumour volumes (from day 9 until resection, seen in **Figure 5.4B**). Interestingly, our previous data showed increases in tumour-associated Ly6G+ cells following BEV administrations, demonstrating the complex function of Ly6G cells in the tumour microenvironment. Various factors, including cytokine and chemokine levels from immune and tumour-associated cells, influence the function of Ly6G+ cells. BEVs may alter the

immune landscape within the tumour and potentially interact directly with Ly6G+ cell receptors, promoting an anti-tumorigenic phenotype. This idea is further supported by the observation that there was no additive effect when BEVs were combined with anti-Ly6G, suggesting that BEVs exert their protective effects through a Ly6G+ cell-driven mechanism.

The percentage of myeloid (CD11b+) cells relative to total immune (CD45+) cells in the blood did not significantly change between groups despite Ly6G+ depletion. However, groups receiving anti-Ly6G+ treatment showed an increased ratio of Ly6C+ monocytes. In the anti-Ly6G+ groups, BEV-treated mice exhibited significantly higher levels of blood Ly6C+ cells, possibly indicating that when Ly6G cells are absent, BEVs enhance Ly6C recruitment. There were no significant differences in tumour volumes between the two Ly6G depleted groups, despite this increase in Ly6C cells, indicating that these BEV-induced Ly6C cell infiltrations have no effect on tumour growth. Effects of Ly6G depletion on immune cells within the tumour microenvironment could not be assessed due to limited size of tumour samples, and thus insufficient number of cells for flow cytometry.

Spleen weight, as a percentage of body weight, was compared to assess inflammation and other conditions. Spleens in the BEV plus anti-Ly6G group were significantly enlarged compared to the respective isotype control, likely due to neutrophil depletion, as neutrophils contribute to clearing old/damaged red blood cells and pathogens in the spleen. BEVs alone did not result in spleen enlargement, suggesting that BEVs do not induce chronic or severe inflammation that could impair organ function and tissue homeostasis.
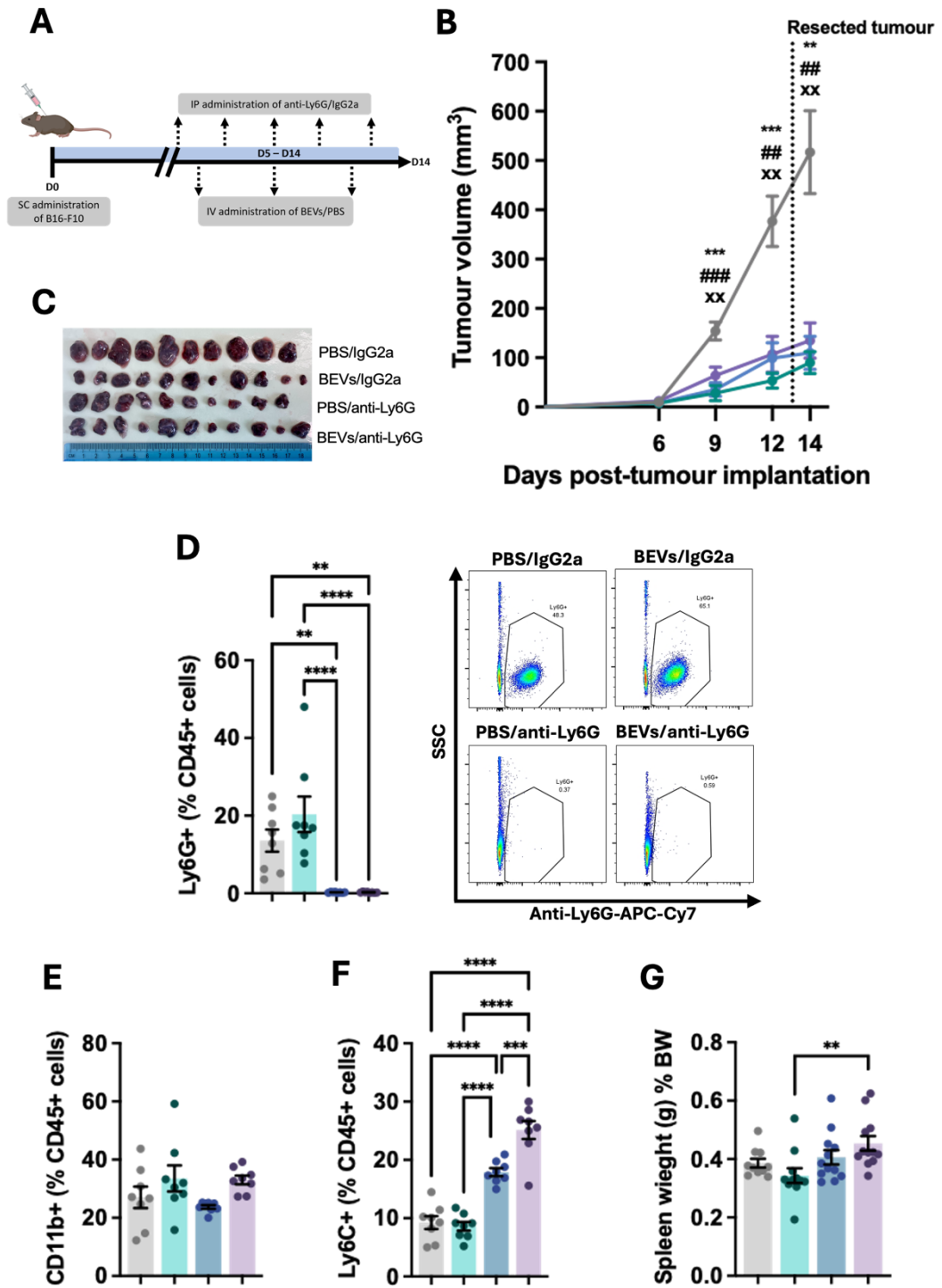
Figure 5.4 Depletion of Ly6G+ granulocytes in vivo inhibited the growth of B16-F10 melanoma tumours. Despite prior increases in tumour-associated Ly6G+ cells, administration of BEVs also resulted in a reduction in B16-F10 tumour growth. Combining Ly6G depletion with BEV administration did not exert any additive effect, suggesting that BEVs may polarise Ly6G+ cells towards an anti-tumorigenic phenotype to confer their benefit. (A) Illustration of B16-F10 melanoma model. Tumour cells were subcutaneously injected (day 0), and anti-Ly6G antibody or the associated isotype control (IgG2a) was injected intraperitoneally on day 5, one day before BEV administrations commenced (day 6). Anti-Ly6G/IgG2a was administered every 2 days and BEVs/PBS every 3 days, before mice were sacrificed (day 14). (B) Average tumour volumes (mm^3) (+/- SEM) in live mice (days 6, 9 and 12) and on resected tumours (day 14) in PBS/IgG2a (n=10); BEVs/IgG2a (n=11); PBS/anti-Ly6G (n=10); BEVs/anti-Ly6G (n=11). Two-way ANOVA was performed with Tukey's multiple comparisons test. "*" denotes the difference between PBS/IgG2a and BEVs/IgG2a. "#" denotes the difference between PBS/IgG2a and PBS/anti-Ly6G. "X" denotes the difference between PBS/IgG2a and BEVs/anti-Ly6G. **/##/xx p<0.01, ***/### p<0.001. (C) Image of resected tumours in each treatment groups. Tumour volumes were measured by tumour width^2 X tumour length X 0.52. (D) Ly6G+ cells were quantified in the blood from each treatment group by flow cytometry (n=8/group). Dot plot visually confirms Ly6G depletion in representative samples in anti-Ly6G groups compared to isotype controls. Quantification by flow cytometry of (E) total myeloid cells (CD11b-positive) and (F) monocytes (Ly6C-positive) out of total immune cells (CD45-positive) in blood from each treatment group (n=8/treatment). Bars represent average percentage immune population (+/-SEM). Two-way ANOVA was performed with Tukey's multiple comparisons test. Statistical significance is denoted by ** (p<0.01), *** (p<0.001), **** (p<0.0001). (G) Resected spleens were weighed (grams) and expressed as a percentage of the corresponding total body weight (BW). Ordinary one-way ANOVA was performed with Tukey's multiple comparisons test. Statistical significance is denoted by ** (p<0.01).

5.5 BEVs MODIFY CELL MARKER EXPRESSION ON BONE MARROW CELLS.

The bone marrow harbours a large repertoire of immune cells, including a significant proportion of Ly6G+ granulocytes, and is primarily comprised of immature cells that can differentiate into mature immune cells. After maturation, immune cells enter circulation and migrate systemically, including to the tumour site.

To investigate whether *Bif*210 BEVs could activate and polarise bone marrow-derived immune cells, murine bone marrow cells were incubated with BEVs (10^9 dose) for five hours. Flow cytometry analysis revealed a significant polarisation towards CD11b+ Ly6G+ cells (depicted in **Figure 5.5**). In control-treated cells, approximately 10% of total immune cells were CD11b+ Ly6G+, whereas this percentage increased to almost 60% in samples incubated with BEVs. Additionally, there was a notable increase (>40%) in the expression of the adhesion marker, ICAM-1, on these Ly6G+ cells after BEV incubation. Studies such as Woodfin et al. (2016) found that ICAM-1 expression regulated neutrophil effector function. In

the context of cancer, enhanced ICAM-1 expression is associated with N1 neutrophils, a subset known for their anti-tumorigenic properties (Ohms et al., 2020). This could mean BEVs not only promote granulopoiesis, the process of granulocyte maturation and proliferation in the bone marrow, but also BEVs may modify Ly6G effector function and inflammatory pathways.
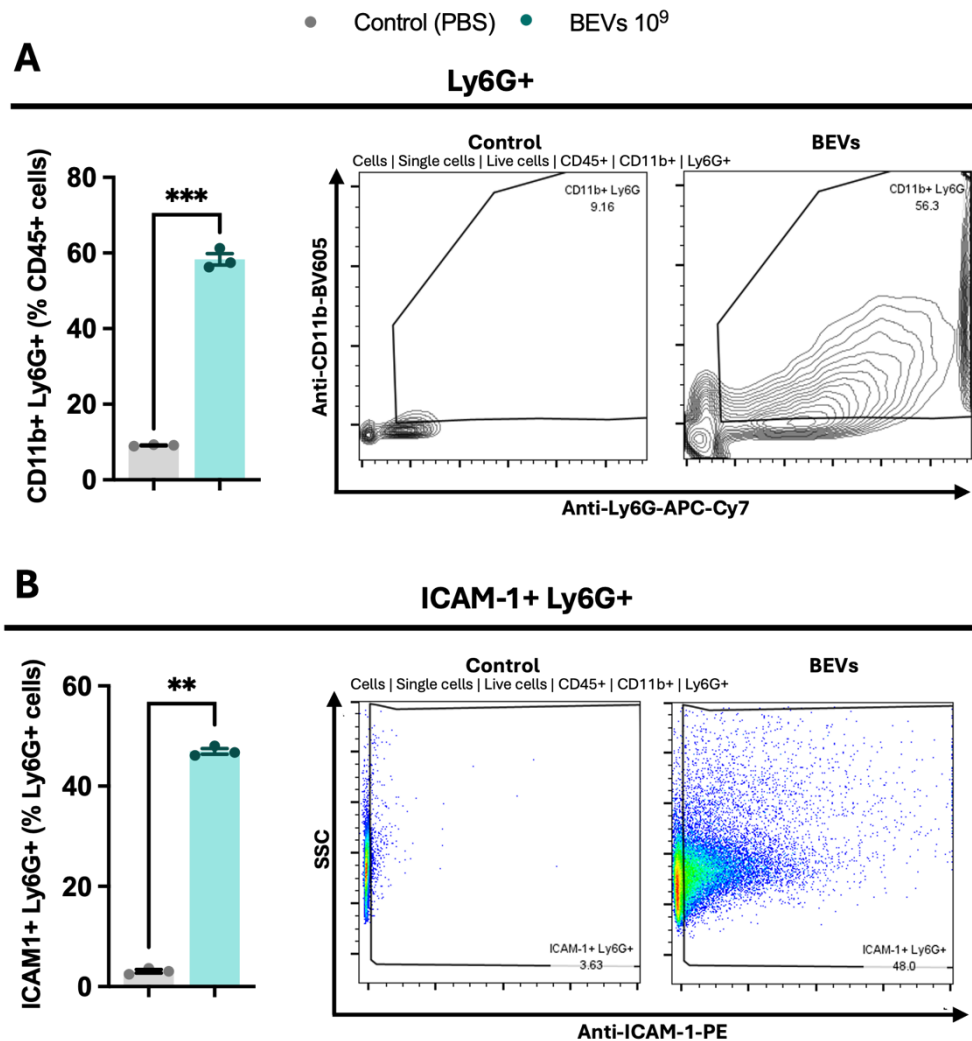
Figure 5.5. Differential expression of markers on bone marrow derived immune cells upon exposure to *Bif*210 BEVs. Bone marrow cells ($1 \times 10^6/100$ µL) isolated from C57BL/6 mice (n=3) were either incubated with PBS (control) or BEVs (final concentration 10^9) for five hours then cellular marker expression was assessed by flow cytometry. (A) Bars represent average (+/- SEM) CD11b-positive, Ly6G-positive cells as a percentage of total immune cells (CD45-positive). Contour plot demonstrates the shift in CD11b+ Ly6G+ cells in a representative BEV-treated sample compared to the corresponding control. (B) Bars represent average (+/- SEM) ICAM-1-positive, Ly6G-positive cells as a percentage of total Ly6G-positive cells. Dot plot demonstrates the shift in ICAM-1 expression in a representative BEV-treated sample compared to the corresponding control. Two-tailed paired T tests were performed, and statistical significance is denoted by *** ($p < 0.001$), **** ($p < 0.0001$).

5.6 FURTHER WORK IS REQUIRED TO ASSESS CELL MARKER EXPRESSION ON TUMOUR-ASSOCIATED LY6G+ GRANULOCYTES *IN VIVO.*

As I have demonstrated that BEVs are associated with differential marker expression on bone marrow-derived Ly6G+ cells *ex vivo,* I wanted to assess whether BEVs modified tumour-associated Ly6G+ cell marker expression *in vivo*. Marker expression on immune cells in tumours from PBS- or BEV-treated mice in a melanoma experiment previously described, were analysed by flow cytometry. Expression of ICAM-1 and ARG1 were quantified as these represent anti-tumourigenic and pro-tumourigenic Ly6G+ cell functions, respectively. In recent years, the cytosolic enzyme, ARG1, has gained a lot of attention as a key driver of immunosuppression on myeloid derived suppressor cells (MDSC), which leads to impaired T cell function (Su et al., 2021). High ARG1 expression has been a prognostic factor for worse clinical outcome in numerous cancer types (Grzywa et al., 2020). Results showed that there were no changes in cell marker expression levels on Ly6G cells in BEV- and PBS-treated mice (**Figure 5.6**). Of note, it is important to highlight that BEVs were administered on days 6, 9 and 12, then tumours were harvested on day 14. Ly6G granulocytes are extremely short lived, with a half-life of 13.7 hours in mice (Pillay et al., 2010). Therefore, the 2-day gap may have resulted in a loss of the polarising activity of the BEVs.
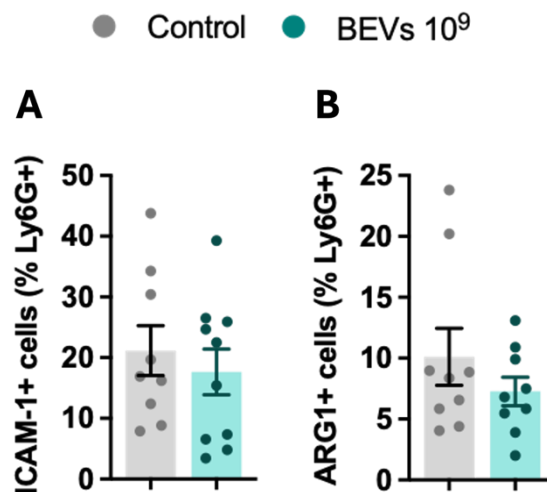
Figure 5.6 No differences in key marker expression on Ly6G+ granulocytes in tumours after BEV exposures. Mice were administered PBS/BEVs 6, 9 and 12 days post-B16-F10 cell subcutaneous injection then tumours harvested on day 14. Flow cytometric analysis on B16-F10 tumours identified (A) Intercellular Adhesion Molecule 1 (ICAM-1)-positive Ly6G cells and (B) the cytosolic enzyme, ARG1-positive Ly6G cells as a percentage of total Ly6G-positive granulocytes.

5.7 METABOLIC ACTIVITY OF BONE MARROW CELLS INCREASED WITH BEV INCUBATION BUT WAS UNALTERED IN TUMOUR CELLS CULTURED WITH BEV-TREATED BONE MARROW CELLS.

As I have shown enhanced polarisation of CD11b+ Ly6G+ cells in the bone marrow after BEV exposures, I sought to further examine whether BEVs may affect this integral component of the immune system. I employed an MTS assay to assess the metabolic activity of bone marrow cells incubated for five hours with either PBS (control) or BEVs. In the MTS assay, BEVs significantly enhanced bone marrow cell metabolic activity (as seen in **Figure 5.7A**). Enhanced cell metabolic activity is indicative of immune cell activation, which ultimately leads to increased cellular migration and proliferation factors. From the MTS results it was therefore likely that BEVs stimulated haematopoiesis. Taken together with the previous findings that BEVs induced Ly6G+ expression on bone marrow cells, this supports the idea of increased Ly6G+ stores, which could be responsible for increased infiltration into the tumour. The MTS assay was performed on all cells within the bone marrow therefore it cannot be concluded whether Ly6G cells experienced increased cell metabolic activity, however, Ly6G cells contribute to a considerable proportion of bone marrow cells.

As I previously hypothesised BEVs polarise Ly6G granulocytes to an anti-tumourigenic phenotype, evident with our findings of increased expression of the N1 marker, ICAM-1, I wanted to assess the cell viability of B16-F10 tumour cells co-cultured with bone marrow cells incubated with PBS (control) or BEVs. There was no difference in cell viability, assessed by MTS assay (**Figure 5.7B**). However, bone marrow-derived cells may lack the tumour killing abilities compared to fully mature immune cells polarised by growth factors in the tumour microenvironment.
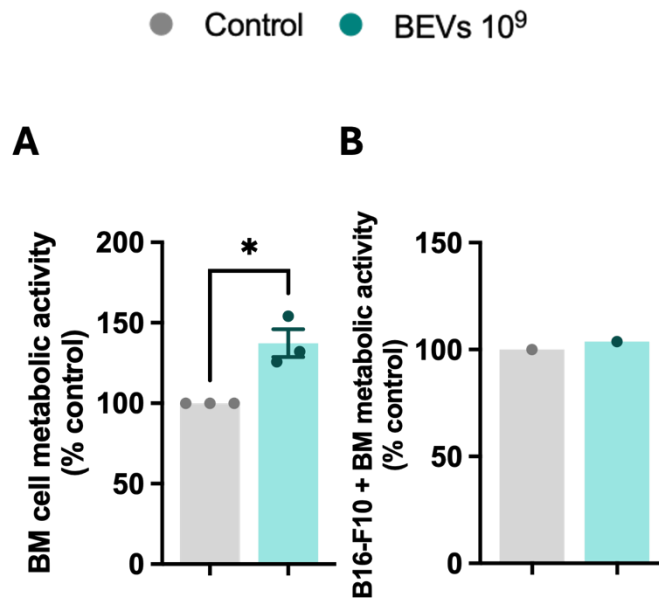
Figure 5.7 *Bif*210 BEVs increased cell metabolic activity of bone marrow cells but had no effect on priming bone marrow cells to have anti-cancer activity. (A) Bone marrow cells ($1 \times 10^6/100$ µL) isolated from C57BL/6 mice (n=3) were either incubated with PBS (control) or BEVs (final concentration 10^9) for five hours then MTS assay was performed to assess cell metabolic activity (in replicates of 3). Bars represent average cell metabolic activity (+/-SEM) expressed as a percentage of optical density (OD) at 492 nm of BEV-treated cells to OD of control cells (PBS-treated). (B) MTS assay on B16-F10 and murine bone marrow cell co-cultures incubated with either PBS (control) or (BEVs) for five hours (averaged over 5 replicates). Bars represent average cell metabolic activity (+/-SEM) expressed as a percentage of optical density (OD) at 492 nm of BEV-treated cells to OD of control cells (PBS-treated). Two-tailed paired T test was performed, and statistical significance is denoted by * ($p<0.05$).

5.8 BEVs INDUCE PRODUCTION OF CYTOKINES INVOLVED IN Ly6G+ GRANULOCYTE BIOLOGY

Cytokines and chemokines, produced by many different cell types, including immune cells and tumour-associated cells, orchestrate immune responses and migration of immune cells to the tumour. I hypothesised that BEVs may be modulating cytokine and chemokine levels that in-turn influence Ly6G polarisation. To test this, our collaborator, Anne Jordan (Unpublished thesis, 2024, Quadram Institute Bioscience, UK), quantified various cytokines involved in Ly6G responses using Enzyme Linked Immunosorbent Assays (ELISAs). To explain the increases in tumour-associated Ly6G+ cells, we measured levels of the neutrophil-attracting chemokines: KC (mouse source) and IL-8 (human source), produced by various immune cell types. Murine spleenocytes produced significantly elevated levels of KC after BEV incubation, surpassing levels induced by the strong immune

stimulator, lipopolysaccharide (LPS) (as seen in **Figure 5.8A**). Similarly, macrophages differentiated from the human leukaemia monocytic cell line, THP-1 cells, as well as reporter THP-1 monocytes showed increased production of the human equivalent, IL-8, following BEV incubation, although to a lesser extent compared to LPS (as seen in **Figure 5.8B**).

The polarisation of Ly6G+ cells, and thus their activity in the tumour microenvironment, is influenced by numerous cytokines. TNFα, for instance, has been demonstrated to prime Ly6G+ cells toward a tumour-suppressive phenotype (Comen et al., 2016). Our findings show that *Bif*210 BEVs stimulated higher levels of TNFα production from human peripheral blood mononuclear cells (PBMCs) compared to LPS. PBMCs are a collection of immune cells with a mononucleated nucleus and include lymphocytes (T cells, B cells, and natural killer cells), monocytes, and dendritic cells. However, of note, it is important to consider that cells were isolated from healthy humans. PBMCs from cancer patients, and thus challenged with tumour antigens, may respond differently to BEV exposures.
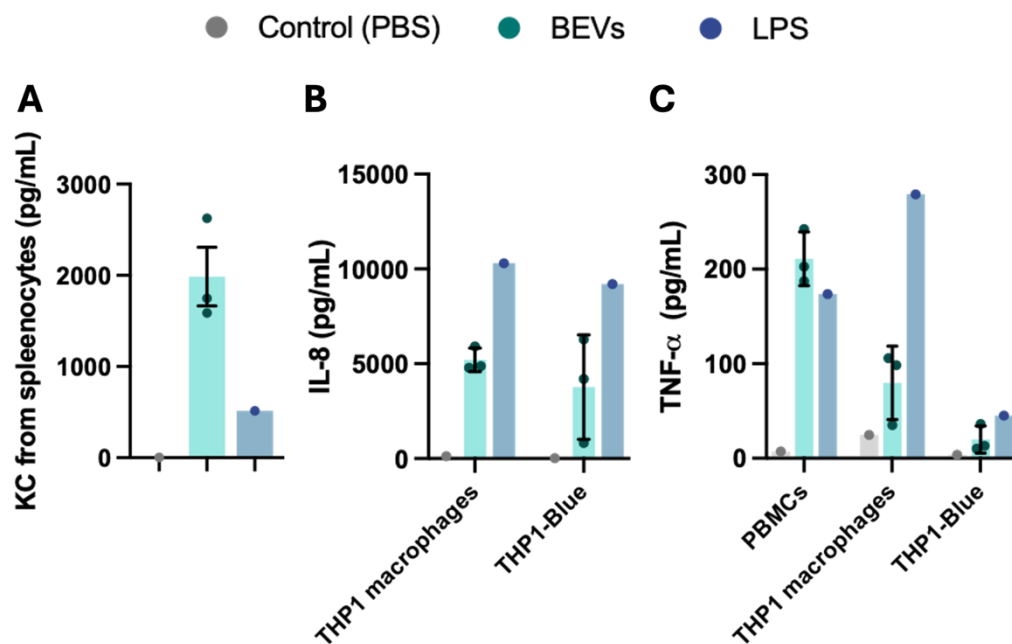
Figure 5.8 BEVs induce production of KC/IL-8 and TNF-α from numerous immune cell types. Immune cell-types were incubated with PBS (control), BEVs (1×10^{10} per well), or positive control (10% LPS at 200 ng/mL) for 24 hours and cytokines were quantified in cell-free supernatant using Enzyme Linked Immunosorbent Assays (ELISAs). Bars represent average level (pg/mL) (+/- SEM) of (A) keratinocyte-derived cytokine (KC) from murine spleenocytes and (B) IL-8 and (C) tumour necrosis factor- alpha (TNF-α) from macrophages derived from THP1 cells, and THP1-XBlue™ (human monocyte cell line with reporter for NFκB/AP-1). TNF-α from human peripheral blood mononuclear cells (PBMCs) was also quantified.

5.9 BEVs ACTIVATE TOLL-LIKE RECEPTOR 2 (TLR2) IN A DOSE-DEPENDENT MANNER.

TLR2, a receptor found on various immune cell types, including Ly6G+ granulocytes, recognises conserved pattern-associated molecular patterns (PAMPs) on microbiological agents. As discussed, specific bacterial products can activate distinct TLRs. *Bifidobacterium*, a Gram-positive bacterium, have cell walls composed of components such as peptidoglycan and lipoteichoic acid, which are known TLR2 activators. Given that BEVs contain cell wall components, I examined whether *Bif*210 BEVs elicit a TLR2 response using a reporter cell line (HEK-Blue™-hTLR2 cells). LPS, a common activator of TLR4, is present in Gram-negative bacteria but absent in Gram-positive. To confirm that BEVs were free from bacterial contaminants, the TLR4 reporter cell-line, HEK-Blue™-hTLR4, was also tested. Results in **Figure 5.9C** confirmed that BEVs were free from Gram-negative bacteria-derived contaminants. Thus, the observed modulations in immune responses are most likely attributable to the biological activity of purified *Bif*210 BEVs. This finding enhances the safety profile of these BEVs, as LPS, a potent endotoxin, is known to trigger immune dysregulation and conditions such as sepsis.

Our findings in **Figure 5.9A** confirm that *Bif*210 BEVs (from 10^9/mL) activate TLR2 through a dose dependent manner. The highest BEV dose (10^{11}/mL) was able to induce a stronger TLR2 response than the positive control (LTA derived from *Bacillus subtilis*). The dose used in our *in vivo* experiments (10^{10}/mL) displayed similar levels of activation as LTA. Therefore, BEVs are likely to activate the transcription factors, NF-κB and AP-1, in the TLR2 signaling pathway that orchestrate pro-inflammatory responses, such as production of cytokines and chemokines.

TLR2 signalling has been shown to display a positive feedback mechanism, by which expression of TLR2 increases upon activation, amplifying pro-inflammatory responses (J et al., 2021). To examine whether BEVs were activating Ly6G cells through a TLR2-dependent mechanism, expression of TLR2 on total Ly6G cells was quantified by flow cytometry. Bone marrow-derived Ly6G+ granulocytes that were incubated with BEVs for five hours had significantly upregulated expression of TLR2, as **Figure 5.9B** shows that TLR2 expression in BEV-treated Ly6G cells were around 20% higher than control-treated.

A

HEK-Blue™-hTLR2

B

C

HEK-Blue™-hTLR4

Control
BEVs (10^{10}/mL)
+Ve Control
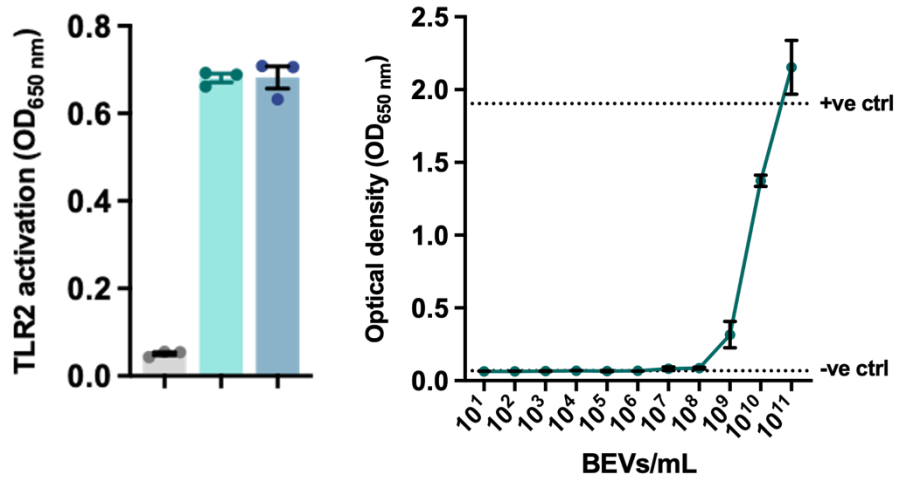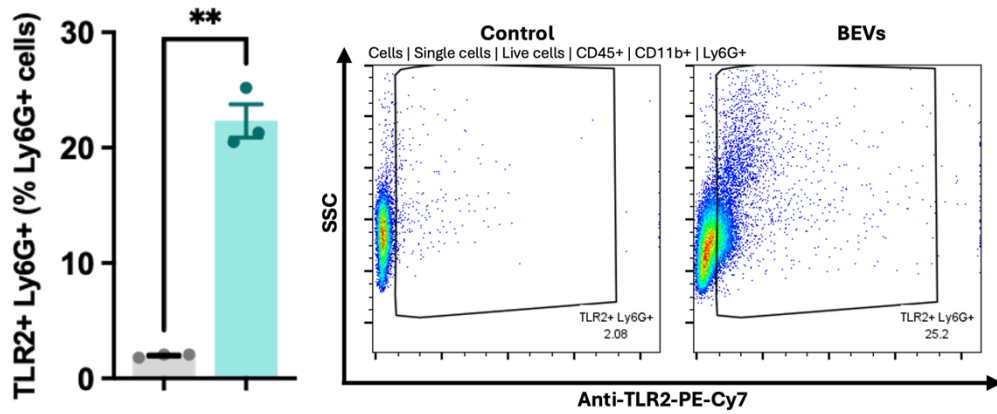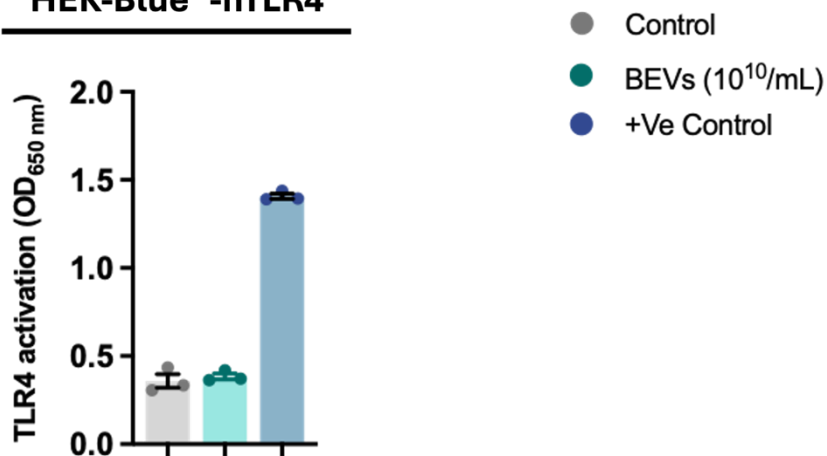
Figure 5.9 *Bif*210 BEVs specifically activate toll-like receptor 2 (TLR2) and upregulate expression on bone-marrow derived Ly6G+ cells. (A) Toll-like receptor 2 (TLR2) activation in human embryonic kidney reporter cell-line, HEK-Blue™-hTLR2, after incubation with PBS (control), BEVs at concentrations indicated, and *Bacillus subtilis* lipoteichoic acid (LTA-BS) for the positive control. Bars represent mean (+/-SEM) optical density at 650 nm (N=3) which is proportional to level of TLR2 activation. (B) TLR2 expression on bone marrow-derived Ly6G+ cells were assessed by flow cytometry after five-hour incubation with PBS (control) or BEVs (10^{10}/mL). Dot plots display the shift in TLR2-positive Ly6G+ granulocytes when stimulated with *Bif*210 BEVs. Unpaired T test was performed, and statistical significance is denoted by ** (P<0.01). (C) *Bif*210 BEVs did not activate toll-like receptor 4 (TLR4) in human embryonic kidney reporter cell-line, HEK-Blue™-hTLR4, after 24-hour incubation. BEV-mediated immune responses are therefore not due to Gram-negative bacterial contaminations. Bars represent mean (+/-SEM) (N=3) optical density at 650 nm which is proportional to level of activation. Lipopolysaccharides (LPS) was used as a positive control.

5.10 BEVS ARE UNLIKELY TO INDUCE NETOSIS.

TLR2 activation in certain instances can induce Ly6G granulocytes to release neutrophil extracellular traps (NETs) in a process known as NETosis (Cacciotto et al., 2016). This process involves a breakdown of the nuclear envelope and chromatin decondensing. Granular proteins, such as myeloperoxidase (MPO) and elastase, subsequently mix with genetic material, which is then released through cellular pores. NETosis has been shown to accelerate tumour progression and facilitate metastasis. To investigate whether *Bifidobacterial* BEVs induce NETosis, I performed several experiments, assessing MPO activity and quantifying extracellular DNA release by flow cytometry with SYTOX green staining.

There were no differences in MPO activity in B16-F10 tumours from BEV-stimulated mice compared to control (PBS) (as seen in **Figure 5.10A**). Of note, the final BEV administration occurred 24 hours before sacrifice, which was shortened from the previously implemented routine of 48 hours. However, assessing MPO activity at timepoints closer to the final BEV administration may need to be investigated due to the short half-life of granulocytes. However, blood isolated from C57BL/6 mice incubated with BEVs *ex vivo* for five hours also showed no differences in MPO activity, as seen in **Figure 5.10B**. Taken together, this suggests that BEVs do not stimulate MPO release.

To further assess NETosis in the presence of BEVs, I incubated bone marrow cells with BEVs and stained with SYTOX Green to assess extracellular DNA release. BEV-treated cells had significantly fewer SYTOX Green-positive cells compared to control (PBS-treated) cells. In contrast, the positive control, cells treated with phorbol-12-myristate-13-acetate (PMA), significantly increased extracellular DNA release, which is indicative of immune cell activation and cell death. The reduction

in SYTOX Green-positive cells with BEV treatment may also suggest increased cell viability, which aligns with results obtained from the MTS assay (**Figure 5.7**). Taken together, there was no evidence to suggest *Bif*210 BEVs induce NETosis in tumours, blood, or bone marrow-derived immune cells.
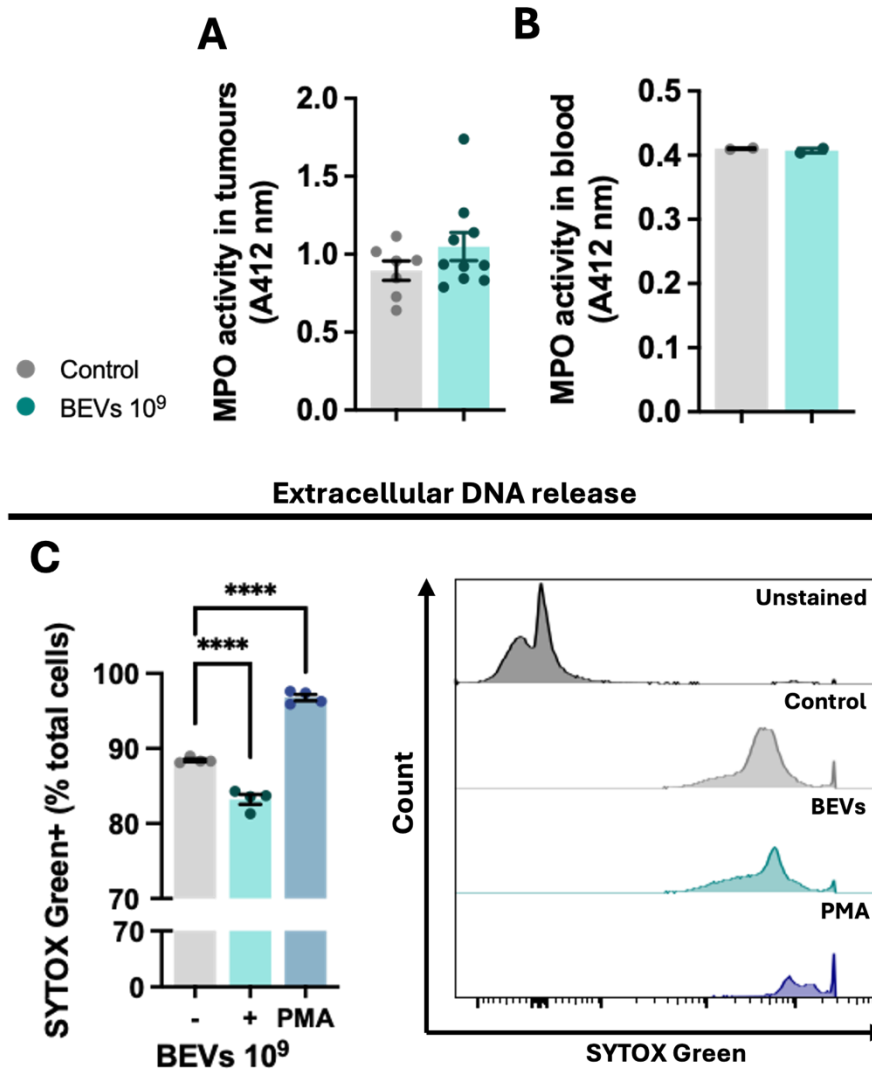
Figure 5.10 BEVs are unlikely to trigger the release of neutrophil extracellular traps (NETs) in B16-F10 tumours, mouse blood, and bone marrow cells. (A) Myeloperoxidase (MPO) activity was measured using a colorimetric assay kit in B16-F10 tumours from mice treated with either PBS (n=7) or BEVs (n=10). (B) MPO activity was also assessed in mouse blood samples (n=2) incubated with either PBS (control) or BEVs (10^9 dose) *ex vivo.* Bars represent mean absorbance (A412 nm) values (+/-SEM), which are proportional to MPO activity. (B) Extracellular DNA release from murine bone marrow cells was evaluated by flow cytometry. Bars represent the mean percentage of SYTOX Green-positive cells (+/-SEM) out of total cells (n=4). One-way ANOVA with Dunnett's multiple comparisons test was performed and statistical significance is denoted with **** ($p < 0.0001$).

5.11 Fluorescence-activated cell sorting (FACS) Ly6G+ granulocytes from tumours and blood for characterisation requires further optimisation.

Our previous findings have shown that BEVs modulate cellular marker expression on bone marrow-derived Ly6G granulocytes, therefore it was vital to assess the polarisation of tumour-associated Ly6G granulocytes in the presence of BEVs. It was hypothesised that BEV-treated Ly6G cells had a distinct transcriptome and functional activity, as we have previously shown BEV-associated increases in cytokines and chemokines (**Figure 5.8**). The aim therefore was to isolate Ly6G granulocytes from tumours from PBS- and BEV-treated mice. To do this, tumours were harvested, and a single cell suspension was prepared as previously described, under sterile conditions to prevent immune activation. To further optimise the method, a CD45+ bead positive selection step was employed pre-antibody staining to increase the proportion of immune cells. CD45-positive bead enrichment was successful as >90% of live cells were CD45+ (**Figure 5.11A**). Despite around a quarter of all CD11b+ (myeloid) cells being Ly6G+, FACS only yielded around 3000 Ly6G cells in total. RNA extraction on isolated cells accrued very low concentrations (1.2 ng/μL), therefore further analysis could not be performed. As sample preparation obtained less than 50% live cells, further optimisation to reduce cell death is also required. Allowing tumours to grow larger would also yield more cells. In addition, a Ly6G+ bead positive selection could be performed.

Isolation of Ly6G granulocytes from blood was also performed (as seen in **Figure 5.11B**), as the vast majority of granulocytes in the blood are mature. The blood also has a higher frequency of CD45+ cells compared to B16-F10 tumours therefore assumed to yield more granulocytes. Compared to the previous attempt to isolate tumour-associated cells, a higher quantity of cells are required for *ex vivo* BEV assays, including tumour cell co-cultures. Around 20,000 CD11b+ Ly6G+ cells were isolated from the blood. Extraction of cellular proteins for Western blots, microscopy, co-cultures with tumour cells and plate-based assays required >20,000 cells, therefore additional optimisation steps to the isolation method is required. For example, a positive selection for Ly6G+ cells using a bead enrichment kit could be incorporated.
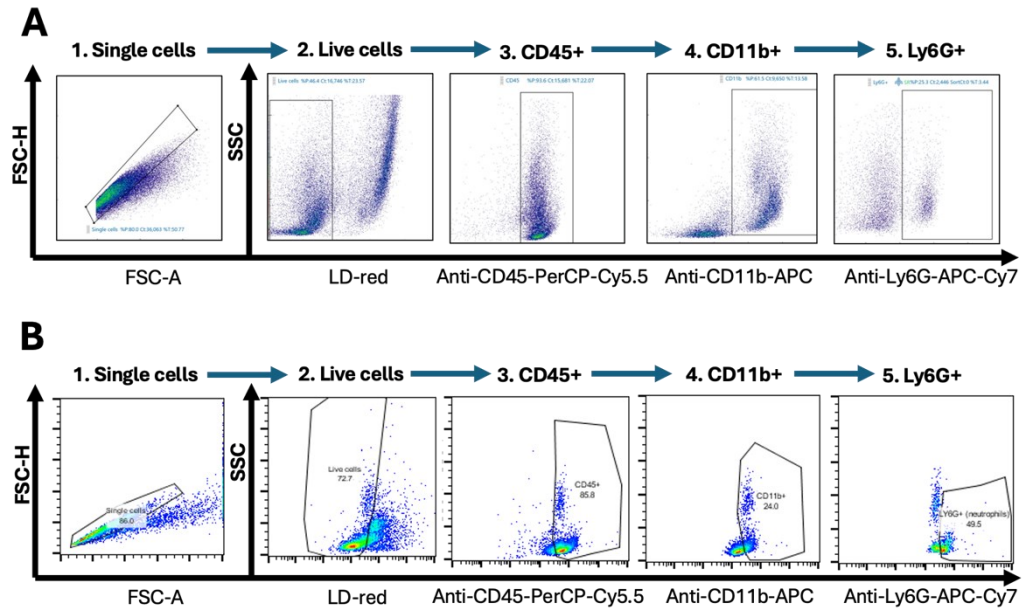
Figure 5.11 Attempt to isolate Ly6G+ cells from B16-F10 tumours and murine blood. Gating strategy for single cell suspensions from (A) B16-F10 tumours using the Bigfoot spectral cell sorter (Invitrogen) and (B) blood using the SONY SH800 cell sorter. Ly6G+ cell isolation was optimised by using a CD45 positive bead enrichment step in (A). Cells were first gated by forward scatter area (FSC-A) vs forward scatter height (FSC-H) to identify single cells; Live/Dead Red-negative for live cells; CD45-positive for immune cells; CD11b-positive for myeloid cells; and Ly6G-positive for Ly6G+ granulocytes.

5.12 *BIF*210 BEV ADMINISTRATION HAS FEW EFFECTS ON METASTATIC BURDEN AND TUMOUR-ASSOCIATED ANGIOGENESIS DESPITE INCREASED INFILTRATION OF Ly6G+ GRANULOCYTES.

As previously discussed, the role Ly6G+ granulocytes play in the context of cancer is complex and research is often contradictory. There has been mounting research to suggest Ly6G+ granulocytes support metastasis by releasing extracellular components to facilitate tumour cell dissemination and shaping the premetastatic niche. To further support metastasis, neutrophils have also been shown to release blood vessel stimulating products such as VEGF and MMPs. Angiogenesis is crucial for tumour cell circulation and dissemination to surrounding tissues and organs. As results have previously shown BEV-associated increased infiltration of Ly6G granulocytes to the tumour, I aimed to assess whether there were any detrimental host effects because of this, including increased metastatic burden.

An experimental metastasis model that involved IV injection of B16-F10 cells was utilised. Circulating tumour cells disseminate first to the lungs then the liver, which

makes for an efficient model to assess lesion growth. BEV IV treatment began 3 days post-tumour cell injection, allowing time for tumour cells to disseminate to the premetastatic niche. As seen in **Figure 5.12A**, there were no significant differences in number of lung nodules between PBS- and BEV-treated mice. There was high intragroup heterogeneity, as the number of lung nodules exceeded 120 in one sample compared to none in another. Lungs with no metastatic nodules were included if the liver nodules were observed, confirming successful IV administration of tumour cells. Due to the liver usually being the secondary site for metastatic growth, there were fewer nodules on average than in the lung samples. As an observation, some samples had more nodules in the liver than the lung, but this could not be compared between treatments due to small sample sizes. On average, there were fewer nodules in the BEV-treated group, albeit this was not significant. To see whether BEV treatments specifically affected liver lesion growth, number of liver lesions were calculated as a percentage of total nodules however no significant differences between treatments were observed (not shown).

There were also no differences in tumour angiogenesis from PBS- and BEV-treated mice. Angiogenesis was compared by counting endomucin-positive vessels, (endomucin is an endothlelial marker), in a total of six regions of interest per tumour section (two sections per tumour).

Altogether, there is no evidence to suggest that BEV treatment affects tumour lesion growth or tumour angiogenesis, both of which drive metastasis. This observation may reinforce the hypothesis that while BEV administrations increased tumour-associated Ly6G+ granulocytes, and previous studies have indicated that these cells promote metastasis, BEVs are priming the cells to an anti-tumourigenic phenotype.
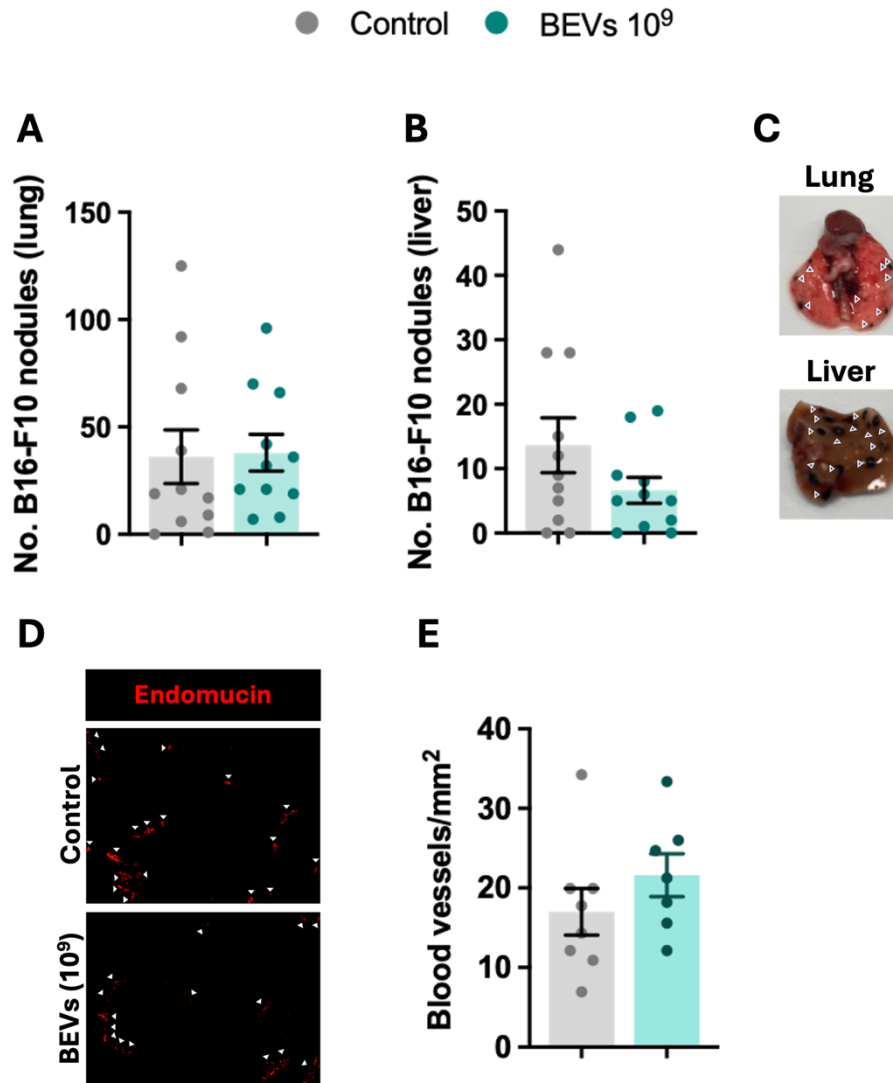
Figure 5.12 BEVs unlikely to accelerate metastasis or tumour angiogenesis. Experimental B16-F10 metastasis model - C57BL/6 mice were treated with PBS (control) or BEVs (10^9 dose). Visible B16-F10 nodules on (A) lungs and (B) liver were counted. Bars represent average (+/- SEM) number of nodules in control- (n=11) and BEV- (n=11) treated mice. (C) Images of a representative lung and liver with visible B16-F10 nodules labelled. (D) Immunofluorescence images (x20 magnification) of tumour sections stained with anti-endomucin (red). Endomucin-positive sections are labelled with white arrows and represent blood vessels. (E) Blood vessel quantification per mm^2 was the average of 3 representative ROI per tumour section with 2 sections per tumour analysed. Bars represent average blood vessels/mm^2 in tumours from control (n=8) and BEV (n=7) treatment groups.

5.13 DISCUSSION

Harnessing the full potential of microbial-based therapeutics for immunological based diseases is an exciting treatment avenue as it offers a relatively inexpensive and efficient drug production option. Cancer, a disease which has defective immune responses, has been harnessing the power of immunotherapy for over a century. The first record of immunotherapy to treat cancer was from 1891 when William Coley injected patients suffering from bone and soft tissue sarcoma with killed bacteria, *Streptococcus pyogenes* and *Serratia marcescens*. To improve the safety profile and reduce the adverse health effects, a filtered mixture of toxins from these bacteria, termed Coley's toxins, was later administered to patients. For decades Coley's toxins were administered to inoperable cancer patients in a New York clinic (Hoption Cann et al., 2003). Together with our current understanding of innate immune responses, this was the first example of how bacterial products could activate the immune system to target cancer cells. The aim was to adapt this basic principle of microbial product-induced immune activation in the treatment of cancer.

As discussed, one of the biggest obstacles in using bacterial products in cancer treatment is the overstimulation of the immune system which can cause adverse side effects. To combat this, I utilised nano-sized particles derived from the outer cell membrane, deemed bacterial extracellular vesicles from the genus *Bifidobacterium*. Members of *Bifidobacterium* are often classed as having 'probiotic' status and have far less virulence factors than non-commensal and pathogenic bacteria. Isolated BEVs from a strain of *Bifidobacterium (Bif*210*)* significantly reduced melanoma (B16-F10) tumour volumes in C57BL/6 mice in a dose dependent mechanism. Intravenous administration of BEVs at a concentration of 10^9 BEVs per mouse was concluded to be the most effective dose compared to lower doses tested.

Consistent with other research on Gram-positive bacterial products, our findings show that *Bif*210 BEVs activate innate immune responses, and thus result in increased infiltration of Ly6G granulocytes to the tumour. However, the results further confirm the complex nature of Ly6G granulocytes in relation to cancer progression. The proposed anti-cancer mechanism of *Bif*210 BEVs is that they activate immune responses that specifically polarise Ly6G granulocytes to an anti-tumourigenic phenotype, confirmed through the *in vivo* Ly6G depletion experiment. As Ly6G cells in the absence of BEVs exhibited pro-tumourigenic responses. In addition, bone marrow cellular marker expression, including increased levels of

171

ICAM-1, were observed with *ex vivo* BEV incubations. The increased production of cytokines and chemokines by various immune cells in the presence of BEVs contributes to the mechanism by which BEVs enhance Ly6G cell infiltration.

Further work to characterise tumour-associated Ly6G granulocytes after BEV exposures is, however, vital. RNA-sequencing of the isolated cells would uncover any gene expression fold changes. Importantly, BEV-primed Ly6G granulocyte-tumour cell co-cultures would be optimal for evaluating whether BEVs modulate the direct cytotoxicity of granulocytes. It would also be important to quantify cytokine and chemokines levels within the tumour, as these are key mediators that bridge the gap between innate and adaptive immunity. Further investigating whether the changes in innate immune responses feed into the adaptive response is vital. For example, CD8 T cells are among the most studied immune cells known to suppress tumour growth. Assessing the activity of tumour-associated CD8 T cells, rather than just their infiltration levels, could further elucidate the *Bif*210 BEV mechanism. Granzyme B, perforin as well as key cytokines involved in CD8 T cell polarisation such as IFNy, TNFα and IL-2, could all be quantified.

To further delineate BEV-associated Ly6G polarising mechanisms, in depth signalling pathway characterisation could be investigated. Even though BEVs, at certain doses, are strong TLR2 activators, the cellular function of this interaction and thus biological relevance in the context of tumour biology is unknown. TLR2 antagonists in the presence of BEVs could therefore be utilised *in vivo* and in cell culture-based assays. This would uncover the effects of additional immune receptor signalling pathways, including NOD-like receptors (NLRs), scavenger receptors, and C-type lectin receptors (CLRs), that all recognise conserved molecular patterns on Gram-positive bacterial cell walls (Kieser and Kagan, 2017). The type of receptor together with the specific structure and dose of bacterial stimuli tailors immune signalling pathways in cells, leading to a unique, complex immune landscape. In addition, it is important to measure cytokines such as IL-6 and chemokines shortly after BEV exposures to assess whether there is an infection-like response. However, as discussed mice had no obvious signs of distress or increased spleen weight compared to control mice. Unearthing BEV receptor signalling is vital, therefore future work could target specific pathways to either amplify or dampen immune responses.

The non-proliferative nature of Ly6G granulocytes means that assessing their activity *ex vivo* or *in vitro* is difficult/not possible. Yielding adequate cell numbers

from tumours is vital and needs to be improved by using larger tumours, as well as using different tumour models which have higher proportions of Ly6G cells.

BEVs contain molecules part of the parent bacterium's cell wall capable of stimulating immune receptors. As discussed, I have successfully shown that *Bif*210 BEVs stimulated TLR2, a common activation target of Gram-positive bacteria. However, since BEVs are non-living, there is little risk of an active infection, and their immunogenicity can be controlled by the dose administered. BEVs also contain less virulence factors than the whole bacterium. Though antibiotic resistance genes can be transferred to other bacteria, the rate is reduced compared to live bacteria (Caruana and Walper, 2020). Mice showed no obvious signs of sickness or intolerability to *Bif*210 BEVs. However, humans, and specifically cancer patients, differ in metabolism, physiological processes, and immune responses, therefore the tolerability in humans needs to be fully assessed.

As discussed in Chapter 3, the immunomodulatory effects are likely to be different depending on the species and even strain of the parent *Bifidobacterium*. To fully elucidate the *Bif*210 BEV-specific mechanism, *Bifidobacterium* BEVs from other strains could be tested and ones that do not elicit anti-tumourigenic activity compared. Comparing the different constituents of the BEV cargos by proteomic and lipidomic analysis could therefore highlight key molecules responsible for the *Bif*210-specific immune activation. If key components are identified, efforts could be made to purify and isolate them, and thus assess if they elicit similar anti-tumourigenic responses in isolation, when not in the BEV-matrix. In addition, attempts to genetically modify *Bif*210 to increase production of chosen molecules, as well reducing adverse side effects, could be employed. One study successfully deleted the gene, phosphoglycerol transferase, responsible for lipoteichoic acid (LTA) biosynthesis, in the potential probiotic, *Lactobacillus acidophilus* (Mohamadzadeh et al., 2011). Perturbations in immune responses were observed in mice, including modulations to DC and thus T cell activity. *Bif*210 could also be genetically modified to increase the rate of BEV production, increasing yields during large-scale production. Turner et al. (2015) found that targeting the *tolR* gene increased outer membrane blebbing in Gram-negative bacteria. However, since Gram-positive bacteria produce BEVs through differing mechanisms, additional research is therefore required. In addition, the high GC content in the *Bifidobacterium* genome make genetic engineering challenging.

Combing results from the BEV dose-response melanoma model with the TLR activation assay using different BEV doses, I have shown that the anti-tumourigenic-immune activity of BEVs is dose dependent, with the higher doses tested being most effective. Due to availability of isolated BEVs throughout this project, the highest dose chosen to test was 10^9 BEVs per mouse. It was unknown whether BEVs accumulated in tissues and whether they favoured certain tissues, therefore concentrations attained in tumours was also unknown. BEVs may have accumulated in tumours which is why there are consistent increases in Ly6G cells in the tumour rather than blood. To examine the physical localisation of *Bif*210 BEVs, future experiments could include administering BEVs tagged with a small reporter system such as NanoLuciferase, then assessing bioluminescence levels in various tissues.

Since Ly6G granulocytes have been implicated in facilitating metastatic lesion growth in pre-metastatic niches, it was encouraging to see that BEV administration did not increase B16-F10 metastatic lesion count in lungs and livers. This may be that *Bif*210 BEVs were not accumulating in these tissues and thus not increasing Ly6G cells. However, it may be hypothesised that Ly6G cells were primed by BEVs in a manner that did not promote metastatic growth. Further supporting this is our evidence that BEVs do not induce NETosis, a process known to drive metastasis. The release of NETs can trap circulating cancer cells, facilitating their invasion and extravasation. In addition, proteases in the NETs can degrade extracellular matrix in primary tumours, adjacent tissue as well as distant organs, which drives metastasis. As previously discussed, there are many ways to model metastasis and tail vein injections of cancer cells are good to assess metastatic lesion growth rate, but they cannot model processes involved in tumour extravasation from the primary tumour to the systemic circulation. Therefore, additional tumour resection models with BEV treatments could be utilised to fully assess metastasis pathogenesis.

Commonly prescribed cancer treatment options, chemotherapy and radiotherapy, often result in neutropenia (low neutrophil counts). The reason for this being that these treatments can damage the bone marrow, the site of Ly6G granulocyte production and maturation. Neutropenia can leave cancer patients at increased risk of infections (Lustberg, 2012). *Bif*210 BEVs may therefore offer a supportive treatment which may restore neutrophil levels by increasing their production and survival. However, the anti-tumourigenic activity of BEVs alongside these treatments is unknown. Since we hypothesise that *Bif*210 BEVs rely on the function

of Ly6G granulocytes to reduce tumour volumes, a loss of these cells may reduce treatment effectiveness. Additional pre-clinical models assessing the therapeutic response of BEVs in combination with chemotherapy and/or radiotherapy need to be assessed to aid clinical translation.

CHAPTER SIX.

6 GENERAL DISCUSSION

6.1 KEY FINDINGS

- Using murine models, *Bifidobacterium* slows primary breast tumour growth in a species-specific manner.

- *Bif*210 oral administration has little effect on the murine gut metagenome or metabolome, and there is no evidence of a tumour microbiome. A possible mechanism proposed is that *Bif*210 is directly interacting with gut mucosal immune cells.

- *Bif*210 could be used as a postbiotic, as non-viable, acid-killed *Bif*210 has been shown to reduce tumour volumes in a murine model of breast cancer.

- *Bif*210 oral administration may slow breast cancer initiation.

- No evidence to suggest that *Bif*210 offers protection for breast cancer metastasis.

- BEVs isolated from *Bif*210, and administered intravenously, slow melanoma tumour growth in mice.

- BEVs do not directly interact with tumour cells.

- *Bif*210 BEVs increased the infiltration of Ly6G granulocytes in tumours and appeared to polarise them to an anti-tumourigenic phenotype.
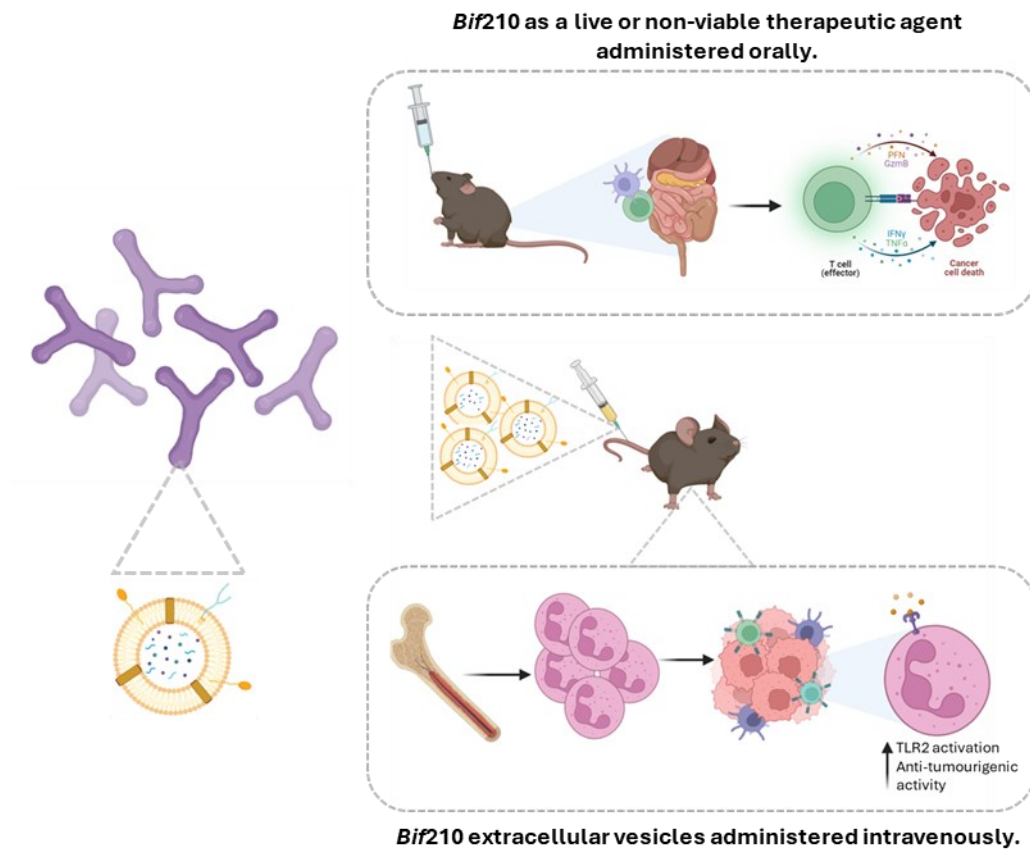
Figure 6.1. Graphical summary of the cancer therapeutic potential of a particular strain of *Bifidobacteria* (*Bif*210) and the isolated bacterial extracellular vesicles (BEVs). Murine models of breast cancer and melanoma were used and *Bif*210 or *Bif*210 BEVs were administered orally or intravenously, respectively. Key findings include treatment-induced immunomodulatory modulation. Created in part using BioRender.com.

6.2 MAIN DISCUSSION

The global cancer burden exerts immense threat to all aspects of human health, encompassing physical, emotional, societal, and economical devastation. Cancer is currently the first, or second, cause of mortality in most countries, however, a large proportion of cancer cases are proposed to be preventable (Cancer Research UK, 2019, Bray et al., 2024). Additionally, there are large discrepancies in treatment efficacy, with high variability in response rates between patients to treatments such as ICIs (Rager et al., 2022, Pavlick et al., 2023). Taken together, the overarching aim of this thesis was to develop microbial-based therapeutics to mitigate all aspects of cancer progression, including initiation, primary tumour growth, and metastasis.

Over recent years, the gut microbiome has proven to have a prominent role in cancer progression and treatment efficacy. However, the clinical success of microbiome-based therapies for the treatment of cancer and other diseases has been relatively low (Ratner, 2016, Young, 2021). To date, the only U.S. Food and Drug Administration (FDA)-approved microbiota treatments are for recurrent *C. difficile* infection (Gonzales-Luna et al., 2023). A prominent barrier to the success of microbiota-based therapies is the lack of mechanistic data. In addition, human and pre-clinical studies often use donor faecal matter, which contain an undefined consortium of bacteria that greatly differ between treatments (Baruch et al., 2021, Davar et al., 2021, Huang et al., 2022). As discussed, research has begun to focus on investigating the anti-tumourigenic effects of targeted microbiota members, such as members of the genus: *Bifidobacteria, Lactobacillus, and Akkermansia (Hibberd et al., 2017, Round and Mazmanian, 2009, Routy et al., 2018)*. Our collaborators, the Hall lab (Quadram Institute Biosciences, UK/Technical University of Munich, Germany) hold one of the largest banks of newly discovered *Bifidobacteria* strains. Our lab aimed to assess whether any of these *Bifidobacterium* strains, along with their associated microbial products, exhibited cancer-protective effects and to investigate the underlying host-modulatory mechanisms.

Our findings underscore *Bifidobacterium's* immunomodulatory effects, which play a pivotal role in cancer therapy. This chapter has showcased that the treatment potential of *Bifidobacterium* is not only limited to live bacteria, but also non-viable, structurally intact cells and bacterial extracellular vesicles. Though to fully capture *Bif*210's anti-tumourigenic effects, oral and intravenous administrations of whole cells and BEVs, respectively, were examined. The immunomodulatory

mechanisms appeared to differ. *Bif*210 oral administrations were shown to enhance CD8 T cell responses, including increasing systemic immunological memory cells in circulation. The few studies that have investigated microbial supplementation in murine cancer models, have commonly reported enhanced cytotoxic T cell responses (Viaud et al., 2013, Wang et al., 2018, Vétizou et al., 2015). On the contrary, BEVs were shown to enhance the tumour-associated myeloid cell population, Ly6G granulocytes. An *in vivo* Ly6G granulocyte depletion experiment suggested that BEVs were polarising Ly6G granulocytes to an anti-tumourigenic phenotype. Adapting myeloid cells within the TME is a relatively understudied area compared to the breadth of emerging T cell research. Iida et al. (2013) also found that microbial members influenced the function of granulocytes in mice that were receiving platinum-based chemotherapy. Granulocyte depletion reduced the production of myeloid cell–derived ROS, which were essential for the chemotherapy's anti-tumourigenic activity.

Results presented in this thesis further highlight how the high genetic diversity amongst *Bifidobacterial* strains significantly influences their immunological activity. In parallel, the study by Yoon et al. (2021) illustrates that different strains of *B. breve* exhibited varying levels of efficacy in enhancing anti-cancer immune responses in a murine colon carcinogenesis (MC38) model during chemotherapy. Similarly, a strain of *B. breve* successfully ameliorated colitis in mice receiving anti–CTLA-4 therapy but other strains of the species: *B. bifidum, B. longum, B. lactis* exerted no effects (Sun et al., 2020). Mechanistically, the study found that *B. breve* enhanced colonic Treg function during CTLA-4 blockade treatment. Strain discrepancies highlight the need for a more refined treatment approach when using microbial-based agents. There should be a focus on the desired immunomodulatory outcome and interactions with other therapies and microbial members.

Strain discrepancies also warrant the need for microbiome-based therapies to be prescribed in clinical settings. To treat a disease, such as cancer, any microbiome therapy would need approval under the appropriate legal regulatory framework. However, the ever-expanding probiotic market is large and there is currently no legal definition for probiotics in the UK (Merenstein et al., 2023). This poses the risk of patients 'self-medicating'. Numerous factors, such as the unknown host effects depending on tumour type, bacterial strain, and existing therapy regimens, pose potential health risks for over-the-counter probiotic use. An example study that reinforces this threat, found that members of the common 'probiotic' genera,

Lactobacillus, attenuated the efficacy of the cancer immunotherapeutic, CpG-oligodeoxynucleotide (Iida et al., 2013).

The effects of microbiome modification to cancer progression are likely to be dependent on cancer type. A range of murine breast cancer (BRPKp110, PyMT-Bo1 and MMTV-PyMT) and B16-F10 melanoma models were utilised for *Bif*210 and *Bif*210 BEV treatments, respectively. The breast cancer models vary in proliferation rate, immune profiles, HER2 status and, although both are ER and PR-positive, luminal B tumours often have reduced expression of these hormone receptors. The melanoma model, generally regarded as an immunogenic model, is often used to divulge mechanisms of possible cancer immunotherapeutics. The preponderance of microbiome-cancer research has focussed on gastro-associated cancers, which is why research conducted in this thesis adds valuable knowledge to the understudied microbiome-breast/melanoma cancer axis.

Importantly, identifying the differences that drive responses to microbiome interventions can add valuable insights into the cancer-protective mechanism. For example, one study found that in humans, a TLR5 polymorphism, that alters host responses to specific microbial members, influenced survival outcomes depending on tumour type (Rutkowski et al., 2015). TLR5 signalling, activated by flagellin on host microbial species, resulted in increased IL-6 levels and tumour-associated inflammation, with higher levels of MDSCs and galectin+ γδ T cells. All of which promoted tumour progression. Antibiotic administrations abrogated TLR5 signalling and therefore reduced tumour volumes. Abrogating TLR5 signalling through the use TLR5-/- mice, tumour progression was also slowed in most cases. However, tumours that were unresponsive to IL-6 had elevated tumour growth in TLR5 deficient tumour-bearing mice. Taken together this shows how the individual cytokines and polymorphisms in signalling pathways form complex interactions with implications to tumour progression. In another study, *B. pseudolongum* abundance was enriched in pancreatic ductal adenocarcinoma (PDA)-bearing mice compared to WT mice (Pushalkar et al., 2018). The study found contrasting results to ours, that being, *B. pseudolongum* accelerated oncogenesis in a TLR dependent manner whilst antibiotic use offered cancer protection (contrary to previous work in the Robinson lab, published by (McKee et al., 2021)). Taken together, these findings suggest the importance of considering tumour type, patient polymorphisms, cytokine environment, and commensal microbiota when using microbial-based interventions in cancer treatment.

The study by Pushalkar and colleagues (2018), reported the presence of a pancreatic tumour microbiome, with distinct microbial composition compared to the healthy tissue. As previously discussed, other studies have uncovered distinct microbial communities that exist within tumours, both in humans and in pre-clinical studies (Banerjee et al., 2018, Nejman et al., 2020, Smith et al., 2019). Contrastingly, the thorough investigation through culturing, qPCR, and gut permeability assessments, has shown that MMTV-PyMT breast tumours are, to our knowledge, sterile. It has therefore been hypothesised that the anti-tumourigenic effects are acting locally to the gastrointestinal tract. Taken together with the results showing that *Bif*210 supplementation exerts little modulation to the gut metagenome and metabolome, *Bif*210 is likely directly interacting with the gastro-mucosal immune cells, which is then modulating systemic, and tumour, immune responses. Some studies have postulated the contrary, being that the immunomodulatory effects are metabolite driven. One such study found that IFNγ+ CD8 T cells accumulated in the colon after administration of a live 11-strain bacterial consortium, but not when this was heat-killed, suggesting the need for metabolically active bacteria (Tanoue et al., 2019). As discussed, heat killing can denature key proteins involved in interactions with immune receptors. Our results observed anti-tumorigenic effects of non-viable *Bif*210, however, the bacteria were acid-killed, which should preserve the structural integrity of these proteins. In addition, Mager et al. (2020) suggested that the ICI enhancing effects of a *B. pseudolongum* strain was dependent on the microbial-metabolite, inosine. Inosine was found to travel systemically, whereby it enhanced cDC-dependent Th1 cell responses.

The study by Mager et al. (2020) also demonstrated that the anti-tumourigenic effects of *B. pseudolongum* were dependent on anti-CTLA-4 therapy, as this allowed the translocation of inosine to the systemic circulation. Also, in a separate study, a mix of four *Bifidobacterium* species did not alter tumour weight compared to the control in a B16-F10 model, but had synergistic effects when combined with anti-CTLA-4 therapy (Wang et al., 2018). Our study therefore demonstrates that *Bif*210 may be modulating the immune system differently or with stronger effects, as the microbial treatment was showing anti-tumourigenic activity independently of an immunotherapy. However, from work presented in this thesis, the effects of *Bif*210 when combined with conventional cancer therapies are unknown. Other neo adjuvant therapies include chemotherapy, radiotherapy and antibiotics, all of which have been shown to induce gut dysbiosis. Will the immunomodulatory effects of

*Bif*210 and BEVs differ when combined with such therapies? As previously discussed, there are numerous studies to suggest microbial members enhance the efficacy of cancer therapies (Di Luccia et al., 2024, Zhao et al., 2023, Vétizou et al., 2015, Iida et al., 2013, Sivan et al., 2015). On the contrary, one study found that the antitumour activity of radiotherapy was enhanced by vancomycin administration in a murine melanoma model (Uribe-Herranz et al., 2020). Vancomycin selectively targets Gram-positive bacteria, which includes *Bifidobacteria.* In the study, depletion of Gram-positive bacteria enhanced the antigen presentation ability of CD11c⁺ DCs in the TDLNs of mice that received radiotherapy. Delving deeper into the mechanism, sodium butyrate, a common Gram-positive microbial metabolite, abrogated DC antigen presentation and IFNγ and IL-12 production in mice. To fully assess the clinical translatability of *Bif*210 and BEVs, additional work should assess the immunomodulatory host effects when these microbial treatments are combined with conventional therapies.

The immunostimulatory properties of *Bif*210 and their isolated BEVs showcased in this thesis, may have unlocked potential for use as adjuvants in cancer immunotherapies. There have been numerous clinical trials testing DC-based vaccines for cancers, all with limited success (Hato et al., 2024). A significant limitation of DC vaccines has been the use of poorly immunogenic DCs. These cells often exhibit reduced expression of chemokine receptors, co-stimulatory molecules, and cytokine production, which ultimately results in inadequate or ineffective T cell activation. Combining DC-based therapies with BEVs or *Bif*210 may therefore prime DCs to enhance their immunostimulatory capabilities.

The International Agency for Research on Cancer (IARC) have expressed their concern that the cancer burden disproportionally affects people of low-socioeconomic status. For instance, breast cancer patients from countries with a high Human Development Index (HDI) have 1 in 71 chances of dying from the disease, compared to 1 in 48 patients from countries with low HDI (World Health Organization, 2024). This highlights the unmet need for treatment equality amongst patients. Compared to other cancer immunotherapies, such as ICI-blockade and CAR T-cell therapy, gut microbiota intervention is a relatively cost-effective option. Oral administrations are non-invasive, do not require trained professionals, and do not need to be taken within healthcare settings. However, as discussed, *Bifidobacteria* treatment would need to be combined alongside conventional therapies and should not replace existing therapies to save treatment costs.

The majority of the epidemiology data suggesting associations between the gut microbiome and cancer were based on non-Hispanic white subjects. Studies have shown microbiome discrepancies between different ethnic minorities. There are also differences in cancer risk amongst people from different ethnic backgrounds. Multiple common factors could be responsible for altered cancer risk, however, there could also be a direct microbiome-cancer link in certain populations. Diet, the largest microbiome influencer, varies significantly between communities. One study found distinct differences in microbial composition in the breast tumour tissue between non-Hispanic Black and non-Hispanic White women (Smith et al., 2019). However, the study had far fewer non-Hispanic Black patients, possibly skewing statistical power and meaningful results. This further highlights the need for representation of all ethnic groups in cancer-microbiome epidemiology studies and inclusion during human clinical trials.

6.3 FUTURE RESEARCH AVENUES

6.3.1 Delving into the anti-tumourigenic host effects of *Bif*210 and *Bif*210 BEVs

Future studies should delve deeper into the mechanisms by which *Bif*210 and *Bif*210 BEVs modulate host immune responses. Advanced techniques, such as scRNA-Seq and proteomics of immune cells, both in the tumour, lymphoid organs and gastrointestinal tract, could assess whether *Bif*210 and BEVs modify cellular signalling pathways and gene expression profiles. Of particular importance, techniques to isolate Ly6G cells from tumours so that downstream signalling analysis can be performed is imperative. Additionally, using organoid cultures and advanced *in vitro* models, such as gut-on-chip systems, can provide insights into how *Bif*210 and BEVs interact with cells within a specific microenvironment, for example immune cells within the lamina propria. In addition, the functional activity of gastrointestinal immune cells could be compared in *Bif*210 gnotobiotic mouse models (GF mice that have been colonized by *Bif*210, only) against GF and SPF mice. Flow cytometry and cytokine analysis could then assess the functional activity and polarisation of gastro-associated immune cells.

A remaining question that is imperative to answer is whether the gastrointestinal immune cells are travelling to the tumour microenvironment or TDLN? Transgenic Kaede mice could be used in future experiments involving immune cell tracking. The Kaede mouse model is genetically engineered to express the photoconvertible

fluorescence protein, Kaede, that changes colour (green to red) upon exposure to light of specific wavelengths (Dean et al., 2024). Photoconverted cells can therefore be tracked and the response to interventions and interaction with other cells can be monitored. The experimental premise would involve administering *Bif*210 or PBS (control) in Kaede mice post photoconversion of cells within the gastrointestinal tract. Flow cytometric analysis could then identify the proportion and marker expression of photoconverted cells in the blood, lymphoid tissues, and tumour.

6.3.2 Developing *Bifidobacterium*-based precision therapies

Recognising that different *Bifidobacterium* strains can exert distinct host effects, there is a need to develop precision microbial therapies tailored to individual patients based on their microbiomes, cancer types, treatment regimens, genetic polymorphisms and immune responses. Future research should focus on high-throughput screening of various *Bifidobacterium* strains, and their BEVs, to identify those with the most potent anti-tumour and CD8 T cell inducing effects. Similarly, Tanoue et al. (2019) utilised a screening protocol to identify an 11-strain consortium of bacteria, derived from human faecal matter, that promoted CD8 T cell responses in GF mice. Similarly, to improve the translatability potential of *Bifidobacterium* for cancer treatment, efforts could be employed to screen CD8 T cell-priming *Bifidobacterial* strains isolated from ICI responders. This is a targeted, more refined approach compared to the successful FMT clinical trials that used faecal matter from ICI responders to treat metastatic melanoma (Baruch et al., 2021, Davar et al., 2021). Additionally, once the anti-tumour mechanistic data has been revealed, strains could be genetically engineered to enhance their therapeutic properties.

6.3.3 Exploring the optimal cancer combinational therapies

As previously discussed, the interactions between *Bifidobacterium*-based therapies and existing cancer treatments should be a focus of future research. Given existing research suggesting that some bacterial strains can enhance the efficacy of immune checkpoint inhibitors, comprehensive studies are needed to understand the optimal bacterial strain and cancer therapy combinations. Additional work should also focus on finding the optimal *Bif*210/BEVs treatment regime, including timing, dosing, and potential adverse effects.

In addition, *Bif*210 supplementation did not show any effects to metastasis in the murine models, however, treating metastasis is extremely difficult. It is therefore

even more vital to assess whether *Bif*210 or BEVs could slow metastasis progression when combined with existing therapies, to assess if there is a synergistic effect.

A potential final approach could involve evaluating the therapeutic efficacy of oral administration of *Bif*210 (either live or non-viable) in combination with intravenous administration of *Bif*210 BEVs. As previously discussed, these treatments operate through distinct immunomodulatory mechanisms, targeting lymphoid and myeloid cell responses, respectively. Similarly, orally administering a defined consortium of *Bifidobacteria* strains, with distinct immunomodulatory effects, may offer additive or synergistic effects, which is why, as discussed, an immune-based screening assay of different strains would be beneficial. Our previous findings show that a 'cocktail' of *Bifidobacterial* species did not affect tumour growth, however, one of these strains, when administered independently, also did not alter tumour growth. Further highlighting the need for careful consideration of the optimal combination. The objective would be to identify a synergistic combination of *Bifidobacterium*-based therapeutics that effectively reduces tumour burden.

6.3.4   Characterising *Bifidobacterial*-derived molecules and components

We have previously hypothesised that *Bif*210, when orally administered, is acting locally in the gastrointestinal tract, which is modifying systemic and tumour-specific immune responses. It is vital to uncover the *Bifidobacterium*-derived active compound or cell wall structural component that could be activating these immune cell receptors. Amongst these cell surface components, exopolysaccharides and sortase-dependent pili have been associated with modulation to host immune responses (Alessandri et al., 2019, O'Connell Motherway et al., 2011, Ma et al., 2023, Hickey et al., 2021). The immunomodulatory properties of both also are reported to be species-specific (Gavzy et al., 2023).

Previous research has highlighted that the cargo load/composition of BEVs influence host immune responses, therefore future experiments, involving proteomic and lipidomic analysis, should assess the composition of *Bif*210 BEVs (Stentz et al., 2018, Chang et al., 2021, Caruana and Walper, 2020). It would be beneficial to compare the composition of *Bif*210 BEVs against (genetically similar) *Bifidobacterial* BEVs that exert no anti-tumorigenic activity. Key differences would highlight the molecule/s or unique molecular structure responsible for the immunomodulatory effects.

6.3.5 Additional experiments to overcome limitations in pre-clinical cancer models

The current study's limitations regarding the translation from murine models to human clinical settings highlight the need for more advanced and representative models of human cancer. Future research should invest in optimising models that better replicate human microbiome complexity, immune system function, and tumour initiation and progression. This could include humanised mouse models, patient-derived xenografts and organ-on-a-chip technology that incorporates patient-specific cells and microbiota. Animal models that more closely mimic cancer metastasis initiation and progression in humans is especially paramount. Taken together, such models could provide some predictions of how *Bifidobacterial* therapies will perform in humans prior to clinical trials.

6.3.6 Clinical trials

Ultimately, the success of microbial-based cancer therapies will depend on human clinical trials. Future efforts should focus on designing and conducting well-controlled clinical trials to evaluate the safety, efficacy, and optimal use of *Bifidobacterium* strains and BEVs for the treatment of cancer. These trials should include diverse patient populations to account for variability in microbiome composition, genetic factors, and cancer types, ensuring that findings are broadly applicable. Furthermore, long-term outcomes and side effects in patients receiving *Bifidobacterium*-based therapies should be monitored.

6.4 CONCLUSION

Our findings have showcased the therapeutic potential of a newly discovered strain of *Bifidobacteria* (*Bif*210) and their isolated BEVs for the treatment of breast cancer and melanoma, respectively. Both *Bifidobacterium*-based therapies were shown to modulate tumour-associated immune responses, by which *Bif*210 oral administration enhanced CD8 T cell activity, whilst BEVs increased the infiltration of Ly6G granulocytes. Whilst the results present a promising avenue for cancer treatment, careful consideration of strain-specific effects, potential interactions with existing therapies, and patient-specific factors are crucial for optimising clinical outcomes. In addition, this thesis has highlighted the particularly understudied area of postbiotic research in cancer therapy. Utilising non-viable *Bif*210 and *Bif*210 BEVs in clinical settings offers significant safety advantages over live bacteria, particularly for cancer patients who commonly suffer from cancer- and treatment-

related immunodeficiencies. Future research into the microbiome-cancer axis is essential to uncover immunomodulatory pathways in more detail. Uncovering the immune-driven mechanism will further develop the opportunity for treatment personalisation, with the overarching aim being to deliver safe cancer therapies with high efficacy.

7 REFERENCES.

ADAMS, S., SCHMID, P., RUGO, H., WINER, E., LOIRAT, D., AWADA, A., CESCON, D., IWATA, H., CAMPONE, M. & NANDA, R. 2019. Pembrolizumab monotherapy for previously treated metastatic triple-negative breast cancer: cohort A of the phase II KEYNOTE-086 study. *Annals of Oncology,* 30**,** 397-404.

AKIRA, S., TAKEDA, K. & KAISHO, T. 2001. Toll-like receptors: critical proteins linking innate and acquired immunity. *Nature Immunology,* 2**,** 675-680.

AL-NEDAWI, K., MIAN, M. F., HOSSAIN, N., KARIMI, K., MAO, Y. K., FORSYTHE, P., MIN, K. K., STANISZ, A. M., KUNZE, W. A. & BIENENSTOCK, J. 2015. Gut commensal microvesicles reproduce parent bacterial signals to host immune and enteric nervous systems. *Faseb j,* 29**,** 684-95.

AL-SADI, R., DHARMAPRAKASH, V., NIGHOT, P., GUO, S., NIGHOT, M., DO, T. & MA, T. Y. 2021. Bifidobacterium bifidum Enhances the Intestinal Epithelial Tight Junction Barrier and Protects against Intestinal Inflammation by Targeting the Toll-like Receptor-2 Pathway in an NF-κB-Independent Manner. *Int J Mol Sci,* 22.

ALESSANDRI, G., OSSIPRANDI, M. C., MACSHARRY, J., VAN SINDEREN, D. & VENTURA, M. 2019. Bifidobacterial Dialogue With Its Human Host and Consequent Modulation of the Immune System. *Front Immunol,* 10**,** 2348.

ALMEIDA-DA-SILVA, C. L. C., SAVIO, L. E. B., COUTINHO-SILVA, R. & OJCIUS, D. M. 2023. The role of NOD-like receptors in innate immunity. *Frontiers in Immunology,* 14.

ALSAIED, A., ISLAM, N. & THALIB, L. 2020. Global incidence of Necrotizing Enterocolitis: a systematic review and Meta-analysis. *BMC Pediatrics,* 20**,** 344.

ALTORKI, N. K., MARKOWITZ, G. J., GAO, D., PORT, J. L., SAXENA, A., STILES, B., MCGRAW, T. & MITTAL, V. 2019. The lung microenvironment: an important regulator of tumour growth and metastasis. *Nat Rev Cancer,* 19**,** 9-31.

ALVAREZ, C. S., BADIA, J., BOSCH, M., GIMÉNEZ, R. & BALDOMÀ, L. 2016. Outer Membrane Vesicles and Soluble Factors Released by Probiotic Escherichia coli Nissle 1917 and Commensal ECOR63 Enhance Barrier Function by Regulating Expression of Tight Junction Proteins in Intestinal Epithelial Cells. *Front Microbiol,* 7**,** 1981.

ALVAREZ, C. S., GIMÉNEZ, R., CAÑAS, M. A., VERA, R., DÍAZ-GARRIDO, N., BADIA, J. & BALDOMÀ, L. 2019. Extracellular vesicles and soluble factors secreted by Escherichia coli Nissle 1917 and ECOR63 protect against enteropathogenic E. coli-induced intestinal epithelial barrier dysfunction. *BMC Microbiol,* 19**,** 166.

ALVES-SANTOS, A. M., SUGIZAKI, C. S. A., LIMA, G. C. & NAVES, M. M. V. 2020. Prebiotic effect of dietary polyphenols: A systematic review. *Journal of Functional Foods,* 74**,** 104169.

ALVES, N. J., TURNER, K. B., DANIELE, M. A., OH, E., MEDINTZ, I. L. & WALPER, S. A. 2015. Bacterial Nanobioreactors--Directing Enzyme Packaging into Bacterial Outer Membrane Vesicles. *ACS Appl Mater Interfaces,* 7**,** 24963-72.

AMATYA, S. B., SALMI, S., KAINULAINEN, V., KARIHTALA, P. & REUNANEN, J. 2021. Bacterial Extracellular Vesicles in Gastrointestinal Tract Cancer: An Unexplored Territory. *Cancers* [Online], 13. [Accessed 2021/10//].

ANANIA, C., DI MARINO, V. P., OLIVERO, F., DE CANDITIIS, D., BRINDISI, G., IANNILLI, F., DE CASTRO, G., ZICARI, A. M. & DUSE, M. 2021. Treatment with a probiotic mixture containing Bifidobacterium animalis subsp. Lactis BB12 and Enterococcus faecium L3 for the prevention of allergic rhinitis symptoms in children: a randomized controlled trial. *Nutrients,* 13**,** 1315.

ANASSI, E. & NDEFO, U. A. 2011. Sipuleucel-T (provenge) injection: the first immunotherapy agent (vaccine) for hormone-refractory prostate cancer. *P t,* 36**,** 197-202.

ANDREWS, M. C., DUONG, C. P. M., GOPALAKRISHNAN, V., IEBBA, V., CHEN, W.-S., DEROSA, L., KHAN, M. A. W., COGDILL, A. P., WHITE, M. G., WONG, M. C., FERRERE, G., FLUCKIGER, A., ROBERTI, M. P., OPOLON, P., ALOU, M. T., YONEKURA, S., ROH, W., SPENCER, C. N., CURBELO, I. F., VENCE, L., REUBEN, A., JOHNSON, S., ARORA, R., MORAD, G., LASTRAPES, M., BARUCH, E. N., LITTLE, L., GUMBS, C., COOPER, Z. A., PRIETO, P. A., WANI, K., LAZAR, A. J., TETZLAFF, M. T., HUDGENS, C. W., CALLAHAN, M. K., ADAMOW, M., POSTOW, M. A., ARIYAN, C. E., GAUDREAU, P.-O., NEZI, L., RAOULT, D., MIHALCIOIU, C., ELKRIEF, A., PEZO, R. C., HAYDU, L. E., SIMON, J. M., TAWBI, H. A., MCQUADE, J., HWU, P., HWU, W.-J., AMARIA, R. N., BURTON, E. M., WOODMAN, S. E., WATOWICH, S., DIAB, A., PATEL, S. P., GLITZA, I. C., WONG, M. K., ZHAO, L., ZHANG, J., AJAMI, N. J., PETROSINO, J., JENQ, R. R., DAVIES, M. A., GERSHENWALD, J. E., FUTREAL, P. A., SHARMA, P., ALLISON, J. P., ROUTY, B., ZITVOGEL, L. & WARGO, J. A. 2021. Gut microbiota signatures are associated with toxicity to combined CTLA-4 and PD-1 blockade. *Nature Medicine,* 27**,** 1432-1441.

AQBI, H. F., WALLACE, M., SAPPAL, S., PAYNE, K. K. & MANJILI, M. H. 2018. IFN-γ orchestrates tumor elimination, tumor dormancy, tumor escape, and progression. *J Leukoc Biol*.

ARTHUR, J. C., PEREZ-CHANONA, E., MÜHLBAUER, M., TOMKOVICH, S., URONIS, J. M., FAN, T.-J., CAMPBELL, B. J., ABUJAMEL, T., DOGAN, B., ROGERS, A. B., RHODES, J. M., STINTZI, A., SIMPSON, K. W., HANSEN, J. J., KEKU, T. O., FODOR, A. A. & JOBIN, C. 2012. Intestinal Inflammation Targets Cancer-Inducing Activity of the Microbiota. *Science,* 338**,** 120-123.

ASADOLLAHI, P., GHANAVATI, R., ROHANI, M., RAZAVI, S., ESGHAEI, M. & TALEBI, M. 2020. Anti-cancer effects of Bifidobacterium species in colon cancer cells and a mouse model of carcinogenesis. *PLoS One,* 15**,** e0232930.

AVGERINOS, K. I., SPYROU, N., MANTZOROS, C. S. & DALAMAGA, M. 2019. Obesity and cancer risk: Emerging biological mechanisms and perspectives. *Metabolism,* 92**,** 121-135.

BACHEM, A., MAKHLOUF, C., BINGER, K. J., DE SOUZA, D. P., TULL, D., HOCHHEISER, K., WHITNEY, P. G., FERNANDEZ-RUIZ, D., DÄHLING, S., KASTENMÜLLER, W., JÖNSSON, J., GRESSIER, E., LEW, A. M., PERDOMO, C., KUPZ, A., FIGGETT, W., MACKAY, F., OLESHANSKY, M., RUSS, B. E., PARISH, I. A., KALLIES, A., MCCONVILLE, M. J., TURNER, S. J., GEBHARDT, T. & BEDOUI, S. 2019. Microbiota-Derived Short-Chain Fatty Acids Promote the Memory Potential of Antigen-Activated CD8+ T Cells. *Immunity,* 51**,** 285-297.e5.

BACHIER, C., BORTHAKUR, G., HOSING, C., BLUM, W., ROTTA, M., OJERAS, P., BARNETT, B., RAJANGAM, K., MAJHAIL, N. S. & NIKIFOROW, S. 2020. A phase 1 study of NKX101, an allogeneic CAR natural killer (NK) cell therapy, in subjects with relapsed/refractory (R/R) acute myeloid leukemia (AML) or higher-risk myelodysplastic syndrome (MDS). *Blood,* 136**,** 42-43.

BAHAR-TOKMAN, H., DEMIRCI, M., KESKIN, F. E., CAGATAY, P., TANER, Z., OZTURK-BAKAR, Y., OZYAZAR, M., KIRAZ, N. & KOCAZEYBEK, B. S. 2022. Firmicutes/Bacteroidetes Ratio in the Gut Microbiota and IL-1β, IL-6, IL-8, TLR2, TLR4, TLR5 Gene Expressions in Type 2 Diabetes. *Clin Lab,* 68.

BAKER, C. & MANSFIELD, Z. 2023. Cancer statistics for England. commonslibrary.parliament.uk: House of Commons Library.

BAKER, J. L., CHEN, L., ROSENTHAL, J. A., PUTNAM, D. & DELISA, M. P. 2014. Microbial biosynthesis of designer outer membrane vesicles. *Curr Opin Biotechnol,* 29**,** 76-84.

BANERJEE, S., TIAN, T., WEI, Z., SHIH, N., FELDMAN, M. D., PECK, K. N., DEMICHELE, A. M., ALWINE, J. C. & ROBERTSON, E. S. 2018. Distinct Microbial Signatures Associated With Different Breast Cancer Types. *Front Microbiol,* 9**,** 951.

BARNABA, V. 2022. T Cell Memory in Infection, Cancer, and Autoimmunity. *Frontiers in Immunology,* 12.

BARRATT, M. J., NUZHAT, S., AHSAN, K., FRESE, S. A., ARZAMASOV, A. A., SARKER, S. A., ISLAM, M. M., PALIT, P., ISLAM, M. R., HIBBERD, M. C., NAKSHATRI, S., COWARDIN, C. A., GURUGE, J. L., BYRNE, A. E., VENKATESH, S., SUNDARESAN, V., HENRICK, B., DUAR, R. M., MITCHELL, R. D., CASABURI, G., PRAMBS, J., FLANNERY, R., MAHFUZ, M., RODIONOV, D. A., OSTERMAN, A. L., KYLE, D., AHMED, T. & GORDON, J. I. 2022. <i>Bifidobacterium infantis</i> treatment promotes weight gain in Bangladeshi infants with severe acute malnutrition. *Science Translational Medicine,* 14**,** eabk1107.

BARROS, L. R. C., COUTO, S. C. F., DA SILVA SANTURIO, D., PAIXÃO, E. A., CARDOSO, F., DA SILVA, V. J., KLINGER, P., RIBEIRO, P., RÓS, F. A., OLIVEIRA, T. G. M., REGO, E. M., RAMOS, R. N. & ROCHA, V. 2022. Systematic Review of Available CAR-T Cell Trials around the World. *Cancers (Basel),* 14.

BARUCH, E. N., YOUNGSTER, I., BEN-BETZALEL, G., ORTENBERG, R., LAHAT, A., KATZ, L., ADLER, K., DICK-NECULA, D., RASKIN, S., BLOCH, N., ROTIN, D., ANAFI, L., AVIVI, C., MELNICHENKO, J., STEINBERG-SILMAN, Y., MAMTANI, R., HARATI, H., ASHER, N., SHAPIRA-FROMMER, R., BROSH-NISSIMOV, T., ESHET, Y., BEN-SIMON, S., ZIV, O., KHAN, M. A. W., AMIT, M., AJAMI, N. J., BARSHACK, I., SCHACHTER, J., WARGO, J. A., KOREN, O., MARKEL, G. & BOURSI, B. 2021. Fecal microbiota transplant promotes response in immunotherapy-refractory melanoma patients. *Science,* 371**,** 602-609.

BASAVAIAH, R. & GURUDUTT, P. S. 2021. Prebiotic Carbohydrates for Therapeutics. *Endocr Metab Immune Disord Drug Targets,* 21**,** 230-245.

BASU, A., RAMAMOORTHI, G., ALBERT, G., GALLEN, C., BEYER, A., SNYDER, C., KOSKI, G., DISIS, M. L., CZERNIECKI, B. J. & KODUMUDI, K. 2021. Differentiation and Regulation of TH Cells: A Balancing Act for Cancer Immunotherapy. *Frontiers in Immunology,* 12.

BEDARF, J. R., BERAZA, N., KHAZNEH, H., ÖZKURT, E., BAKER, D., BORGER, V., WÜLLNER, U. & HILDEBRAND, F. 2021. Much ado about nothing? Off-target amplification can lead to false-positive bacterial brain microbiome detection in healthy and Parkinson's disease individuals. *Microbiome,* 9**,** 75.

BEER, T. M., KWON, E. D., DRAKE, C. G., FIZAZI, K., LOGOTHETIS, C., GRAVIS, G., GANJU, V., POLIKOFF, J., SAAD, F., HUMANSKI, P., PIULATS, J. M., MELLA, P. G., NG, S. S., JAEGER, D., PARNIS, F. X., FRANKE, F. A., PUENTE, J., CARVAJAL, R., SENGELØV, L., MCHENRY, M. B., VARMA, A., EERTWEGH, A. J. V. D. & GERRITSEN, W. 2017. Randomized, Double-Blind, Phase III Trial of Ipilimumab Versus Placebo in Asymptomatic or Minimally Symptomatic Patients With Metastatic Chemotherapy-Naive Castration-Resistant Prostate Cancer. *Journal of Clinical Oncology,* 35**,** 40-47.

BEHZADI, E., MAHMOODZADEH HOSSEINI, H. & IMANI FOOLADI, A. A. 2017. The inhibitory impacts of Lactobacillus rhamnosus GG-derived extracellular vesicles on the growth of hepatic cancer cells. *Microb Pathog,* 110**,** 1-6.

BENDER, M. J., MCPHERSON, A. C., PHELPS, C. M., PANDEY, S. P., LAUGHLIN, C. R., SHAPIRA, J. H., MEDINA SANCHEZ, L., RANA, M., RICHIE, T. G., MIMS, T. S., GOCHER-DEMSKE, A. M., CERVANTES-BARRAGAN, L., MULLETT, S. J., GELHAUS, S. L., BRUNO, T. C., CANNON, N., MCCULLOCH, J. A., VIGNALI, D. A. A., HINTERLEITNER, R., JOGLEKAR, A. V., PIERRE, J. F., LEE, S. T. M., DAVAR, D., ZAROUR, H. M. & MEISEL, M. 2023. Dietary tryptophan metabolite released by intratumoral Lactobacillus reuteri facilitates immune checkpoint inhibitor treatment. *Cell,* 186**,** 1846-1862.e26.

BENICHOU, G., GONZALEZ, B., MARINO, J., AYASOUFI, K. & VALUJSKIKH, A. 2017. Role of Memory T Cells in Allograft Rejection and Tolerance. *Frontiers in Immunology,* 8.

BERGANTINI, L., D'ALESSANDRO, M., CAMELI, P., VIETRI, L., VAGAGGINI, C., PERRONE, A., SESTINI, P., FREDIANI, B. & BARGAGLI, E. 2020. Effects

of rituximab therapy on B cell differentiation and depletion. *Clinical Rheumatology,* 39**,** 1415-1421.

BERGHOLTZ, H., LIEN, T. G., SWANSON, D. M., FRIGESSI, A., BATHEN, T. F., BORGEN, E., BØRRESEN-DALE, A. L., ENGEBRÅTEN, O., GARRED, Ø., GEISLER, J., GEITVIK, G. A., HARTMANN-JOHNSEN, O. J., HOFVIND, S., KRISTENSEN, V. N., LANGERØD, A., LINGJÆRDE, O. C., MÆLANDSMO, G. M., NAUME, B., RUSSNES, H., SAUER, T., SCHLICHTING, E., SKJERVEN, H. K., DAIDONE, M. G., TOST, J., WÄRNBERG, F., SØRLIE, T. & OSLO BREAST CANCER RESEARCH, C. 2020. Contrasting DCIS and invasive breast cancer by subtype suggests basal-like DCIS as distinct lesions. *npj Breast Cancer,* 6**,** 26.

BEUTLER, B. 2002. Toll-like receptors: how they work and what they do. *Current opinion in hematology,* 9**,** 2-10.

BIZZARRI, M., DINICOLA, S., BEVILACQUA, A. & CUCINA, A. 2016. Broad Spectrum Anticancer Activity of Myo-Inositol and Inositol Hexakisphosphate. *Int J Endocrinol,* 2016**,** 5616807.

BLOEMEN, J. G., VENEMA, K., VAN DE POLL, M. C., OLDE DAMINK, S. W., BUURMAN, W. A. & DEJONG, C. H. 2009. Short chain fatty acids exchange across the gut and liver in humans measured at surgery. *Clin Nutr,* 28**,** 657-61.

BLOMBERG, O. S., SPAGNUOLO, L., GARNER, H., VOORWERK, L., ISAEVA, O. I., VAN DYK, E., BAKKER, N., CHALABI, M., KLAVER, C., DUIJST, M., KERSTEN, K., BRÜGGEMANN, M., PASTOORS, D., HAU, C. S., VRIJLAND, K., RAEVEN, E. A. M., KALDENBACH, D., KOS, K., AFONINA, I. S., KAPTEIN, P., HOES, L., THEELEN, W., BAAS, P., VOEST, E. E., BEYAERT, R., THOMMEN, D. S., WESSELS, L. F. A., DE VISSER, K. E. & KOK, M. 2023. IL-5-producing CD4(+) T cells and eosinophils cooperate to enhance response to immune checkpoint blockade in breast cancer. *Cancer Cell,* 41**,** 106-123.e10.

BLUMBERG, R. & POWRIE, F. 2012. Microbiota, disease, and back to health: a metastable journey. *Science translational medicine,* 4**,** 137rv7-137rv7.

BOMBERGER, J. M., MACEACHRAN, D. P., COUTERMARSH, B. A., YE, S., O'TOOLE, G. A. & STANTON, B. A. 2009. Long-Distance Delivery of Bacterial Virulence Factors by Pseudomonas aeruginosa Outer Membrane Vesicles. *PLOS Pathogens,* 5**,** e1000382.

BONFRATE, L., DI PALO, D. M., CELANO, G., ALBERT, A., VITELLIO, P., DE ANGELIS, M., GOBBETTI, M. & PORTINCASA, P. 2020. Effects of Bifidobacterium longum BB536 and Lactobacillus rhamnosus HN001 in IBS patients. *Eur J Clin Invest,* 50**,** e13201.

BRABLETZ, T., KALLURI, R., NIETO, M. A. & WEINBERG, R. A. 2018. EMT in cancer. *Nature Reviews Cancer,* 18**,** 128-134.

BRAY, F., LAVERSANNE, M., SUNG, H., FERLAY, J., SIEGEL, R. L., SOERJOMATARAM, I. & JEMAL, A. 2024. Global cancer statistics 2022: GLOBOCAN estimates of incidence and mortality worldwide for 36 cancers in 185 countries. *CA: A Cancer Journal for Clinicians,* 74**,** 229-263.

BRISKEN, C. 2013. Progesterone signalling in breast cancer: a neglected hormone coming into the limelight. *Nature Reviews Cancer,* 13**,** 385-396.

BRYANT, W. A., STENTZ, R., LE GALL, G., STERNBERG, M. J. E., CARDING, S. R. & WILHELM, T. 2017. In Silico Analysis of the Small Molecule Content of Outer Membrane Vesicles Produced by Bacteroides thetaiotaomicron Indicates an Extensive Metabolic Link between Microbe and Host. *Front Microbiol,* 8**,** 2440.

BUZAS, E. I. 2023. The roles of extracellular vesicles in the immune system. *Nature Reviews Immunology,* 23**,** 236-250.

CABRITA, R., LAUSS, M., SANNA, A., DONIA, M., SKAARUP LARSEN, M., MITRA, S., JOHANSSON, I., PHUNG, B., HARBST, K., VALLON-CHRISTERSSON, J., VAN SCHOIACK, A., LÖVGREN, K., WARREN, S., JIRSTRÖM, K., OLSSON, H., PIETRAS, K., INGVAR, C., ISAKSSON, K., SCHADENDORF, D., SCHMIDT, H., BASTHOLT, L., CARNEIRO, A., WARGO, J. A., SVANE, I. M. & JÖNSSON, G. 2020. Tertiary lymphoid structures improve immunotherapy and survival in melanoma. *Nature,* 577**,** 561-565.

CACCIOTTO, C., CUBEDDU, T., ADDIS, M. F., ANFOSSI, A. G., TEDDE, V., TORE, G., CARTA, T., ROCCA, S., CHESSA, B., PITTAU, M. & ALBERTI, A. 2016. lipoproteins are major determinants of neutrophil extracellular trap formation. *Cellular Microbiology,* 18**,** 1751-1762.

CALDER, P. C. 2013. Feeding the immune system. *Proceedings of the Nutrition Society,* 72**,** 299-309.

CAMERON, D., PICCART-GEBHART, M. J., GELBER, R. D., PROCTER, M., GOLDHIRSCH, A., DE AZAMBUJA, E., CASTRO, G., JR., UNTCH, M., SMITH, I., GIANNI, L., BASELGA, J., AL-SAKAFF, N., LAUER, S., MCFADDEN, E., LEYLAND-JONES, B., BELL, R., DOWSETT, M. & JACKISCH, C. 2017. 11 years' follow-up of trastuzumab after adjuvant chemotherapy in HER2-positive early breast cancer: final analysis of the HERceptin Adjuvant (HERA) trial. *Lancet,* 389**,** 1195-1205.

CANCER, I. A. F. R. O. 2024. *IARC MONOGRAPHS ON THE IDENTIFICATION OF CARCINOGENIC HAZARDS TO HUMANS* [Online]. Human Cancer: Known Causes and Prevention by Organ Site – IARC Monographs on the Identification of Carcinogenic Hazards to Humans (who.int): *The Lancet Oncology*. [Accessed].

CANCER RESEARCH UK 2019. Breast Cancer Mortality. Breast cancer statistics | Cancer Research UK.

CANYELLES, M., BORRÀS, C., ROTLLAN, N., TONDO, M., ESCOLÀ-GIL, J. C. & BLANCO-VACA, F. 2023. Gut Microbiota-Derived TMAO: A Causal Factor Promoting Atherosclerotic Cardiovascular Disease? *Int J Mol Sci,* 24.

CARRIQUIRIBORDE, F., MARTIN AISPURO, P., AMBROSIS, N., ZURITA, E., BOTTERO, D., GAILLARD, M. E., CASTUMA, C., RUDI, E., LODEIRO, A. & HOZBOR, D. F. 2021. Pertussis Vaccine Candidate Based on Outer Membrane Vesicles Derived From Biofilm Culture. *Front Immunol,* 12**,** 730434.

CARUANA, J. C. & WALPER, S. A. 2020. Bacterial Membrane Vesicles as Mediators of Microbe - Microbe and Microbe - Host Community Interactions. *Front Microbiol,* 11**,** 432.

CARUSO, R., WARNER, N., INOHARA, N. & NÚÑEZ, G. 2014. NOD1 and NOD2: signaling, host defense, and inflammatory disease. *Immunity,* 41**,** 898-908.

CHANG, W. H., CERIONE, R. A. & ANTONYAK, M. A. 2021. Extracellular Vesicles and Their Roles in Cancer Progression. *Methods Mol Biol,* 2174**,** 143-170.

CHAPUT, N., LEPAGE, P., COUTZAC, C., SOULARUE, E., LE ROUX, K., MONOT, C., BOSELLI, L., ROUTIER, E., CASSARD, L., COLLINS, M., VAYSSE, T., MARTHEY, L., EGGERMONT, A., ASVATOURIAN, V., LANOY, E., MATEUS, C., ROBERT, C. & CARBONNEL, F. 2017. Baseline gut microbiota predicts clinical response and colitis in metastatic melanoma patients treated with ipilimumab. *Annals of Oncology,* 28**,** 1368-1379.

CHEN, C., LIAO, J., XIA, Y., LIU, X., JONES, R., HARAN, J., MCCORMICK, B., SAMPSON, T. R., ALAM, A. & YE, K. 2022. Gut microbiota regulate Alzheimer's disease pathologies and cognitive disorders via PUFA-associated neuroinflammation. *Gut,* 71**,** 2233.

CHEN, G., GAO, C., JIANG, S., CAI, Q., LI, R., SUN, Q., XIAO, C., XU, Y., WU, B. & ZHOU, H. 2024. Fusobacterium nucleatum outer membrane vesicles activate autophagy to promote oral cancer metastasis. *J Adv Res,* 56**,** 167-179.

CHEN, J., CHEN, X. & HO, C. L. 2021. Recent development of probiotic bifidobacteria for treating human diseases. *Frontiers in bioengineering and biotechnology,* 9**,** 770248.

CHEN, Y., CAO, P., SU, W., ZHAN, N. & DONG, W. 2020. Fusobacterium nucleatum facilitates ulcerative colitis through activating IL-17F signaling to NF-κB via the upregulation of CARD3 expression. *J Pathol,* 250**,** 170-182.

CHEON, S., KIM, G., BAE, J. H., LEE, D. H., SEONG, H., KIM, D. H., HAN, J. S., LIM, S. Y. & HAN, N. S. 2023. Comparative analysis of prebiotic effects of four oligosaccharides using in vitro gut model: digestibility, microbiome, and metabolome changes. *FEMS Microbiol Ecol,* 99.

CHISTIAKOV, D. A., MYASOEDOVA, V. A., REVIN, V. V., OREKHOV, A. N. & BOBRYSHEV, Y. V. 2018. The impact of interferon-regulatory factors to macrophage differentiation and polarization into M1 and M2. *Immunobiology,* 223**,** 101-111.

CHOI, H.-I., CHOI, J.-P., SEO, J., KIM, B. J., RHO, M., HAN, J. K. & KIM, J. G. 2017. Helicobacter pylori-derived extracellular vesicles increased in the gastric juices of gastric adenocarcinoma patients and induced inflammation mainly via specific targeting of gastric epithelial cells. *Experimental & Molecular Medicine,* 49**,** e330-e330.

CLUFF, C. W. 2010. Monophosphoryl lipid A (MPL) as an adjuvant for anti-cancer vaccines: clinical results. *Adv Exp Med Biol,* 667**,** 111-23.

COICO, R. 2005. Gram staining. *Curr Protoc Microbiol,* Appendix 3**,** Appendix 3C.

COLEMAN, W. B. & TSONGALIS, G. J. 2001. *The molecular basis of human cancer*, Springer Science & Business Media.

COMEN, E., WOJNAROWICZ, P., SESHAN, V. E., SHAH, R., COKER, C., NORTON, L. & BENEZRA, R. 2016. TNF is a key cytokine mediating neutrophil cytotoxic activity in breast cancer patients. *npj Breast Cancer, 2***,** 16009.

COPELAND, J. K., CHAO, G., VANDERHOUT, S., ACTON, E., WANG, P. W., BENCHIMOL, E. I., EL SOHAMI, A., CROITORU, K., GOMMERMAN, J. L. & GUTTMAN, D. S. 2021. The Impact of Migration on the Gut Metagenome of South Asian Canadians. *Gut Microbes, 13***,** 1-29.

COX, M. A., HARRINGTON, L. E. & ZAJAC, A. J. 2011. Cytokines and the inception of CD8 T cell responses. *Trends Immunol, 32***,** 180-6.

DANIELPOUR, D. 2024. Advances and Challenges in Targeting TGF-β Isoforms for Therapeutic Intervention of Cancer: A Mechanism-Based Perspective. *Pharmaceuticals (Basel), 17.*

DARFEUILLE-MICHAUD, A., NEUT, C., BARNICH, N., LEDERMAN, E., DI MARTINO, P., DESREUMAUX, P., GAMBIEZ, L., JOLY, B., CORTOT, A. & COLOMBEL, J. F. 1998. Presence of adherent Escherichia coli strains in ileal mucosa of patients with Crohn's disease. *Gastroenterology, 115***,** 1405-13.

DAVAR, D., DZUTSEV, A. K., MCCULLOCH, J. A., RODRIGUES, R. R., CHAUVIN, J.-M., MORRISON, R. M., DEBLASIO, R. N., MENNA, C., DING, Q., PAGLIANO, O., ZIDI, B., ZHANG, S., BADGER, J. H., VETIZOU, M., COLE, A. M., FERNANDES, M. R., PRESCOTT, S., COSTA, R. G. F., BALAJI, A. K., MORGUN, A., VUJKOVIC-CVIJIN, I., WANG, H., BORHANI, A. A., SCHWARTZ, M. B., DUBNER, H. M., ERNST, S. J., ROSE, A., NAJJAR, Y. G., BELKAID, Y., KIRKWOOD, J. M., TRINCHIERI, G. & ZAROUR, H. M. 2021. Fecal microbiota transplant overcomes resistance to anti–PD-1 therapy in melanoma patients. *Science, 371***,** 595-602.

DAVID, L., TAIEB, F., PÉNARY, M., BORDIGNON, P.-J., PLANÈS, R., BAGAYOKO, S., DUPLAN-ECHE, V., MEUNIER, E. & OSWALD, E. 2022. Outer membrane vesicles produced by pathogenic strains of Escherichia coli block autophagic flux and exacerbate inflammasome activation. *Autophagy, 18***,** 2913-2925.

DE CLERCQ, E. 2015. AMD3100/CXCR4 Inhibitor. *Front Immunol, 6***,** 276.

DE FILIPPO, C., DI PAOLA, M., RAMAZZOTTI, M., ALBANESE, D., PIERACCINI, G., BANCI, E., MIGLIETTA, F., CAVALIERI, D. & LIONETTI, P. 2017. Diet, environments, and gut microbiota. A preliminary investigation in children living in rural and urban Burkina Faso and Italy. *Frontiers in microbiology, 8***,** 1979.

DE GOFFAU, M. C., LAGER, S., SOVIO, U., GACCIOLI, F., COOK, E., PEACOCK, S. J., PARKHILL, J., CHARNOCK-JONES, D. S. & SMITH, G. C. S. 2019. Human placenta has no microbiome but can contain potential pathogens. *Nature, 572***,** 329-334.

DE MANZONI, G., PELOSI, G., PAVANEL, F., DI LEO, A., PEDRAZZANI, C., DURANTE, E., CORDIANO, C. & PASINI, F. 2002. The presence of bone marrow cytokeratin-immunoreactive cells does not predict outcome in gastric cancer patients. *British Journal of Cancer,* 86**,** 1047-1051.

DE MARTEL, C., FERLAY, J., FRANCESCHI, S., VIGNAT, J., BRAY, F., FORMAN, D. & PLUMMER, M. 2012. Global burden of cancers attributable to infections in 2008: a review and synthetic analysis. *The Lancet Oncology,* 13**,** 607-615.

DEAN, I., KENNEDY, B. C., LI, Z., BERDITCHEVSKI, F. & WITHERS, D. R. 2024. Protocol for transcutaneous tumor photolabeling to track immune cells in vivo using Kaede mice. *STAR Protocols,* 5**,** 102956.

DEROSA, L., IEBBA, V., SILVA, C. A. C., PICCINNO, G., WU, G., LORDELLO, L., ROUTY, B., ZHAO, N., THELEMAQUE, C., BIREBENT, R., MARMORINO, F., FIDELLE, M., MESSAOUDENE, M., THOMAS, A. M., ZALCMAN, G., FRIARD, S., MAZIERES, J., AUDIGIER-VALETTE, C., SIBILOT, D. M., GOLDWASSER, F., SCHERPEREEL, A., PEGLIASCO, H., GHIRINGHELLI, F., BOUCHARD, N., SOW, C., DARIK, I., ZOPPI, S., LY, P., RENI, A., DAILLÈRE, R., DEUTSCH, E., LEE, K. A., BOLTE, L. A., BJÖRK, J. R., WEERSMA, R. K., BARLESI, F., PADILHA, L., FINZEL, A., ISAKSEN, M. L., ESCUDIER, B., ALBIGES, L., PLANCHARD, D., ANDRÉ, F., CREMOLINI, C., MARTINEZ, S., BESSE, B., ZHAO, L., SEGATA, N., WOJCIK, J., KROEMER, G. & ZITVOGEL, L. 2024. Custom scoring based on ecological topology of gut microbiota associated with cancer immunotherapy outcome. *Cell,* 187**,** 3373-3389.e16.

DEROSA, L., ROUTY, B., THOMAS, A. M., IEBBA, V., ZALCMAN, G., FRIARD, S., MAZIERES, J., AUDIGIER-VALETTE, C., MORO-SIBILOT, D. & GOLDWASSER, F. 2022. Intestinal Akkermansia muciniphila predicts clinical response to PD-1 blockade in patients with advanced non-small-cell lung cancer. *Nature medicine,* 28**,** 315-324.

DI LUCCIA, B., MOLGORA, M., KHANTAKOVA, D., JAEGER, N., CHANG, H.-W., CZEPIELEWSKI, R. S., HELMINK, B. A., ONUFER, E. J., FACHI, J. L., BHATTARAI, B., TRSAN, T., RODRIGUES, P. F., HOU, J., BANDO, J. K., DA SILVA, C. S., CELLA, M., GILFILLAN, S., SCHREIBER, R. D., GORDON, J. I. & COLONNA, M. 2024. TREM2 deficiency reprograms intestinal macrophages and microbiota to enhance anti–PD-1 tumor immunotherapy. *Science Immunology,* 9**,** eadi5374.

DITSCH, N., FUNKE, I., MAYER, B. & UNTCH, M. 2002. [Detection of disseminated tumor cells in bone marrow--currently of no practical therapeutic value]. *MMW Fortschr Med,* 144**,** 37-9.

DOMÍNGUEZ RUBIO, A. P., MARTÍNEZ, J. H., MARTÍNEZ CASILLAS, D. C., COLUCCIO LESKOW, F., PIURI, M. & PÉREZ, O. E. 2017. Lactobacillus casei BL23 Produces Microvesicles Carrying Proteins That Have Been Associated with Its Probiotic Effect. *Front Microbiol,* 8**,** 1783.

DOTTERUD, C. K., STORRØ, O., JOHNSEN, R. & OIEN, T. 2010. Probiotics in pregnant women to prevent allergic disease: a randomized, double-blind trial. *Br J Dermatol,* 163**,** 616-23.

EARLY BREAST CANCER TRIALISTS' COLLABORATIVE GROUP (EBCTCG) 2005. Effects of chemotherapy and hormonal therapy for early breast cancer on recurrence and 15-year survival: an overview of the randomised trials. *Lancet,* 365**,** 1687-717.

ELMI, A., NASHER, F., JAGATIA, H., GUNDOGDU, O., BAJAJ-ELLIOTT, M., WREN, B. & DORRELL, N. 2016. Campylobacter jejuni outer membrane vesicle-associated proteolytic activity promotes bacterial invasion by mediating cleavage of intestinal epithelial cell E-cadherin and occludin. *Cell Microbiol,* 18**,** 561-72.

ENOMOTO, T., SOWA, M., NISHIMORI, K., SHIMAZU, S., YOSHIDA, A., YAMADA, K., FURUKAWA, F., NAKAGAWA, T., YANAGISAWA, N. & IWABUCHI, N. 2014. Effects of bifidobacterial supplementation to pregnant women and infants in the prevention of allergy development in infants and on fecal microbiota. *Allergology International,* 63**,** 575-585.

FACKENTHAL, J. D. & OLOPADE, O. I. 2007. Breast cancer risk associated with BRCA1 and BRCA2 in diverse populations. *Nature Reviews Cancer,* 7**,** 937-948.

FANNING, S., HALL, L. J., CRONIN, M., ZOMER, A., MACSHARRY, J., GOULDING, D., O'CONNELL MOTHERWAY, M., SHANAHAN, F., NALLY, K., DOUGAN, G. & VAN SINDEREN, D. 2012. Bifidobacterial surface-exopolysaccharide facilitates commensal-host interaction through immune modulation and pathogen protection. *Proceedings of the National Academy of Sciences,* 109**,** 2108-2113.

FENG, T. Y., AZAR, F. N., DREGER, S. A., ROSEAN, C. B., MCGINTY, M. T., PUTELO, A. M., KOLLI, S. H., CAREY, M. A., GREENFIELD, S., FOWLER, W. J., ROBINSON, S. D. & RUTKOWSKI, M. R. 2022. Reciprocal Interactions Between the Gut Microbiome and Mammary Tissue Mast Cells Promote Metastatic Dissemination of HR+ Breast Tumors. *Cancer Immunol Res,* 10**,** 1309-1325.

FILLATREAU, S., SWEENIE, C. H., MCGEACHY, M. J., GRAY, D. & ANDERTON, S. M. 2002. B cells regulate autoimmunity by provision of IL-10. *Nature Immunology,* 3**,** 944-950.

FISHER, B., ANDERSON, S., BRYANT, J., MARGOLESE, R. G., DEUTSCH, M., FISHER, E. R., JEONG, J. H. & WOLMARK, N. 2002. Twenty-year follow-up of a randomized trial comparing total mastectomy, lumpectomy, and lumpectomy plus irradiation for the treatment of invasive breast cancer. *N Engl J Med,* 347**,** 1233-41.

FLUCK, M. M. & SCHAFFHAUSEN, B. S. 2009. Lessons in signaling and tumorigenesis from polyomavirus middle T antigen. *Microbiol Mol Biol Rev,* 73**,** 542-63, Table of Contents.

FRIDLENDER, Z. G., SUN, J., KIM, S., KAPOOR, V., CHENG, G., LING, L., WORTHEN, G. S. & ALBELDA, S. M. 2009. Polarization of tumor-associated neutrophil phenotype by TGF-beta: "N1" versus "N2" TAN. *Cancer Cell,* 16**,** 183-94.

FU, A., YAO, B., DONG, T., CHEN, Y., YAO, J., LIU, Y., LI, H., BAI, H., LIU, X., ZHANG, Y., WANG, C., GUO, Y., LI, N. & CAI, S. 2022. Tumor-resident

intracellular microbiota promotes metastatic colonization in breast cancer. *Cell,* 185**,** 1356-1372.e26.

FU, L. Q., DU, W. L., CAI, M. H., YAO, J. Y., ZHAO, Y. Y. & MOU, X. Z. 2020. The roles of tumor-associated macrophages in tumor angiogenesis and metastasis. *Cell Immunol,* 353**,** 104119.

FU, Q., FU, T. M., CRUZ, A. C., SENGUPTA, P., THOMAS, S. K., WANG, S., SIEGEL, R. M., WU, H. & CHOU, J. J. 2016. Structural Basis and Functional Role of Intramembrane Trimerization of the Fas/CD95 Death Receptor. *Mol Cell,* 61**,** 602-613.

GAINOR, J. F., SHAW, A. T., SEQUIST, L. V., FU, X., AZZOLI, C. G., PIOTROWSKA, Z., HUYNH, T. G., ZHAO, L., FULTON, L., SCHULTZ, K. R., HOWE, E., FARAGO, A. F., SULLIVAN, R. J., STONE, J. R., DIGUMARTHY, S., MORAN, T., HATA, A. N., YAGI, Y., YEAP, B. Y., ENGELMAN, J. A. & MINO-KENUDSON, M. 2016. EGFR Mutations and ALK Rearrangements Are Associated with Low Response Rates to PD-1 Pathway Blockade in Non-Small Cell Lung Cancer: A Retrospective Analysis. *Clin Cancer Res,* 22**,** 4585-93.

GAMA, L. A., ROCHA MACHADO, M. P., BECKMANN, A. P. S., MIRANDA, J. R. D. A., CORÁ, L. A. & AMÉRICO, M. F. 2020. Gastrointestinal motility and morphology in mice: Strain-dependent differences. *Neurogastroenterology & Motility,* 32**,** e13824.

GAO, Y., SHANG, Q., LI, W., GUO, W., STOJADINOVIC, A., MANNION, C., MAN, Y. G. & CHEN, T. 2020. Antibiotics for cancer treatment: A double-edged sword. *J Cancer,* 11**,** 5135-5149.

GAVZY, S. J., KENSISKI, A., LEE, Z. L., MONGODIN, E. F., MA, B. & BROMBERG, J. S. 2023. Bifidobacterium mechanisms of immune modulation and tolerance. *Gut Microbes,* 15**,** 2291164.

GELLINGS, P., GALEAS-PENA, M. & MORICI, L. A. 2023. Mycobacterium bovis bacille Calmette-Guerin-derived extracellular vesicles as an alternative to live BCG immunotherapy. *Clin Exp Med,* 23**,** 519-527.

GIBSON, G. R. & ROBERFROID, M. B. 1995. Dietary modulation of the human colonic microbiota: introducing the concept of prebiotics. *J Nutr,* 125**,** 1401-12.

GIHAWI, A., COOPER, C. S. & BREWER, D. S. 2023. Caution regarding the specificities of pan-cancer microbial structure. *Microb Genom.* England.

GOEDERT, J. J., HUA, X., BIELECKA, A., OKAYASU, I., MILNE, G. L., JONES, G. S., FUJIWARA, M., SINHA, R., WAN, Y., XU, X., RAVEL, J., SHI, J., PALM, N. W. & FEIGELSON, H. S. 2018. Postmenopausal breast cancer and oestrogen associations with the IgA-coated and IgA-noncoated faecal microbiota. *Br J Cancer,* 118**,** 471-479.

GOEDERT, J. J., JONES, G., HUA, X., XU, X., YU, G., FLORES, R., FALK, R. T., GAIL, M. H., SHI, J., RAVEL, J. & FEIGELSON, H. S. 2015. Investigation of the association between the fecal microbiota and breast cancer in postmenopausal women: a population-based case-control pilot study. *J Natl Cancer Inst,* 107.

GONZALES-LUNA, A. J., CARLSON, T. J. & GAREY, K. W. 2023. Gut microbiota changes associated with Clostridioides difficile infection and its various treatment strategies. *Gut Microbes,* 15**,** 2223345.

GONZÁLEZ-MERCADO, V. J., SARKAR, A., PENEDO, F. J., PÉREZ-SANTIAGO, J., MCMILLAN, S., MARRERO, S. J., MARRERO-FALCÓN, M. A. & MUNRO, C. L. 2020. Gut microbiota perturbation is associated with acute sleep disturbance among rectal cancer patients. *J Sleep Res,* 29**,** e12915.

GONZÁLEZ, M. F., DÍAZ, P., SANDOVAL-BÓRQUEZ, A., HERRERA, D. & QUEST, A. F. G. 2021. Helicobacter pylori Outer Membrane Vesicles and Extracellular Vesicles from Helicobacter pylori-Infected Cells in Gastric Disease Development. *International Journal of Molecular Sciences,* 22**,** 4823.

GREATHOUSE, K. L., WYATT, M., JOHNSON, A. J., TOY, E. P., KHAN, J. M., DUNN, K., CLEGG, D. J. & REDDY, S. 2022. Diet-microbiome interactions in cancer treatment: Opportunities and challenges for precision nutrition in cancer. *Neoplasia,* 29**,** 100800.

GREENWALT, I., ZAZA, N., DAS, S. & LI, B. D. 2020. Precision Medicine and Targeted Therapies in Breast Cancer. *Surg Oncol Clin N Am,* 29**,** 51-62.

GRINDE, M. T., SKRBO, N., MOESTUE, S. A., RØDLAND, E. A., BORGAN, E., KRISTIAN, A., SITTER, B., BATHEN, T. F., BØRRESEN-DALE, A. L., MÆLANDSMO, G. M., ENGEBRAATEN, O., SØRLIE, T., MARANGONI, E. & GRIBBESTAD, I. S. 2014. Interplay of choline metabolites and genes in patient-derived breast cancer xenografts. *Breast Cancer Res,* 16**,** R5.

GROEGER, D., O'MAHONY, L., MURPHY, E. F., BOURKE, J. F., DINAN, T. G., KIELY, B., SHANAHAN, F. & QUIGLEY, E. M. 2013. Bifidobacterium infantis 35624 modulates host inflammatory processes beyond the gut. *Gut Microbes,* 4**,** 325-39.

GRZYWA, T. M., SOSNOWSKA, A., MATRYBA, P., RYDZYNSKA, Z., JASINSKI, M., NOWIS, D. & GOLAB, J. 2020. Myeloid Cell-Derived Arginase in Cancer Immune Response. *Frontiers in Immunology,* 11.

GUAN, W., SONG, X., YANG, S., ZHU, H., LI, F. & LI, J. 2022. Observation of the Gut Microbiota Profile in BALB/c Mice Induced by Plasmodium yoelii 17XL Infection. *Front Microbiol,* 13**,** 858897.

GUR, C., IBRAHIM, Y., ISAACSON, B., YAMIN, R., ABED, J., GAMLIEL, M., ENK, J., BAR-ON, Y., STANIETSKY-KAYNAN, N., COPPENHAGEN-GLAZER, S., SHUSSMAN, N., ALMOGY, G., CUAPIO, A., HOFER, E., MEVORACH, D., TABIB, A., ORTENBERG, R., MARKEL, G., MIKLIĆ, K., JONJIC, S., BRENNAN, C. A., GARRETT, W. S., BACHRACH, G. & MANDELBOIM, O. 2015. Binding of the Fap2 protein of Fusobacterium nucleatum to human inhibitory receptor TIGIT protects tumors from immune cell attack. *Immunity,* 42**,** 344-355.

GURUNG, M., MOON, D. C., CHOI, C. W., LEE, J. H., BAE, Y. C., KIM, J., LEE, Y. C., SEOL, S. Y., CHO, D. T., KIM, S. I. & LEE, J. C. 2011. Staphylococcus aureus Produces Membrane-Derived Vesicles That Induce Host Cell Death. *PLOS ONE,* 6**,** e27958.

GUZMAN, G., REED, M. R., BIELAMOWICZ, K., KOSS, B. & RODRIGUEZ, A. 2023. CAR-T Therapies in Solid Tumors: Opportunities and Challenges. *Curr Oncol Rep,* 25**,** 479-489.

HAN, Y. W., SHEN, T., CHUNG, P., BUHIMSCHI, I. A. & BUHIMSCHI, C. S. 2009. Uncultivated bacteria as etiologic agents of intra-amniotic inflammation leading to preterm birth. *J Clin Microbiol,* 47**,** 38-47.

HANAHAN, D. 2022. Hallmarks of Cancer: New Dimensions. *Cancer Discovery,* 12**,** 31-46.

HANAHAN, D. & WEINBERG, R. A. 2000. The Hallmarks of Cancer. *Cell,* 100**,** 57-70.

HANAHAN, D. & WEINBERG, ROBERT A. 2011. Hallmarks of Cancer: The Next Generation. *Cell,* 144**,** 646-674.

HARTKOPF, A. D., TARAN, F. A., WALLWIENER, M., HAHN, M., BECKER, S., SOLOMAYER, E. F., BRUCKER, S. Y., FEHM, T. N. & WALLWIENER, D. 2014. Prognostic relevance of disseminated tumour cells from the bone marrow of early stage breast cancer patients - results from a large single-centre analysis. *Eur J Cancer,* 50**,** 2550-9.

HATO, L., VIZCAY, A., EGUREN, I., PÉREZ-GRACIA, J. L., RODRÍGUEZ, J., GÁLLEGO PÉREZ-LARRAYA, J., SAROBE, P., INOGÉS, S., DÍAZ DE CERIO, A. L. & SANTISTEBAN, M. 2024. Dendritic Cells in Cancer Immunology and Immunotherapy. *Cancers,* 16**,** 981.

HE, Z., GHARAIBEH, R. Z., NEWSOME, R. C., POPE, J. L., DOUGHERTY, M. W., TOMKOVICH, S., PONS, B., MIREY, G., VIGNARD, J., HENDRIXSON, D. R. & JOBIN, C. 2019. Campylobacter jejuni promotes colorectal tumorigenesis through the action of cytolethal distending toxin. *Gut,* 68**,** 289.

HELGUERO, L. A., FAULDS, M. H., GUSTAFSSON, J.-Å. & HALDOSEN, L.-A. 2005. Estrogen receptors alfa (ERα) and beta (ERβ) differentially regulate proliferation and apoptosis of the normal murine mammary epithelial cell line HC11. *Oncogene,* 24**,** 6605-6616.

HELMINK, B. A., KHAN, M. A. W., HERMANN, A., GOPALAKRISHNAN, V. & WARGO, J. A. 2019. The microbiome, cancer, and cancer therapy. *Nature Medicine,* 25**,** 377-388.

HERRMANN, I. K., WOOD, M. J. A. & FUHRMANN, G. 2021. Extracellular vesicles as a next-generation drug delivery platform. *Nature Nanotechnology,* 16**,** 748-759.

HIBBERD, A. A., LYRA, A., OUWEHAND, A. C., ROLNY, P., LINDEGREN, H., CEDGÅRD, L. & WETTERGREN, Y. 2017. Intestinal microbiota is altered in patients with colon cancer and modified by probiotic intervention. *BMJ Open Gastroenterology,* 4**,** e000145.

HICKEY, A., STAMOU, P., UDAYAN, S., RAMÓN-VÁZQUEZ, A., ESTEBAN-TORRES, M., BOTTACINI, F., WOZNICKI, J. A., HUGHES, O., MELGAR, S., VENTURA, M., VAN SINDEREN, D., ROSSINI, V. & NALLY, K. 2021. Bifidobacterium breve Exopolysaccharide Blocks Dendritic Cell Maturation and Activation of CD4(+) T Cells. *Front Microbiol,* 12**,** 653587.

HILDEBRANDT, M. A., HOFFMANN, C., SHERRILL–MIX, S. A., KEILBAUGH, S. A., HAMADY, M., CHEN, Y. Y., KNIGHT, R., AHIMA, R. S., BUSHMAN, F. & WU, G. D. 2009. High-fat diet determines the composition of the murine gut microbiome independently of obesity. *Gastroenterology,* 137**,** 1716-1724. e2.

HOFFMANN, J. A., KAFATOS, F. C., JANEWAY JR, C. A. & EZEKOWITZ, R. 1999. Phylogenetic perspectives in innate immunity. *Science,* 284**,** 1313-1318.

HOOPER, L. V., LITTMAN, D. R. & MACPHERSON, A. J. 2012. Interactions between the microbiota and the immune system. *science,* 336**,** 1268-1273.

HOOPER, L. V., WONG, M. H., THELIN, A., HANSSON, L., FALK, P. G. & GORDON, J. I. 2001. Molecular analysis of commensal host-microbial relationships in the intestine. *Science,* 291**,** 881-884.

HOPTION CANN, S. A., VAN NETTEN JP FAU - VAN NETTEN, C. & VAN NETTEN, C. 2003. Dr William Coley and tumour regression: a place in history or in the future. *Postgraduate Medical Journal*.

HORIMOTO, Y., POLANSKA, U. M., TAKAHASHI, Y. & ORIMO, A. 2012. Emerging roles of the tumor-associated stroma in promoting tumor metastasis. *Cell Adh Migr,* 6**,** 193-202.

HUANG, J., ZHENG, X., KANG, W., HAO, H., MAO, Y., ZHANG, H., CHEN, Y., TAN, Y., HE, Y., ZHAO, W. & YIN, Y. 2022. Metagenomic and metabolomic analyses reveal synergistic effects of fecal microbiota transplantation and anti-PD-1 therapy on treating colorectal cancer. *Front Immunol,* 13**,** 874922.

IIDA, N., DZUTSEV, A., STEWART, C. A., SMITH, L., BOULADOUX, N., WEINGARTEN, R. A., MOLINA, D. A., SALCEDO, R., BACK, T., CRAMER, S., DAI, R. M., KIU, H., CARDONE, M., NAIK, S., PATRI, A. K., WANG, E., MARINCOLA, F. M., FRANK, K. M., BELKAID, Y., TRINCHIERI, G. & GOLDSZMID, R. S. 2013. Commensal bacteria control cancer response to therapy by modulating the tumor microenvironment. *Science,* 342**,** 967-70.

IMAI, C., IWAMOTO, S. & CAMPANA, D. 2005. Genetic modification of primary natural killer cells overcomes inhibitory signals and induces specific killing of leukemic cells. *Blood,* 106**,** 376-83.

IRVING, A. T., MIMURO, H., KUFER, T. A., LO, C., WHEELER, R., TURNER, L. J., THOMAS, B. J., MALOSSE, C., GANTIER, M. P., CASILLAS, L. N., VOTTA, B. J., BERTIN, J., BONECA, I. G., SASAKAWA, C., PHILPOTT, D. J., FERRERO, R. L. & KAPARAKIS-LIASKOS, M. 2014. The immune receptor NOD1 and kinase RIP2 interact with bacterial peptidoglycan on early endosomes to promote autophagy and inflammatory signaling. *Cell Host Microbe,* 15**,** 623-35.

ISHIDA, Y., AGATA, Y., SHIBAHARA, K. & HONJO, T. 1992. Induced expression of PD‐1, a novel member of the immunoglobulin gene superfamily, upon programmed cell death. *The EMBO Journal,* 11**,** 3887-3895.

ISOLAURI, E., ARVOLA, T., SÜTAS, Y., MOILANEN, E. & SALMINEN, S. 2000. Probiotics in the management of atopic eczema. *Clin Exp Allergy,* 30**,** 1604-10.

J, N. H., K, L. P., SELVARAJ, A., CHINNARAJ, S. & LUKE ELIZABETH, H. 2021. Toll like receptor (2 and 4) expression and cytokine release by human neutrophils during tuberculosis treatment-A longitudinal study. *Mol Immunol,* 140**,** 136-143.

JACKSON, M. A., VERDI, S., MAXAN, M. E., SHIN, C. M., ZIERER, J., BOWYER, R. C. E., MARTIN, T., WILLIAMS, F. M. K., MENNI, C., BELL, J. T., SPECTOR, T. D. & STEVES, C. J. 2018. Gut microbiota associations with common diseases and prescription medications in a population-based cohort. *Nat Commun,* 9**,** 2655.

JAFARI, S. H., SAADATPOUR, Z., SALMANINEJAD, A., MOMENI, F., MOKHTARI, M., NAHAND, J. S., RAHMATI, M., MIRZAEI, H. & KIANMEHR, M. 2018. Breast cancer diagnosis: Imaging techniques and biochemical markers. *Journal of cellular physiology,* 233**,** 5200-5213.

JAHROMI, L. P. & FUHRMANN, G. 2021. Bacterial extracellular vesicles: Understanding biology promotes applications as nanopharmaceuticals. *Advanced Drug Delivery Reviews,* 173**,** 125-140.

JAYNES, J. M., SABLE, R., RONZETTI, M., BAUTISTA, W., KNOTTS, Z., ABISOYE-OGUNNIYAN, A., LI, D., CALVO, R., DASHNYAM, M., SINGH, A., GUERIN, T., WHITE, J., RAVICHANDRAN, S., KUMAR, P., TALSANIA, K., CHEN, V., GHEBREMEDHIN, A., KARANAM, B., BIN SALAM, A., AMIN, R., ODZORIG, T., AIKEN, T., NGUYEN, V., BIAN, Y., ZARIF, J. C., DE GROOT, A. E., MEHTA, M., FAN, L., HU, X., SIMEONOV, A., PATE, N., ABU-ASAB, M., FERRER, M., SOUTHALL, N., OCK, C. Y., ZHAO, Y., LOPEZ, H., KOZLOV, S., DE VAL, N., YATES, C. C., BALJINNYAM, B., MARUGAN, J. & RUDLOFF, U. 2020. Mannose receptor (CD206) activation in tumor-associated macrophages enhances adaptive and innate antitumor immune responses. *Sci Transl Med,* 12.

JIANG, T., ZHOU, C. & REN, S. 2016. Role of IL-2 in cancer immunotherapy. *Oncoimmunology,* 5**,** e1163462.

JIANG, Y., LI, Y. & ZHU, B. 2015. T-cell exhaustion in the tumor microenvironment. *Cell Death & Disease,* 6**,** e1792-e1792.

JIMÉNEZ, E., FERNÁNDEZ, L., MARÍN, M. L., MARTÍN, R., ODRIOZOLA, J. M., NUENO-PALOP, C., NARBAD, A., OLIVARES, M., XAUS, J. & RODRÍGUEZ, J. M. 2005. Isolation of Commensal Bacteria from Umbilical Cord Blood of Healthy Neonates Born by Cesarean Section. *Current Microbiology,* 51**,** 270-274.

JIN, J. S., KWON, S.-O., MOON, D. C., GURUNG, M., LEE, J. H., KIM, S. I. & LEE, J. C. 2011. Acinetobacter baumannii secretes cytotoxic outer membrane protein A via outer membrane vesicles. *PloS one,* 6**,** e17027.

JUNGERSEN, M., WIND, A., JOHANSEN, E., CHRISTENSEN, J. E., STUER-LAURIDSEN, B. & ESKESEN, D. 2014. The Science behind the Probiotic Strain Bifidobacterium animalis subsp. lactis BB-12(®). *Microorganisms,* 2**,** 92-110.

JUNICK, J. & BLAUT, M. 2012. Quantification of human fecal bifidobacterium species by use of quantitative real-time PCR analysis targeting the groEL gene. *Appl Environ Microbiol,* 78**,** 2613-22.

KAPARAKIS-LIASKOS, M. & FERRERO, R. L. 2015. Immune modulation by bacterial outer membrane vesicles. *Nature Reviews Immunology,* 15**,** 375-387.

KELLINGRAY, L., TAPP, H. S., SAHA, S., DOLEMAN, J. F., NARBAD, A. & MITHEN, R. F. 2017. Consumption of a diet rich in Brassica vegetables is associated with a reduced abundance of sulphate-reducing bacteria: A randomised crossover study. *Mol Nutr Food Res,* 61.

KIESER, K. J. & KAGAN, J. C. 2017. Multi-receptor detection of individual bacterial products by the innate immune system. *Nature Reviews Immunology,* 17**,** 376-390.

KILKKINEN, A., RISSANEN, H., KLAUKKA, T., PUKKALA, E., HELIÖVAARA, M., HUOVINEN, P., MÄNNISTÖ, S., AROMAA, A. & KNEKT, P. 2008. Antibiotic use predicts an increased risk of cancer. *International Journal of Cancer,* 123**,** 2152-2155.

KIM, J.-H., JEUN, E.-J., HONG, C.-P., KIM, S.-H., JANG, M. S., LEE, E.-J., MOON, S. J., YUN, C. H., IM, S.-H. & JEONG, S.-G. 2016. Extracellular vesicle–derived protein from Bifidobacterium longum alleviates food allergy through mast cell suppression. *Journal of Allergy and Clinical Immunology,* 137**,** 507-516. e8.

KIM, J. Y., DOODY, A. M., CHEN, D. J., CREMONA, G. H., SHULER, M. L., PUTNAM, D. & DELISA, M. P. 2008. Engineered bacterial outer membrane vesicles with enhanced functionality. *J Mol Biol,* 380**,** 51-66.

KIM, J. Y., KWON, J. H., AHN, S. H., LEE, S. I., HAN, Y. S., CHOI, Y. O., LEE, S. Y., AHN, K. M. & JI, G. E. 2010. Effect of probiotic mix (Bifidobacterium bifidum, Bifidobacterium lactis, Lactobacillus acidophilus) in the primary prevention of eczema: a double‐blind, randomized, placebo‐controlled trial. *Pediatric Allergy and Immunology,* 21**,** e386-e393.

KIM, S. W., LEE, J. S., PARK, S. B., LEE, A. R., JUNG, J. W., CHUN, J. H., LAZARTE, J. M. S., KIM, J., SEO, J. S., KIM, J. H., SONG, J. W., HA, M. W., THOMPSON, K. D., LEE, C. R., JUNG, M. & JUNG, T. S. 2020. The Importance of Porins and β-Lactamase in Outer Membrane Vesicles on the Hydrolysis of β-Lactam Antibiotics. *Int J Mol Sci,* 21.

KLEIN-BRILL, A., AMAR-FARKASH, S., ROSENBERG-KATZ, K., BRENNER, R., BECKER, J. C. & ARAN, D. 2024. Comparative efficacy of combined CTLA-4 and PD-1 blockade vs. PD-1 monotherapy in metastatic melanoma: a real-world study. *BJC Reports,* 2**,** 14.

KOH, C.-H., LEE, S., KWAK, M., KIM, B.-S. & CHUNG, Y. 2023. CD8 T-cell subsets: heterogeneity, functions, and therapeutic potential. *Experimental & Molecular Medicine,* 55**,** 2287-2299.

KOUTSOUMANIS, K., ALLENDE, A., ÁLVAREZ-ORDÓÑEZ, A., BOLTON, D., BOVER-CID, S., CHEMALY, M., DAVIES, R., DE CESARE, A., HERMAN, L., HILBERT, F., LINDQVIST, R., NAUTA, M., RU, G., SIMMONS, M., SKANDAMIS, P., SUFFREDINI, E., ARGÜELLO, H., BERENDONK, T.,

CAVACO, L. M., GAZE, W., SCHMITT, H., TOPP, E., GUERRA, B., LIÉBANA, E., STELLA, P. & PEIXE, L. 2021. Role played by the environment in the emergence and spread of antimicrobial resistance (AMR) through the food chain. *Efsa j,* 19**,** e06651.

KRUMMEL, M. F. & ALLISON, J. P. 1995. CD28 and CTLA-4 have opposing effects on the response of T cells to stimulation. *The Journal of experimental medicine,* 182**,** 459-465.

KULKARNI, T., MAJARIKAR, S., DESHMUKH, M. A.-O., ANANTHAN, A., BALASUBRAMANIAN, H., KEIL, A. & PATOLE, S. 2019. Probiotic sepsis in preterm neonates-a systematic review.

KURATA, A., YAMASAKI-YASHIKI, S., IMAI, T., MIYAZAKI, A., WATANABE, K. & UEGAKI, K. 2022. Enhancement of IgA production by membrane vesicles derived from Bifidobacterium longum subsp. infantis. *Biosci Biotechnol Biochem,* 87**,** 119-128.

KWEE, B. J., BUDINA, E., NAJIBI, A. J. & MOONEY, D. J. 2018. CD4 T-cells regulate angiogenesis and myogenesis. *Biomaterials,* 178**,** 109-121.

LA GIOIA, A., FIORINI, F. & LA GIOIA, N. 2022. Bone marrow involvement by metastatic invasive lobular breast cancer. *Int J Lab Hematol,* 44**,** 40-41.

LANITIS, E., DANGAJ, D., IRVING, M. & COUKOS, G. 2017. Mechanisms regulating T-cell infiltration and activity in solid tumors. *Annals of Oncology,* 28**,** xii18-xii32.

LE MAGNEN, C., DUTTA, A. & ABATE-SHEN, C. 2016. Optimizing mouse models for precision cancer prevention. *Nat Rev Cancer,* 16**,** 187-96.

LEE, C. Y. C., KENNEDY, B. C., RICHOZ, N., DEAN, I., TUONG, Z. K., GASPAL, F., LI, Z., WILLIS, C., HASEGAWA, T., WHITESIDE, S. K., POSNER, D. A., CARLESSO, G., HAMMOND, S. A., DOVEDI, S. J., ROYCHOUDHURI, R., WITHERS, D. R. & CLATWORTHY, M. R. 2024. Tumour-retained activated CCR7+ dendritic cells are heterogeneous and regulate local anti-tumour cytolytic activity. *Nature Communications,* 15**,** 682.

LEE, J., LEE, J. E., KIM, S., KANG, D. & YOO, H. M. 2020. Evaluating Cell Death Using Cell-Free Supernatant of Probiotics in Three-Dimensional Spheroid Cultures of Colorectal Cancer Cells. *J Vis Exp.*

LEE, J. H. & O'SULLIVAN, D. J. 2010. Genomic insights into bifidobacteria. *Microbiol Mol Biol Rev,* 74**,** 378-416.

LEEMING, E. R., JOHNSON, A. J., SPECTOR, T. D. & LE ROY, C. I. 2019. Effect of Diet on the Gut Microbiota: Rethinking Intervention Duration. *Nutrients,* 11.

LEI, X., KHATRI, I., DE WIT, T., DE RINK, I., NIEUWLAND, M., KERKHOVEN, R., VAN EENENNAAM, H., SUN, C., GARG, A. D., BORST, J. & XIAO, Y. 2023. CD4+ helper T cells endow cDC1 with cancer-impeding functions in the human tumor micro-environment. *Nature Communications,* 14**,** 217.

LEMAITRE, B., NICOLAS, E., MICHAUT, L., REICHHART, J.-M. & HOFFMANN, J. A. 1996. The Dorsoventral Regulatory Gene Cassette späätzle/Toll/cactus Controls the Potent Antifungal Response in Drosophila Adults. *Cell,* 86**,** 973-983.

LEWIS, Z. T., SHANI, G., MASARWEH, C. F., POPOVIC, M., FRESE, S. A., SELA, D. A., UNDERWOOD, M. A. & MILLS, D. A. 2016. Validating bifidobacterial species and subspecies identity in commercial probiotic products. *Pediatric Research,* 79**,** 445-452.

LI, M., LEE, K., HSU, M., NAU, G., MYLONAKIS, E. & RAMRATNAM, B. 2017. Lactobacillus-derived extracellular vesicles enhance host immune responses against vancomycin-resistant enterococci. *BMC Microbiol,* 17**,** 66.

LI, Q., LEI, X., ZHU, J., ZHONG, Y., YANG, J., WANG, J. & TAN, H. 2023. Radiotherapy/Chemotherapy-Immunotherapy for Cancer Management: From Mechanisms to Clinical Implications. *Oxid Med Cell Longev,* 2023**,** 7530794.

LI, X., SU, C., JIANG, Z., YANG, Y., ZHANG, Y., YANG, M., ZHANG, X., DU, Y., ZHANG, J., WANG, L., JIANG, J. & HONG, B. 2021. Berberine attenuates choline-induced atherosclerosis by inhibiting trimethylamine and trimethylamine-N-oxide production via manipulating the gut microbiome. *NPJ Biofilms Microbiomes,* 7**,** 36.

LIANG, J. Q., ZENG, Y., LAU, E. Y. T., SUN, Y., HUANG, Y., ZHOU, T., XU, Z., YU, J., NG, S. C. & CHAN, F. K. L. 2023. A Probiotic Formula for Modulation of Colorectal Cancer Risk via Reducing CRC-Associated Bacteria. *Cells,* 12.

LIN, W. Y., LIN, J. H., KUO, Y. W., CHIANG, P. R. & HO, H. H. 2022. Probiotics and their Metabolites Reduce Oxidative Stress in Middle-Aged Mice. *Curr Microbiol,* 79**,** 104.

LIND, N. A., RAEL, V. E., PESTAL, K., LIU, B. & BARTON, G. M. 2022. Regulation of the nucleic acid-sensing Toll-like receptors. *Nature Reviews Immunology,* 22**,** 224-235.

LIU, E., TONG, Y., DOTTI, G., SHAIM, H., SAVOLDO, B., MUKHERJEE, M., ORANGE, J., WAN, X., LU, X., REYNOLDS, A., GAGEA, M., BANERJEE, P., CAI, R., BDAIWI, M. H., BASAR, R., MUFTUOGLU, M., LI, L., MARIN, D., WIERDA, W., KEATING, M., CHAMPLIN, R., SHPALL, E. & REZVANI, K. 2018. Cord blood NK cells engineered to express IL-15 and a CD19-targeted CAR show long-term persistence and potent antitumor activity. *Leukemia,* 32**,** 520-531.

LIU, S., GALAT, V., GALAT, Y., LEE, Y. K. A., WAINWRIGHT, D. & WU, J. 2021. NK cell-based cancer immunotherapy: from basic biology to clinical development. *J Hematol Oncol,* 14**,** 7.

LIU, S., WU, W., DU, Y., YIN, H., CHEN, Q., YU, W., WANG, W., YU, J., LIU, L., LOU, W. & PU, N. 2023. The evolution and heterogeneity of neutrophils in cancers: origins, subsets, functions, orchestrations and clinical applications. *Mol Cancer,* 22, 148.

LORDAN, C., THAPA, D., ROSS, R. P. & COTTER, P. D. 2020. Potential for enriching next-generation health-promoting gut bacteria through prebiotics and other dietary components. *Gut Microbes,* 11**,** 1-20.

LOZUPONE, C. A., STOMBAUGH, J. I., GORDON, J. I., JANSSON, J. K. & KNIGHT, R. 2012. Diversity, stability and resilience of the human gut microbiota. *Nature,* 489**,** 220-30.

LUGLI, G. A., MILANI, C., TURRONI, F., DURANTI, S., FERRARIO, C., VIAPPIANI, A., MANCABELLI, L., MANGIFESTA, M., TAMINIAU, B., DELCENSERIE, V., VAN SINDEREN, D. & VENTURA, M. 2014. Investigation of the evolutionary development of the genus Bifidobacterium by comparative genomics. *Appl Environ Microbiol,* 80**,** 6383-94.

LUO, C., HANG, X., LIU, X., ZHANG, M., YANG, X. & YANG, H. 2015. Detection of erm(X)-mediated antibiotic resistance in Bifidobacterium longum subsp. longum. *Annals of Microbiology,* 65**,** 1985-1991.

LUSTBERG, M. B. 2012. Management of neutropenia in cancer patients. *Clin Adv Hematol Oncol,* 10**,** 825-6.

LUU, T. H., MICHEL, C., BARD, J. M., DRAVET, F., NAZIH, H. & BOBIN-DUBIGEON, C. 2017. Intestinal Proportion of Blautia sp. is Associated with Clinical Stage and Histoprognostic Grade in Patients with Early-Stage Breast Cancer. *Nutr Cancer,* 69**,** 267-275.

LV, B., ZHANG, X., YUAN, J., CHEN, Y., DING, H., CAO, X. & HUANG, A. 2021. Biomaterial-supported MSC transplantation enhances cell-cell communication for spinal cord injury. *Stem Cell Res Ther,* 12**,** 36.

LV, Y., WANG, H. & LIU, Z. 2019. The Role of Regulatory B Cells in Patients with Acute Myeloid Leukemia. *Med Sci Monit,* 25**,** 3026-3031.

MA, B., GAVZY, S. J., SAXENA, V., SONG, Y., PIAO, W., LWIN, H. W., LAKHAN, R., IYYATHURAI, J., LI, L., FRANCE, M., PALUSKIEVICZ, C., SHIRKEY, M. W., HITTLE, L., MUNAWWAR, A., MONGODIN, E. F. & BROMBERG, J. S. 2023. Strain-specific alterations in gut microbiome and host immune responses elicited by tolerogenic Bifidobacterium pseudolongum. *Sci Rep,* 13**,** 1023.

MA, J., LI, Z., ZHANG, W., ZHANG, C., ZHANG, Y., MEI, H., ZHUO, N., WANG, H., WANG, L. & WU, D. 2020. Comparison of gut microbiota in exclusively breast-fed and formula-fed babies: a study of 91 term infants. *Scientific Reports,* 10**,** 15792.

MACIA, L., NANAN, R., HOSSEINI-BEHESHTI, E. & GRAU, G. E. 2020. Host- and Microbiota-Derived Extracellular Vesicles, Immune Function, and Disease Development. *International Journal of Molecular Sciences,* 21**,** 107.

MAGER, L. F., BURKHARD, R., PETT, N., COOKE, N. C. A., BROWN, K., RAMAY, H., PAIK, S., STAGG, J., GROVES, R. A., GALLO, M., LEWIS, I. A., GEUKING, M. B. & MCCOY, K. D. 2020. Microbiome-derived inosine modulates response to checkpoint inhibitor immunotherapy. *Science,* 369**,** 1481-1489.

MAHMOOD, R. D., MORGAN, R. D., EDMONDSON, R. J., CLAMP, A. R. & JAYSON, G. C. 2020. First-Line Management of Advanced High-Grade Serous Ovarian Cancer. *Current Oncology Reports,* 22**,** 64.

MAMIDI, S., HÖNE, S. & KIRSCHFINK, M. 2017. The complement system in cancer: Ambivalence between tumour destruction and promotion. *Immunobiology,* 222**,** 45-54.

MANNING, A. J. & KUEHN, M. J. 2011. Contribution of bacterial outer membrane vesicles to innate bacterial defense. *BMC Microbiology,* 11**,** 258.

MANOME, A., ABIKO, Y., KAWASHIMA, J., WASHIO, J., FUKUMOTO, S. & TAKAHASHI, N. 2019. Acidogenic Potential of Oral Bifidobacterium and Its High Fluoride Tolerance. *Frontiers in Microbiology,* 10.

MANTOVANI, A., ALLAVENA, P., MARCHESI, F. & GARLANDA, C. 2022. Macrophages as tools and targets in cancer therapy. *Nature Reviews Drug Discovery,* 21**,** 799-820.

MARTÍN, M. & RAMOS, S. 2021. Impact of Dietary Flavanols on Microbiota, Immunity and Inflammation in Metabolic Diseases. *Nutrients,* 13.

MARTINEZ, F. O. & GORDON, S. 2014. The M1 and M2 paradigm of macrophage activation: time for reassessment. *F1000Prime Rep,* 6**,** 13.

MASENGA, S. K., HAMOOYA, B., HANGOMA, J., HAYUMBU, V., ERTUGLU, L. A., ISHIMWE, J., RAHMAN, S., SALEEM, M., LAFFER, C. L., ELIJOVICH, F. & KIRABO, A. 2022. Recent advances in modulation of cardiovascular diseases by the gut microbiota. *Journal of Human Hypertension,* 36**,** 952-959.

MASHIAH, J., KARADY, T., FLISS-ISAKOV, N., SPRECHER, E., SLODOWNIK, D., ARTZI, O., SAMUELOV, L., ELLENBOGEN, E., GODNEVA, A., SEGAL, E. & MAHARSHAK, N. 2022. Clinical efficacy of fecal microbial transplantation treatment in adults with moderate-to-severe atopic dermatitis. *Immun Inflamm Dis,* 10**,** e570.

MASUCCI, M. T., MINOPOLI, M., DEL VECCHIO, S. & CARRIERO, M. V. 2020. The Emerging Role of Neutrophil Extracellular Traps (NETs) in Tumor Progression and Metastasis. *Front Immunol,* 11**,** 1749.

MATSON, V., FESSLER, J., BAO, R., CHONGSUWAT, T., ZHA, Y., ALEGRE, M. L., LUKE, J. J. & GAJEWSKI, T. F. 2018. The commensal microbiome is associated with anti-PD-1 efficacy in metastatic melanoma patients. *Science,* 359**,** 104-108.

MCKEE, A. M., KIRKUP, B. M., MADGWICK, M., FOWLER, W. J., PRICE, C. A., DREGER, S. A., ANSORGE, R., MAKIN, K. A., CAIM, S., LE GALL, G., PAVELEY, J., LECLAIRE, C., DALBY, M., ALCON-GINER, C., ANDRUSAITE, A., FENG, T. Y., DI MODICA, M., TRIULZI, T., TAGLIABUE, E., MILLING, S. W. F., WEILBAECHER, K. N., RUTKOWSKI, M. R., KORCSMÁROS, T., HALL, L. J. & ROBINSON, S. D. 2021. Antibiotic-induced disturbances of the gut microbiota result in accelerated breast tumor growth. *iScience,* 24**,** 103012.

MCNABNEY, S. M. & HENAGAN, T. M. 2017. Short chain fatty acids in the colon and peripheral tissues: a focus on butyrate, colon cancer, obesity and insulin resistance. *Nutrients,* 9**,** 1348.

MCRITCHIE, B. R. & AKKAYA, B. 2022. Exhaust the exhausters: Targeting regulatory T cells in the tumor microenvironment. *Front Immunol,* 13**,** 940052.

MÉNARD, O., BUTEL, M. J., GABORIAU-ROUTHIAU, V. & WALIGORA-DUPRIET, A. J. 2008. Gnotobiotic mouse immune response induced by Bifidobacterium sp. strains isolated from infants. *Appl Environ Microbiol,* 74**,** 660-6.

MERENSTEIN, D., POT, B., LEYER, G., OUWEHAND, A. C., PREIDIS, G. A., ELKINS, C. A., HILL, C., LEWIS, Z. T., SHANE, A. L., ZMORA, N.,

PETROVA, M. I., COLLADO, M. C., MORELLI, L., MONTOYA, G. A., SZAJEWSKA, H., TANCREDI, D. J. & SANDERS, M. E. 2023. Emerging issues in probiotic safety: 2023 perspectives. *Gut Microbes,* 15**,** 2185034.

MIHAILA, A. C., CIORTAN, L., MACARIE, R. D., VADANA, M., CECOLTAN, S., PREDA, M. B., HUDITA, A., GAN, A. M., JAKOBSSON, G., TUCUREANU, M. M., BARBU, E., BALANESCU, S., SIMIONESCU, M., SCHIOPU, A. & BUTOI, E. 2021. Transcriptional Profiling and Functional Analysis of N1/N2 Neutrophils Reveal an Immunomodulatory Effect of S100A9-Blockade on the Pro-Inflammatory N1 Subpopulation. *Front Immunol,* 12**,** 708770.

MILLS, C. D., KINCAID, K., ALT, J. M., HEILMAN, M. J. & HILL, A. M. 2000. M-1/M-2 macrophages and the Th1/Th2 paradigm. *J Immunol,* 164**,** 6166-73.

MIN, H. Y. & LEE, H. Y. 2023. Cellular Dormancy in Cancer: Mechanisms and Potential Targeting Strategies. *Cancer Res Treat,* 55**,** 720-736.

MIRAGLIA DEL GIUDICE, M., INDOLFI, C., CAPASSO, M., MAIELLO, N., DECIMO, F. & CIPRANDI, G. 2017. Bifidobacterium mixture (B longum BB536, B infantis M-63, B breve M-16V) treatment in children with seasonal allergic rhinitis and intermittent asthma. *Ital J Pediatr,* 43**,** 25.

MIRET, J. J., KIRSCHMEIER, P., KOYAMA, S., ZHU, M., LI, Y. Y., NAITO, Y., WU, M., MALLADI, V. S., HUANG, W., WALKER, W., PALAKURTHI, S., DRANOFF, G., HAMMERMAN, P. S., PECOT, C. V., WONG, K.-K. & AKBAY, E. A. 2019. Suppression of Myeloid Cell Arginase Activity leads to Therapeutic Response in a NSCLC Mouse Model by Activating Anti-Tumor Immunity. *Journal for ImmunoTherapy of Cancer,* 7**,** 32.

MIYAWAKI, T., KENMOTSU, H., DOSHITA, K., KODAMA, H., NISHIOKA, N., IIDA, Y., MIYAWAKI, E., MAMESAYA, N., KOBAYASHI, H., OMORI, S., KO, R., WAKUDA, K., ONO, A., NAITO, T., MURAKAMI, H., MORI, K., HARADA, H., ENDO, M., TAKAHASHI, K. & TAKAHASHI, T. 2023. Clinical impact of tumour burden on the efficacy of PD-1/PD-L1 inhibitors plus chemotherapy in non-small-cell lung cancer. *Cancer Med,* 12**,** 1451-1460.

MOHAMADZADEH, M., PFEILER, E. A., BROWN, J. B., ZADEH, M., GRAMAROSSA, M., MANAGLIA, E., BERE, P., SARRAJ, B., KHAN, M. W., PAKANATI, K. C., ANSARI, M. J., O'FLAHERTY, S., BARRETT, T. & KLAENHAMMER, T. R. 2011. Regulation of induced colonic inflammation by <i>Lactobacillus acidophilus</i> deficient in lipoteichoic acid. *Proceedings of the National Academy of Sciences,* 108**,** 4623-4630.

MONTASSIER, E., VALDÉS-MAS, R., BATARD, E., ZMORA, N., DORI-BACHASH, M., SUEZ, J. & ELINAV, E. 2021. Probiotics impact the antibiotic resistance gene reservoir along the human GI tract in a person-specific and antibiotic-dependent manner. *Nat Microbiol,* 6**,** 1043-1054.

MOTEI, D. E., BETERI, B., HEPSOMALI, P., TZORTZIS, G., VULEVIC, J. & COSTABILE, A. 2023. Supplementation with postbiotic from Bifidobacterium Breve BB091109 improves inflammatory status and

endocrine function in healthy females: a randomized, double-blind, placebo-controlled, parallel-groups study. *Frontiers in Microbiology,* 14.

MOWAT, A. M. 2003. Anatomical basis of tolerance and immunity to intestinal antigens. *Nature Reviews Immunology,* 3**,** 331-341.

MURPHY, T. L. & MURPHY, K. M. 2022. Dendritic cells in cancer immunology. *Cell Mol Immunol,* 19**,** 3-13.

NAVEGANTES, K. C., DE SOUZA GOMES, R., PEREIRA, P. A. T., CZAIKOSKI, P. G., AZEVEDO, C. H. M. & MONTEIRO, M. C. 2017. Immune modulation of some autoimmune diseases: the critical role of macrophages and neutrophils in the innate and adaptive immunity. *Journal of Translational Medicine,* 15**,** 36.

NEJMAN, D., LIVYATAN, I., FUKS, G., GAVERT, N., ZWANG, Y., GELLER, L. T., ROTTER-MASKOWITZ, A., WEISER, R., MALLEL, G., GIGI, E., MELTSER, A., DOUGLAS, G. M., KAMER, I., GOPALAKRISHNAN, V., DADOSH, T., LEVIN-ZAIDMAN, S., AVNET, S., ATLAN, T., COOPER, Z. A., ARORA, R., COGDILL, A. P., KHAN, M. A. W., OLOGUN, G., BUSSI, Y., WEINBERGER, A., LOTAN-POMPAN, M., GOLANI, O., PERRY, G., ROKAH, M., BAHAR-SHANY, K., ROZEMAN, E. A., BLANK, C. U., RONAI, A., SHAOUL, R., AMIT, A., DORFMAN, T., KREMER, R., COHEN, Z. R., HARNOF, S., SIEGAL, T., YEHUDA-SHNAIDMAN, E., GAL-YAM, E. N., SHAPIRA, H., BALDINI, N., LANGILLE, M. G. I., BEN-NUN, A., KAUFMAN, B., NISSAN, A., GOLAN, T., DADIANI, M., LEVANON, K., BAR, J., YUST-KATZ, S., BARSHACK, I., PEEPER, D. S., RAZ, D. J., SEGAL, E., WARGO, J. A., SANDBANK, J., SHENTAL, N. & STRAUSSMAN, R. 2020. The human tumor microbiome is composed of tumor type–specific intracellular bacteria. *Science,* 368**,** 973-980.

NG, S. L., TEO, Y. J., SETIAGANI, Y. A., KARJALAINEN, K. & RUEDL, C. 2018. Type 1 Conventional CD103(+) Dendritic Cells Control Effector CD8(+) T Cell Migration, Survival, and Memory Responses During Influenza Infection. *Front Immunol,* 9**,** 3043.

NICKEL, W. 2010. Pathways of unconventional protein secretion. *Current opinion in biotechnology,* 21**,** 621-626.

NIKKARI, S., MCLAUGHLIN, I. J., BI, W., DODGE, D. E. & RELMAN, D. A. 2001. Does blood of healthy subjects contain bacterial ribosomal DNA? *J Clin Microbiol,* 39**,** 1956-9.

NOGUEIRA, J. C. R. & GONÇALVES, M. D. C. R. 2011. Probiotics in allergic rhinitis. *Brazilian Journal of otorhinolaryngology,* 77**,** 129-134.

O'CALLAGHAN, A. & VAN SINDEREN, D. 2016. Bifidobacteria and Their Role as Members of the Human Gut Microbiota. *Front Microbiol,* 7**,** 925.

O'CONNELL MOTHERWAY, M., ZOMER, A., LEAHY, S. C., REUNANEN, J., BOTTACINI, F., CLAESSON, M. J., O'BRIEN, F., FLYNN, K., CASEY, P. G., MUNOZ, J. A., KEARNEY, B., HOUSTON, A. M., O'MAHONY, C., HIGGINS, D. G., SHANAHAN, F., PALVA, A., DE VOS, W. M., FITZGERALD, G. F., VENTURA, M., O'TOOLE, P. W. & VAN SINDEREN, D. 2011. Functional genome analysis of Bifidobacterium breve UCC2003 reveals type IVb tight adherence (Tad) pili as an essential and

conserved host-colonization factor. *Proc Natl Acad Sci U S A,* 108**,** 11217-22.

OBIERO, C. W., GUMBI, W., MWAKIO, S., MWANGUDZAH, H., SEALE, A. C., TANIUCHI, M., LIU, J., HOUPT, E. & BERKLEY, J. A. 2022. Detection of pathogens associated with early-onset neonatal sepsis in cord blood at birth using quantitative PCR. *Wellcome Open Res,* 7**,** 3.

OHMS, M., MÖLLER, S. & LASKAY, T. 2020. An Attempt to Polarize Human Neutrophils Toward N1 and N2 Phenotypes in vitro. *Front Immunol,* 11**,** 532.

OPPEZZO, A. & ROSSELLI, F. 2021. The underestimated role of the microphthalmia-associated transcription factor (MiTF) in normal and pathological haematopoiesis. *Cell & Bioscience,* 11**,** 18.

OU, S., WANG, H., TAO, Y., LUO, K., YE, J., RAN, S., GUAN, Z., WANG, Y., HU, H. & HUANG, R. 2022. Fusobacterium nucleatum and colorectal cancer: From phenomenon to mechanism. *Frontiers in Cellular and Infection Microbiology,* 12.

PADMANABHAN, P., GROSSE, J., ASAD, A. B., RADDA, G. K. & GOLAY, X. 2013. Gastrointestinal transit measurements in mice with 99mTc-DTPA-labeled activated charcoal using NanoSPECT-CT. *EJNMMI Res,* 3**,** 60.

PAGE, A., CHUVIN, N., VALLADEAU-GUILEMOND, J. & DEPIL, S. 2024. Development of NK cell-based cancer immunotherapies through receptor engineering. *Cellular & Molecular Immunology,* 21**,** 315-331.

PAGET, S. 1889. The distribution of secondary growths in cancer of the breast. *The Lancet,* 133**,** 571-573.

PAÏSSÉ, S., VALLE, C., SERVANT, F., COURTNEY, M., BURCELIN, R., AMAR, J. & LELOUVIER, B. 2016. Comprehensive description of blood microbiome from healthy donors assessed by 16S targeted metagenomic sequencing. *Transfusion,* 56**,** 1138-47.

PAN, H., GRAY, R., BRAYBROOKE, J., DAVIES, C., TAYLOR, C., MCGALE, P., PETO, R., PRITCHARD, K. I., BERGH, J., DOWSETT, M. & HAYES, D. F. 2017. 20-Year Risks of Breast-Cancer Recurrence after Stopping Endocrine Therapy at 5 Years. *N Engl J Med,* 377**,** 1836-1846.

PARK, H.-S., HAN, J.-H., PARK, J. W., LEE, D.-H., JANG, K.-W., LEE, M., HEO, K.-S. & MYUNG, C.-S. 2021. Sodium propionate exerts anticancer effect in mice bearing breast cancer cell xenograft by regulating JAK2/STAT3/ROS/p38 MAPK signaling. *Acta Pharmacologica Sinica,* 42**,** 1311-1323.

PARK, J. Y., CHOI, J., LEE, Y., LEE, J. E., LEE, E. H., KWON, H. J., YANG, J., JEONG, B. R., KIM, Y. K. & HAN, P. L. 2017. Metagenome Analysis of Bodily Microbiota in a Mouse Model of Alzheimer Disease Using Bacteria-derived Membrane Vesicles in Blood. *Exp Neurobiol,* 26**,** 369-379.

PARK, S.-Y. & NAM, J.-S. 2020. The force awakens: metastatic dormant cancer cells. *Experimental & Molecular Medicine,* 52**,** 569-581.

PASARE, C. & MEDZHITOV, R. 2004. Toll-like receptors: linking innate and adaptive immunity. *Microbes and infection,* 6**,** 1382-1387.

PATEL, Y., SONI, V., RHEE, K. Y. & HELMANN, J. D. 2023. Mutations in rpoB That Confer Rifampicin Resistance Can Alter Levels of Peptidoglycan Precursors and Affect β-Lactam Susceptibility. *mBio,* 14**,** e0316822.

PAVLICK, A. C., ARIYAN, C. E., BUCHBINDER, E. I., DAVAR, D., GIBNEY, G. T., HAMID, O., HIEKEN, T. J., IZAR, B., JOHNSON, D. B., KULKARNI, R. P., LUKE, J. J., MITCHELL, T. C., MOORADIAN, M. J., RUBIN, K. M., SALAMA, A. K., SHIRAI, K., TAUBE, J. M., TAWBI, H. A., TOLLEY, J. K., VALDUEZA, C., WEISS, S. A., WONG, M. K. & SULLIVAN, R. J. 2023. Society for Immunotherapy of Cancer (SITC) clinical practice guideline on immunotherapy for the treatment of melanoma, version 3.0. *J Immunother Cancer,* 11.

PENG, D., FU, M., WANG, M., WEI, Y. & WEI, X. 2022. Targeting TGF-β signal transduction for fibrosis and cancer therapy. *Mol Cancer,* 21**,** 104.

PETERSEN JILLIAN, M. & OSVATIC, J. 2018. Microbiomes In Natura: Importance of Invertebrates in Understanding the Natural Variety of Animal-Microbe Interactions. *mSystems,* 3**,** 10.1128/msystems.00179-17.

PETITPREZ, F., DE REYNIÈS, A., KEUNG, E. Z., CHEN, T. W.-W., SUN, C.-M., CALDERARO, J., JENG, Y.-M., HSIAO, L.-P., LACROIX, L., BOUGOÜIN, A., MOREIRA, M., LACROIX, G., NATARIO, I., ADAM, J., LUCCHESI, C., LAIZET, Y. H., TOULMONDE, M., BURGESS, M. A., BOLEJACK, V., REINKE, D., WANI, K. M., WANG, W.-L., LAZAR, A. J., ROLAND, C. L., WARGO, J. A., ITALIANO, A., SAUTÈS-FRIDMAN, C., TAWBI, H. A. & FRIDMAN, W. H. 2020. B cells are associated with survival and immunotherapy response in sarcoma. *Nature,* 577**,** 556-560.

PICCARD, H., MUSCHEL, R. J. & OPDENAKKER, G. 2012. On the dual roles and polarized phenotypes of neutrophils in tumor development and progression. *Critical Reviews in Oncology/Hematology,* 82**,** 296-309.

PILLAY, J., RAMAKERS, B. P., KAMP, V. M., LOI, A. L. T., LAM, S. W., HIETBRINK, F., LEENEN, L. P., TOOL, A. T., PICKKERS, P. & KOENDERMAN, L. 2010. Functional heterogeneity and differential priming of circulating neutrophils in human experimental endotoxemia. *Journal of Leukocyte Biology,* 88**,** 211-220.

POORE, G. D., KOPYLOVA, E., ZHU, Q., CARPENTER, C., FRARACCIO, S., WANDRO, S., KOSCIOLEK, T., JANSSEN, S., METCALF, J., SONG, S. J., KANBAR, J., MILLER-MONTGOMERY, S., HEATON, R., MCKAY, R., PATEL, S. P., SWAFFORD, A. D. & KNIGHT, R. 2024. Retraction Note: Microbiome analyses of blood and tissues suggest cancer diagnostic approach. *Nature,* 631**,** 694-694.

PROCTOR, L. M., CREASY, H. H., FETTWEIS, J. M., LLOYD-PRICE, J., MAHURKAR, A., ZHOU, W., BUCK, G. A., SNYDER, M. P., STRAUSS, J. F., WEINSTOCK, G. M., WHITE, O., HUTTENHOWER, C. & THE INTEGRATIVE, H. M. P. R. N. C. 2019. The Integrative Human Microbiome Project. *Nature,* 569**,** 641-648.

PUSCHHOF, J., PLEGUEZUELOS-MANZANO, C. & CLEVERS, H. 2021. Organoids and organs-on-chips: Insights into human gut-microbe interactions. *Cell Host Microbe,* 29**,** 867-878.

PUSHALKAR, S., HUNDEYIN, M., DALEY, D., ZAMBIRINIS, C. P., KURZ, E., MISHRA, A., MOHAN, N., AYKUT, B., USYK, M., TORRES, L. E., WERBA, G., ZHANG, K., GUO, Y., LI, Q., AKKAD, N., LALL, S., WADOWSKI, B., GUTIERREZ, J., KOCHEN ROSSI, J. A., HERZOG, J. W., DISKIN, B., TORRES-HERNANDEZ, A., LEINWAND, J., WANG, W., TAUNK, P. S., SAVADKAR, S., JANAL, M., SAXENA, A., LI, X., COHEN, D., SARTOR, R. B., SAXENA, D. & MILLER, G. 2018. The Pancreatic Cancer Microbiome Promotes Oncogenesis by Induction of Innate and Adaptive Immune Suppression. *Cancer Discov,* 8**,** 403-416.

QIN, J., LI, R., RAES, J., ARUMUGAM, M., BURGDORF, K. S., MANICHANH, C., NIELSEN, T., PONS, N., LEVENEZ, F., YAMADA, T., MENDE, D. R., LI, J., XU, J., LI, S., LI, D., CAO, J., WANG, B., LIANG, H., ZHENG, H., XIE, Y., TAP, J., LEPAGE, P., BERTALAN, M., BATTO, J.-M., HANSEN, T., LE PASLIER, D., LINNEBERG, A., NIELSEN, H. B., PELLETIER, E., RENAULT, P., SICHERITZ-PONTEN, T., TURNER, K., ZHU, H., YU, C., LI, S., JIAN, M., ZHOU, Y., LI, Y., ZHANG, X., LI, S., QIN, N., YANG, H., WANG, J., BRUNAK, S., DORÉ, J., GUARNER, F., KRISTIANSEN, K., PEDERSEN, O., PARKHILL, J., WEISSENBACH, J., ANTOLIN, M., ARTIGUENAVE, F., BLOTTIERE, H., BORRUEL, N., BRULS, T., CASELLAS, F., CHERVAUX, C., CULTRONE, A., DELORME, C., DENARIAZ, G., DERVYN, R., FORTE, M., FRISS, C., VAN DE GUCHTE, M., GUEDON, E., HAIMET, F., JAMET, A., JUSTE, C., KACI, G., KLEEREBEZEM, M., KNOL, J., KRISTENSEN, M., LAYEC, S., LE ROUX, K., LECLERC, M., MAGUIN, E., MELO MINARDI, R., OOZEER, R., RESCIGNO, M., SANCHEZ, N., TIMS, S., TORREJON, T., VARELA, E., DE VOS, W., WINOGRADSKY, Y., ZOETENDAL, E., BORK, P., EHRLICH, S. D., WANG, J. & META, H. I. T. C. 2010a. A human gut microbial gene catalogue established by metagenomic sequencing. *Nature,* 464**,** 59-65.

QUIGLEY, E. 2017. Bifidobacterium animalis spp. lactis. *The microbiota in gastrointestinal pathophysiology*. Elsevier.

RAGER, T., ECKBURG, A., PATEL, M., QIU, R., GANTIWALA, S., DOVALOVSKY, K., FAN, K., LAM, K., ROESLER, C., RASTOGI, A., GAUTAM, S., DUBE, N., MORGAN, B., NASIFUZZAMAN, S. M., RAMASWAMI, D., GNANASEKAR, V., SMITH, J., MERCHANT, A. & PURI, N. 2022. Treatment of Metastatic Melanoma with a Combination of Immunotherapies and Molecularly Targeted Therapies. *Cancers (Basel),* 14.

RAMIREDDY, L., TSEN, H. Y., CHIANG, Y. C., HUNG, C. Y., WU, S. R., YOUNG, S. L., LIN, J. S., HUANG, C. H., CHIU, S. H. & CHEN, C. C. 2021. Molecular Identification and Selection of Probiotic Strains Able to Reduce the Serum TMAO Level in Mice Challenged with Choline. *Foods,* 10.

RASTRELLI, M., TROPEA, S., ROSSI, C. R. & ALAIBAC, M. 2014. Melanoma: epidemiology, risk factors, pathogenesis, diagnosis and classification. *In Vivo,* 28**,** 1005-11.

RATNER, M. 2016. Seres's pioneering microbiome drug fails mid-stage trial. *Nat Biotechnol,* 34**,** 1004-1005.

REBUFFET, L., MELSEN, J. E., ESCALIÈRE, B., BASURTO-LOZADA, D., BHANDOOLA, A., BJÖRKSTRÖM, N. K., BRYCESON, Y. T., CASTRICONI, R., CICHOCKI, F., COLONNA, M., DAVIS, D. M., DIEFENBACH, A., DING, Y., HANIFFA, M., HOROWITZ, A., LANIER, L. L., MALMBERG, K.-J., MILLER, J. S., MORETTA, L., NARNI-MANCINELLI, E., O'NEILL, L. A. J., ROMAGNANI, C., RYAN, D. G., SIVORI, S., SUN, D., VAGNE, C. & VIVIER, E. 2024. High-dimensional single-cell analysis of human natural killer cell heterogeneity. *Nature Immunology*.

REDELMAN-SIDI, G., GLICKMAN, M. S. & BOCHNER, B. H. 2014. The mechanism of action of BCG therapy for bladder cancer—a current perspective. *Nature Reviews Urology,* 11**,** 153-162.

RHODES, D. R., YU, J., SHANKER, K., DESHPANDE, N., VARAMBALLY, R., GHOSH, D., BARRETTE, T., PANDER, A. & CHINNAIYAN, A. M. 2004. ONCOMINE: A Cancer Microarray Database and Integrated Data-Mining Platform. *Neoplasia,* 6**,** 1-6.

RIVERA, C. A. & LENNON-DUMÉNIL, A.-M. 2023. Gut immune cells and intestinal niche imprinting. *Seminars in Cell & Developmental Biology,* 150-151**,** 50-57.

RIVIÈRE, A., SELAK, M., LANTIN, D., LEROY, F. & DE VUYST, L. 2016. Bifidobacteria and Butyrate-Producing Colon Bacteria: Importance and Strategies for Their Stimulation in the Human Gut. *Front Microbiol,* 7**,** 979.

ROBERTSON, C., SAVVA, G. M., CLAPUCI, R., JONES, J., MAIMOUNI, H., BROWN, E., MINOCHA, A., HALL, L. J. & CLARKE, P. 2020. Incidence of necrotising enterocolitis before and after introducing routine prophylactic Lactobacillus and Bifidobacterium probiotics. *Archives of Disease in Childhood - Fetal and Neonatal Edition,* 105**,** 380.

RODRIGUES, M. L., NAKAYASU, E. S., ALMEIDA, I. C. & NIMRICHTER, L. 2014. The impact of proteomics on the understanding of functions and biogenesis of fungal extracellular vesicles. *Journal of Proteomics,* 97**,** 177-186.

ROUANET, A., BOLCA, S., BRU, A., CLAES, I., CVEJIC, H., GIRGIS, H., HARPER, A., LAVERGNE, S. N., MATHYS, S., PANE, M., POT, B., SHORTT, C., ALKEMA, W., BEZULOWSKY, C., BLANQUET-DIOT, S., CHASSARD, C., CLAUS, S. P., HADIDA, B., HEMMINGSEN, C., JEUNE, C., LINDMAN, B., MIDZI, G., MOGNA, L., MOVITZ, C., NASIR, N., OBERREITHER, M., SEEGERS, J., STERKMAN, L., VALO, A., VIEVILLE, F. & CORDAILLAT-SIMMONS, M. 2020. Live Biotherapeutic Products, A Road Map for Safety Assessment. *Front Med (Lausanne),* 7**,** 237.

ROUND, J. L. & MAZMANIAN, S. K. 2009. The gut microbiota shapes intestinal immune responses during health and disease. *Nature Reviews Immunology,* 9**,** 313-323.

ROUTY, B., LE CHATELIER, E., DEROSA, L., DUONG, C. P. M., ALOU, M. T., DAILLÈRE, R., FLUCKIGER, A., MESSAOUDENE, M., RAUBER, C., ROBERTI, M. P., FIDELLE, M., FLAMENT, C., POIRIER-COLAME, V., OPOLON, P., KLEIN, C., IRIBARREN, K., MONDRAGÓN, L., JACQUELOT,

N., QU, B., FERRERE, G., CLÉMENSON, C., MEZQUITA, L., MASIP, J. R., NALTET, C., BROSSEAU, S., KADERBHAI, C., RICHARD, C., RIZVI, H., LEVENEZ, F., GALLERON, N., QUINQUIS, B., PONS, N., RYFFEL, B., MINARD-COLIN, V., GONIN, P., SORIA, J.-C., DEUTSCH, E., LORIOT, Y., GHIRINGHELLI, F., ZALCMAN, G., GOLDWASSER, F., ESCUDIER, B., HELLMANN, M. D., EGGERMONT, A., RAOULT, D., ALBIGES, L., KROEMER, G. & ZITVOGEL, L. 2018. Gut microbiome influences efficacy of PD-1–based immunotherapy against epithelial tumors. *Science,* 359**,** 91-97.

RUTKOWSKI, M. R., ALLEGREZZA, M. J., SVORONOS, N., TESONE, A. J., STEPHEN, T. L., PERALES-PUCHALT, A., NGUYEN, J., ZHANG, P. J., FIERING, S. N., TCHOU, J. & CONEJO-GARCIA, J. R. 2014. Initiation of metastatic breast carcinoma by targeting of the ductal epithelium with adenovirus-cre: a novel transgenic mouse model of breast cancer. *J Vis Exp*.

RUTKOWSKI, M. R., STEPHEN, T. L., SVORONOS, N., ALLEGREZZA, M. J., TESONE, A. J., PERALES-PUCHALT, A., BRENCICOVA, E., ESCOVAR-FADUL, X., NGUYEN, J. M., CADUNGOG, M. G., ZHANG, R., SALATINO, M., TCHOU, J., RABINOVICH, G. A. & CONEJO-GARCIA, J. R. 2015. Microbially driven TLR5-dependent signaling governs distal malignant progression through tumor-promoting inflammation. *Cancer Cell,* 27**,** 27-40.

SAGIV, JITKA Y., MICHAELI, J., ASSI, S., MISHALIAN, I., KISOS, H., LEVY, L., DAMTI, P., LUMBROSO, D., POLYANSKY, L., SIONOV, RONIT V., ARIEL, A., HOVAV, A.-H., HENKE, E., FRIDLENDER, ZVI G. & GRANOT, Z. 2015. Phenotypic Diversity and Plasticity in Circulating Neutrophil Subpopulations in Cancer. *Cell Reports,* 10**,** 562-573.

SAI, B. & XIANG, J. 2018. Disseminated tumour cells in bone marrow are the source of cancer relapse after therapy. *J Cell Mol Med,* 22**,** 5776-5786.

SALMINEN, S., COLLADO, M. C., ENDO, A., HILL, C., LEBEER, S., QUIGLEY, E. M., SANDERS, M. E., SHAMIR, R., SWANN, J. R. & SZAJEWSKA, H. 2021. The International Scientific Association of Probiotics and Prebiotics (ISAPP) consensus statement on the definition and scope of postbiotics. *Nature Reviews Gastroenterology & Hepatology,* 18**,** 649-667.

SCHMIDT, H., BASTHOLT, L., GEERTSEN, P., CHRISTENSEN, I. J., LARSEN, S., GEHL, J. & VON DER MAASE, H. 2005. Elevated neutrophil and monocyte counts in peripheral blood are associated with poor survival in patients with metastatic melanoma: a prognostic model. *British Journal of Cancer,* 93**,** 273-278.

SCUDELLARI, M. 2017. News Feature: Cleaning up the hygiene hypothesis. *Proc Natl Acad Sci U S A*. United States.

SHANG, F., JIANG, X., WANG, H., GUO, S., KANG, S., XU, B., WANG, X., CHEN, S., LI, N., LIU, B. & ZHAO, Z. 2024. Bifidobacterium longum suppresses colorectal cancer through the modulation of intestinal microbes and immune function. *Frontiers in Microbiology,* 15.

SHEN, Y., GIARDINO TORCHIA, M. L., LAWSON, G. W., KARP, C. L., ASHWELL, J. D. & MAZMANIAN, S. K. 2012. Outer membrane vesicles of a human commensal mediate immune regulation and disease protection. *Cell Host Microbe,* 12**,** 509-20.

SHIEN, T. & IWATA, H. 2020. Adjuvant and neoadjuvant therapy for breast cancer. *Jpn J Clin Oncol,* 50**,** 225-229.

SHROUT, M. R., MADISON, A. A., RENNA, M. E., ALFANO, C. M., POVOSKI, S. P., LIPARI, A. M., AGNESE, D. M., CARSON, W. E., 3RD, MALARKEY, W. B., BAILEY, M. T. & KIECOLT-GLASER, J. K. 2022. The gut connection: Intestinal permeability as a pathway from breast cancer survivors' relationship satisfaction to inflammation across treatment. *Brain Behav Immun,* 100**,** 145-154.

SILHAVY, T. J., KAHNE, D. & WALKER, S. 2010. The bacterial cell envelope. *Cold Spring Harb Perspect Biol,* 2**,** a000414.

SIVAN, A., CORRALES, L., HUBERT, N., WILLIAMS, J. B., AQUINO-MICHAELS, K., EARLEY, Z. M., BENYAMIN, F. W., LEI, Y. M., JABRI, B., ALEGRE, M. L., CHANG, E. B. & GAJEWSKI, T. F. 2015. Commensal Bifidobacterium promotes antitumor immunity and facilitates anti-PD-L1 efficacy. *Science,* 350**,** 1084-9.

SLEEMAN, J. P., NAZARENKO, I. & THIELE, W. 2011. Do all roads lead to Rome? Routes to metastasis development. *Int J Cancer,* 128**,** 2511-26.

SMITH, A., PIERRE, J. F., MAKOWSKI, L., TOLLEY, E., LYN-COOK, B., LU, L., VIDAL, G. & STARLARD-DAVENPORT, A. 2019. Distinct microbial communities that differ by race, stage, or breast-tumor subtype in breast tissues of non-Hispanic Black and non-Hispanic White women. *Sci Rep,* 9**,** 11940.

SMITH, P. M., HOWITT, M. R., PANIKOV, N., MICHAUD, M., GALLINI, C. A., BOHLOOLY-Y, M., GLICKMAN, J. N. & GARRETT, W. S. 2013. The Microbial Metabolites, Short-Chain Fatty Acids, Regulate Colonic T$_{reg}$ Cell Homeostasis. *Science,* 341**,** 569-573.

SOBHANI, N., TARDIEL-CYRIL, D., DAVTYAN, A., GENERALI, D., ROUDI, R. & LI, Y. 2021. CTLA-4 in Regulatory T Cells for Cancer Immunotherapy. *Cancers*.

SONG, J., LI, M., LI, C., LIU, K., ZHU, Y. & ZHANG, H. 2022. Friend or foe: RIG- I like receptors and diseases. *Autoimmun Rev,* 21**,** 103161.

SORRENTI, V., ALI, S., MANCIN, L., DAVINELLI, S., PAOLI, A. & SCAPAGNINI, G. 2020. Cocoa Polyphenols and Gut Microbiota Interplay: Bioavailability, Prebiotic Effect, and Impact on Human Health. *Nutrients,* 12.

SRIVASTAVA, S., BASAK, U., NAGHIBI, M., VIJAYAKUMAR, V., PARIHAR, R., PATEL, J., JADON, P. S., PANDIT, A., DARGAD, R. R., KHANNA, S., KUMAR, S. & DAY, R. 2024. A randomized double-blind, placebo-controlled trial to evaluate the safety and efficacy of live Bifidobacterium longum CECT 7347 (ES1) and heat-treated Bifidobacterium longum CECT 7347 (HT-ES1) in participants with diarrhea-predominant irritable bowel syndrome. *Gut Microbes,* 16**,** 2338322.

STEEG, P. S. 2006. Tumor metastasis: mechanistic insights and clinical challenges. *Nat Med,* 12**,** 895-904.

STENTZ, R., CARVALHO, A. L., JONES, E. J. & CARDING, S. R. 2018. Fantastic voyage: the journey of intestinal microbiota-derived microvesicles through the body. *Biochem Soc Trans,* 46**,** 1021-1027.

STENTZ, R., JONES, E., JUODEIKIS, R., WEGMANN, U., GUIRRO, M., GOLDSON ANDREW, J., BRION, A., BOOTH, C., SUDHAKAR, P., BROWN IAN, R., KORCSMÁROS, T. & CARDING SIMON, R. 2022a. The Proteome of Extracellular Vesicles Produced by the Human Gut Bacteria Bacteroides thetaiotaomicron In Vivo Is Influenced by Environmental and Host-Derived Factors. *Applied and Environmental Microbiology,* 88**,** e00533-22.

STENTZ, R., MIQUEL-CLOPÉS, A. & CARDING, S. R. 2022b. Production, Isolation, and Characterization of Bioengineered Bacterial Extracellular Membrane Vesicles Derived from Bacteroides thetaiotaomicron and Their Use in Vaccine Development. *Bacterial Vaccines: Methods and Protocols.* New York, NY: Springer US.

STIEMSMA, L. T., REYNOLDS, L. A., TURVEY, S. E. & FINLAY, B. B. 2015. The hygiene hypothesis: current perspectives and future therapies. *Immunotargets Ther,* 4**,** 143-57.

STRISCIUGLIO, C., VITALE, A., PERNA, F., GARZIANO, F., DOLCE, P., VITALE, S., MICILLO, T., OGLIO, F., DEL GIUDICE, M. M. & MATARESE, G. 2023. Bifidobacteria modulate immune response in pediatric patients with cow's milk protein allergy. *Pediatric Research,* 94**,** 1111-1118.

STUIVENBERG, G. A., BURTON, J. P., BRON, P. A. & REID, G. 2022. Why Are Bifidobacteria Important for Infants? *Microorganisms,* 10.

SU, W., CHEN, Y., CAO, P., GUO, Y., WANG, S. & DONG, W. 2020. Fusobacterium nucleatum Promotes the Development of Ulcerative Colitis by Inducing the Autophagic Cell Death of Intestinal Epithelial. *Front Cell Infect Microbiol,* 10**,** 594806.

SU, X., XU, Y., FOX, G. C., XIANG, J., KWAKWA, K. A., DAVIS, J. L., BELLE, J. I., LEE, W. C., WONG, W. H., FONTANA, F., HERNANDEZ-AYA, L. F., KOBAYASHI, T., TOMASSON, H. M., SU, J., BAKEWELL, S. J., STEWART, S. A., EGBULEFU, C., KARMAKAR, P., MEYER, M. A., VEIS, D. J., DENARDO, D. G., LANZA, G. M., ACHILEFU, S. & WEILBAECHER, K. N. 2021. Breast cancer-derived GM-CSF regulates arginase 1 in myeloid cells to promote an immunosuppressive microenvironment. *J Clin Invest,* 131.

SUCHANEK, O., FERDINAND, J. R., TUONG, Z. K., WIJEYESINGHE, S., CHANDRA, A., CLAUDER, A.-K., ALMEIDA, L. N., CLARE, S., HARCOURT, K., WARD, C. J., BASHFORD-ROGERS, R., LAWLEY, T., MANZ, R. A., OKKENHAUG, K., MASOPUST, D. & CLATWORTHY, M. R. 2023. Tissue-resident B cells orchestrate macrophage polarisation and function. *Nature Communications,* 14**,** 7081.

SUDHAKAR, A. 2009. History of cancer, ancient and modern treatment methods. *Journal of cancer science & therapy,* 1**,** 1.

SUN, S., LI, X., REN, A., DU, M., DU, H., SHU, Y., ZHU, L. & WANG, W. 2016. Choline and betaine consumption lowers cancer risk: a meta-analysis of epidemiologic studies. *Sci Rep,* 6**,** 35547.

SUN, S., LUO, L., LIANG, W., YIN, Q., GUO, J., RUSH, A. M., LV, Z., LIANG, Q., FISCHBACH, M. A., SONNENBURG, J. L., DODD, D., DAVIS, M. M. & WANG, F. 2020. Bifidobacterium alters the gut microbiota and modulates the functional metabolism of T regulatory cells in the context of immune checkpoint blockade. *Proceedings of the National Academy of Sciences,* 117**,** 27509-27515.

SURVE, M. V., ANIL, A., KAMATH, K. G., BHUTDA, S., STHANAM, L. K., PRADHAN, A., SRIVASTAVA, R., BASU, B., DUTTA, S., SEN, S., MODI, D. & BANERJEE, A. 2016. Membrane Vesicles of Group B Streptococcus Disrupt Feto-Maternal Barrier Leading to Preterm Birth. *PLOS Pathogens,* 12**,** e1005816.

SWANSON, K. S., GIBSON, G. R., HUTKINS, R., REIMER, R. A., REID, G., VERBEKE, K., SCOTT, K. P., HOLSCHER, H. D., AZAD, M. B., DELZENNE, N. M. & SANDERS, M. E. 2020. The International Scientific Association for Probiotics and Prebiotics (ISAPP) consensus statement on the definition and scope of synbiotics. *Nat Rev Gastroenterol Hepatol,* 17**,** 687-701.

SWIERCZAK, A. & POLLARD, J. W. 2020. Myeloid Cells in Metastasis. *Cold Spring Harb Perspect Med,* 10.

TAN, J., MCKENZIE, C., POTAMITIS, M., THORBURN, A. N., MACKAY, C. R. & MACIA, L. 2014. Chapter Three - The Role of Short-Chain Fatty Acids in Health and Disease. *In:* ALT, F. W. (ed.) *Advances in Immunology.* Academic Press.

TANG, W. H., WANG, Z., LEVISON, B. S., KOETH, R. A., BRITT, E. B., FU, X., WU, Y. & HAZEN, S. L. 2013. Intestinal microbial metabolism of phosphatidylcholine and cardiovascular risk. *N Engl J Med,* 368**,** 1575-84.

TANOUE, T., MORITA, S., PLICHTA, D. R., SKELLY, A. N., SUDA, W., SUGIURA, Y., NARUSHIMA, S., VLAMAKIS, H., MOTOO, I., SUGITA, K., SHIOTA, A., TAKESHITA, K., YASUMA-MITOBE, K., RIETHMACHER, D., KAISHO, T., NORMAN, J. M., MUCIDA, D., SUEMATSU, M., YAGUCHI, T., BUCCI, V., INOUE, T., KAWAKAMI, Y., OLLE, B., ROBERTS, B., HATTORI, M., XAVIER, R. J., ATARASHI, K. & HONDA, K. 2019. A defined commensal consortium elicits CD8 T cells and anti-cancer immunity. *Nature,* 565**,** 600-605.

TATUSOV, R. L., GALPERIN, M. Y., NATALE, D. A. & KOONIN, E. V. 2000. The COG database: a tool for genome-scale analysis of protein functions and evolution. *Nucleic Acids Res,* 28**,** 33-6.

TAY, R. E., RICHARDSON, E. K. & TOH, H. C. 2021. Revisiting the role of CD4+ T cells in cancer immunotherapy—new insights into old paradigms. *Cancer Gene Therapy,* 28**,** 5-17.

THAY, B., DAMM, A., KUFER, T. A., WAI, S. N. & OSCARSSON, J. 2014. Aggregatibacter actinomycetemcomitans outer membrane vesicles

are internalized in human host cells and trigger NOD1- and NOD2-dependent NF-κB activation. *Infect Immun, 82,* 4034-46.

TSATSARONIS, J. A., FRANCH-ARROYO, S., RESCH, U. & CHARPENTIER, E. 2018. Extracellular Vesicle RNA: A Universal Mediator of Microbial Communication? *Trends in Microbiology, 26,* 401-410.

TURKINA, M. V., OLOFSSON, A., MAGNUSSON, K. E., ARNQVIST, A. & VIKSTRÖM, E. 2015. Helicobacter pylori vesicles carrying CagA localize in the vicinity of cell-cell contacts and induce histone H1 binding to ATP in epithelial cells. *FEMS Microbiol Lett, 362.*

TURNBAUGH, P. J., HAMADY, M., YATSUNENKO, T., CANTAREL, B. L., DUNCAN, A., LEY, R. E., SOGIN, M. L., JONES, W. J., ROE, B. A., AFFOURTIT, J. P., EGHOLM, M., HENRISSAT, B., HEATH, A. C., KNIGHT, R. & GORDON, J. I. 2009. A core gut microbiome in obese and lean twins. *Nature, 457,* 480-4.

TURNER, L., PRASZKIER, J., HUTTON, M. L., STEER, D., RAMM, G., KAPARAKIS‐LIASKOS, M. & FERRERO, R. L. 2015. Increased outer membrane vesicle formation in a Helicobacter pylori tolB mutant. *Helicobacter, 20,* 269-283.

UK, C. R. 2021. Melanoma skin cancer incidence statistics | Cancer Research UK. Available: https://www.cancerresearchuk.org/health-professional/cancer-statistics/statistics-by-cancer-type/melanoma-skin-cancer/incidence#ref- [Accessed 03/04/24].

UK., C. R. 2015. *Cancer risk statistics* [Online]. Cancer risk statistics | Cancer Research UK. [Accessed 30/05/2024].

URIBE-HERRANZ, M., RAFAIL, S., BEGHI, S., GIL-DE-GÓMEZ, L., VERGINADIS, I., BITTINGER, K., PUSTYLNIKOV, S., PIERINI, S., PERALES-LINARES, R., BLAIR, I. A., MESAROS, C. A., SNYDER, N. W., BUSHMAN, F., KOUMENIS, C. & FACCIABENE, A. 2020. Gut microbiota modulate dendritic cell antigen presentation and radiotherapy-induced antitumor immune response. *J Clin Invest, 130,* 466-479.

VALENCIA, J. C., ERWIN-COHEN, R. A., CLAVIJO, P. E., ALLEN, C., SANFORD, M. E., DAY, C. P., HESS, M. M., JOHNSON, M., YIN, J., FENIMORE, J. M., BETTENCOURT, I. A., TSUNEYAMA, K., ROMERO, M. E., KLARMANN, K. D., JIANG, P., BAE, H. R., MCVICAR, D. W., MERLINO, G., EDMONDSON, E. F., ANANDASABAPATHY, N. & YOUNG, H. A. 2021. Myeloid-Derived Suppressive Cell Expansion Promotes Melanoma Growth and Autoimmunity by Inhibiting CD40/IL27 Regulation in Macrophages. *Cancer Res, 81,* 5977-5990.

VAN DER AA, L. B., VAN AALDEREN, W. M., HEYMANS, H. S., HENK SILLEVIS SMITT, J., NAUTA, A. J., KNIPPELS, L. M., BEN AMOR, K. & SPRIKKELMAN, A. B. 2011. Synbiotics prevent asthma-like symptoms in infants with atopic dermatitis. *Allergy, 66,* 170-7.

VAN HOEK, A. H. A. M., MAYRHOFER, S., DOMIG, K. J. & AARTS, H. J. M. 2008a. Resistance determinant erm(X) is borne by transposon Tn5432 in Bifidobacterium thermophilum and Bifidobacterium animalis subsp. lactis. *International Journal of Antimicrobial Agents, 31,* 544-548.

VANAJA, S. K., RUSSO, A. J., BEHL, B., BANERJEE, I., YANKOVA, M., DESHMUKH, S. D. & RATHINAM, V. A. 2016. Bacterial outer membrane vesicles mediate cytosolic localization of LPS and caspase-11 activation. *Cell,* 165**,** 1106-1119.

VANGAY, P., JOHNSON, A. J., WARD, T. L., AL-GHALITH, G. A., SHIELDS-CUTLER, R. R., HILLMANN, B. M., LUCAS, S. K., BEURA, L. K., THOMPSON, E. A., TILL, L. M., BATRES, R., PAW, B., PERGAMENT, S. L., SAENYAKUL, P., XIONG, M., KIM, A. D., KIM, G., MASOPUST, D., MARTENS, E. C., ANGKURAWARANON, C., MCGREADY, R., KASHYAP, P. C., CULHANE-PERA, K. A. & KNIGHTS, D. 2018. US Immigration Westernizes the Human Gut Microbiome. *Cell,* 175**,** 962-972.e10.

VENTURA, M., CANCHAYA, C., CASALE, A. D., DELLAGLIO, F., NEVIANI, E., FITZGERALD, G. F. & VAN SINDEREN, D. 2006. Analysis of bifidobacterial evolution using a multilocus approach. *Int J Syst Evol Microbiol,* 56**,** 2783-2792.

VENTURA, M., CANCHAYA, C., TAUCH, A., CHANDRA, G., FITZGERALD GERALD, F., CHATER KEITH, F. & VAN SINDEREN, D. 2007. Genomics of Actinobacteria: Tracing the Evolutionary History of an Ancient Phylum. *Microbiology and Molecular Biology Reviews,* 71**,** 495-548.

VÉTIZOU, M., PITT, J. M., DAILLÈRE, R., LEPAGE, P., WALDSCHMITT, N., FLAMENT, C., RUSAKIEWICZ, S., ROUTY, B., ROBERTI, M. P., DUONG, C. P. M., POIRIER-COLAME, V., ROUX, A., BECHAREF, S., FORMENTI, S., GOLDEN, E., CORDING, S., EBERL, G., SCHLITZER, A., GINHOUX, F., MANI, S., YAMAZAKI, T., JACQUELOT, N., ENOT, D. P., BÉRARD, M., NIGOU, J., OPOLON, P., EGGERMONT, A., WOERTHER, P.-L., CHACHATY, E., CHAPUT, N., ROBERT, C., MATEUS, C., KROEMER, G., RAOULT, D., BONECA, I. G., CARBONNEL, F., CHAMAILLARD, M. & ZITVOGEL, L. 2015. Anticancer immunotherapy by CTLA-4 blockade relies on the gut microbiota. *Science,* 350**,** 1079-1084.

VIAUD, S., SACCHERI, F., MIGNOT, G., YAMAZAKI, T., DAILLÈRE, R., HANNANI, D., ENOT, D. P., PFIRSCHKE, C., ENGBLOM, C., PITTET, M. J., SCHLITZER, A., GINHOUX, F., APETOH, L., CHACHATY, E., WOERTHER, P.-L., EBERL, G., BÉRARD, M., ECOBICHON, C., CLERMONT, D., BIZET, C., GABORIAU-ROUTHIAU, V., CERF-BENSUSSAN, N., OPOLON, P., YESSAAD, N., VIVIER, E., RYFFEL, B., ELSON, C. O., DORÉ, J., KROEMER, G., LEPAGE, P., BONECA, I. G., GHIRINGHELLI, F. & ZITVOGEL, L. 2013. The Intestinal Microbiota Modulates the Anticancer Immune Effects of Cyclophosphamide. *Science,* 342**,** 971-976.

VIGNALI, D. A. A., COLLISON, L. W. & WORKMAN, C. J. 2008. How regulatory T cells work. *Nature Reviews Immunology,* 8**,** 523-532.

VITHEEJONGJAROEN, P., KASORN, A., PUTTARAT, N., LOISON, F. & TAWEECHOTIPATR, M. 2022. Bifidobacterium animalis MSMC83 Improves Oxidative Stress and Gut Microbiota in D-Galactose-Induced Rats. *Antioxidants,* 11**,** 2146.

VLEMS, F. A., RUERS, T. J., PUNT, C. J., WOBBES, T. & VAN MUIJEN, G. N. 2003. Relevance of disseminated tumour cells in blood and bone marrow of

patients with solid epithelial tumours in perspective. *Eur J Surg Oncol,* 29**,** 289-302.

WAHL, A., YAO, W., LIAO, B., CHATEAU, M., RICHARDSON, C., LING, L., FRANKS, A., SENTHIL, K., DOYON, G., LI, F., FROST, J., WHITEHURST, C. B., PAGANO, J. S., FLETCHER, C. A., AZCARATE-PERIL, M. A., HUDGENS, M. G., ROGALA, A. R., TUCKER, J. D., MCGOWAN, I., SARTOR, R. B. & GARCIA, J. V. 2024. A germ-free humanized mouse model shows the contribution of resident microbiota to human-specific pathogen infection. *Nature Biotechnology,* 42**,** 905-915.

WALDMAN, A. D., FRITZ, J. M. & LENARDO, M. J. 2020. A guide to cancer immunotherapy: from T cell basic science to clinical practice. *Nature Reviews Immunology,* 20**,** 651-668.

WALKER, A. W., INCE, J., DUNCAN, S. H., WEBSTER, L. M., HOLTROP, G., ZE, X., BROWN, D., STARES, M. D., SCOTT, P., BERGERAT, A., LOUIS, P., MCINTOSH, F., JOHNSTONE, A. M., LOBLEY, G. E., PARKHILL, J. & FLINT, H. J. 2011. Dominant and diet-responsive groups of bacteria within the human colonic microbiota. *Isme j,* 5**,** 220-30.

WALSH, T. R., GALES, A. C., LAXMINARAYAN, R. & DODD, P. C. 2023. Antimicrobial Resistance: Addressing a Global Threat to Humanity. *PLOS Medicine,* 20**,** e1004264.

WANG, F., YIN, Q., CHEN, L. & DAVIS, M. M. 2018. Bifidobacterium can mitigate intestinal immunopathology in the context of CTLA-4 blockade. *Proceedings of the National Academy of Sciences,* 115**,** 157-161.

WANG, Z., MCWILLIAMS-KOEPPEN, H. P., REZA, H., OSTBERG, J. R., CHEN, W., WANG, X., HUYNH, C., VYAS, V., CHANG, W. C., STARR, R., WAGNER, J. R., AGUILAR, B., YANG, X., WU, X., WANG, J., KOELKER-WOLFE, E., SEET, C. S., MONTEL-HAGEN, A., CROOKS, G. M., FORMAN, S. J. & BROWN, C. E. 2022. 3D-organoid culture supports differentiation of human CAR(+) iPSCs into highly functional CAR T cells. *Cell Stem Cell,* 29**,** 515-527.e8.

WATANABE, Y., CUI, L., KATAYAMA, Y., KOZUE, K. & HIRAMATSU, K. 2011. Impact of rpoB Mutations on Reduced Vancomycin Susceptibility in Staphylococcus aureus. *Journal of Clinical Microbiology,* 49**,** 2680-2684.

WEISS, J. M., GUÉRIN, M. V., REGNIER, F., RENAULT, G., GALY-FAUROUX, I., VIMEUX, L., FEUILLET, V., PERANZONI, E., THOREAU, M., TRAUTMANN, A. & BERCOVICI, N. 2017. The STING agonist DMXAA triggers a cooperation between T lymphocytes and myeloid cells that leads to tumor regression. *Oncoimmunology,* 6**,** e1346765.

WESTENEND, P. J., MEURS, C. J. & DAMHUIS, R. A. 2005. Tumour size and vascular invasion predict distant metastasis in stage I breast cancer. Grade distinguishes early and late metastasis. *J Clin Pathol,* 58**,** 196-201.

WESTFALL, S., CARRACCI, F., ESTILL, M., ZHAO, D., WU, Q.-L., SHEN, L., SIMON, J. & PASINETTI, G. M. 2021. Optimization of probiotic therapeutics using machine learning in an artificial human gastrointestinal tract. *Scientific Reports,* 11**,** 1067.

WINER, E. P., LIPATOV, O., IM, S.-A., GONCALVES, A., MUÑOZ-COUSELO, E., LEE, K. S., SCHMID, P., TAMURA, K., TESTA, L., WITZEL, I., OHTANI, S., TURNER, N., ZAMBELLI, S., HARBECK, N., ANDRE, F., DENT, R., ZHOU, X., KARANTZA, V., MEJIA, J. & CORTES, J. 2021. Pembrolizumab versus investigator-choice chemotherapy for metastatic triple-negative breast cancer (KEYNOTE-119): a randomised, open-label, phase 3 trial. *The Lancet Oncology,* 22**,** 499-511.

WINKLER, J., ABISOYE-OGUNNIYAN, A., METCALF, K. J. & WERB, Z. 2020. Concepts of extracellular matrix remodelling in tumour progression and metastasis. *Nat Commun,* 11**,** 5120.

WOO, J., GWAK, G., PARK, I., BAE, B. N., LEE, S. K., CHAE, B. J., YU, J., LEE, J. E., KIM, S. W., NAM, S. J. & RYU, J. M. 2021. Preoperative diagnosis of BRCA1/2 mutation impacts decision-making for risk-reducing mastectomy in breast cancer patients. *Sci Rep,* 11**,** 14747.

WOTHERSPOON, A. C., ORTIZ-HIDALGO, C., FALZON, M. R. & ISAACSON, P. G. 1991. Helicobacter pylori-associated gastritis and primary B-cell gastric lymphoma. *Lancet,* 338**,** 1175-6.

WOUTERS, M. C. A. & NELSON, B. H. 2018. Prognostic Significance of Tumor-Infiltrating B Cells and Plasma Cells in Human Cancer. *Clinical Cancer Research,* 24**,** 6125-6135.

WU, H., GANGULY, S. & TOLLEFSBOL, T. O. 2022. Modulating Microbiota as a New Strategy for Breast Cancer Prevention and Treatment. *Microorganisms* [Online], 10.

WU, W. K., CHEN, C. C., LIU, P. Y., PANYOD, S., LIAO, B. Y., CHEN, P. C., KAO, H. L., KUO, H. C., KUO, C. H., CHIU, T. H. T., CHEN, R. A., CHUANG, H. L., HUANG, Y. T., ZOU, H. B., HSU, C. C., CHANG, T. Y., LIN, C. L., HO, C. T., YU, H. T., SHEEN, L. Y. & WU, M. S. 2019. Identification of TMAO-producer phenotype and host-diet-gut dysbiosis by carnitine challenge test in human and germ-free mice. *Gut,* 68**,** 1439-1449.

WU, W. K., PANYOD, S., LIU, P. Y., CHEN, C. C., KAO, H. L., CHUANG, H. L., CHEN, Y. H., ZOU, H. B., KUO, H. C., KUO, C. H., LIAO, B. Y., CHIU, T. H. T., CHUNG, C. H., LIN, A. Y., LEE, Y. C., TANG, S. L., WANG, J. T., WU, Y. W., HSU, C. C., SHEEN, L. Y., OREKHOV, A. N. & WU, M. S. 2020. Characterization of TMAO productivity from carnitine challenge facilitates personalized nutrition and microbiome signatures discovery. *Microbiome,* 8**,** 162.

XIONG, F., WANG, Q., WU, G.-H., LIU, W.-Z., WANG, B. & CHEN, Y.-J. 2022. Direct and indirect effects of IFN-α2b in malignancy treatment: not only an archer but also an arrow. *Biomarker Research,* 10**,** 69.

XU, X., GAMMON, M. D., ZEISEL, S. H., BRADSHAW, P. T., WETMUR, J. G., TEITELBAUM, S. L., NEUGUT, A. I., SANTELLA, R. M. & CHEN, J. 2009. High intakes of choline and betaine reduce breast cancer mortality in a population-based study. *Faseb j,* 23**,** 4022-8.

YANABA, K., BOUAZIZ, J.-D., MATSUSHITA, T., TSUBATA, T. & TEDDER, T. F. 2009. The Development and Function of Regulatory B Cells Expressing IL-10 (B10 Cells) Requires Antigen Receptor Diversity and TLR Signals1. *The Journal of Immunology,* 182**,** 7459-7472.

YANG, D., CHEN, X., WANG, J., LOU, Q., LOU, Y., LI, L., WANG, H., CHEN, J., WU, M. & SONG, X. 2019a. Dysregulated lung commensal bacteria drive interleukin-17B production to promote pulmonary fibrosis through their outer membrane vesicles. *Immunity,* 50**,** 692-706. e7.

YANG, J., HWANG, I., LEE, E., SHIN, S. J., LEE, E.-J., RHEE, J. H. & YU, J.-W. 2020. Bacterial Outer Membrane Vesicle-Mediated Cytosolic Delivery of Flagellin Triggers Host NLRC4 Canonical Inflammasome Signaling. *Frontiers in Immunology,* 11.

YANG, X., CHENG, X., TANG, Y., QIU, X., WANG, Y., KANG, H., WU, J., WANG, Z., LIU, Y. & CHEN, F. 2019b. Bacterial endotoxin activates the coagulation cascade through gasdermin D-dependent phosphatidylserine exposure. *Immunity,* 51**,** 983-996. e6.

YATSUNENKO, T., REY, F. E., MANARY, M. J., TREHAN, I., DOMINGUEZ-BELLO, M. G., CONTRERAS, M., MAGRIS, M., HIDALGO, G., BALDASSANO, R. N., ANOKHIN, A. P., HEATH, A. C., WARNER, B., REEDER, J., KUCZYNSKI, J., CAPORASO, J. G., LOZUPONE, C. A., LAUBER, C., CLEMENTE, J. C., KNIGHTS, D., KNIGHT, R. & GORDON, J. I. 2012. Human gut microbiome viewed across age and geography. *Nature,* 486**,** 222-7.

YE, W., CHEW, M., HOU, J., LAI, F., LEOPOLD, S. J., LOO, H. L., GHOSE, A., DUTTA, A. K., CHEN, Q., OOI, E. E., WHITE, N. J., DONDORP, A. M., PREISER, P. & CHEN, J. 2018. Microvesicles from malaria-infected red blood cells activate natural killer cells via MDA5 pathway. *PLoS Pathog,* 14**,** e1007298.

YEHYA, A. H. S., ASIF, M., PETERSEN, S. H., SUBRAMANIAM, A. V., KONO, K., MAJID, A. & OON, C. E. 2018. Angiogenesis: Managing the Culprits behind Tumorigenesis and Metastasis. *Medicina (Kaunas),* 54.

YERSAL, O. & BARUTCA, S. 2014. Biological subtypes of breast cancer: Prognostic and therapeutic implications. *World J Clin Oncol,* 5**,** 412-24.

YERUSHALMI, R., WOODS, R., RAVDIN, P. M., HAYES, M. M. & GELMON, K. A. 2010. Ki67 in breast cancer: prognostic and predictive potential. *The lancet oncology,* 11**,** 174-183.

YIN, H., GAO, S., CHEN, Q., LIU, S., SHOUCAIR, S., JI, Y., LOU, W., YU, J., WU, W. & PU, N. 2022. Tumor-associated N1 and N2 neutrophils predict prognosis in patients with resected pancreatic ductal adenocarcinoma: A preliminary study. *MedComm (2020),* 3**,** e183.

YOON, Y., KIM, G., JEON, B. N., FANG, S. & PARK, H. 2021. Bifidobacterium Strain-Specific Enhances the Efficacy of Cancer Therapeutics in Tumor-Bearing Mice. *Cancers (Basel),* 13.

YOUNG, V. B. 2021. Unexpected Results From a Phase 2 Trial of a Microbiome Therapeutic for Clostridioides difficile Infection: Lessons for the Future. *Clin Infect Dis,* 72**,** 2141-2143.

YU, K., LI, Q., SUN, X., PENG, X., TANG, Q., CHU, H., ZHOU, L., WANG, B., ZHOU, Z., DENG, X., YANG, J., LV, J., LIU, R., MIAO, C., ZHAO, W., YAO, Z. & WANG, Q. 2023. Bacterial indole-3-lactic acid affects epithelium–macrophage crosstalk to regulate intestinal homeostasis. *Proceedings of the National Academy of Sciences,* 120**,** e2309032120.

YU, W., HUA, Y., QIU, H., HAO, J., ZOU, K., LI, Z., HU, S., GUO, P., CHEN, M., SUI, S., XIONG, Y., LI, F., LU, J., GUO, W., LUO, G. & DENG, W. 2020. PD-L1 promotes tumor growth and progression by activating WIP and β-catenin signaling pathways and predicts poor prognosis in lung cancer. *Cell Death & Disease,* 11**,** 506.

YUAN, Z., LI, Y., ZHANG, S., WANG, X., DOU, H., YU, X., ZHANG, Z., YANG, S. & XIAO, M. 2023. Extracellular matrix remodeling in tumor progression and immune escape: from mechanisms to treatments. *Mol Cancer,* 22**,** 48.

ZETTER, B. R. 1998. Angiogenesis and tumor metastasis. *Annu Rev Med,* 49**,** 407-24.

ZHANG, Q., ZHAO, Q., LI, T., LU, L., WANG, F., ZHANG, H., LIU, Z., MA, H., ZHU, Q., WANG, J., ZHANG, X., PEI, Y., LIU, Q., XU, Y., QIE, J., LUAN, X., HU, Z. & LIU, X. 2023. Lactobacillus plantarum-derived indole-3-lactic acid ameliorates colorectal tumorigenesis via epigenetic regulation of CD8+ T cell immunity. *Cell Metabolism,* 35**,** 943-960.e9.

ZHANG, X., ZHANG, M., HO, C.-T., GUO, X., WU, Z., WENG, P., YAN, M. & CAO, J. 2018. Metagenomics analysis of gut microbiota modulatory effect of green tea polyphenols by high fat diet-induced obesity mice model. *Journal of Functional Foods,* 46**,** 268-277.

ZHAO, L.-Y., MEI, J.-X., YU, G., LEI, L., ZHANG, W.-H., LIU, K., CHEN, X.-L., KOŁAT, D., YANG, K. & HU, J.-K. 2023. Role of the gut microbiota in anticancer therapy: from molecular mechanisms to clinical applications. *Signal Transduction and Targeted Therapy,* 8**,** 201.

ZHENG, Y., WANG, T., TU, X., HUANG, Y., ZHANG, H., TAN, D., JIANG, W., CAI, S., ZHAO, P., SONG, R., LI, P., QIN, N. & FANG, W. 2019. Gut microbiome affects the response to anti-PD-1 immunotherapy in patients with hepatocellular carcinoma. *Journal for ImmunoTherapy of Cancer,* 7**,** 193.

ZHU, J., LIAO, M., YAO, Z., LIANG, W., LI, Q., LIU, J., YANG, H., JI, Y., WEI, W., TAN, A., LIANG, S., CHEN, Y., LIN, H., ZHU, X., HUANG, S., TIAN, J., TANG, R., WANG, Q. & MO, Z. 2018. Breast cancer in postmenopausal women is associated with an altered gut metagenome. *Microbiome,* 6**,** 136.

8 ABBREVIATIONS.

^{1}H NMR: Proton nuclear magnetic resonance

A2AR: Adenosine 2A receptor

AMP: Anti-microbial protein

AMR: Anti-microbial resistance

APC: Antigen-presenting cell

ARG1: Arginase 1

BCG: Bacillus Calmette-Guérin

BEV: Bacterial extracellular vesicle

BHI: Brain heart infusion

Bif: *Bifidobacterium*

Bif cocktail: *Bifidobacterium* cocktail

BrCa: Breast cancer

CAF: Cancer-associated fibroblast

CAR: Chimeric antigen receptor

cDCs: Convention dendritic cell

CFU: Colony forming unit

CK: Cytokeratin

COGs: Cluster of Orthologous Genes

CRC: Colorectal cancer

C-section: Caesarean section

CT: Cycle threshold

CTCs: Circulating tumour cells

CTLA-4: Cytotoxic T-lymphocyte-associated protein 4

CVD: Cardiovascular disease

CXCL: C-X-C motif chemokine ligand

CXCR: C-X-C motif chemokine receptor

DAMP: Damage associated molecular pattern

DC: Dendritic cell

DCIS: Ductal carcinoma in situ

ECM: Extracellular matrix

EPS: Exopolysaccharide

ER: Oestrogen receptor

EV: Extracellular vesicle

FACS: Fluorescence-activated cell sorting

FFPE: Formaldehyde fixed paraffin embedded

FITC: Fluorescein isothiocyanate

FMO: Fluorescence minus one

FMT: Faecal microbiota transplant

FOXP3: Forkhead box protein P3

FSC: Forward scatter

GABA: Glutamate into γ-amino butyric acid

GALT: Gut-associated lymphoid tissue

GF: Germ-free

GFP: Green fluorescent protein

GIT: Gastrointestinal tract

GM-CSF: Granulocyte-macrophage colony stimulating factor

GPCR: G-protein coupled receptor

GRAS: Generally recognised as safe

H&E: Haematoxylin & eosin

HER2: human epidermal growth factor receptor

HMO: Human milk oligosaccharide

HR: Hormone receptor

HSC: Haematopoietic stem cell

IBD: Inflammatory bowel disease

IBS: Irritable bowel syndrome

ICAM-1: Intercellular Adhesion Molecule 1

ICI: Immune checkpoint inhibitor

IDO: indoleamine 2, 3-dioxygenase

IFN: Interferon

Ig: Immunoglobulin

IL: Interleukin

ILA: Indole-3-lactic acid

iNOS: Inducible nitric oxide synthase

IP: Intraperitoneal

IV: Intravenous

LCIS: Lobular carcinoma in situ

LC-MS – liquid chromatography mass spectrometry

LPS: Lipopolysaccharide

LTA: Lipoteichoic acid

LumA: Luminal A

LumB: Luminal B

MAMP: Microbe-associated molecular pattern

MAPK: Mitogen-activated protein kinase

M-cells: Microfold cells

MDSC: Myeloid derived suppressor cell

MDSC: Myeloid-derived suppressor cell

MHC: Major histocompatibility complex

MLN: Mesenteric lymph node

M-MDSC: Monocytic myeloid derived suppressor cell

MMP: Matrix metalloproteinase

MMTV-PyMT: Mouse mammary tumour virus - polyoma middle T antigen

MPL: Monophosphoryl lipid A

MPO: Myeloperoxidase

MRS: Man Rogosa Sharpe

MRSc: Man Rogosa Sharpe-cysteine

NEC: Necrotising enterocolitis

NETs: Neutrophil extracellular traps

NF-κB: Nuclear factor kappa-light-chain-enhancer of activated B cells

NK: Natural killer (cell)

NMR: Nuclear magnetic resonance

NO: Nitric oxide

NOD: Nucleotide-binding oligomerization domain-containing protein

NSCLC: Non-small cell lung cancer

OD: Optical density

OG: Oral gavage

OMV: Outer membrane vesicle

PAMP: Pathogen associated molecular pattern

PBMC: Peripheral blood mononuclear cell

PBS: Phosphate-buffered saline

PCR: Polymerase chain reaction

PD: Parkinson's disease

PD-1: Programmed death receptor

PDGF: Platelet-derived growth factor

PD-L1: Programmed death receptor ligand

PG: Peptidoglycan

PMAA: Partially methylated alditol acetate

PP: Peyer's patch

PR: Progesterone receptor

PRR: Pattern recognition receptor

PYGS: Peptone Yeast Extract Glucose Starch

qPCR: Quantitative polymerase chain reaction

ROS: Reactive oxygen species

SCFA: Short chain fatty acid

ScRNA-Seq: Single-cell RNA-sequencing

SED: Subepithelial dome

SEM: Standard error of the mean

SNPs: Single nucleotide polymorphisms

SSC: Side scatter

TAA: Tumour-associated antigen

TAM: Tumour-associated macrophage

Tcm: T central memory cells

TCR: T cell receptor

TDLN: Tumour-draining lymph node

Tem: T effector memory

TGFβ: Transforming growth factor beta

Th1: T helper 1 cell

Th17: T helper 17 cell

Th2: T helper 2 cell

TLR: Toll-like receptor

TMAO: Trimethylamine-N-oxide

TME: Tumour microenvironment

Treg: T regulatory cell

Trm: Resident memory T cell

TSG: Tumour suppressor gene

VEGF: Vascular endothelial growth factor

VNMAA: Vancomycin, neomycin, metronidazole, amphotericin, and ampicillin

WHO: World Health Organisation

9 SUPPLEMENTARY.

Supplementary table 9.1. Gating strategy for identifying cell populations including immune cell subsets.

| Immune cell	Gating strategy
T cell	Singlet, Live, CD45+, CD3+
T helper cell	Singlet, Live, CD45+, CD3+, CD4+
T regulatory cell	Singlet, Live, CD45+, CD3+, CD4+, FOXP3+
CD8+ T cell	Singlet, Live, CD45+, CD3+, CD8+
CD8+ T effector memory	Singlet, Live, CD45+, CD3+, CD8+, CD44+, CD62L-
CD8+ T central memory	Singlet, Live, CD45+, CD3+, CD8+, CD44+, CD62L+
CD8+ T resident memory	Singlet, Live, CD45+, CD3+, CD8+, CD44+, CD62L-, CD103+, CD69+
NK T cell	Singlet, Live, CD45+, CD3+, NK1.1+
B cell	Singlet, Live, CD45+, CD3-, CD19+
NK cell	Singlet, Live, CD45+, CD3-, NK1.1+
Dendritic cells	Singlet, Live, CD45+, CD11c+
cDC1	Singlet, Live, CD45+, CD11c+, MHCII+, CD103^{hi}, CD11b^{lo}
cDC2	Singlet, Live, CD45+, CD11c+, MHCII+, CD103^{lo}, CD11b^{hi}
Myeloid cells	Singlet, Live, CD45+, CD11b+
Monocytes	Singlet, Live, CD45+, CD11b+, Ly6G-, Ly6C+
Granulocytes	Singlet, Live, CD45+, CD11b+, Ly6G+
N1 neutrophils	Singlet, Live, CD45+, CD11b+, Ly6G+, I-CAM1+
N2 neutrophils	Singlet, Live, CD45+, CD11b+, Ly6G+, ARG1+
Macrophages	Singlet, Live, CD45+, CD11b+, Ly6C-, F4/80+
M1 macrophages	Singlet, Live, CD45+, CD11b+, Ly6C-, F4/80+, MHCII+
M2 macrophages	Singlet, Live, CD45+, CD11b+, Ly6C-, F4/80+, CD206+
Tumour cells	Singlet, Live, CD45-, GFP+, Luc+
	Singlet, Live, CD45-, Cytokeratin+
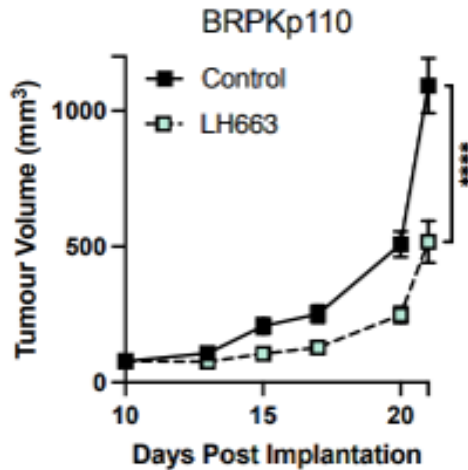
Supplementary figure 9.1. Bif210 reduces breast tumour volume in a BRPKp110 model. Data presented was planned, performed and analysed by Christopher Price (unpublished thesis, Quadram Institute Bioscience, UK, 2024). Bif210 or PBS (control) were orally administered 10 days post BRPKp110 orthotopic injection into the mammary gland. Oral administrations and tumour volume measuring occurred three times per week. Data shows mean tumour volumes (mm3) +/- SEM. **** (p<0.0001) denotes the statistical significance difference between control and Bif210-treated mice calculated by two-tailed unpaired T test.
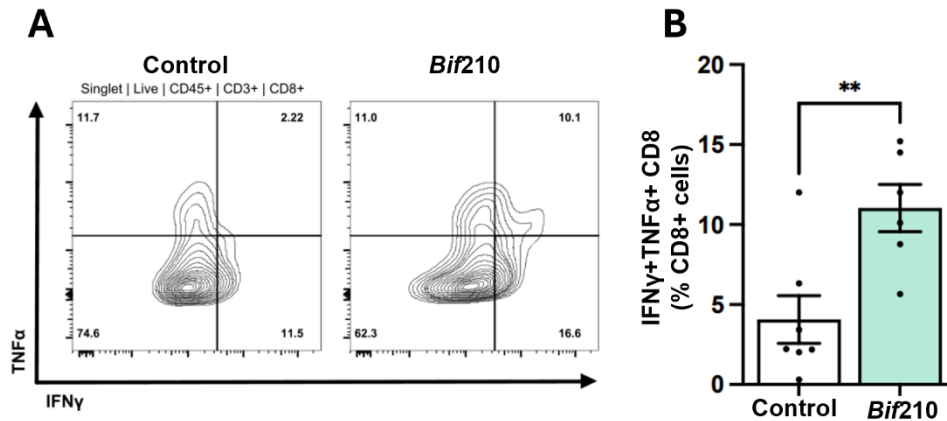

Supplementary figure 9.2. Bif210 increases activity of tumour-associated CD8 T cells. Data presented was planned, performed and analysed by Christopher Price (unpublished thesis, Quadram Institute Bioscience, UK, 2024). (A) Flow cytometry plot shows the polarisation of BRPKp110 infiltrating CD8+ T cells. (B) Data shows the mean percentage (+/- SEM) of CD8 T cells expressing the inflammatory cytokines, TNFα and IFNγ, as a percentage of total tumour-infiltrating CD8 T cells. * (p<0.05) denotes the statistical significance difference between control and Bif210-treated mice calculated by two-tailed unpaired T test.
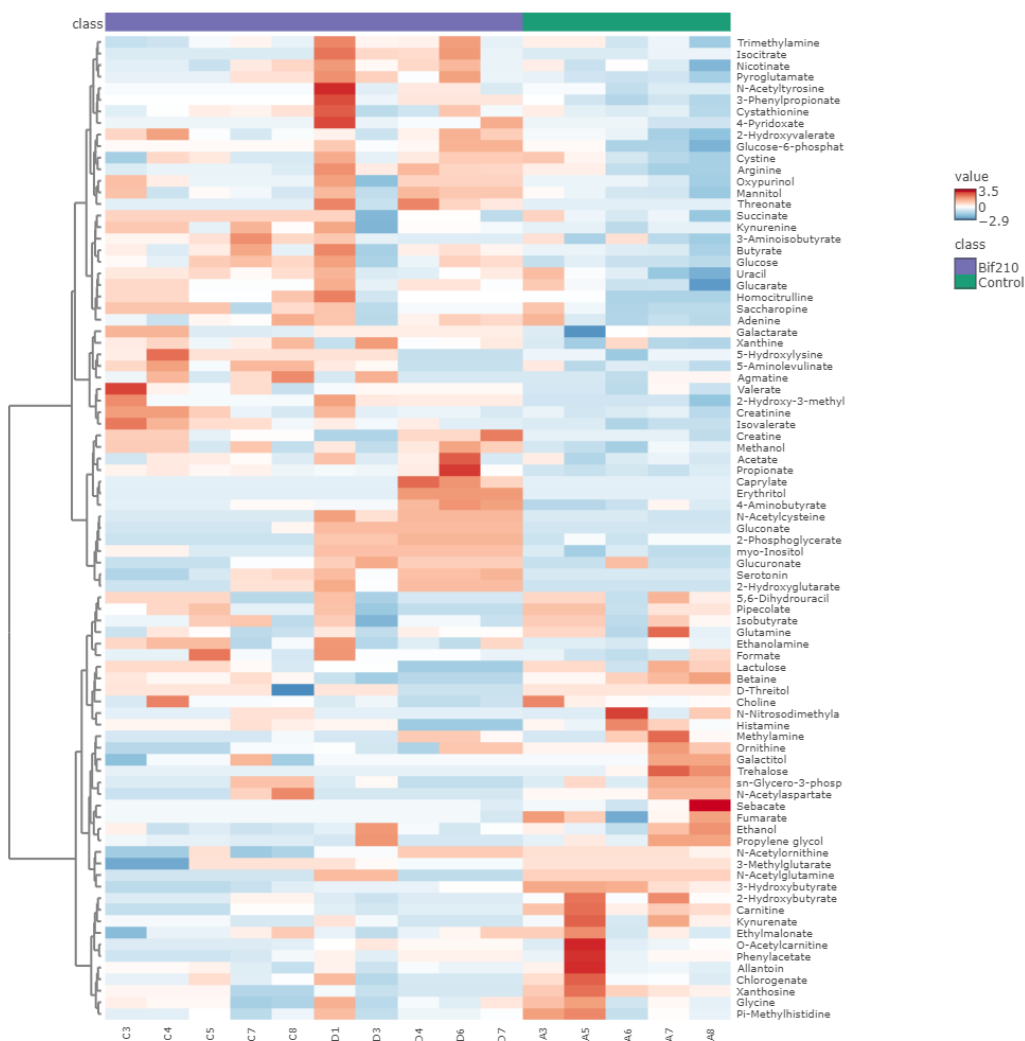
Supplementary figure 9.3. All caecal metabolites identified in tumour-burdened mice. Mice were orally administered PBS (control) or Bif210 for the duration of the BRPKp110 model (total of five treatments total). Caecal metabolites were analysed by ^{1}H NMR. Heatmap and cluster analysis of T-test (Wilcoxon rank-sum test) of all differentially abundant metabolites in caecum samples from control (n=5) and Bif210-treated (n=10) mice.
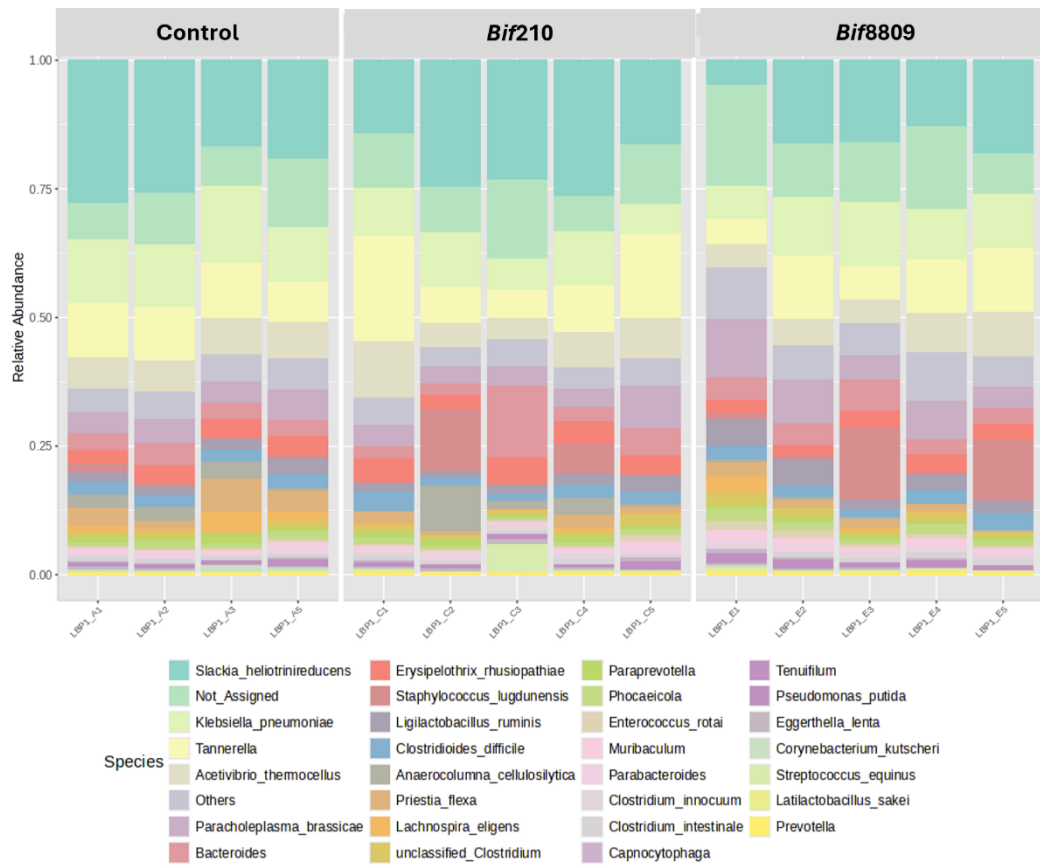
Supplementary figure 9.4 Stacked bar chart of the relative abundance of the top 30 most prevalent bacterial species present in caecal samples from control (n=4), *Bif*210 (n=5) and Bif8809 (n=5) supplemented mice.
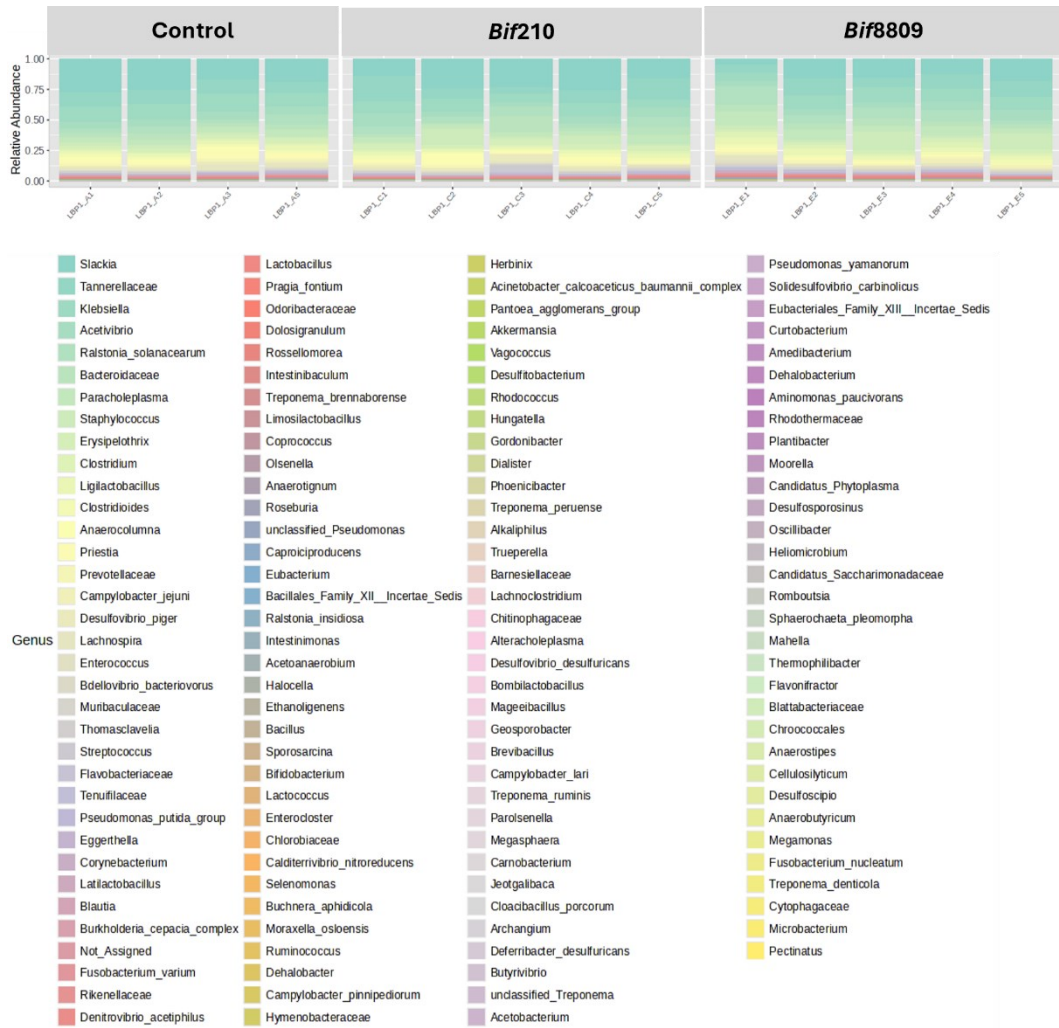
Supplementary figure 9.5 Stacked bar chart of the relative abundance of all the bacterial genera present in caecal samples from control (n=4), *Bif*210 (n=5) and Bif8809 (n=5) supplemented mice.